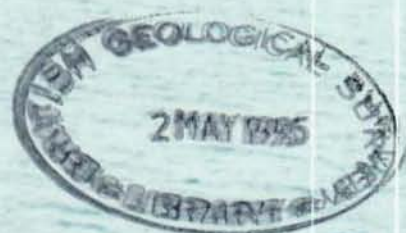


LONG RANGE SHOCK WAVE PROPAGATION (LORASWAP) FROM AN UNDERWATER EXPLOSION IN THE NORTH SEA

Handwritten signature

1: THE EXPERIMENT AND THE DATA



EXTREMELY RARE
NOT AVAILABLE
FOR STAFF LOAN

This report has been generated from a scanned image of the document with any blank pages removed at the scanning stage.
Please be aware that the pagination and scales of diagrams or maps in the resulting report may not appear as in the original



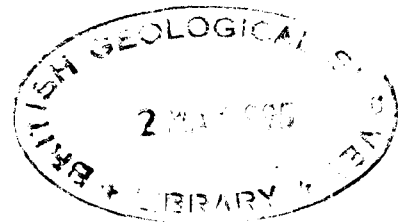
This page is blank

GLOBAL SEISMOLOGY
Report No. WL/89/7

LONG RANGE SHOCK WAVE PROPAGATION (LORASWAP)
FROM AN UNDERWATER EXPLOSION IN THE NORTH SEA.
I: THE EXPERIMENT AND THE DATA

by

P. W. Burton, A. Miller, C. M. Allen
and A. S. Mould
February 1989



Crown Copyright

Copyright is reserved for the contents of this report, no part of which may be reproduced without permission from the Director of the British Geological Survey.

LONG RANGE SHOCK WAVE PROPAGATION (LORASWAP) FROM AN UNDERWATER
EXPLOSION IN THE NORTH SEA. I: THE EXPERIMENT AND THE DATA

by Paul W. Burton, Alistair Miller, Carolyn M. Allen and Alan S. Mould*

Keywords: pull up shallow water seismometer, shock wave propagation,
underwater explosion, acoustic wave, seismic wave,
experimental record

Global Seismology Research Group
British Geological Survey
Murchison House
West Mains Road
Edinburgh
EH9 3LA
031-667-1000

* Marine Geophysics and Offshore Services, BGS

CONTENTS

Table of contents	i
List of Tables	iv
List of Figures	v
Summary	1
1. Introduction	2
2. Planning the experiment	5
2.1 REQUIREMENTS AND OBJECTIVES	5
2.2 CHOICE OF EXPERIMENT SITE	7
2.3 OUTLINE PLAN OF THE EXPERIMENT	9
2.4 CHARGE CONFIGURATION	11
2.5 PREDICTED SIGNAL AMPLITUDES AND EXPLOSION SOURCE PARAMETERS.....	12
2.5.1 Pressure waves	12
2.5.2 Seismic waves	14
2.5.3 Optimum depth	15
2.5.4 Bubble radius (and frequency)	16
2.6 ADDITIONAL SCIENTIFIC BENEFITS EXPECTED FROM THE EXPERIMENT	16
3. Methods and equipment	19
3.1 RECORDING PACKAGES AND TRANSDUCERS	19
3.1.1 Pressure gauges	19
3.1.2 Shot timing	19
3.1.3 Vertical hydrophone strings (VHS)	20
3.1.4 BGS sea bottom package (BGS SBP)	20
3.1.5 Pull-up sea bottom seismometers (PUSSes)	20
3.1.6 Onshore seismometers	21
3.2 REMOTELY OPERATED VEHICLE: SEA OWL	22
3.3 NAVIGATIONAL AIDS	22
3.3.1 SERCEL SYLEDIS B	23
3.3.2 QUBIT TRAC-IV	23
4. Operations at sea	25
4.1 SHOT SITE	25
4.2 PUSS DEPLOYMENT	25
4.3 BGS STATION	25
4.4 POSITION-FIXING PROCEDURES	26
4.4.1 PUSS location	26
4.4.2 SBP/VHS location	26
5. Shot firing	27
6. Simplified properties of the propagation paths and sites occupied .	28
6.1 MODELS OF THE ACOUSTIC PROPAGATION PATHS	29
6.1.1 Water layer	29
6.1.2 Sea-bed	29
6.1.3 Acoustic models and range of applicability	32
6.2 MODELS OF THE SEISMIC PROPAGATION PATHS	32
6.2.1 Shot-point central model	33
6.2.1.1 Water layer	33
6.2.1.2 Sea-bed	33
6.2.1.3 Shallow upper crust	34
6.2.1.4 Upper, mid and lower crust	34
6.2.1.5 Density	35

6.2.1.6	<i>Specific attenuation factors</i>	35
6.2.2	<i>Geophysical constraints on seismic models and range of applicability</i>	35
6.2.2.1	<i>BGS site model</i>	37
6.2.2.2	<i>Tentsmuir hard rock site model</i>	37
7.	The data	38
7.1	DATA FORMAT	38
7.2	DISPLAY OF THE DATA	39
7.3	PREPROCESSING OF THE DATA FILES	39
7.3.1	<i>Despiking</i>	39
7.3.2	<i>Zeroing</i>	40
7.3.3	<i>Low gain</i>	40
7.4	PRELIMINARY ANALYSIS	40
7.4.1	<i>Travel time determinations</i>	40
7.4.2	<i>Amplitude determinations</i>	41
7.4.3	<i>Magnitude M_L</i>	41
8.	Discussion	42
8.1	MAJOR CHARACTERISTICS OF THE ACOUSTIC AND SEISMIC WAVEFORMS	42
8.2	OBSERVED SHOCK WAVE AMPLITUDE: EFFICIENCY OF THE SOURCE	42
9.	Conclusion	44
	Acknowledgements	45
	References	46
	Tables	52
	Figures	72
	Appendices:	101
	Appendix A: Planned schedule for the LORASWAP experiment	101
	Appendix B: Log of deployment of sea bed instruments	103
	1: BGS sea-bottom package 22:Sep:1987	103
	2: Redeployment of Pusses 27-28:Sep:1987	105
	Appendix C: Syledis determination of site locations at the final (second) deployment	112
	1: Shot point	112
	2: PUSSES	114
	3: BGS/ARE listening site	117
	Appendix D: Models for computer simulations	119
	1: Acoustic	120
	2: Seismic	121
	Appendix E: Data inventory	127
	1: List of sites known to have detected the 4500lb explosion	127
	2: Inventory of PUSS data from 4500lb and 900lb explosions	129
	Appendix F: Display of the data	133
	1: whole record	135
	2: acoustic arrivals	150
	3: seismic arrivals	168

Appendix G: Picking list for travel time determinations	183
Appendix H: Photographic record of the experiment	190
1: Photograph Captions	190
2: Plates	192

Tables

Table 2.1	Proposed spacings for instrumentation at sea.	52
Table 2.2	Table of proposed position for PUSSES and other offshore equipment.	53
Table 2.3	Expected maximum pressure (kPa), time constant (ms) and impulse (kPa-ms) for the direct shock wave and first surface reflection from a 4500 lb TNT (2041.17 kg) charge at 75 m depth in water.	54
Table 2.4	Estimated upper bounds to seismic ground motion expected at distance r km from a 4500 lb TNT (2041.17 kg) underwater explosion.	55
Table 3.1	ARE pressure gauge deployment (a) Dimensions of the system; (b) Spacing of pressure gauges on the cable.	56
Table 3.2	ARE pressure gauge calibrations.	57
Table 3.3	BGS Vertical Hydrophone String (VHS) specifications.	58
Table 3.4	BGS Sea Bottom Package (SBP) specifications.	59
Table 3.5	Calibration of Pull up Shallow - water Seismometers.	60
Table 3.6	PUSS specifications; (a) PUSS geophones, (b) PUSS hydrophones.	61
Table 3.7	Seismometer coastal sites installed temporarily on "soft" rock.	62
Table 4.1	Revised shot windows for second deployment.	64
Table 4.2	Offshore site location details (2nd deployment)	65
Table 5.1	Explosion shot times on 29th September 1987 and pressure pulse arrival recorded at RMAS Goosander.	66
Table 6.1	Geological characteristics of offshore sites determined from British Geological survey maps.	67
Table 6.2	Geological column and seismic velocities to 2000 m depth at 56°51' 305"N 00°22'20.2"W from Amoco Well 27/3-1, September 1967.	68
Table 7.1	Data file header block configuration (a) and example (b).	69
Table 7.2	Preliminary results from ARE pressure gauges (a) 4500lb explosion; (b) 900lb explosion.	70
Table 8.1	Comparison of measured extreme pressures with those calculated for the direct wave using equation 2.4. after Britt (1984).	71

Figures

- Fig. 2.1** The selected shot point at about 57°7'N, 0°45'W. The position of shallow boreholes is taken from Thomson & Eden (1977), the deepest penetrates to 81 m. The AMOCO Well 27/3-1 penetrates to about 2 km. HBF: Highland Boundary Fault. SUF: Southern Upland Fault. The coarse dashed line represents probable offshore extension of the HBF and the SUF, and significant offshore faulting. The fine dashed line represents the 50 m isobath. Page
72
- Fig. 2.2** Plan of the experiment. The ragged star shows the 2 ton shot point, about 80 km east of Aberdeen. Recording packages were placed at the locations 1-4, BGS, 5 and 6 along the great circle from the shot point to Tentsmuir, in Fife. The triangles on-shore show the positions of vertical component seismometer sites, squares show three-component seismometer sites, associated with LOWNET and additional "soft" rock coastal seismic installations. 73
- Fig. 2.3** Cross-section of the experiment. The ragged star shows the 2 ton shot point in 75 m water depth. 1-6 represent the positions of Pull-up sea bottom seismometers (PUSSes), each of which contains one three-component geophone and a hydrophone. Each PUSS is ship independent. BGS represents the position of the BGS Sea Bottom Package, which contained one three-component accelerometer and one hydrophone, cabled to the Salmaster. BGS also represents the position of the vertical hydrophone string (VHS), consisting of 10 hydrophones at 5 m intervals from the sea-bed, and of other hydrophones; all of which are cabled to the Salmaster. Tentsmuir is the position of a three-component seismometer in a "soft" rock site onshore but near to the coast. 74
- Fig. 2.4** Charge configuration and shot point moorings. The shackle ring is the shot point identifier at sea; it is the mid-point of the cable held under tension between the two Class 5 mooring buoys. It was intended to detonate the 2 ton charge at 5 m above the sea-bed using floats to create positive buoyancy for the charge anchored to the sea-bed. Sponge shaped floats give buoyancy to the detonation cable which should be slack or strain relieved to avoid snapping. The stand-off distance Goosander to shot point is of order 500 m. 75
- Fig. 2.5** Local magnitude, ML, versus charge size for underwater explosions (adapted from Jacob and Neilson 1977). Enveloping curves and mean trend (dashed line) are eyeball fits. 76
- Fig. 3.1** Shot timing system configurations. 77
- Fig. 3.2** Three-dimensional impression of the configuration of the equipment deployed at sea by BGS, i.e. BGS Sea Bottom Package, Vertical Hydrophone String, Pull Up Shallow-water Seismometer. 78

Fig. 3.3	General system configuration and recording scheme for VHS output, MSF and DCF radio time onto two Store 14s operating at different record levels.	79
Fig. 3.4	Amplitude response to the Geospace MP-24H1 hydrophone used in the BGS Vertical Hydrophone String (VHS). (3900 Ω ; 45%)	80
Fig. 3.5	Schematic representation of the deployment method used for the BGS Vertical Hydrophone String.	81
Fig. 3.6	Block diagram of the recording and digital systems of the BGS Sea Bottom Package. The digital system is contained in the pressure tube which rests on the sea-bed and is cable linked to a surface recorder. Outputs selected in this experiment were three-component digital seismic acceleration and velocity and FM hydrophone. The digital data on channel 13 consists of multiplexed three-component seismic acceleration on Deck 1 and seismic velocity on Deck 2. The hydrophone output is FM recorded. MSF and DCF radio time are recorded on both decks.	82
Fig. 3.7	The amplitude-frequency response of the BGS Sea Bottom Package Teledyne Geotech S-500 accelerometers and Graseby Dynamics 770/401 PZT-4 hydrophone system. The S-500 accelerometer response is given for both velocity and acceleration output. Where only the solid line is shown it is common to all three responses.	83
Fig. 3.8	Plan of the system arrangement at the BGS listening station.	84
Fig. 3.9	The amplitude-frequency response of the PUSS geophone and hydrophone system. The geophone response is identical for Z, X and Y components. The geophone and hydrophone are identically low pass filtered. Where only the solid line is shown it is common to both responses.	85
Fig. 3.10	The phase-frequency response of the PUSS geophone and hydrophone system.	86
Fig. 4.1	Ribbon diagram illustrating the distribution of recording windows programmed into the PUSSES.	87
Fig. 4.2	Plan view of PUSS deployment procedure at site 3.	88
Fig. 6.1	Geological cross-section interpreted between the shot-point (57°06.984'N 00°45.030'W) and Tentsmuir (TMA at 56°24.456'N 02°48.72'E).	89
Fig. 7.1	Map showing sites in the U.K. and Eire known to have detected the 4500lb explosion.	90
Fig. 7.2	Plot of travel time against range for all picked arrivals. (4500lb explosion)	91

Fig. 7.3	Plot of travel time against range for all picked arrivals. (900lb explosion)	92
Fig. 7.4	Plot of apparent velocity against range for all picked arrivals. (4500 lb explosion)	93
Fig. 7.5	Plot of apparent velocity against range for all picked arrivals. (900 lb explosion)	94
Fig. 7.6	Plot of maximum amplitude against range (km) - seismic velocity (4500lb explosion)	95
Fig. 7.7	Plot of maximum amplitude against range (km) - seismic velocity (900lb explosion)	96
Fig. 7.8	Plot of maximum amplitude against range (km) - pressure (4500lb explosion)	97
Fig. 7.9	Plot of maximum amplitude against range (km) - pressure (900lb explosion)	98
Fig. 8.1	Comparison of measured peak pressures with those calculated from the similitude equations. (4500lb explosion)	99
Fig. 8.2	Comparison of measured peak pressures with those calculated from the similitude equations. (900lb explosion)	100

Summary

Two large explosions were detonated in the North Sea about 80 km east of Aberdeen on 29 September, 1987, as part of a collaborative project between the British Geological Survey and the Admiralty Research Establishment. Both charges were deployed and detonated on the sea bed by RMAS Goosander at 57°06.98'N 00°45.04'W in water depth 76.125 m. The 4500 lb (2041.27 kg) TNT charge was detonated at 11h 52m 33.225s GMT and the 900 lb (408.2 kg) TNT charge at 15h 22m 30.591s GMT.

The majority of offshore recording equipment was deployed and retrieved by RMAS Salmaster. Shock waves from both explosions were recorded by a variety of instruments, both offshore and onshore.

Vertical arrays of pressure gauges and shot timing equipment recorded the shock waves in the water near to the shot point, ranges being about 550 m and 230 m respectively for the two shots. Five Pull-up Shallow Water Seismometers (PUSSes) were deployed at ranges from about 10 to 85 km. Each PUSS contained one three-component geophone and one hydrophone and operated independently of any ship but was restricted to recording within nine pre-set time windows, each of 10 minutes duration. At 60 km range three instrument packages were deployed and connected by cable to RMAS Salmaster: two vertical strings of hydrophones, sensitive to higher and lower frequencies respectively and the BGS sea-bed package containing a three component accelerometer and one hydrophone. Four onshore near coastal seismograph stations were installed and recorded at "soft" sites to investigate sediment to hard rock propagation effects of the seismic waves. Seismic recordings were obtained at land stations in the UK and Eire, the latter by the Dublin Institute of Advanced Studies for investigations into the deep crust and lithosphere.

Predicted pressures from a 4500 lb explosion detonated at 5m above the sea-bed were 818kPa at 0.5km range, 28kPa at 10km (closest planned PUSS site) and 2kPa at 85km (furthest planned PUSS site). The pressures observed at 0.55km over a range of depths were 210-660kPa; 8kPa was observed on the sea-bed at 9.98km and .09kPa at 85.29km.

Seismic local magnitude estimated from onshore seismic stations are 2.9 ML and 2.3 ML for the 4500 lb and 900 lb TNT charge respectively.

1. Introduction

This report describes an experiment in the North Sea designed to record the LOnG RAnge Shock WAVE Propagation (LORASWAP) from the detonation of a large charge in shallow water. The experiment was carried out successfully at sea during 18 September to 1 October 1987. In practice two explosions were detonated on the sea-bed at a depth of 76m. in the North Sea at a point about 80 km east of Aberdeen. The experiment and equipment used to observe the various shock waves are described herein. The data obtained are described, catalogued and displayed with a minimum of analysis. Analysis and information included concentrates on the most basic and pertinent aspects: shot timing; properties of the propagation paths and observation sites occupied; and, most fundamentally, the pressure wave observations in the sea water. More detailed data analysis will be the subject of subsequent reports.

The *raison-d'etre* of the experiment is to assist with the prediction of pressure waves at long range from large underwater explosions in shallow water by synthesising the time histories and estimating gross properties e.g. pressure in the water, seismic wave velocities in the shallow crust, reflection and interaction of the waves with sea-bed sediments.

A previous report (MacBeth 1985) reviews the methods used in seismology for synthesising pressure waveforms, and seismic waves propagating through the earth. The methods reviewed were:

1. The Ray Series Method or Asymptotic Ray Theory.
2. Fully numerical methods: Finite Difference and Finite Element techniques.
3. Transform methods: Generalised Ray Theory, Reflectivity and the Thomson- Haskell method.

The Reflectivity method was favoured eventually because overall it was judged to have more advantages than disadvantages compared with the other methods. The Reflectivity method is very efficient in layered media, and includes multiple and converted wave types. Complex wave velocities allow for intrinsic absorption and the compilations are stable at high frequencies. The method used (Kennett & Kerry 1979) considers the

response of a layered half-space in terms of reflection and transmission properties of the medium, for both up- and down-going waves. The method therefore includes all possible reflections and reverberations. The disadvantages are that Reflectivity is computationally expensive, CPU being proportional to the square of the number of layers; secondly, ray training support is required to help in the interpretation of wave arrivals. Reflectivity has already been used to model typical explosion/shallow sea scenarios (MacBeth 1985) appropriate to the North Sea.

Shock waves from an underwater explosion are modified in both shape and wave velocity by the geometrical arrangement and physical properties of sediments and strata (including the sea) through which the waves propagate. After attempting theoretical modelling using Reflectivity, the need to compare observational data with theory became apparent. The need was for an experiment which would provide pressure data, for example, recorded at an array of sensors from a large explosion (say 2 ton) near to the Firth of Forth. This would serve to "calibrate" the modelling software and correlations between the improved modelling, using realistic sea-bed parameters, and observational data would be sought. Pressure observations would also allow evaluation of similitude equations used by Britt (1984) to model the maximum direct shock or free-field pressure wave.

Improved modelling also relies on evaluation of realistic sea-bed parameters, because of the need to consider reflections and shock wave/sea-bed interactions. Sea-bed sediment properties relevant to seismo-acoustic modelling, with the emphasis on the North Sea, have been reviewed by Allen (1988). A simple structural seismic velocity-depth model of the Firth of Forth region, including the effect of sea-bed sediments on seismic propagation, has been obtained by MacBeth and Burton (1988) for the analysis of seismic surface waves generated by underwater explosions (in Kirkcaldy Bay, offshore Scotland). This model can be improved and extended into the North Sea using the seismic data obtained from the controlled explosion experiment described herein. The ultimate aim is to combine knowledge of the sea-bed sediment properties and

realistic sea-bed structure to obtain improved modelling, with perturbations from these sources reduced to a minimum or taken into account. It is then of fundamental importance to compare observed pressures in the water waves with those modelled. Existing models of expected pressures, such as those of Britt (1984), can also be considered.

The report is divided into several sections. The experiment as originally envisaged is described first, including the planned configuration of explosive charge and its location with respect to recording instrumentation position, and the forecast amplitudes of acoustic and seismic waves. The various instruments used to record both acoustic and seismic waves on the sea-bed are briefly described, particularly with respect to instrument response and ensuing acquisition of digital data from analogue, where appropriate. This section also describes the Syledis and Qubit Trac-IV navigational aid used for positioning at sea. A further section then describes the experiment itself, as dictated by circumstances at sea. The following sections then describe simplified models of the geological and seismic parameters of the sites occupied and the propagation paths sampled, information required for subsequent computer modelling; accurate measurement of the time of detonation of the explosions and then an inventory and brief commentary on the total data obtained. A display of much of the data obtained forms a substantial appendix for reference purposes. The discussion centres on the quality and types of data obtained. It emphasises the information obtained on the shock waves through the water, the pressures observed both as a function of range from the explosion and of depth in the water. It compares the observed pressure values with those forecast at the planning and feasibility study stage of the experiment.

2. Planning the experiment

This section deals with the motivation behind various aspects of the experiment and how this relates to the choice of site and equipment. Essential equipment was obviously selected prior to going to sea and allowed only limited scope for adaptation on board ship. The setting up of equipment, for example, sensitivity and dynamic range, was mostly predetermined by expectations arising from estimates of shock wave sizes.

Inevitably, there were changes to the envisaged plan perforce circumstances at sea. Modus operandi had to be adapted to meet specific difficulties and growing first hand experience. These changes and circumstances are described in Chapter 4.

2.1 REQUIREMENTS AND OBJECTIVES

The fundamental objective was to obtain observations of the shock or pressure wave from a large underwater explosion in shallow water to test against the theory.

Ultimately the purpose is to improve modelling of shock waves in water. The time history of the shock wave will be influenced by the charge size, the placement of the charge and interaction of the ensuing pressure waves with sediments on the sea-bed and sea-bed structure. Therefore, fidelity in modelling of real data depends on several components: the theory and software used; precise knowledge of the charge; detailed knowledge of the structure in which the charge is detonated and with which the pressure waves subsequently interact, including models of this structure which can be incorporated into the shock wave modelling at short and long range from the explosion. The software to be used relies on the Reflectivity method to model time histories. Current software uses similitude equations (e.g. examples are cited, Britt (1984)) to scale amplitudes of pressure time histories.

It was also the general objective to use a known charge to test the existing software.

Implicit within this objective is the need to know realistic sea-bed parameters, and to use these in the modelling process. This knowledge falls into two parts. Firstly, there are the soft sediments which constitute the immediate sea-bed at the shot point and along the propagation path. These sediments will perturb reflection coefficients pertinent to pressure wave reverberations and will also influence seismic wave propagation. Secondly, there is the deeper sea-bed structure. Overall, the sea-bed structure may be known partially from in situ measurements, e.g. boreholes, which provides spot sampling. Additional information on the sea-bed structure can also be obtained by recording and interpreting the seismic waves generated in conjunction with an explosion. The analysis of borehole and seismic data has to provide a seismological model of the sea-bed, that is in terms of compressional and shear wave velocities, density and attenuation, with depth.

The experiment is therefore designed to improve pressure wave time history modelling in two ways:

1. by using data on realistic sea-bed structure obtained from both borehole information and from the seismic waves generated by the experiment itself to generate a sea-bed model sufficiently good not to be an uncertainty of significance in the pressure wave modelling,
2. by providing pressure data at an array of sensors from a known explosion, correlations between the improved modelling obtained in 1 and the observational data can be sought.

The eventual combination of 1 and 2 will calibrate the modelling software.

In view of the general objective - to compare observational data with theoretical - the experimental requirements which emerged were:

1. to detonate a known and large quantity of explosive in shallow water, at depth near the sea-bed,
2. to detonate the charge at full yield,

3. to detonate a smaller charge at the same point, in the same circumstances,
4. to choose a point for the explosion which is expected to provide relatively simple propagation paths for both pressure waves and seismic waves - to "simplify" the subsequent interpretation and modelling,
5. to record with good dynamic range the direct shock or pressure wave near the sea-bed at increasing range from the explosion,
6. to record the direct shock or pressure wave at short and long range at different depths in the sea,
7. to record the seismic waves on the sea-bed at increasing range from the explosion.
8. to record the seismic waves at "hard" and "soft" rock seismometer sites at close proximity to the sea (to investigate possible coupling of seismic waves with the softer sediments overlying the deeper sea-bed structure).

An additional objective onshore of predominantly seismological pertinence was:

1. to record the seismic waves in the Scottish Midland Valley, and beyond, at increasing regional distances from the shot point (to investigate crustal structure).

2.2 CHOICE OF EXPERIMENT SITE

The main considerations in site selection were: the amount of structural information available about the site and implicit shock wave propagation paths; simplicity of propagation paths; water depth; navigational precision possible at the site; minimisation of adverse environmental impact, including proximity to centres of population and offshore structures; the logistics of assembling the experiment and deploying equipment at the site.

The Firth of Forth was one possible site. Underwater explosions in the Forth had been observed by seismological stations and a preliminary seismic structure obtained (MacBeth & Burton 1988). Such a site would also have been close to ARE embarkation points at HM Royal Dockyard, Rosyth. This was ruled out because of the large charge size, around 2 tons, which would have been detonated too near to centres of population and relatively busy sea lanes. It would also have been difficult to deploy a sufficiently long linear array of recorders on the sea-bed which traversed structures in a relatively simple manner. At the other extreme, deep water in excess of 150 m compatible with seismically optimum depth detonation of the charge (Jacob 1975), could only be found at considerable distances into the North Sea, or in such anomalous structures as the Devil's Hole Deeps - which would be expected to complicate interpretation, or in the Witch Ground Beds of the South Fladen area - close to oil fields and platforms. These sites were also ruled out on this occasion.

The shot point selected is located within the offshore extension of the Scottish Midland Valley around $57^{\circ}7'N$, $0^{\circ}45'W$ (Fig. 2.1). Seismic propagation paths to the permanent BGS stations of LOWNET and Paisley-net do not traverse the known major geological discontinuities, e.g. the Southern Upland Fault. Therefore, the seismic waves are expected to sample the rocks of geological provinces without being contaminated by many obviously perturbing structures. The size of the shot and distance offshore (110-150 km approximately), ensures sampling to different geological horizons and regimes: in (a) the shallow crust, (b) the deep crust and lithosphere, (c) onshore and (d) offshore geological provinces. Considerable information on geological structure pre-exists (see discussion in chapter 6). The expected water depth at this shot point is around 70-80 m.

Inspection of the summary bathymetry chart given by Holmes (1977) shows that reasonably smoothly varying bathymetry can be found to the south and south-west. Pressure waves recorded at this azimuth should be relatively unperturbed by sea-bed topography.

2.3 OUTLINE PLAN OF THE EXPERIMENT

The central concept of the experiment at sea is shown in the plan in Fig. 2.2 and cross-section in Fig. 2.3. The specific details of the listening equipment packages, such as the , instrument responses, package sizes etc, are described in the next chapter. The logistics of the experiment at sea required two ships: RMAS Salmaster and RMAS Goosander. Many of the underlying reasons and background information for adopting specific details in this plan are explained later in this report.

It was decided to opt for six Pull-up Shallow Water Seismometers (PUSSes) to be deployed on the sea bottom in a line between the coast and the shot point. The chosen shot point was located around 57°7N, 0°45W. The recording great circle line extends from the coastal seismometer station at Tentsmuir in Fife (TMA in Fig. 2.2) , to the shot point. Each PUSS was to be deployed from the Salmaster in about 50-70 m of water. Once deployed each PUSS is self contained but is not disposable and would have to be retrieved after detonating the charge. Each PUSS contains one 3-component geophone and one hydrophone. Each PUSS can record a total of 90 minutes of 4-channel data; this 90 minutes can be divided into pre-selected time windows of arbitrary length and 10 minutes was the selected option. Coordination of PUSS recording time windows and potential firing times of the explosion is obviously vital.

One BGS sea bottom package was to be deployed by the Salmaster on the sea-bed in about 50-70 m of water on the shore-shot line (TMA to explosion in Fig 2.2). This package is not self contained. It would need to be cable-linked to the moored and stationery Salmaster, either directly or via mooring buoys. This cable would carry signals received at the BGS sea bottom package to recorders on board the Salmaster. The BGS sea bottom package contains one 3-component piezo-electric seismometer and one hydrophone. In addition, it was necessary for the recorder on the Salmaster to record an accurate time standard such as MSF transmitted from Rugby.

A vertical hydrophone string (VHS) would also be deployed on the shore-shot line near to the BGS sea bottom package (Fig.2.3) and would be deployed by the Salmaster. The VHS would extend to the sea bottom and

have 10 equally spaced hydrophones. This VHS is not self contained and would have to be cable-linked to the moored and stationery Salmaster, either directly or via mooring buoys. This cable would carry the VHS signals to its own recorder on board the Salmaster. This recorder on the Salmaster would also be required to record accurate MSF radio time.

It is necessary to know the accurate time at which detonation occurred, therefore the times of explosions were to be recorded on Goosander, using hydrophone and geophone detectors, with signals going onto a recorder in parallel with MSF radio time. In order to ensure that accurate shot instants would be obtained, radio time from two different transmitters (MSF and DCF), would be recorded. Additionally, near-field observations of the shock waves were to be obtained using pressure gauges deployed by the Goosander at its chosen stand-off position for detonating the charges.

Instrument gain and sensitivity settings depended on estimates of pressure and impulses from the water pressure and expected seismic ground displacements, velocities and accelerations. These estimates are described in section 2.5.

All the sea bottom packages were to be located on the same great circle, the shore-shot line shown in Fig 2.2, with the spacings and distances from the 2 ton shot point as given in Table 2.1.

Increasing spacing with distance between the sea bottom packages was chosen, rather than equal spacing, because of the expected $1/r^n$ signal decay with distance. The proposed positions for PUSSEs and other offshore equipment are given in Table 2.2. Water depths were read from Admiralty Charts.

The exact position of each package would need to be located using Goosander/Salmaster navigational devices. Accuracy to better than 20 m is desirable. Syledis and QUBIT Trac-IV navigational aids were chosen for temporary installation on Salmaster to achieve this accuracy.

The 2 ton explosive charge would be deployed by the Goosander at about

57°7N, 0°45W, at a precise site previously surveyed by the Salmaster and at which appropriate buoys were moored (precise mooring details as per ARE plans are described in Section 2.4). The charge was to be suspended 5 m above the sea bottom; sea bottom to surface being about 75 m.

Only one 2 ton charge would be available and it was vital that its detonation should be synchronised within the recording time windows of the PUSSES (the BGS sea bottom package and the VHS are continuous recording devices and thus not a constraint). There would be a total of 90 minutes of recording time available for each PUSS and this was to be divided into pre-selected time windows. Once deployed, the PUSS time windows cannot be changed without retrieving, resetting and redeploying them. Ten minute recording time windows were appropriate for the purposes of this experiment, assuming that the 2 ton explosion would be detonated no sooner than 2 minutes and no later than 4 minutes into the time window. This provided nine time windows and a choice of 9 detonation time windows available to the explosives officer. This was designed to allow flexibility for on the spot decisions in the event of bad weather or other delaying factors.

The schedule including potential shot windows, all times stated in GMT, is given in Appendix A.

2.4 CHARGE CONFIGURATION

The two charge sizes adopted were 4500 lb TNT (2041.2 kg TNT nominally referred to as 2 ton elsewhere in this report) and 900 lb TNT (408.2 kg TNT).

The 4500 lb TNT charge was to be constructed from fifteen 300 lb TNT drums placed in an open crate (Plates 24-27), and the 900 lb TNT charge from three 300 lb TNT drums lashed together to be lowered on a pallet (Plate 31). High explosive primers were inserted in the drums prior to deployment in order to attain full yield at detonation (Plate 24).

The intention was to detonate both charges at a position suspended 5 m above the sea-bed. This was to be achieved using a sinker weight attached to the charge, and a large float (constructed from practice contact mines)

with sufficient buoyancy to hold the charge taut at 5m from the sea bed. (Fig 2.4). The purpose of detonation 5 m above the sea-bed is to instigate against energy loss in simple rock fracturing, probable with detonation on the sea-bed. Detonation 5 m above the sea-bed, a distance less than the bubble radius, ought to achieve slap-down of the pressure pulse impulsively on the sea-bed without extensive rock fracturing. This is seismically more efficient.

The shot point for practical purposes at sea was defined as the shackle ring shown in Fig 2.4. The mooring arrangement consisted of two Class 5 buoys wired together with each buoy anchored to the sea-bed so that the whole system was held under tension. The mid-point of the wire connecting the two buoys consisted of a shackle ring which lay below sea level. The shackle ring was connected to a free floating orange marker buoy so that it could easily be retrieved when required, for example, to locate the precise shot point when the charge was to be lowered.

The detonation cable was to be reeled out from a drum with small sponge-like floats attached every few metres (see photographs), and fed through the shackle ring down to the charge. Anticipated stand-off distances for the Goosander at shot-time were 1500' and 750' for the larger and smaller charge size respectively.

2.5 PREDICTED SIGNAL AMPLITUDES AND EXPLOSION SOURCE PARAMETERS

It was expected that the equipment deployed on the sea-bed at different distances from the explosions would need to span a wide range of signal amplitudes. It was necessary to forecast the approximate amplitude of direct pressure waves and seismic ground motions at each proposed site so that instrumental gains could be set accordingly.

2.5.1 Pressure wave:

Standard expressions given by Cole (1948) for the direct shock or pressure wave $P(t)$ MPa from an underwater explosion, detonated at time $t = 0$, are of the form:

$$P(t) = P_m(r) S(t-t_d), \quad (2.1)$$

where the explosive source function, $S(t-t_d)$, and distance between explosion and recorder, r metres, are given by:

$$S(t-t_d) = H(t-t_d) \exp [-(t-t_d)/\theta(r)] \quad (2.2)$$

$$r = [(d_s - d_r)^2 + x^2]^{1/2} \quad (2.3)$$

d_s and d_r are the explosive source and the sensor depth respectively, x their horizontal separation. H is the Heaviside step function. t_d is the shock wave arrival time, assumed to be given approximately by $t_d = r/c$, c being the speed of sound in water. The maximum pressure, $P_m(r)$, and time constant, $\theta(r)$ ms, depend on the type of explosive used but are of general similitude form given by Britt's (1984), equations:

$$P_m(r) = K_p (W^{1/3}/r)^a, \quad (2.4)$$

$$\theta(r) = K_\theta W^{1/3} (W^{1/3}/r)^b. \quad (2.5)$$

W kg is charge weight and values for the constants adopted in (2.4) and (2.5) are those for TNT, viz:

$$K_p = 52.4, \quad a = 1.13; \quad (2.6)$$

$$K_\theta = 0.084, \quad b = -0.23.$$

Integrating equation (2.1) over time gives the impulse, $I(r)$ MPa-ms:

$$I(r) = K_I W^{1/3} (W^{1/3}/r)^c, \quad (2.7)$$

with constants:

$$K_I = 5.75, \quad c = 0.89. \quad (2.8)$$

These constants are for integration carried to 50(r) ms after the main pressure wave.

The preceding discussion closely follows Britt (1984) where further details can be found. Forecasts of the maximum pressure and impulse for both the direct wave and the surface reflected wave as a function of

distance from a 4500 lb TNT (2041.2 Kg) charge are given in Table 2.3. A water depth of 75 m is assumed with the charge on the sea-bed. Values tabulated for the surface reflected wave equal those of the direct wave at 10 km range and are therefore not tabulated at greater ranges.

A maximum of 28 kPa pressure was expected at the closest proposed PUSS at 10 km range and at the furthest proposed at 115 km range the peak pressure should have dropped to about 1.8 kPa. Maximum pressure expected at the pressure gauges close to the shot-point at the Goosander's stand-off position at 0.5 km is about 818 kPa. In view of this expected decay of peak pressure with distances it was decided to set the PUSSes at sites 4-6 at an equal but highest gain, PUSSes at sites 2-3 at an intermediate but equal gain, the PUSS at site 1 was to be set to the lowest gain.

2.5.2 *Seismic waves:*

Jacob & Neilson (1977) investigate the seismic local magnitude (M_L) of underwater explosions as a function of charge weight. Their data (Fig. 2.5) adapted from Jacob & Neilson) show considerable scatter, but the overall trend is very clear, and enveloping curves have been drawn into Fig. 2.5 spanning ranges of observed M_L for given charge size. Examination of Fig. 2.5 shows empirically that the local magnitude generated by a 4500 lb TNT charge lies in the observational range 2.6-3.74 ML. In view of this, a magnitude 3.74 ML was selected as being the largest value compatible with the size of the charge.

Local magnitude is defined in terms of seismic ground motion by the equation (Richter 1958):

$$ML = \log A - \log A_0 \quad (2.9)$$

A and A_0 are ground displacement in mm (notionally on a standard torsion Wood-Anderson seismometer). A is the observed seismic ground displacement and A_0 is a magnitude standardising distance correction term for local magnitude calculation. There are tables of standard A_0 values (see Richter 1958). Forecasts of the extreme upper bound to the seismic displacements, assuming 3.74 ML, are given in Table 2.4. This table also

gives forecasts of extreme upper bounds to the velocity and acceleration of seismic ground motion for sea bed explosions by choosing a representative decay, which is assumed to be of the form $A = \exp(-0.225)$, based on observations of an explosion in the Firth of Forth (Newmark 1984). The calculations in Table 2.4 are truncated at a range of 100 km. The highest values of seismic ground motion expected to be observed at the closest PUSS (10 km range) to the 4500 lb explosion are a displacement of 148 microns with a corresponding velocity of 9.3 mm s^{-1} and acceleration of 584 mm s^{-2} at 10 Hz. The BGS Sea bottom package at 60 km range contains an accelerometer where the expected maximum acceleration is 12 mm s^{-2} .

2.5.3 Optimum depth:

The optimum depth for an underwater explosion to generate maximum peak velocity in the seismic P-waves, is given by Jacob (1975) in the relationship:

$$W = \left[\frac{d(d + 10)^{5/6}}{803} \right]^3 \quad (2.10)$$

d metres being the optimum depth for a W kg TNT charge. For $d \gg 10$, (2.10) may be reduced to approximately

$$d \approx 38.41 W^{2/11} \quad (2.11)$$

for ease of calculation. Optimum depth using (2.11) for the large charge is about 154 m and 115 m for the small charge. Both these values are considerably in excess of the water depth, 75 m, available at the shot-point. Firing at about half optimum depth, as is the case for the large charge, loses about 30-40% of the peak velocity in the P-wave (Jacob, personal communication); never-the-less, the seismic signal-to-noise ratio was expected to be good for these charge sizes. The "optimum" charge in 75 m of water is only about 54 Kg for seismic efficiency which is too small for the overall purposes of this experiment.

2.5.4 Bubble radius (and frequency)

In order to enhance the expected efficiency of the explosion in terms of generation of maximum pressure and seismic waves, the intention was to suspend the charge above the sea-bed, but within the first bubble radius. This should minimise non-linear and unquantifiable energy losses at the source, such as the shattering of rock in the sea-bed, and thus simplify the source to effective 'slap-down' of the pressure pulse impulsively on the sea-bed.

Weston (1960a) gives an expression for the bubble radius, a ft, which follows Arons (1943),

$$a = 12.6 \left(\frac{W}{d_o} \right)^{1/3} \text{ ft}, \quad (2.12)$$

where W is charge in lb TNT and d_o is (depth in feet + 33). Therefore 4500 lb of TNT detonated at 75 m generates a value for bubble radius of $a = 31.8$ ft (9.7 m). The equivalent radius for the 900 lb charge is 18.6 ft (5.7 m). Using the arrangement shown in Fig. 2.4, involving sinker weight, charge and buoy it was anticipated that both charges would be detonated five metres above the sea-bed.

It is worth noting the expected bubble pulse frequencies. Weston (1960b) defines the bubble pulse frequency, F_b Hz, as:

$$F_b = 0.23 d_o^{5/6} W^{-1/3}, \quad (2.13)$$

with W in lb and d_o (depth in feet + 33). (13) gives values of 1.52 and the 2.60 Hz for the 4500 and 900 lb charges respectively, at 75 m (246.1 ft) depth.

2.6 ADDITIONAL SCIENTIFIC BENEFITS

The objectives of the experiment at sea are clear in terms of observing pressure waves from a large underwater explosion and ultimately using the data to calibrate and improve modelling of the shock waves. However, there are other potential benefits expected from the experiment which are of a geological nature.

The experiment provides an opportunity to investigate the deep structure in the Forth Approaches and Scottish Midland Valley using geophysical techniques, some of which have only been developed in recent years.

It should be noted that much of the general distribution of seismic instrumentation in relation to the shot point, lies approximately perpendicular to that used in LISPB (Bamford et al, 1976) and is therefore aligned with the structural "grain" of the Midland Valley. Land based recordings will provide data designed to give an improved 3-D model of the shallow crust in the Midland Valley (top 2 or 3 km). In view of the distance of some onshore seismic stations from the shot point, the seismic phase P_n will be observed allowing refraction studies of the deeper crust and upper mantle. This will contribute to lithospheric studies in Ireland, deeper crustal studies of the southern Midland Valley and improved 3-D models of the Midland Valley, with the opportunity for tie-in to borehole proving, to extend inter-borehole geological interpretation in the shallow crust.

The deployment of offshore seismic recorders in the experiment should help to improve knowledge of the geological transition from a marine environment to a well-surveyed land one, by seismic sampling of appropriate propagation paths. Land based recordings have already proved useful in augmenting marine airgun profiles (Lund et al, 1987).

The possibility exists to correlate offshore propagation paths with borehole data in the Quaternary. There is an abundance of Quaternary borehole data, between the shot point and near-coastal seismic stations (Thomson & Eden, 1977), which will be sampled by ray paths from the shot point (see Fig. 2.1). Correlation of these data with the seismic may help to clarify deeper structures west of the Devils Hole Horst in the extension of the Midland Valley offshore.

There is also a large and growing body of information on the physical properties of rocks (e.g. Carmichael, 1982). The crustal geophysical model, provided by LISPB (Bamford et al, 1976), has already been improved in resolution of shear velocity-depth for the shallow crust in the eastern Midland Valley (MacBeth & Burton, 1986). This refinement may be taken

further by comparing seismically interpreted velocity-depth models with known outcrop or borehole rock physical properties, extending the range of geological interpreted models using physical measurement from seismics. These gradual refinements in measurement should contribute to assessing specific geological provinces, for example, in the present case, the rocks of the Midland Valley Carboniferous (e.g. see Browne et al, 1985, 1987).

Offshore, the deployment of PUSSES will provide an opportunity to observe the interface (Scholte and Stonely) waves which may be generated and hence, to measure the shear wave structure of the unconsolidated sediments. In general the experiment allows further development and application of the use of high frequency Rayleigh waves (1 Hz) in the measurement of physical properties of rocks *in situ*, to help discern the physical properties of deep geological structure.

3. METHODS AND EQUIPMENT

The general layout of the equipment is shown in Figs 2.2 and 2.3, with PUSSEs at sites 1-6 and a vertical hydrophone string and the BGS Sea Bottom Package (SBP) at the site marked BGS. The major items of equipment were photographed and can be seen at the end of the report. MSF Rugby was recorded as a time standard on all BGS systems.

3.1 RECORDING PACKAGES AND TRANSDUCERS

3.1.1 Pressure Gauges

Piezo electric pressure gauges (type: Piezotechnics TX - IAP - CE) were deployed in two vertical arrays of six cable-linked to Goosander. The signal from each gauge was recorded at two different sensitivity levels on a store - 14DS recorder. The general arrangement of the gauges and their sensitivities are given in Tables 3.1 and 3.2 respectively, as provided by ARE. The presentation and analysis of the data will be dealt with in subsequent reports.

3.1.2 Shot Timing Equipment

In order to determine the velocity of seismic arrivals across the array it is essential to know the shot instant accurately. Two independent systems were installed on the Goosander in an attempt to be failsafe. The first system was designed around a Store-7 recorder with a Store-14 as a back-up. The second system was a digital recorder programmed to switch on automatically for each of the scheduled ten minute shot windows. MSF and DCF time standards, along with one geophone, one hydrophone and the shot firing pulse, were recorded on each system. The geophones were fixed to the ships hull and the hydrophones were suspended in the sea. As only the first onset from the shockwave was important the recording sensitivity levels were not critical. The arrival times at the geophones and hydrophones are corrected for the travel-time between the shot and Goosander's stand-off position. The shot instant was also obtained by recording the shot pulse from the firing mechanism. The configuration of the shot timing systems is shown in Fig. 3.1.

3.1.3 Vertical Hydrophone String (VHS)

A general impression of the VHS is shown in Fig. 3.2, (see also Plate 22). At the position marked BGS (Figs 2.2 and 2.3), ten Geospace type MP-24L hydrophones were deployed in a vertical configuration at 5m intervals, with the first hydrophone placed at 5m from the sea-bed. The string was anchored to the sea bed by a sinker weight and held approximately vertical by submerged plastic floats. Signal cables were routed along the sea-bed and up to the recording systems on Salmaster. The cables were terminated in an underwater junction box which, in the event that the ship had to leave station, could be buoyed-off and later retrieved. The recording configuration and response specifications for the VHS are given in Figs 3.3, 3.4 and Table 3.3. The method of deployment (Fig. 3.5), which was devised to eliminate the possibility of entanglement, was successfully implemented at sea.

3.1.4 BGS Sea Bottom Package (SBP)

The SBP was also deployed at the position marked BGS (Figs 2.2 and 2.3). The package was originally designed to monitor earthquakes in the North Sea near to the oil fields (Turbitt et al 1983). The pressure sealed package (Plate 17) contains a 3-component set of piezoelectric seismometers (Teledyne Geotech type S500) and one piezoelectric hydrophone (Graseby Dynamics type 770/401/PZT-4), along with the associated electronics for signal conditioning. The multicore signal cable was routed along the sea-bed and up to the recorders on Salmaster. This cable was also terminated in an underwater junction box (Plate 20) which could be buoyed-off if necessary. The system configuration and response specifications are given in Figs 3.6, 3.7 and Table 3.4. The final arrangement at the BGS station is shown in Fig. 3.8.

3.1.5 Pull-Up Sea-bottom Seismometers (PUSSes)

The complete digital recording system is contained in a 4ft long pressure sealed tube. Each PUSS contains a 3-component set of geophones and an externally mounted piezoelectric hydrophone (Plate 12). The general

impression is shown in Fig. 3.2 and the system details are described in Owen & Barton (1986). For this experiment the 90 minutes of available recording time was divided into nine pre-selected time windows of ten minutes duration (see Appendix A). To allow for any slight loss of synchronisation between PUSS windows and shot times, and also shock-wave travel times across the array, the explosions were to be detonated no sooner than 2 minutes and no later than 4 minutes into any PUSS recording window (Appendix A). This would ensure that, the fastest waves at the closest PUSS (10Km) and the slowest waves at the most distant PUSS (115Km), would be recorded. PUSS sensitivities (Table 3.5) at each site were arranged according to the expected pressures and ground velocities given in Tables 2.3 and 2.4. The specifications for the hydrophone and geophones are given in Tables 3.6 and 3.7.

3.1.6 Onshore Seismic Stations

The explosions were recorded on-shore using standard seismological stations of the BGS. The main network used was LOWNET (Crampin et al 1970) in the Scottish Midland Valley with extensive additional observations coming from other BGS networks (Browitt 1979). All LOWNET stations, which use the Willmore MkIII-A seismometer, are shown in Fig. 2.1. Response specifications are given in Turbitt & Stewart 1982.

For this experiment additional special stations were installed at four coastal sites, the details of which are given in Table 3.7. These sites were chosen near to the sea and deliberately placed in soft sediments in an attempt to obtain the closest coupling to the seismic waves propagating in the sea-bed sediments. Strata were chosen to give the best geological match to the extension of the submarine strata just offshore. At each site, the data from a 3-component set of seismometers placed on soft ground and a vertical reference seismometer on a nearby hard rock site, were recorded on a Geostore which provided one week of continuous recording per tape.

3.2 REMOTELY OPERATED VEHICLE (ROV)

The BGS sealed Package and the PUSSEs do not contain a facility to determine their orientation after deployment, and although they can be held lengthwise, as much as possible, along the array line while lowering them to the sea-bed, the final alignment on the sea-bed is not known. In an attempt to verify the orientation of the instruments, a bright line was painted along the length of each package (Plates 12,17). Subsequently, using a remote controlled submersible (SUTEC: Sea Owl Mk11) (Plate 23), it was anticipated that, by following the PUSS tethering cable or the SBP recovery rope down to the sea-bed and along to the package, the orientation could be determined from the visual lines on the instruments and the compass bearing indicated on the Sea Owl control unit.

By fixing the grab-hand around the cable near the surface the ROV could successfully reach the decoupling weight but could not successfully follow the cable along the sea-bed to the package. This was quite conceivable as the cables between the decoupling weights and the packages were deliberately loose and winding on the sea-bed. It was also apparent that the ROV was under-powered for this particular application, because of the strength of the sea currents.

3.3 NAVIGATIONAL SYSTEMS

The slower seismic surface waves were expected to have a velocity similar to or slightly less than that of the main shock wave in the water, that is about 1.5 km s^{-1} or less. The arrival time of such waves would be resolvable to a few hundredths of a second, implying an uncertainty in path length not exceeding a few tens of meters at most. As phase arrival time resolution could not be usefully improved beyond this, it was concluded that the position-fixing scheme should not introduce a larger error than that implicit in reading the seismic phase arrivals. This meant that position-fixing had to achieve accuracy of the order of a few tens of meters.

Positions were fixed by simultaneous ranging by Sercel Syledis B to any three of four precisely coordinated shore reference stations. Shore

stations were set up specifically for the project by Wimpol Ltd who also supplied shipboard Syledis equipment. Ranges were computed into plan position by the QUBIT TRAC-IVB computer system, owned and operated by the Marine Geophysics/Offshore Services programme of the British Geological Survey.

3.3.1 Sercel Syledis B

Syledis is a transportable ranging system capable of measuring three ranges from shore reference stations. Maximum achievable range is typically 100-120km, dependant on antenna heights, power output and antenna configuration but in any case limited to "three times line-of-sight". For this project, the antennae at the four reference stations were configured to provide at least three reference signals throughout the work area. Ranging accuracies quoted by manufacturers indicate a maximum probable error of 3.6m at 120km providing that bench-calibrated delays for each mobile reference station pair are precise and correctly applied. Residuals on least-squares position calculations obtained at sea, indicated a good level of ranging precision. The expected maximum probable error of 3.6m refers to the antenna on-board ship and loss of accuracy beyond this could only be attributed to any deviations incurred while lowering the packages down to the sea-bed. It was necessary to adopt deployment schemes which placed equipment on the sea-bed in a careful and controlled manner, coordinated with the position fixing procedure. (Plate 5)

3.3.2 Qubit Trac-IVB

TRAC-IVB is a navigation computer system designed to accept line-of-position (LOP) data from a wide variety of navigation sensors, compute any combination of such LOPs into plan position using a least-squares fit, and output the position as a variety of displays designed to facilitate shipboard survey operations. For this project, three Syledis LOPs chosen from the four available, were utilised as the

primary position fix. Decca main chain 2A LOPs were also recorded and computed for comparison. All positions were computed in Airy spheroid, OSGB 36 datum and expressed as latitude and longitude. Data for all fixes were recorded in hard copy on a graphics printer. Vessel guidance was given through a range of steering and target displays on a colour monitor adjacent to the steering position.

4. OPERATIONS AT SEA

Major operations at sea were photographed and filmed throughout the experiment by ARE and BGS photographic personnel. A video of the experiment has been made, and can be made available.

4.1 SHOT SITE

The Salmaster proceeded to the shot position to deploy the mooring buoys for the explosives (Fig.2.4 and Plate 1). Following the deployment of the mooring buoys, the vessel moved very gently forward to the marker buoy using the bow thrusters. With an observer on the walkway between the horns, the marker buoy (Plate 2) was hauled up over the bow until the shackle ring was sighted directly below the observer. The shot position, taken as the shackle ring, was then fixed by Syledis as detailed in Appendix B.

4.2 PUSS DEPLOYMENT

Deployment was carefully co-ordinated by constant communication arrangements between the bridge and operators on deck. All six PUSSES were deployed on schedule in accordance with the logs shown in Appendix A. However, as unfavourable weather conditions delayed the shot firing during the first deployment of the PUSSES, they were retrieved, reset to cover the final set of recording windows (Table 4.1 and Fig. 4.1), and redeployed according to the schedule given in Appendix C.

4.3 BGS STATION

Following the first deployment of the PUSSES the Salmaster sailed to the BGS position and deployed the SBP according to the procedure and log given in Appendix C. The SBP cable was disconnected from the ship and buoyed-off until after the second deployment of the PUSSES. On returning to the BGS station the cable was retrieved using the Gemini. Deployment of the VHS was then carried out as shown in Fig. 3.5. The recording systems had already been installed in a portacabin below the forward deck.

4.4 POSITION FIXING PROCEDURES

Measured distances along and off the ships main axis, along with the vessel-heading taken from a gyrocompass, were manually keyed in by the operator. Offsets from the syledis antenna to the points of deployment, were then computed and applied by Trac IVB. The final positions of the instruments at the times of shot firing are listed in Appendix B and summarised Table 4.2

4.4.1 Puss location

Equipment deployed on the sea-bed was fixed at the time of bottoming with the assumption that the position was vertically below the point of deployment. In order to assess the possibility of the PUSS having been dragged, the vessel movement was closely monitored (Fig.4.2) from the time of bottoming until the release of the buoy. Where drag may have occurred, the vessel locus and seabed equipment configuration were used to estimate a most likely position.

4.4.2 SBP/VHS location

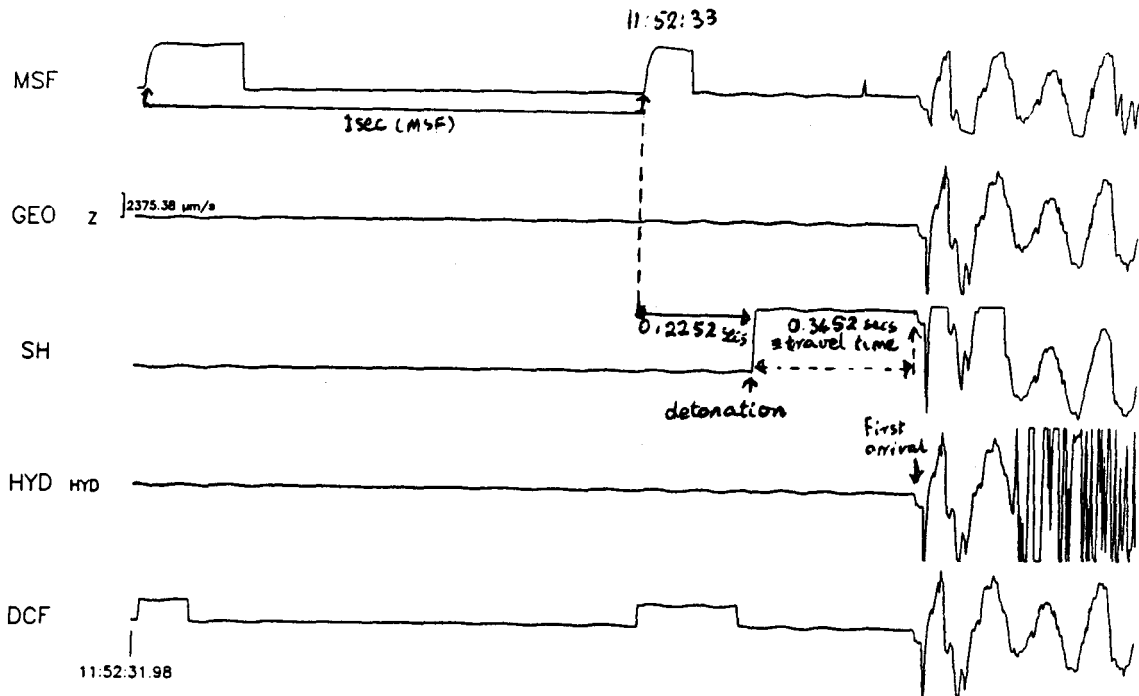
Trac-IVB guidance was used to provide close control over anchor positions hence allowing the various sensors to be closely equidistant from the shot point (Fig.3.8). The BGS sealed package was fixed in the same way as the PUSSES. The vertical hydrophone string was fixed by pulling the surface floats and rope tight and measuring the range to the ship by taut rope, along with a bearing on the ship's gyro compass. The offset was manually computed and applied to the ship's position.

5. SHOT FIRING

Operators on shore were continuously updated on the changing schedules at sea using ship-to-shore communications. All systems were in position and operating prior to the first of the second series of shot windows at 13h 22m on Monday 28 Sept. However, technical problems associated with the deployment of the charge delayed firing until the next day (Sept 29), when both the 4500lb and 900lb charges were detonated at 11h 52m GMT and 15h 22m GMT respectively. The signals from both charges were successfully monitored on Goosander and Salmaster.

The shot times were determined by measurement from the continuous record played out on a jet pen recorder at high speed, using the MSF and DCF time code traces as reference, as illustrated below. The results are listed in Table 5.1.

LORASWAP 1 shot timing



6. Simplified properties of the propagation paths and sites occupied

The major inputs to the computer programs which will be used to model the acoustic and seismic waves are, firstly, source parameters of the explosive source and, secondly, realistic models of the acoustic and seismic propagation paths between the shot-point and the sensor positions (Fig.2.2). Modelling of the observational data will be described in a subsequent report. This chapter will produce the primary acoustic and seismic models which describe the propagation paths used in the experiment.

Plane-layered models are required by the modelling programs (for example, see: Kennett & Kerry 1979; MacBeth 1985). The principal parameters required in these models are: layer thickness; compressional and shear wave velocities, α and β km s^{-1} ; density ρ g cm^{-3} ; specific attenuation factors for both compressional and shear waves, $1/Q_\alpha$ and $1/Q_\beta$ respectively.

Considerable data on the geological stratification of the sea-bed can be obtained from the off-shore geological maps published by the British Geological Survey and by extrapolation from on-shore geological maps. The sheets which were consulted and from which specific inferences were made concerning geological strata at sites PUSS 1-4, BGS and PUSS 5 (of Fig.2.2) are listed in Table 6.1.

The single most important proving evidence for structure in the sea-bed and shallow upper crust (SUC) near to the shot-point was provided by AMOCO Well 27/3-1 of September 1967. This provided direct observation of geological strata and one-way compressional wave travel-times down to 2 km (Table 6.2). Other important evidence from which model parameters could be inferred were provided by MacBeth & Burton's (1988) Model FF1 for the Firth of Forth, Bamford et al's (1976) LISPB models crossing the Scottish Midland Valley, and shallow off-shore borehole data provided in Thomson & Eden (1977) and Holmes (1977). Links between parameters and tables of observed physical properties in unconsolidated sediments are provided by Allen (1988).

The selection of specific parameter values and construction of the acoustic and seismic models appropriate for modelling to different ranges from the shot-point will now be summarised.

6.1 MODELS OF THE ACOUSTIC PROPAGATION PATHS

These models are restricted to a layered sea overlying a sea-bed which will be taken as extending down about 60 m before a half-space may be assumed. The interaction of shock or pressure wave, which propagates through the sea, with the sea-bed, is not influenced by material properties at greater depths for the acoustic frequencies considered. However, the physical properties of the top few tens of metres will significantly influence reflection coefficients and the resulting interference waveform.

6.1.1 Water layer

Three layers will be used to form a modified summer profile based on Fofonoff & Millard (1983) and as discussed by MacBeth (1985). In all cases 1.510 km s^{-1} will be used in 0 - 20 m depth, 1.4902 in 20 - 40 m and 1.480 at all water depths exceeding 40 m down to the sea bottom. $1/Q_\alpha$, $1/Q_\beta$ values are effectively zero. This leads to:

Layer No	Type	Thickness	Depth to base, m	α km/s	β km/s	ρ g/cc	$\frac{1}{Q_\alpha}^*$	$\frac{1}{Q_\beta}^*$
1	Water	20	20	1.5100	0	1.02	0	0
2	Water	20	40	1.4902	0	1.02	0	0
3	Water	40 to sea bed	sea bed	1.4800	0	1.02	0	0

* Use value of $Q^{-1} = 10^{-6}$ to maintain computational stability.

6.1.2 Sea-bed

Three layers will be used, these being two layers of unconsolidated sediments overlying a consolidated half space. Given the borehole evidence provided in Thomson & Eden (1977), Holmes (1977) and BGS 1:250000

offshore maps of Quaternary geology and sea-bed sediments displayed on the Peterhead and Marr Bank sheets, the sediments are divided into an upper sand layer and a lower silty sand layer, the sand layer being twice the thickness of the silty sand layer.

Layer No	Type	Thickness	Depth to base, m	α km/s	β km/s	ρ g/cc	$\frac{1}{Q_\alpha}$	$\frac{1}{Q_\beta}$
4	Recent Pleistocene sand (fine) ¹	20	Depends on sea depth at each site	1.749 ¹	.195 ³	1.941 ⁵	.03 ⁶	.06 ⁷
5	Upper Tertiary silty sand	40		1.838 ²	.751 ⁴	1.772 ⁵	.03 ⁶	.06 ⁷
6	Lower Tertiary gravelly muddy sand	∞ (or remainder of Plio-Pleistocene (to 139m in case of AMOCO)		1.838 ²	.926 ⁸	1.772 ⁵	.03 ⁶	.06 ⁷

All individual physical property values for a specific layer parameter are extracted from review tables in Allen (1988) as follows:

1: Although Thomson & Eden (1977) do not subdivide the "sand" category used in their borehole logs it will be defined as "fine sand" in order to extract α values from Hamilton (1980) and Allen (1988). $\alpha = 1.749$ km/s is similar to Schirmer's (1971) value of $\alpha = 1.725$ km/s for "sand".

2: Velocity calculated from Plio-Pleistocene one-way travel time in AMOCO well after allowing for 20 m of fine sand.

3: Jensen & Schmidt (1986) for sand at 20 m.

4: Calculated using $\alpha/\beta = 2.449$ or a Poisson's ratio, σ , of 0.4.

5: From Hamilton (1980) and Hamilton et al. (1982).

6: From Hamilton (1972).

7: From Hamilton (1976), taking log decrement, δ , ~ 0.2 for both sand and silty sand.

8: Calculated using $\alpha/\beta = 1.985$ or $\sigma = 0.33$, appropriate for soft unconsolidated sediment near to the surface.

It is worth noting possible values which are appropriate for Poisson's ratio. Assumpcao & Bamford's (1978) LISPB results show typically $\sigma = 0.25$ except in the upper crust south of the Southern Uplands fault ($\sigma = 0.231$) and in the middle crust under the Midland Valley ($\sigma = 0.224$). However, higher values are expected near to the surface where there are soft or unconsolidated sediments; this is supported by laboratory and field measurements e.g. $\sigma = 0.33$. Poisson's ratio links α and β as follows:

$$\alpha = [2(1-\sigma)/(1-2\sigma)]^{1/2}\beta, \quad (6.1)$$

$$\alpha = c(\sigma)\beta, \quad (6.2)$$

and typical values are:

σ	$c(\sigma)^2$	$c(\sigma)$	
0.231	2.859	1.691	South of Southern Uplands
0.224	2.812	1.677	Middle crust, Midland Valley
0.25	3.	1.732	
0.27	3.1739	1.7815	
0.33	3.941	1.985	Soft unconsolidated sediment near surface
0.40	6.	2.449	This value assumed for silty sand layer in new acoustics models developed here
0.45	11.	3.3166	
0.49	52.	7.2111	
[0.4921376]	64.583937	8.037035	From the unconsolidated sediment sea-bed layer of Model FFI for the Firth of Forth (MacBeth & Burton 1988)

6.1.3 Acoustic models and range of applicability

One single model cannot be chosen to represent the entire propagation path from the shot-point to Tentsmuir. The above layers and numerical values of parameters are combined to form representative models as follows.

1. The layering given above is good to form a representative model at the shot point and extending to PUSS 1.
2. For sites PUSS 2 and 3 use layer 4 and layer 5 plus the residual thickness of layer 6, similarly layers 1 and 2 plus residual of layer 3.
3. For sites PUSS 4,5 and BGS use layer 4 and residual of layer 6, that is, layer 5 has now been pinched out.

This implies three varieties of preliminary acoustic model, the parameters of which are listed in Table D1 in Appendix D.

6.2 MODELS OF THE SEISMIC PROPAGATION PATHS

In general the construction of the central model representative of the shot point will be guided by the layers and parameters of AMOCO Well 27/3-1. This well is about 20 km southeast of the shot point and given that the general dip of geological strata is to the northeast, with low angle - about 1:50 or 1:100, this well is taken as a good representation of the geological column down to 2 km depth at the shot point. This well projects onto the Tentsmuir to shot point great circle at a point less than 3 km northeast of the shot point. The parameters extracted and derived from the borehole log for the purposes of this model are given in Table 6.2. The number of layers, n , in the ensuing seismic model is constrained by CPU time used in the program REFLECT which is proportional to n^2 and typically 10 layers implies 1000 s.

Most of the seismic excitation propagating to the observational end of the PUSS line, PUSS 5 at 85 km, will be confined to the top few kilometers of the upper crust. However, models will be generated encompassing the crust and lid of the upper mantle to allow eventual modelling throughout

the Scottish Midland Valley and beyond. In view of the relatively small angle of dip of the geological strata downwards northeast along the Tentsmuir to shot point propagation path, one central model will be used to model most of the first order effects. Perturbations and individual changes to this model will be used to investigate lateral inhomogeneities and specific local variations.

6.2.1 Shot-point central model

The central model is designed to have 1 water layer; 1 (or 2) unconsolidated sediment layers; 4 layers corresponding to the AMOCO well down to approximately 2 km; 3 layers in the upper and mid crust within 2 to 18 km; 1 layer in the lower crust extending to the Moho within 18 to 31 km, which will usually be considered as the half space layer, except when an upper mantle lid is needed beneath the Moho for distant modelling. The overall considerations in choosing the Shot-point Central Model are complicated and summarised below, the model which results is given in Table D2a.

6.2.1.1 Water layer: One layer is used to form an average and modified summer model based originally on Fofonoff & Millard Jr.'s (1983) models which are discussed by MacBeth (1985). This is a reduction of the acoustic model water layers from 3 to 1. The representative velocity value used will be 1.4902 km s^{-1} (Kaye & Laby 1973). This value corresponds to a temperature of 10°C and a salinity of 3.5% at surface depth. The $1/Q_{\alpha,\beta}$ values are effectively zero although in practice set to 10^{-6} for computational purposes. The water depth is known to be slightly more than 75 m at the shot point.

6.2.1.2 Sea-bed: The sources of information and assumptions used to model the sediment and solid earth layers are mostly defined as footnotes to the tabulated parameters within the central model table. The broader details are as follows:

Two layers are used which extend to the bottom of the Tertiary Plio-Pleistocene layer of the AMOCO Well at 214 m beneath sea level, whereas the acoustic modelling considered 3 layers. The general borehole evidence for the unconsolidated layer composition is provided by Thomson & Eden

(1977), Holmes (1977) and BGS 1:250,000 offshore maps of "Quaternary Geology" and "Sea-bed Sediments" displayed on the Peterhead and Marr Bank sheets. The two layers used are considered to consist of an upper fine sand layer overlying a silty or gravelly muddy sand, with properties as in the acoustic case, but taken as a single layer. The fine sand layer has compressional and shear wave velocities implying a very high Poisson's ratio in excess of 0.49 and the lower layer implies $\sigma = 0.33$.

6.2.1.3 Shallow upper crust: The horizons and P-wave velocities for these 4 layers extending down to about 2 km are taken directly from the observations in AMOCO Well 27/3-1. Shear wave velocities are computed using an assumed Poisson's ratio of $\sigma = 0.33$. Observational values of σ at these depths could not be found except for Assumpção & Bamford's (1978) comment that high values of σ exist near the surface where there are soft or unconsolidated sediments and their indications that these may persist down to 2 - 3 km in the Scottish Midland Valley (their Fig. 7). A Poisson's ratio of 0.33 is consistent with comparison of their shear wave velocities below 0.6 km in the model FF1 of the Kirkcaldy Bay region of the Firth of Forth (MacBeth & Burton 1988) with compressional wave velocities in the Permian Zechstein and Lower Paleozoic base layers of the AMOCO Well 27/3-1 i.e. comparing mid to lower layers of inshore structure with deeper layers of offshore structure at the shot point, noting that strata slope slightly down dip northeast towards the shot point. The major shallow and upper crustal features of FF1 were determined from inversion of high frequency (~ 2 Hz) fundamental mode Rayleigh wave velocities, observed from explosions in Kirkcaldy Bay and recorded in Edinburgh, to shear-velocity depth profiles (MacBeth & Burton 1988).

6.2.1.4 Upper, mid and lower crust: There is no borehole information available for depths beyond 2 km. Shear wave velocities are modelled for 3 layers within 2 - 18 km (Macbeth & Burton 1985) and compressional wave velocity in the lower crust extending to the Moho at 31 km (Bamford et al. 1978). Poisson's ratio throughout the upper, middle and lower crust are taken from Assumpção & Bamford (1978). Where necessary, a value of 8.1 km s^{-1} is taken for compressional velocity in the lid to the upper mantle, similar to the values indicated by Bamford et al. (1976) for sub-Moho in the Scottish Midland Valley.

6.2.1.5 *Density*: Derivation of density from velocity values follows Stuart's (1978) prescription for the North Sea, specific details are appended as footnotes to tabulated values in the shot-point central model.

6.2.1.6 *Specific attenuation factors*: Regional measurements of attenuation appropriate to Scotland, the Midland Valley in particular, and to the North Sea are in short supply. Allen's (1988) review of physical properties of marine sediments was used to guide selection of attenuation values in different sand types (Hamilton 1976c) in the sea bottom layers. $1/Q_{\beta}$ in the Carboniferous of the Midland Valley has been measured by Evans (1981) down to about 2 km using Rayleigh waves and their values are reasonably consistent with MacBeth & Burton's (1987) general results for attenuation in the upper shallow crust in Scotland. No regionally specific attenuation values for the upper crust through to the upper mantle are available and so values are selected from those generally representative of the continental crust and lithosphere (e.g. Burton 1976).

6.2.2 *Geophysical constraints on seismic models and range of applicability*

The Shot-point Central Model, the derivation of which is mostly described above, is given in Table D2a.

The range of applicability of this model depends on the relative consistency and simplicity of the structure parallel to the shot-point to Tentsmuir great circle. There is considerable other geophysical evidence for simplicity of structure, being valley-like, parallel to the shot-line axis out to the shot-point. Secondly, there is evidence that the AMOCO Well is on the flanks of this structure - this is why deeper layers are used in the shot-point velocity depth model for the shallow upper crust (i.e. the Triassic and Zechstein), as the final adjustment of parameters with respect to those observed at the AMOCO Well.

Examination of the contours on the Aeromagnetic Map of Great Britain (Sheet 1, England, Scotland & Northern Ireland) shows them to be consistent with a synclinal valley with axis parallel to the shot-line.

The gravity data emphasises this fact. The Tay Forth Bouguer Gravity Anomaly Map (Sheet 56°N 04°W) shows the Bell Rock gravity anomaly, a 10 mgal high, just to the southeast of the shot-line. The shot-line itself is parallel to an elongated 5 mgal contour. North of Arbroath, and north of the shot-line, the Bouguer values again rise to a 9 mgal high anomaly (typical of lower Devonian sandstone complex). The Peterhead Bouguer Gravity Anomaly Map (Sheet 57°N 02°W, 1:250000, Provisional Edition) for the northeast of the shot-line still shows the trend of the syncline parallel to the shot-line. All the geophysical evidence indicates that the shot-line is following down the dip or core of the principal syncline in the area and is parallel to the axis of major faulting.

The AMOCO Well, south of the shot-line, is just off to the south of the Peterhead Sheet. It is likely that the structure in the well yields an under-estimate of the thickness of the nearer surface sedimentary layers on the shot-line, because the AMOCO Well is on the southern flanks of the syncline of the shot-line. The Marr Bank Bouguer Gravity Anomaly Map (Sheet 56°N 02°W, 1:250000, Provisional Edition) strengthens this interpretation, showing that the AMOCO Well does lie on the southern flank where the sedimentary layers are thinner, at about 10+mgal, within a 10 mgal contour high.

The Forth Tay Aeromagnetic Anomaly Map (1:250000) helps in the interpretation of structure at the southwest end of the shot-line. This map shows high positive anomalies west of Tentsmuir reaching upto +100 nT. These anomalies extend about 13 km northeast, about 8 km offshore past Tentsmuir. This implies that the Lower Devonian basalts are still sufficiently near to the surface at this distance offshore to cause these anomalies.

Weighing the structural evidence provided by the AMOCO Well (Table 6.2), the geological maps (Table 6.1), the aeromagnetic anomaly and Bouguer gravity anomaly maps, leads to the geological cross-section in Fig. 6.1 for the shallow upper crust. This geological cross-section can be parameterised into two seismic models representative of the BGS sea-bed site and the Tentsmuir hard rock coastal site (see Fig. 2.1), to supplement the shot-point central model described above and in Table D2a.

6.2.2.1 BGS site model: The BGS site model (Table D2b) has a sea thickness of 60 m, thinner than that of the shot-point Central Model. The parameters of the two sea-bed layers are identical in the two models. The significant differences are confined to the shallow upper crust (layers 4-5) and the upper crust (layers 6-8), inspection of Fig. 6.1 underlines the reasons for this. Parameters for the mid crust, starting at 9 km depth, are identical in the two models. Indeed, the seismic parameters of the deepest upper crustal layer (8) are also identical, layer 8 in the BGS site Model simply being thinned to extend from 5.3 to 9.0 km. Differences in seismic properties between the two models are therefore constrained within depth above 4 or 5 km and mainly reflect the thicker Triassic and the identification of Devonian layers.

6.2.2.2 Tentsmuir hard rock site model: This model (Table D2c) obviously excludes a sea layer. The two sea-bed layers of the previous models are also excluded and no matching to the unconsolidated sediment layer in the Firth of Forth model FF1 (MacBeth & Burton 1988) is considered, although a model representative of the three-component seismometer site at TMA on soft rock would need this. The general interpretation of the geological strata at Tentsmuir is shown in Fig. 6.1 for the shallow upper crust down to 2 km depth (layers 1-3).

The 300 m thickness of the Lower Devonian Old Red Sandstone upper layer is inferred from the BGS Arbroath Solid Geology Map (1:250000); similarly inferred are the Lower Devonian volcanics, basalt and sandstone extending down to 2 km and divided into layers 2-3 for seismic parameterisation. Shear wave velocity is drawn from Evans' (1981) inversion of Rayleigh wave velocities in the Old Red Sandstone and in Devonian Lavas. Footnotes to Table D2c explain the derivation of the seismic parameters in the shallow and upper crust. Parameters of the mid and lower crust, and upper mantle down to over 90 km (layers 5-10) are identical to the bottom six layers of the two offshore models previously constructed. Four more layers are added to the Tentsmuir hard rock model extending it to below 12000 km into the upper mantle. The parameters of this extension derive largely from the Jeffreys-Bullen 'A' model and are incorporated simply with an eye to future modelling of the seismic waveforms up to 1 Hz energy at Tentsmuir, a range of 148 km from the shot-point.

7. The data

This chapter describes the data which has been acquired, with particular emphasis on that from the instrumentation at sea.

A list of sites at which the larger of the two explosions is known to have been recorded is given in Appendix E and illustrated on the map in Fig. 7.1. The list includes the sites at sea, and BGS temporary and permanent sites covering the UK and Eire. In addition to the permanent land stations of the various BGS networks and University arrays, a number of temporary stations were deployed for the event by other organisations including The Dublin Institute of Advanced Studies (72 stations), University of Hull (5 stations) and Glasgow University (2 stations).

This report concentrates on the data from the sea bed instrumentation along the great circle path from the shot point to Tentsmuir A (Fig. 2.2). These comprise the PUSSEs and the BGS Sea Bottom Package and the land station at Tentsmuir. These files were subjected to pre-treatment in order that the maximum amount of data could be recovered, and that the final data set files should all be in the same format.

7.1 DATA FORMAT

The format selected for the data files consists of a four line header block containing information on:

- (1) The filename
- (2) The source explosion
- (3) The station, channel and instrument
- (4) The data, e.g. sampling rate, units etc.

followed by the data values for a single channel in double precision fixed format in order that the full number of significant figures could be preserved for data from all sources. An example is given in Table 7.1. The header was designed to contain all the information required by standard time series analysis programs.

The processing of the data required to put the data into the required format is outlined below. The data set is now available on magnetic tape in ASCII format both "as digitised" and after processing. The currently available files are given in Appendix G.

7.2 DISPLAY OF THE DATA

The data obtained from the PUSSEs, the BGS instrumentation at sea and some preliminary results from the land station at Tentsmuir are displayed in Appendix F. In each case, the whole of the data in each data file is displayed graphically in Appendix F1, with the regions of the trace (2 secs) containing the acoustic arrivals in Appendix F2 and those containing the seismic arrivals in Appendix F3.

7.3 PREPROCESSING OF THE DATA FILES.

The preliminary processing to which the data has been subjected is described in the following paragraphs.

7.3.1 Despiking

Close examination of the data files revealed some channels on which spikes were present which were artifacts of the digitisation process. These were removed where one could be confident that they were not part of the data stream. In cases of doubt, they were left in. The criterion for use with the continuously recorded instruments was that the spike should not be present on the jet pen ployout of the data.

With the digitally recorded PUSS instruments, the spikes were usually unambiguous. Two of the PUSS files were found to have a very low amplitude signal which was partly masked by spikes with a very uniform spacing and size, which were not readily susceptible to filtering (Z14G1.DAT, Z14G2.DAT). In order to render this data accessible, a program was written allowing one to zoom in on a spike and remove it. In files other than the two named above, the vast majority were single point

spikes of which the amplitude varied enormously. A significant proportion of the spikes in the digital files were dropouts to zero. This procedure was chosen as the best able to maintain any trends in the data without distorting the background noise level or losing significant signal amplitude. The data files are available on magnetic tape both with and without spike removal.

7.3.2 Zeroing

The PUSS digital files were already normalised to zero when received. The files from the BGS package and land stations were not, each channel having an offset to a greater or lesser degree. The procedure here was to take the average of all points up to the arrival of the seismic signal and to subtract this value from all data points in the file.

7.3.3 Low Gain

The gain on the system at Tentsmuir appeared to have been set too low such that the signal was buried in system noise generated during digitisation. Fortunately, the frequencies in the noise tend to be higher than those in the data, allowing some improvement to be brought about by filtering. For display purposes only, the Tentsmuir data were filtered at 8Hz before plotting (Figs. F1.8 and F1.16). The data files on the magnetic tape are not filtered. Since the original analogue signal is clean, but of low amplitude, it is hoped to be able to achieve better recovery by transcribing the source tape at a higher gain. The graphs of the Tentsmuir data should therefore be regarded as preliminary only.

7.4 PRELIMINARY ANALYSIS

7.4.1 Travel time determinations

A program was written to pick the arrivals from the sea bed instruments and the BGS vertical hydrophone string for both events. The arrival times for both seismic and acoustic signals are listed in Appendix H. Travel times were calculated using the shot times determined at the Goosander (Table 5.1). The travel times are plotted against distance from the shot

point (Range (km)) in Fig. 7.2 and 7.3 for the 4500lb explosion and the 900 lb explosion respectively. All components of all records and both shots are included in order to show the range of values observed. Those from the BGS Sea bed package have been corrected for the instrumentally introduced delay (Table 3.4). The apparent velocities (Range/Travel time) are plotted in Fig. 7.4 and 7.5.

7.4.2 Amplitude determinations

The maximum amplitude of the seismic and acoustic wave forms for the sea bed instruments and hydrophone strings are plotted in Figs. 7.6 and 7.8 for the 4500lb explosion and in Figs 7.7 and 7.9 for the 900lb explosion. Preliminary peak pressure values from the ARE pressure gauges, (Short trot) are given in Table 7.2.

7.4.2 Magnitude M_L

The local magnitudes for the two explosions were estimated from the amplitude of signals received at the LOWNET stations. The 4500lb charge yielded a local magnitude of 2.9 M_L and the 900lb charge, 2.3 M_L . These have been plotted in Fig. 2.5.

8. Discussion

8.1 MAJOR CHARACTERISTICS OF THE ACOUSTIC AND SEISMIC WAVEFORMS

An examination of the BGS vertical hydrophone string records, both the analogue signal recorded on the jet pen and after digitisation at 2011.5 samples per second, has revealed that the signal at long range contains high frequencies in excess of 2kHz in the first 1/10th sec from the first arrival, obscuring any shape. It is apparent from the analogue playout that the onset is not sharp, the maximum values occurring up to 0.2secs after the first arrival. The two hydrophones nearest the sea bed, although losing some sensitivity due to the effects of water pressure, did detect the influence of the seismic waves, albeit weakly.

Unfortunately the only available sea bed instruments (PUSSES) were limited to a digital sampling rate of 256Hz. They also have a limit on the maximum increment between samples. The shape of the pulse at the acoustic arrival is thus open to question. The acoustic arrivals, as recorded by the PUSSES, also exhibit a high frequency component just after the first arrival. Despite the limitations, clear arrival times can be measured, and the peak amplitudes readily determined. It will be possible to generate spectra from this data, bearing in mind the frequency limitation of the instruments. This will be done for the next report.

8.2 OBSERVED SHOCK WAVE AMPLITUDE: EFFICIENCY OF THE SOURCE

The ratio of peak pressures measured for gauge 188 for the two explosions is $0.66/1.5 = 0.44$. Using the similitude equations, the calculated ratio of peak pressures $P_{\max}(4500\text{lb})/P_{\max}(900\text{lb})$ is 0.815 allowing for the differences in distance. This is an indication that the present source theory is inadequate when charges are detonated on the bottom. This may, in part be a result of the differing conditions, in that the 900 lb charge was lowered to the sea bed on a pallet and detonated while still on it, whereas the 4500lb charge was detonated in a frame, allowing the shock wave direct access to the soft sandy sediment of the sea bed. The much reduced efficiency of the large charge could also partly be explained if

some of the energy were expended in digging a crater. This would also lead to the gauges nearer to the sea bed being sheltered from much of the shock wave, more so in the case of the large charge. This is borne out by the observations given in Table 7.2.

The peak pressures measured at the various instruments deployed at sea are compared with the predicted values from equation 2.4 for P_{\max} using the constants for TNT given in equations 2.6 and the measured depth and range of each instrument (Britt 1984). The results are listed in Table 8.1 and displayed in Figs 8.1 and 8.2. It is noted that the measured values do not exceed the the calculated values for the 4500 lb charge but for the 900lb charge, for which the depth was closer to the optimum, calculated maximum pressures were exceeded at the site of the Goosander.

9. Conclusion

The LORASWAP experiment has generated the most comprehensively instrumented and fully documented data set yet available for an underwater explosion, generating pressure, velocity and acceleration data, for the sea bed and pressure in profile through the water column.

The experiment took place in an area where the sea bed geology is structurally simple and is known in greater detail than for similar events in the past, and is thus well suited to the testing of computer models of shock wave propagation in the water and seismic waves through the sea bed.

The emphasis on accurate shot timing will allow this data set to be used for the determination of station corrections for North Sea events in addition its usefulness in determining the deep structure below the offshore extension of the Midland Valley of Scotland, complementing the LISPB data. It has already been used for studies of the deep crust by the Dublin Institute of Advanced Studies.

Acknowledgements

For producing the photographs and film used in the video, thanks are due to Mr F. McTaggart (BGS), Mr J. Erskine and Mr. G. Hydes (ARE) on the RMAS Goosander, and Mr C. Whitem with Mr L. Carter (ARE) on the RMAS Salmaster.

For their work with the PUSSEs we must thank Mr T.R.E. Owen and Miss C. Pierce from Carrack Measurement Technology and Cambridge University.

From ARE we must thank Dr J. Greenhorn, Mr T. Kerrigan, Mr J. Wallace and their staff; especially Mr G. Duncan for operating the Sea Owl, and Mr C.Hall the firing officer and his team.

We should also thank Captain Alistair MacGregor and the crew of the Salmaster, and Captain John Campbell and the crew of the Goosander.

Thanks are also due to the BGS technical personnel: Mr D.L. Petrie, Mr R.M.Young and Mr R. Muir Walker on the Salmaster, Mr D. Stewart who handled the shot timing on the Goosander, Mr D. Houliston at BGS; Mr S.N. Morgan and Mr P.Day for their work on the special coastal stations.

For permission to install the special coastal sites on their land, we are indebted to John Ogilvie and Sons Ltd (Newbarns); Mr J. Stansfeld (Boddin Pt); Mr Robert Dale (Lochhouses); Mr. Main (Whitekirk); BP (Grangemouth); The Forestry Commission (Tentsmuir A) and Mr Finlay (Tentsmuir B).

We would also like to thank Miss A. McCluskie for entering much of this report onto the word processor.

References

- Allen, C.M., 1988. A review of the properties of marine sediments for seismo-acoustic modelling, *Brit.Geol.Surv., Glob.Seism. Report No 348*.
- Arons, A.B., 1948. Secondary pressure pulses due to gas globe oscillations in underwater explosions. II: Selection of adiabatic parameters in the theory of oscillation, *J.acoust.Soc.,Am.*, 20, 277-282.
- Assumpção, M. and Bamford, D., 1978. LISPB V - Studies of crustal shear waves. *Geophys.J.R.astr.Soc.*, 54, 61-73.
- Bamford, D., Faber, S., Jacob, B., Kaminski, W., Nunn, K., Prodehl, C., Fuchs, K., King, R. and Willmore, P., 1976. A lithospheric seismic profile in Britain - I. Preliminary results, *Geophys.J.R.astr.Soc.*, 44, 145-160.
- Bamford, D., Nunn K., Prodehl, C. and Jacob, B., 1978 . LISPB IV - Crustal structure of Northern Britain. *Geophys.J.R.astr.Soc.*, 54, 43-60
- Ben Menahem, A. and Singh S.J., 1981. Seismic waves and sources, *Springer Verlag (New York, Heidelberg, Berlin)*
- Birch, F., 1961. The velocity of compressional waves in rocks to 10 kilobars, Part 2, *J.Geophys.Res.*, 66, 2199-2224.
- Britt, J.R., 1984. SWREF _ Shock wave reflection and submarine response code: Volume I - User Manual, *Applied Research Associates Inc. Report No NSWC TR84-192*.
- Browitt, C.W.A., 1979. Seismograph networks of the Institute of Geological Sciences, UK, *Physics of the Earth and Planetary Interiors*, 18, 127-134

- Browne, M.A.E., Hargreaves, R.L. and Smith, I.F., 1985. The Upper Palaeozoic Basins of the Midland Valley of Scotland, *Invest.geotherm.potent.UK, Brit.Geol.Surv.*
- Browne, M.A.E., Robins, N.S., Evans, R.B., Monro, S.K. and Robson, P.G., 1987. The upper Devonian and Carboniferous sandstones of the Midland valley of Scotland, *Invest.geotherm.potent.UK, Brit.Geol.Surv.*, in press.
- Burton, P.W., 1977. Inversions of high frequency $(1/Q_Y)(f)$, *Geophys.J.R.astr.Soc.*, **48**, 29-51.
- Carmichael, R.S. (editor), 1982. *handbook of physical properties of rocks*, CRC Pres, Florida.
- Cole, R.H., 1948. *Underwater explosions*, Princeton University Press.
- Colette, B.J., Laagay, R.A., Ritsema, A.R. and Schouten, J.A., 1970. Seismic investigation in the North Sea, 3 to 7, *Geophys.J.R.astr.Soc.*, **19**, 183-199.
- Crampin, S., Jacob, A.W.B., Miller, A. and Neilson, G., 1970. The LOWNET radio linked seismometer network. *Geophysical J.* **21**, 207-216
- Evans, A.C., 1981. Propagation and dissipation of VHF Rayleigh waves in Scotland, *PhD thesis, University of Edinburgh.*
- Fofonoff, N.P. and Millard Jr., 1983. Algorithms for computation of fundamental properties of seawater. *Report No. 44, UNESCO Technical Papers in Marine Science.*
- Hamilton, E.L., 1972. Compressional wave attenuation in marine sediments. *Geophysics* **37**, 620-646.
- Hamilton, E.L., 1976. Attenuation of shear waves in marine sediments. *J.Acoust.Soc.Am.* **60**, 334-338.

- Hamilton, E.L., 1980. Geoacoustic modelling of the sea floor. *J. Acoust. Soc. Am.* **68**, 1313-1340
- Hamilton, E.L., Bachman, R.T., Berger W.H., Johnson T.C. and Mayer, L.A., 1982. Acoustic and related properties of calcareous deep sea sediments. *J. Sediment. Petrology.* **52**, 733-753
- Holmes, R., 1977. Quaternary deposits of the central North Sea 5. The Quaternary geology of the UK sector of the North Sea between 56° and 58°N, *Inst. Geol. Sci.* Report No 77/14.
- Jacob, .A.W., 1975. Dispersed shots at optimum depth - an efficient seismic source for lithospheric studies, *J. Geophys.* **41**, 63-70.
- Jacob, A.W.B. and Neilson, G., 1977. Magnitude determination of LOWNET, *Inst. Geol. Sci., Glob. Seism. Unit Report No 86.*
- Jensen, F.B. and Schmidt, H. 1986. Shear properties of ocean sediments determined from numerical modelling of Scholte-wave data. in *Ocean Seismo-Acoustics, NATO Conference Series IV:16; ed. T. Akal and J.M. Berkson, Plenum Press, New York and London.* 683-692.
- Kaye, G.W.C. and Laby, T.H., 1982. *Tables of physical and chemical constants*, Longman, London and New York.
- Kennett, B.L.N. and Kerry, N.J., 1979. Seismic waves in a stratified half-space, *Geophys. J. R. astr. Soc.*, **57**, 557-583.
- Kirk, R.E., Whitmarsh, R.B. and Langford, J.J., 1982. A three-component ocean bottom seismograph for controlled source and earthquake seismology, *Mar. Geophys. Res.*, **5**, 327-341.
- Langford, J.J. and Whitmarsh, R.B., 1977. Pop-up Bottom Seismic Recorder (PUBS) of the Institute of Oceanographic Sciences, U.K., *Mar. Geophys. Res.*, **3**, 235-250.

- Lund, C-E., Roberts, R.G., Johlin, C., Bodvarson, R. and Palm, H., 1987. The use of land recorded long-range marine airgun data in crustal reflection-refraction investigations, *Geophys.J.R.astr.Soc.*, **89**, 365-370.
- MacBeth, C.D., 1985. Long range underwater pressure resulting from the detonation of a large charge in shallow water, *Brit.Geol.Surv. Glob. Seism. Report No 259*.
- MacBeth, C.D. and Burton, P.W., 1985. Upper crustal shear velocity models from higher mode Rayleigh wave dispersion in Scotland. *Geophys.J.R.astr.Soc.*, **83(2)**, 519-540.
- MacBeth, C.D. and Burton, P.W., 1986. Propagation of 0.7-2.5 Hz Rayleigh waves in Scotland, *Geophys.J.R.astr.Soc.*, **84**, 101-120.
- MacBeth, C.D. and Burton, P.W., 1987. Single-station attenuation measurements of high frequency Rayleigh waves in Scotland, *Geophys.J.R.astr.Soc.*, **89**, 757-797.
- MacBeth, C.D. and Burton, P.W., 1988. Surface waves generated by underwater explosions offshore Scotland, *Geophys.J.(R.astr.Soc.)*, **94(2)** 285-294. Also see: *Brit.Geol.Surv. Global Seismology Report No 318 (1987)*.
- MacBeth, C.D. and Panza, G.F., 1989. Modal synthesis of high-frequency waves in Scotland, *Geophys.J.R.astr.Soc.*, **96**, (in press)
- Miller, A., Richards, J.A., McCann, D.M. and Hallam, J.R., 1986. Microseismic investigations in a flooded limestone mine at Daw End: an experimental borehole network, *Brit.Geol. Surv. Glob.Seism. Report No 310*.
- Nafe J.E. and Drake C.L., 1965. In: *Interpretation theory in applied geophysics*, p200, eds Grant F.S. and West G.F. McGraw-Hill

- Newmark, R., 1984. Tables of ground amplitude in microns produced by earthquakes of different depth, range, magnitude, *Brit.Geol.Surv., Glob.Seism.* unpublished report.
- Owen, T.R.E. and Barton, P.J., 1986. *The Cambridge seismic recorder*, Bullard Laboratories, Cambridge University, 4 page pamphlet.
- Peal, K.R. and Kirk, R.E., 1983. An event recording ocean bottom seismograph, *IEEE Proc. Third Working Symposium on Oceanographic Data Systems*, 114-118.
- Richter C.F., 1958. *Elementary Seismology*. W.H.Freeman and Company (San Francisco)
- Schirmer, F., 1971. Eine Untersuchung akustischer Eigenschaften von Sedimenten der Nord-und-Ostsee. *Ph.D. Thesis, Hamburg*
- Sensonics, no date, Willmore MkIIIA seismometer. Operating and servicing instructions, Sensonics Limited HB 064 15/5/77.
- Stuart, G.W., 1978. The upper mantle structure of the North Sea region from Rayleigh wave dispersion. *Geophys.J.R.astr.Soc.*, 52, 367-382.
- Thomson, M.E. and Eden, R.A., 1977. Quaternary deposits of the central North Sea. 3: The Quaternary sequence in the west-central North Sea, *Inst.Geol.Sci.*, Report No 77/12.
- Turbitt, T., Browitt, C.W.A., Morgan, S.N. and Petrie, D.L., 1981. Seismic data acquisition buoy in the North Sea, *Inst.Geol.Sci., Glob. Seism. Unit Report No 142*.
- Turbitt, T. and Stewart, D.A., 1982. Calibration of the Willmore MkIIIA/Geostore seismic recording system, *Inst.Geol.Sci., Glob. Seism. Unit Report No 158*.

Turbitt, T., Browitt, C.W.A., Morgan, S.N., Newmark, R.H. and Petrie, D.L., 1983. Instrumentation for North Sea seismic data acquisition system, In: *Seismicity and Seismic Risk in the Offshore North Sea Area*, editors R. Ritsema and A. Gurpinar, Reidel Publishing Co, 155-171.

Turbitt, T., Petrie, D.L. and Stewart, D.L., 1988. An improved North Sea seismic data acquisition system at Statfjord A, *Brit.Geol.Surv., Glob. Seism. Report No 350*.

Teledyne Geotech, 1981. Operation and maintenance manual short-period seismometer, model S-500, Teledyne Geotech CPT 187.

Weston, D.E., 1960a. Underwater explosions as acoustic sources, *Proc. Phys.Soc.*, 75, 233-249.

Weston, D.E., 1960b. The low-frequency scaling laws and source levels for underground explosions and other disturbances, *Geophys.J.R.astr.Soc.*, 3, 191-202.

Table 2.1 Proposed spacing for instrumentation at sea

Distance r, for shot point km	Spacing between sea bottom packages km	Package type
10	5	PUSS
15	10	PUSS
25	15	PUSS
40	20	PUSS
60	25	BGS Sea Bottom package, VHS
85	30	PUSS
115		PUSS

Table 2.2 Prospective positions for PUSSEs and other offshore equipment. Positions are calculated along the great circle from the proposed explosion site at 57°07'N, 00°45'W and the land site at Tents Muir at 56°24'27.4"N, 2°48'43.2"W based on an Earth equivalent sphere radius of 6371 km. Positional accuracy: 0.1" = 3.11m = 0.000028°.

Site	Range (km)	Latitude		Longitude		Depth (m)	
		North	West	North	West	LW	TR
Shot	0	57.11667	0.75000	57° 07' 00.0"	00° 45' 00.0"	68	3.0
1 PUSS	10	57.06995	0.89145	57° 04' 11.8"	00° 53' 29.2"	65	3.1
2 PUSS	15	57.04653	0.96204	57° 02' 47.5"	00° 57' 43.4"	64	3.2
3 PUSS	25	56.99958	1.10296	56° 59' 58.5"	01° 06' 10.6"	65	3.3
4 PUSS	40	56.92885	1.31366	56° 55' 43.9"	01° 18' 49.2"	62	3.5
	BGS 60	56.83399	1.59336	56° 50' 02.4"	01° 35' 36.1"	60	3.7
5 PUSS	85	56.71455	1.94099	56° 42' 52.4"	01° 56' 27.6"	50	4.1
6 PUSS	115	56.56995	2.35523	56° 34' 11.8"	02° 21' 18.8"	50	4.6
Tents Muir	148.35	56.4076	2.8120	56° 24' 27.4"	02° 48' 43.2"	0	

LW = lowest astronomical tide;

TR = tidal range correction to mean high water spring tide given to the next 0.1 m above (from Admiralty co-tidal chart no. 5058).

Note. Water depths are given relative to Admiralty Chart datum, which is the lowest astronomical tide. For mean high water spring tide (MHWS), a correction has to be applied (TR). For the highest astronomical tide, a further 0.7m should be added. A further 1.0 m should be allowed for atmospheric effects.

Table 2.3 Expected maximum pressure (kPa), time constant (ms) and impulse (kPa-ms) for the direct shock wave and first surface reflection from a 4500 lb TNT (2041.17 kg) charge detonated at 75 m depth in water.

	Range km	Depth m	Direct wave			Surface reflected wave		
			kPa	ms	kPa-ms	kPa	ms	kPa-ms
01	0.2000	75.00	2322.	2.009	6266.	-837.1**	2.115	5137.
02	0.5000	75.00	824.5	2.481	2772.	-785.4*	2.505	2668.
03	1.000	75.00	376.7	2.909	1496.	-372.0*	2.917	1481.
04	2.000	75.00	172.1	3.412	807.2	-171.6*	3.415	805.2
05	3.000	75.00	108.9	3.746	562.7	-108.7*	3.747	562.0
06	4.000	75.00	78.65	4.002	435.6	-78.59	4.003	435.3
07	5.000	75.00	61.12	4.213	357.1	-61.09	4.213	357.0
PUSS	10.00	75.00	27.93	4.941	192.7	-27.93%	4.941%	192.7%
PUSS	15.00	75.00	17.66	5.424	134.3			
10	20.00	75.00	12.76	5.795	104.0			
PUSS	25.00	75.00	9.917	6.100	85.26			
12	30.00	75.00	8.071	6.361	72.49			
13	35.00	75.00	6.780	6.591	63.19			
PUSS	40.00	75.00	5.831	6.797	56.11			
15	45.00	75.00	5.104	6.983	50.53			
16	50.00	75.00	4.531	7.154	46.01			
17	55.00	75.00	4.069	7.313	42.26			
BGS	60.00	75.00	3.688	7.461	39.11			
19	65.00	75.00	3.369	7.600	36.42			
20	70.00	75.00	3.098	7.730	34.10			
21	75.00	75.00	2.866	7.854	32.07			
22	80.00	75.00	2.664	7.971	30.28			
PUSS	85.00	75.00	2.488	8.083	28.69			
24	90.00	75.00	2.332	8.190	27.27			
25	95.00	75.00	2.194	8.293	25.98			
26	100.0	75.00	2.070	8.391	24.83			
PUSS	115.0	75.00	1.768	8.665	21.92			

** : where the size of the negative pressure exceeds the hydrostatic pressure for the depth of the gauge, -the hydrostatic pressure is given.

* : these negative pressures exceed atmospheric pressure at the surface (1 atmosphere = 101.3kPa).

% : at 10 km range and beyond, the values of maximum pressure etc. in the direct and surface reflected wave are equal. The surface reflected wave is not tabulated beyond this point. The surface reflection coefficient is assumed to be -1.

NB : proposed ranges for occupation of sea-bed sites indicated by PUSS and BGS.

Table 2.4 Estimated upper bounds to seismic ground motion (x=displacement, v=velocity, a=acceleration) expected at distance r km from a 4500lb TNT (2041.17 kg) underwater explosion. The calculations assume a local seismic magnitude value, ML, of 3.74. This value is selected as the largest compatible with the size of the charge.

Site	Range d km	-log A ₀	log A	A mm	x microns	v mm/s	a mm/s ²
	0	1.4	2.34	3742.59	1336.64	83.9835	5276.84
	5	1.4	2.34	1245.80	444.93	27.9557	1756.51
PUSS 1	10	1.5	2.24	414.69	148.10	9.3056	584.69
PUSS 2	15	1.6	2.14	138.04	49.30	3.0976	194.63
	20	1.7	2.04	109.65	39.16	2.4605	154.60
PUSS 3	25	1.9	1.84	69.18	24.71	1.5525	97.54
	30	2.1	1.64	43.65	15.59	0.9795	61.55
	35	2.3	1.44	27.54	9.84	0.6180	38.83
PUSS 4	40	2.4	1.34	21.88	7.81	0.4909	30.85
	45	2.5	1.24	17.38	6.21	0.3900	24.50
	50	2.6	1.14	13.80	4.93	0.3098	19.46
	55	2.7	1.04	10.96	3.92	0.2460	15.46
BGS/VHS	60	2.8	0.94	8.71	3.11	0.1954	12.28
	65	2.8	0.94	8.71	3.11	0.1954	12.28
	70	2.8	0.94	8.71	3.11	0.1954	12.28
	75	2.9	0.84	6.92	2.47	0.1552	9.75
	80	2.9	0.84	6.92	2.47	0.1552	9.75
PUSS 5	85	2.9	0.84	6.92	2.47	0.1552	9.75
	90	3.0	0.74	5.50	1.96	0.1233	7.75
	95	3.0	0.74	5.50	1.96	0.1233	7.75
	100	3.0	0.74	5.50	1.96	0.1233	7.75

Note: A is displacement in mm on a standard torsion seismometer and A₀ is a standardising distance correction term for local magnitude calculation (see text for details).

Table 3.1 ARE pressure gauge deployment.

(a) Dimensions of system

Overall length	Long Trot 189.6m	Short trot ~100m
standoff at surface	1) 505.97m (1660ft) 2) 173.74m (570ft)	1) 541.93m (1778ft) 2) 219.46m (720ft)
approx length from buoy to topmost gauge	70.2m (shot 1) (230ft)	
approx length from buoy to RMAS Goosander	63.4m (shot 1) (208ft)	

(b) Spacing of pressure gauges on cable

	spacing m		spacing m
gauge 290		gauge 188	
	9.8		9.44
292		189	
	9.6		9.21
294		190	
	9.7		9.4
296		191	
	9.5		9.1
300		192	
	9.41		9.7
302		193	
	8.0		8.0
weight		weight	

Table 3.2 ARE pressure gauge calibrations.

	Gauge Number (pC/psi)	Sensitivity (aC/Pa)	Sensitivity
Short	188	0.580	84.12
Trot	188	0.598	86.73
	190	0.597	86.59
	191	0.590	85.57
	192	0.585	84.85
	193	0.594	86.15
Long	290	0.578	83.83
Trot	292	0.554	80.35
	294	0.574	83.25
	296	0.612	88.76
	300	0.558	80.93
	302	0.596	86.44
Nominal disc sensitivity		(0.55)	80.0
Max. peak pressure		40 kpsi	275MPa

Table 3.3

VHS - SPECIFICATIONS

Hydrophone sensitivity.....	15v/bar
Natural frequency \pm 15%.....	12Hz
frequency response \pm 1db.....	12 - 1000Hz
Sensitivity change with depth.....	< 1.5db 10-150ft
Impedance.....	250 ohms
DC resistance.....	150 ohms
Amplifier gains.....	\times 10
System response.....	DC - 2.5KHz
Record/replay gain at 10v peak.....	+ 2 \equiv 5
Record/replay gain at 5v peak.....	\times 1 \equiv 10
Record/replay gain at 2v peak.....	\times 2.5 \equiv 25

Table 3.4

SBP SPECIFICATIONS

S500 acceleration channel:

Sensitivity.....50v/m/s²
 Attenuator.....÷ 33
 Amplification.....× 390
 Frequency response.....1 - 30Hz

S500 velocity channel:

Sensitivity.....450v/m/s
 amplification.....× 48.8
 Frequency response.....1 - 30Hz

Hydrophone channel:

Sensitivity.....79.4v/MPa
 Pre-amp gain.....× 0.94
 Amp/Mod gain.....× 4
 Frequency response.....1.5 - 30Hz
 Transcription gain.....× 5

NOTE:

The digital system introduces a delay to the acceleration and velocity channels, relative to the FM hydrophone channel as follows:

FREQUENCY Hz	DELAY msec
5.5	45.6
10.8	46.3
16.1	46.6
21.3	46.9
26.2	47.7
30.6	49.0

Table 3.5 Calibration of Pull Up Shallow-water Seismometers

Puss id.	Range		Pressure Pa/count	Velocity microns/sec/count
	Planned	Meas.		
10	10	9.982	0.0191	0.0116
11	15	14.543	0.1411	0.0116
09	25	25.002	0.1910	0.0470
13	40	39.705	0.1910	0.0484
14	85	85.291	0.1910	0.0484
12 [*]	115	0.0191	0.0484

* not used in 2nd deployment

Table 3.6 PUSS SPECIFICATIONS

(a) Geophone channels:

Type.....Sensor SM1/A

Sensitivity.....25.2 V/M/S

Natural frequency.....3Hz

Coil resistance.....280 ohms

Damping.....750 Ω ϕ for 60%

(b) Hydrophone channels:

Type.....Barium titanato zirconate

Sensitivity.....78 micro v/Pa

Element dimensions....25mm O.D.
38mm long
3.15 wall thickness

Table 3.7 Seismometer coastal sites installed temporarily on soft rock. The seismometers used are Willmore Mk IIIA recording as analogue on Geostores at 15/320 in s^{-1} giving a maximum frequency of 16 Hz.

Code	Site	Components	Latitude North	Longitude West	Ht m	Geology
GMA	Grangemouth ¹	Z,N-S,E-W	56.0348	-3.6943	2	reclaimed land,
GMB	Grangemouth ¹	Z	56.0337	-3.6952	2	coarse conglomerate on top of late glacial estuarine alluvial sediment, mostly clayey silt
LHS	Lochhouses ²	Z,N-S,E-W	56.0274	-2.6221	42	soft rock - late glacial estuarine alluvial; clay, silt sand & gravel
WHK	Whitekirk ³	Z	56.0267	-2.6491	180	hard rock - basalt
LUA	Newbarns ⁴	Z,N-S,E-W	56.6328	-2.5158	55	soft rock - raised beach glacial sediments
LUB	Boddin point ⁵	Z	56.6723	-2.4692	3	hard rock - upper Old Red Sandstone
TMA	Tentsmuir ⁶	Z,N-S,E-W	56.4076	-2.8120	3	soft rock - blown sand
TMB	Tentsmuir ⁷	Z	56.4211	-2.8633	10	hard rock - basalt

1: Airdrie sheet 31 1:63360 series Drift Edition for onshore. Correlation to offshore structure using Tay-Forth sheet 56°N-04°W, 1:250000 series Solid Geology. Two instruments were used, placed a short distance apart, since the site is potentially noisy. The ground is reclaimed land consisting mostly of boulders, shale fragments and sand

2: Dunbar sheet 33E & part of 41, 1:50000 series Drift Edition for onshore. Correlation to offshore structure using Tay-Forth sheet 56°N-04°W, 1:250000

series Solid Geology.

- 3: Dunbar sheet 33E & part of 41, 1:50000 series Solid Edition for onshore. Correlation to offshore structure using Tay-Forth sheet 56°N-04°W, 1:250000 series Solid Geology.
- 4: Forfar sheet 57, 1:63360 series Solid Geology (publ. 1887) for onshore. Drift edition and sediment details are not available. Correlation to offshore structure using Tay-Forth sheet 56°N-04°W, 1:250000 series Solid Geology.
- 5: Forfar sheet 57, 1:63360 series Solid Geology for onshore. Correlation to offshore structure using Tay-Forth sheet 56°N-04°W, 1:250000 series Solid Geology.
- 6: Arbroath sheet 49, 1:50000 series Drift Edition for onshore. Correlation to offshore structure using Tay-Forth sheet 56°N-04°W, 1:250000 series Solid Geology.
- 7: Arbroath sheet 49, 1:50000 series Solid Edition for onshore. Correlation to offshore structure using Tay-Forth sheet 56°N-04°W, 1:250000 series Solid Geology.

Table 4.1 Revised shot windows for second deployment

Monday 28th September 1987	13 ^h 22 ^m 30 ^s 15 ^h 22 ^m 30 ^s
Tuesday 29th September 1987	11 ^h 02 ^m 30 ^s 11 ^h 52 ^m 30 ^s 13 ^h 17 ^m 30 ^s 14 ^h 02 ^m 30 ^s 15 ^h 22 ^m 30 ^s 16 ^h 02 ^m 30 ^s 16 ^h 32 ^m 30 ^s

Table 4.2 Offshore site location details (second deployment)

Site ^a	Instrument ^a		Latitude N ^b		Longitude W ^b		Depth ^c	Range from ^d	Great circle ^e
	Type	No	deg min		deg min		m	km	m
Shotpoint	-	-	57 ⁰ 06.984'	(+.010' = +9m)	00 ⁰ 45.036'	(+.009' = +5m)	76.125 (+.125)	-	-
1	PUSS	10	57 ⁰ 04.141'	(+.002' = +2m)	00 ⁰ 53.424'	(+.003' = +1.5m)	74	9.982	-116
2	PUSS	11	57 ⁰ 02.882'	(+.004' = +4m)	00 ⁰ 57.298'	(+.010' = +5m)	70	14.543	- 75
3	PUSS	9	56 ⁰ 59.974'	(+.002' = +2m)	01 ⁰ 06.151'	(+.001' = +.5m)	70	25.002	- 11
4	PUSS	13	56 ⁰ 55.794'	(+.002' = +2m)	01 ⁰ 18.472'	(+.003' = +1.5m)	67	39.705	- 82
BGS(1)	Sea Bottom Package		56 ⁰ 50.073'	(+.002' = +2m)	01 ⁰ 35.537'	(+.006' = +3m)	61	60.035	+ 21
BGS(2)	VHS		56 ⁰ 50.123'		01 ⁰ 35.625'		61.5	60.062	+147
BGS(3)	ARE/VHS (Shot 1)		56 ⁰ 50.140'		01 ⁰ 35.715'		61.5	60.123	+222
BGS(4)	ARE/VHS (Shot 2)		56 ⁰ 50.141'		01 ⁰ 35.729'		61.5	60.091	+235
5	PUSS	14	56 ⁰ 42.810'	(+.001' = +1m)	01 ⁰ 56.500'	(+.007' = +3.5m)	54	85.291	- 76
6	Not occupied		-		-		-	-	-

a: each PUSS and the BGS sea bottom package contains one hydrophone and three component geophone; VHS = vertical hydrophone string; BGS(1) and (2) are packages deployed on the sea bottom and recorded onboard ship, (3) and (4) are deployed from and recorded onboard ship. b: Syledis measurement. c: Sonar measurement. d: Calculated from mean of two positions of shackle ring, first with ship's heading of 080⁰ and second with 185-190⁰, closure distance between two positions is 45m (44m latitude, 8m longitude). e: perpendicular distance from great circle from shot point to Tentsmuir (TMA: 56⁰24.456'N, 02⁰48.720'W) measured positive clockwise.

Table 5.1 Explosion shot times on 29 September 1987 and pressure pulse arrival recorded at RMAS Goosander

Shot	Charge size lb	Water depth ^a m	Shot time ^b GMT h:m:s	Pressure pulse		Goosander standoff m	Comments
				Travel time s	Distance ^c m		
1	4500	76.13(+.1)	11:52:33.2252(+1ms)	0.3452	514.44	508.78	a precursor arrives about 18.8 ms before the main pressure pulse and extends up to it, the start of the main pressure pulse is therefore arbitrary to a few ms.
2	900	76.13(+.1)	15:22:30.5910(+1ms)	0.1759	262.19	250.89	a tiny precursor arrives about 9.1 ms before the very sharp onset of the main compression pulse.

- a. Both explosions were detonated at the same position. A sonar depth of 76.25 m was measured on September 20 and 76 m on September 29. Depth of 76.125 m used to calculate standoff. All Table entries are rounded to less than the precision used in the calculations.
- b. Measured from jet pen playout of the shot sequence timer channel recorded on Store 7 on RMAS Goosander. Individual measurements taken from the jet pen playout good to ± 0.25 ms. Maximum alignment difference between second markers noted on playout of MSF and DCF radio time channels from Store 7 recorder was 2 ms. The main pressure pulse was recorded sharply on sequence timer, hydrophone, geophone, MSF and DCF channels of Store 7; the largest difference between shot time measured on any of these channels and the above is 0.8 ms.
- c. Calculated using 1.4902 km s^{-1} as the velocity of sound in sea water at 10°C (Kaye & Laby 198?).

Table 6.1 Geological characteristics of offshore sites determined from British Geological Survey maps

Site	Water depth m	Quaternary thickness m	Depth to top of Permo-Triassic Boundary m	Comment on solid geology
Shotpoint	75 ²	105-206 ^{1,*}	1125 ³	In Palaeocene sediments, bottom of Quaternary ³
PUSS 1	74 ²	78-80 ¹	900 ³	Between Palaeocene and Upper Cretaceous ³
PUSS 2	71 ²	72-73 ¹	800 ³	Upper Cretaceous ³
PUSS 3	69 ⁵	63 ⁴	610 ⁶	Upper Cretaceous ⁶
PUSS 4	64 ⁵	45 ⁴	- ⁶	Lower Cretaceous ⁶
BGS Package	61 ⁵	21-22 ⁴	- ⁶	Triassic ⁶
PUSS 5	55 ⁵	<10 ⁴	- ⁶	Triassic ⁶

BGS maps:

- 1 : Peterhead sheet 57°N 02°W Quaternary geology 1:250 000
 - 2 : Peterhead sheet 57°N 02°W Sea bed sediments 1:250 000
 - 3 : Peterhead sheet 57°N 02°W Solid geology 1:250 000
 - 4 : Marr Bank sheet 56°N 02°W Quaternary geology 1:250 000
 - 5 : Marr Bank sheet 56°N 02°W Sea bed sediments 1:250 000
 - 6 : Marr Bank sheet 56°N 02°W Solid geology 1:250 000 (no depth contours)
- * : Amoco Well 27/3-1 at 20 km southeast of shot point indicates 139 m of Plio-Pleistocene

Table 6.2 Geologic column and seismic velocities to 2000 m depth at 56°57'30.5"N 00°32'20.2"W
from Amoco Well 27/3-1, September 1967

Layer No	Geology ^e		Depth to ^a base m	Thickness m	One way t-time s	Interval time Dt s	P-velocity km s ⁻¹	S-velocity km s ⁻¹
1	Water		75.0	75.0	(.0503) ^b	(.0505) ^b	(1.4902) ^b	-
2	Tertiary	Plio-Pleistocene	214.0	139.0	.1265	.0762	1.824	.919
3		Eocene-Palaeocene	338.0	124.0	.1935	.0670	1.851	1.039
4	Upper Cretaceous	Maestrichtian/ Campanian	643.7	305.7	.2990	.1055	2.898	1.625
5		Undiff. Upper Cretaceous	707.1	63.4	.3200	.0210	3.019	1.694
6	Lower Cretaceous	Albian-Aptian	729.4	22.3	.3300	.0100	2.230	1.251
7		Barremian- Hauterivian	779.1	49.7	.3515	.0215	2.312	1.297
8	Triassic	Undifferentiated	867.2	88.1	.3878	.0363	2.427	1.362
9	Permian	Zechstein ^c	1352.1	484.9	.4826	.0948	5.115	2.870
10	Lower Palaeozoics	Undifferentiated	1963.5	611.4	.6034	.1208	5.061	2.840

a : From mean sea level. b : Assumed velocity in sea water = 1.4902 km s⁻¹. c : Contains approximately three cycles of anhydrite, dolomite, halite. e : Principal unconformities exist between layers 3-4, 9-10 and within layer 7.

Table 7.1 Header block configuration (a) and example (b).

(a)

fname

event_id__ source source source _____source timing_____ source
 latitude longitude altitude year mm dd hh mm ss.ssss information

site_id cpt site site site site site (instrument)
 latitude longitude altitude range azimuth (information)

start of data sample
 hh mm ss.ss npts rate scale units

sd.ddddd sd.ddddd sd.ddddd sd.ddddd sd.ddddd sd.ddddd
 sd.ddddd sd.ddddd sd.ddddd sd.ddddd sd.ddddd sd.ddddd

(b)

X10G1S.

LORASWAP 1 57.11660 -0.75060 -76.125 1987 9 29 11 52 33.2252 4500 lb TNT
 PUSS 10 X 57.06902 -0.89040 -74.000 9.98 239.21
 11 52 5.00 23040 256.00 0.10000E-05 METRES/SEC
 0.00000 3.94400 -0.46400 -0.46400 -3.24800 -1.85600
 -0.69600 2.08800 4.87200 2.32000 2.55200 3.01600

Table 7.2 Preliminary results from ARE pressure gauges

a) 4500lb explosion

Gauge No	Depth	Measured [*] Standoff	Surface Cutoff (ms)	Long Sample Time Approximate Pressure (MPa)
188			5.5	0.66
189			7.6	0.66
190			9.0	0.69
191			10.0	0.59
192			12.8	0.37
193			14.2	0.21

Precursor appears 27.5ms before main pressure pulse

Measured bubble period: 711 ms

a) 900lb explosion

Gauge No	Depth	Measured Standoff	Surface Cutoff (ms)	Long Sample Time Approximate Pressure (MPa)
188			10.9	1.50
189			15.6	1.73
190			20.1	1.55
191			24.1	1.36
192			27.9	1.10
193			30.8	0.89

Precursor appears approx. 3ms before main pressure pulse

Measured bubble period: 388.7 ms

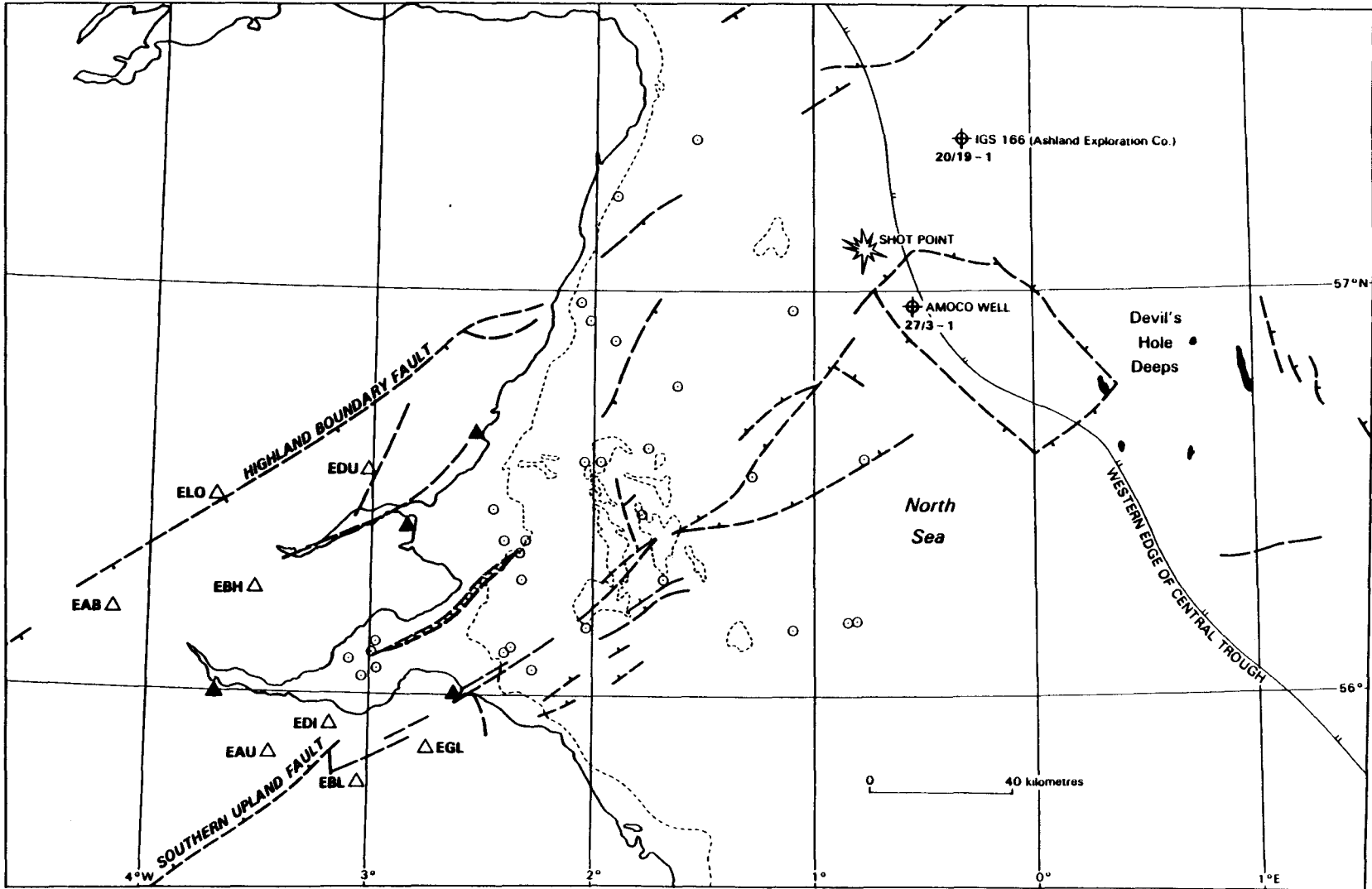
* Calculated, based on an assumed velocity in sea water of 5000 ft/s
(1.5240 m/s)

Table 8.1 Comparison of measured extreme pressures with those calculated for the direct wave using equation 2.4. after Britt (1984)

Inst.	Event	Range(km)	Depth(m)	Peak Pressure (Pa)	
				Measured	Calculated
ARE188	1	0.540	25.9	660000.00	747546.6
ARE189	1	0.540	35.4	660000.00	748776.8
ARE190	1	0.540	44.6	690000.00	749726.7
ARE191	1	0.540	57.1	590000.00	750632.9
ARE192	1	0.540	63.2	370000.00	750913.1
ARE193	1	0.540	72.6	210000.00	751135.5
PUSS10	1	9.982	74.0	8136.3	27985.7
PUSS11	1	14.543	70.0	5562.7	18291.7
PUSS09*	1	25.002	70.0	794.6	9916.1
PUSS13	1	39.705	67.0	1134.4	5879.7
BGSSBP	1	60.035	61.0	3726.9	3685.2
VHS01	1	60.062	11.5	1933.6	3683.3
VHS02	1	60.062	16.5	2086.9	3683.3
VHS03	1	60.062	21.5	1822.9	3683.3
VHS04	1	60.062	26.5	1494.4	3683.3
VHS05	1	60.062	31.5	1750.9	3683.3
VHS06	1	60.062	36.5	1836.1	3683.3
VHS07	1	60.062	41.5	2152.7	3683.3
VHS08	1	60.062	46.5	1731.8	3683.3
VHS09	1	60.062	51.5	1713.6	3683.3
VHS10	1	60.062	56.5	781.2	3683.3
PUSS14	1	85.291	54.0	89.2	2478.2
ARE188	2	0.22403	25.9	1500000.0	1083816.9
ARE189	2	0.21946	35.4	1730000.0	1121317.1
ARE190	2	0.21550	44.6	1550000.0	1147275.1
ARE191	2	0.21330	57.1	1360000.0	1174230.6
ARE192	2	0.21330	63.2	1100000.0	1177067.5
ARE193	2	0.21550	72.6	890000.0	1166945.9
PUSS10	2	9.982	74.0	4224.6	15263.6
PUSS11	2	14.543	70.0	2853.6	9976.4
PUSS09*	2	25.002	70.0	458.4	5408.3
PUSS13	2	39.705	67.0	518.3	3206.8
BGSSBP	2	60.035	61.0	2744.5	2009.9
VHS01	2	60.062	11.5	1116.8	2008.9
VHS02	2	60.062	16.5	1066.7	2008.9
VHS03	2	60.062	21.5	1083.7	2008.9
VHS04	2	60.062	26.5	945.5	2008.9
VHS05	2	60.062	31.5	1233.5	2008.9
VHS06	2	60.062	36.5	1253.4	2008.9
VHS07	2	60.062	41.5	1075.9	2008.9
VHS08	2	60.062	46.5	858.5	2008.9
VHS09	2	60.062	51.5	1006.4	2008.9
VHS10	2	60.062	56.5	534.5	2008.9
PUSS14	2	85.291	54.0	55.0	1351.6

* Instrument dragged, value suspect

Fig. 2.1



- | | | | | | |
|---|--------------------------|-------|----------------------------|-----|------------|
| △ | LOWNET seismometer site | ----- | 50 metre isobathic contour | --- | Fault |
| ▲ | Special seismometer site | ■ | Depth > 150 metres | ▨ | Fault zone |
| ○ | Deep soil boring | | | | |

Fig. 2.2

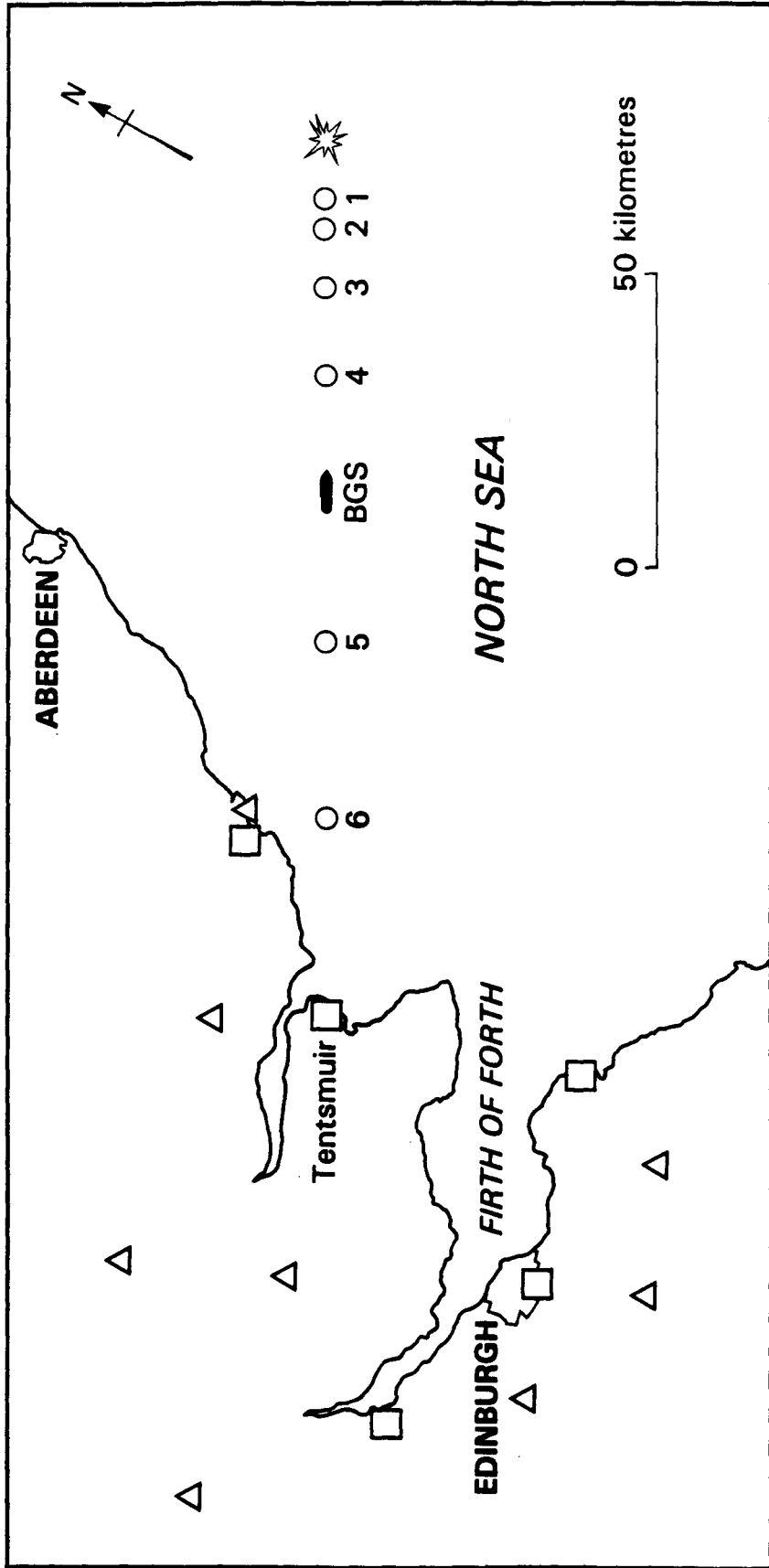
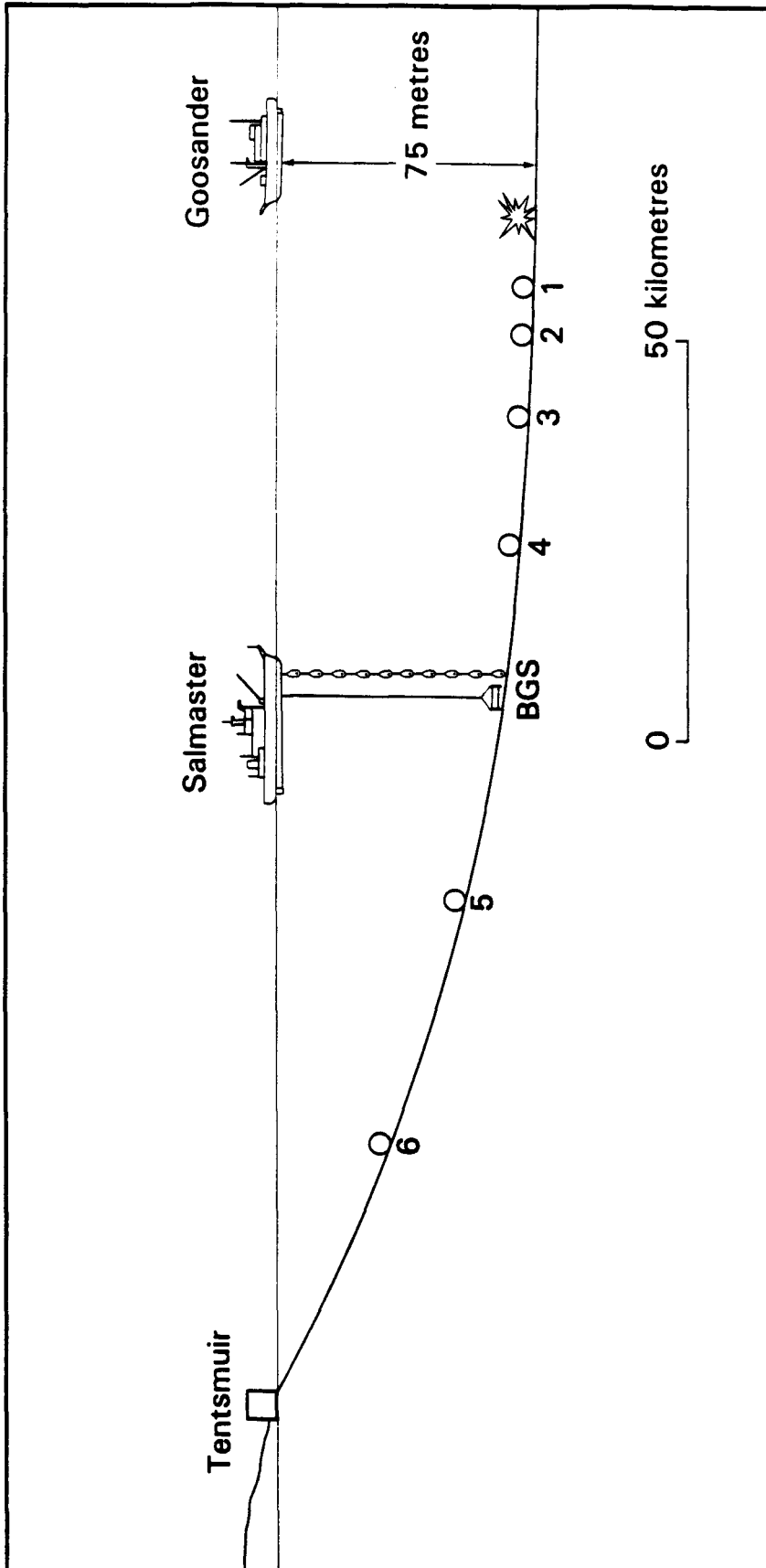


Fig. 2.3



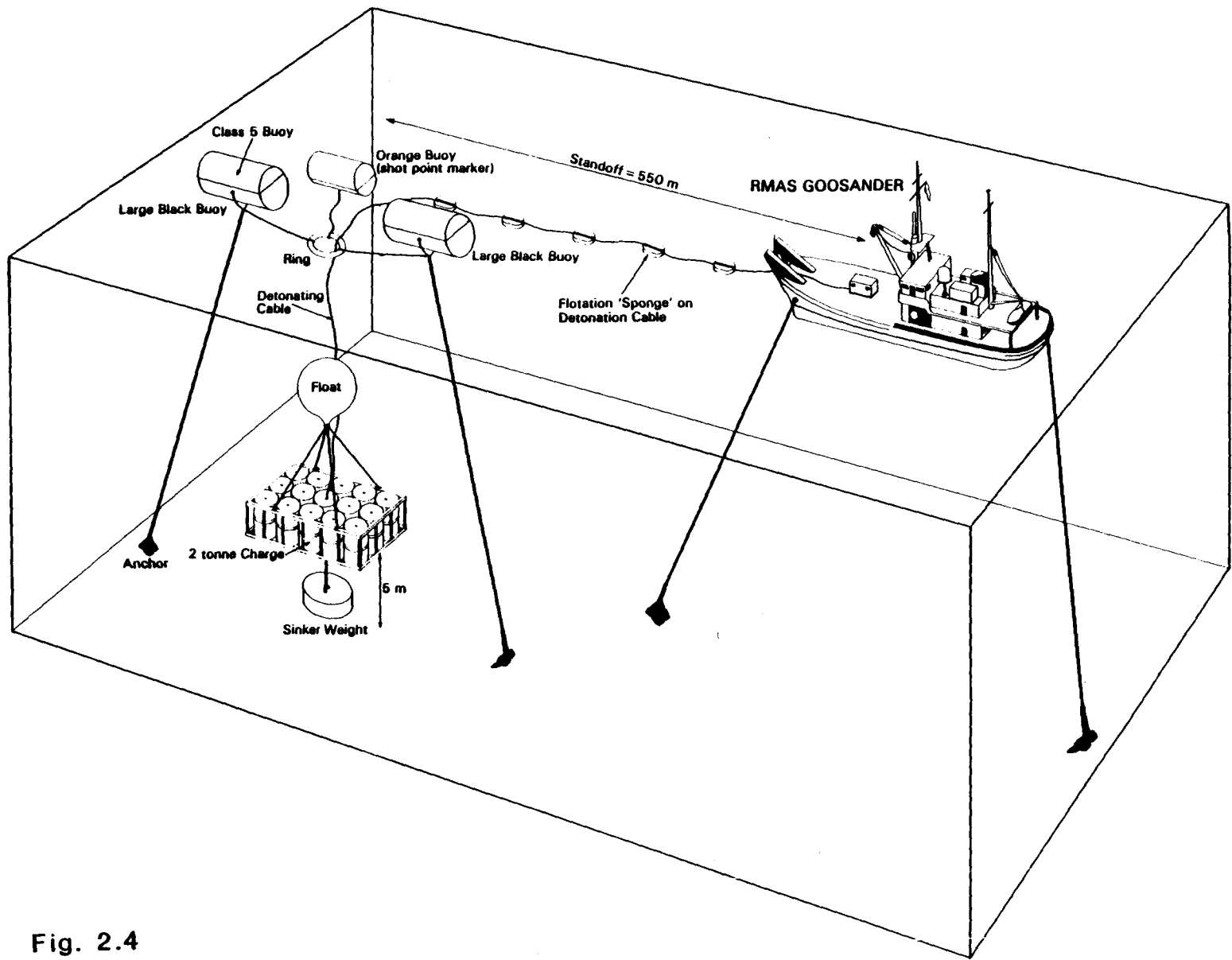


Fig. 2.4

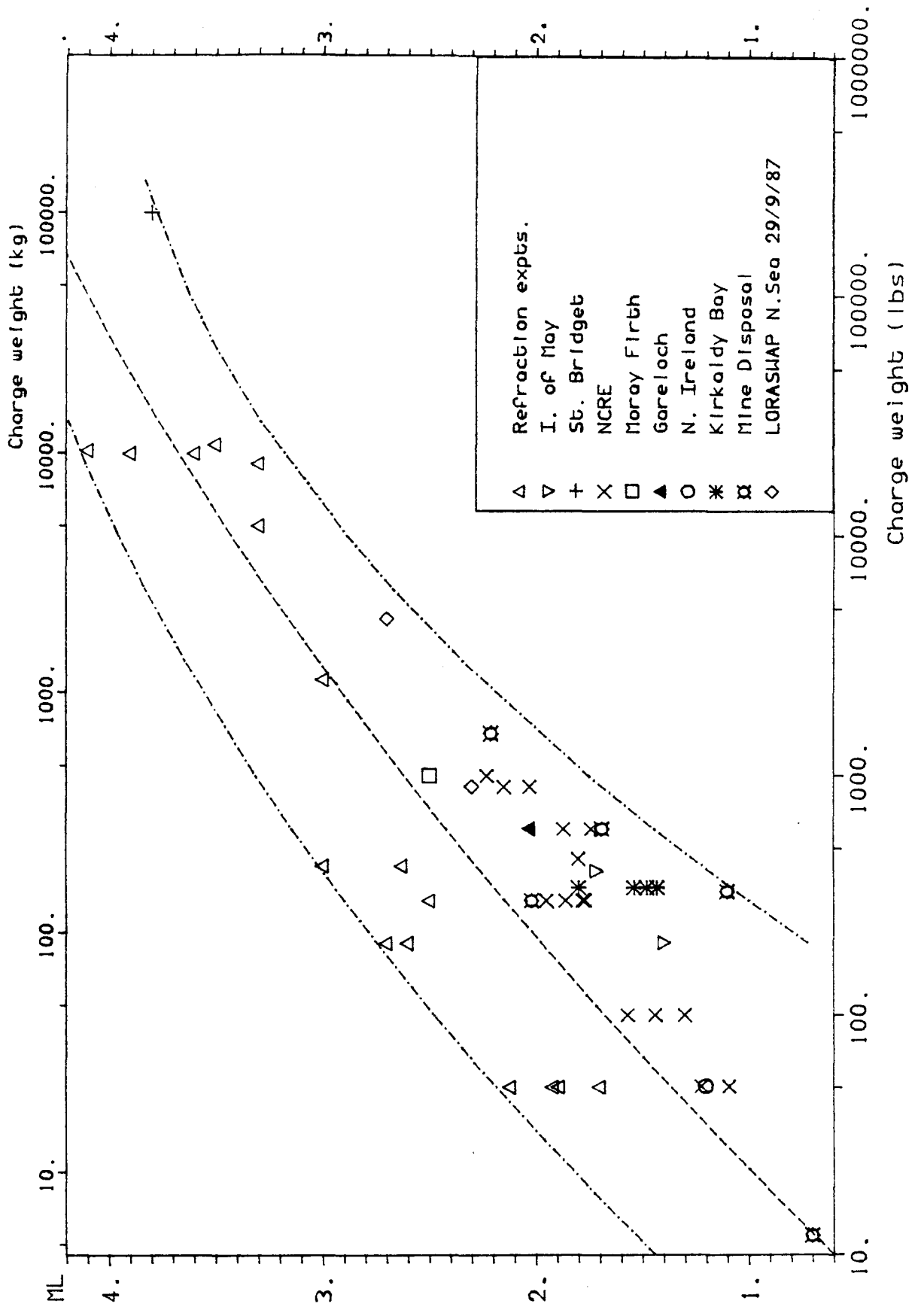
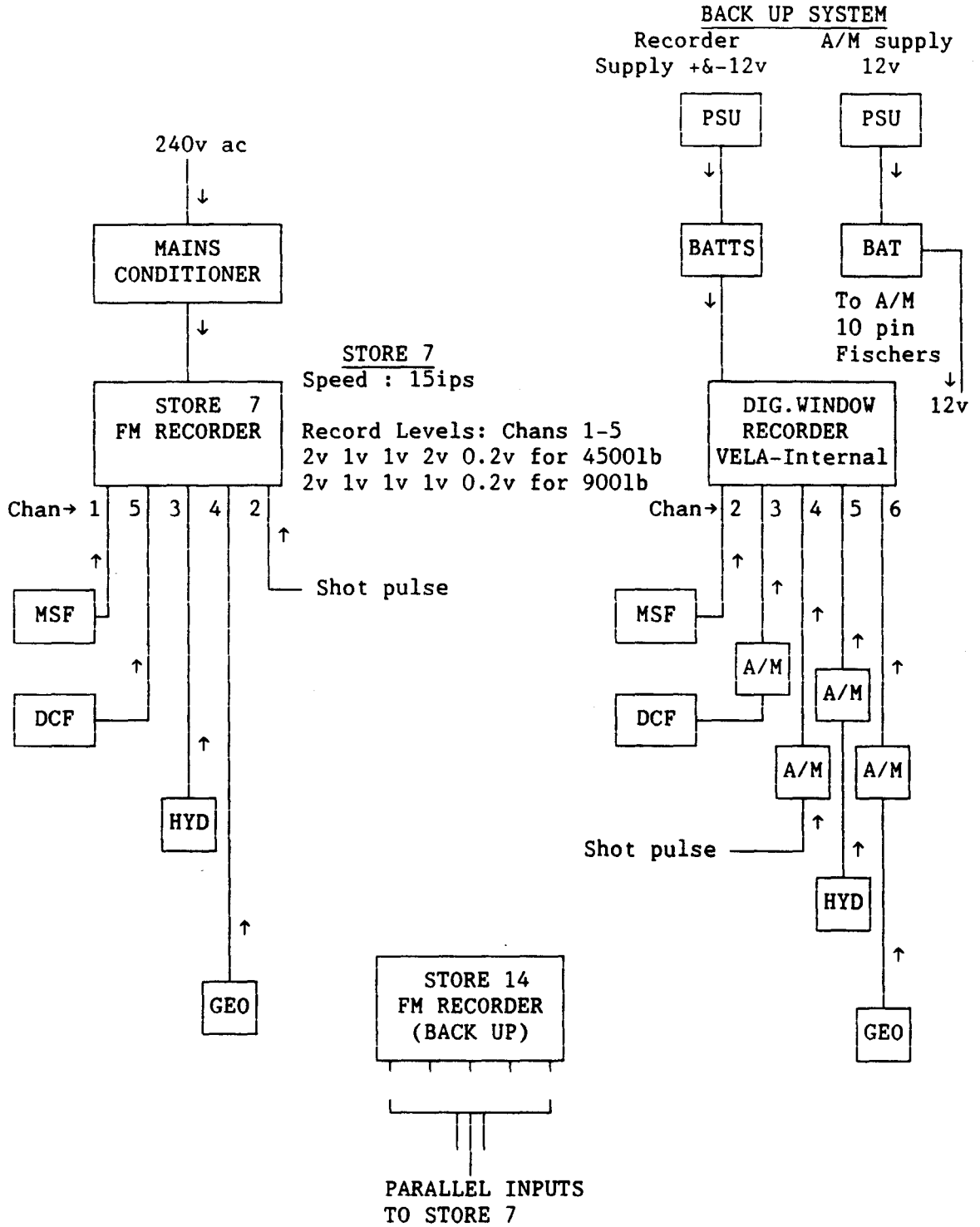


Fig. 2.5

Fig. 3.1

SHOT TIME - SYSTEM CONFIGURATIONS



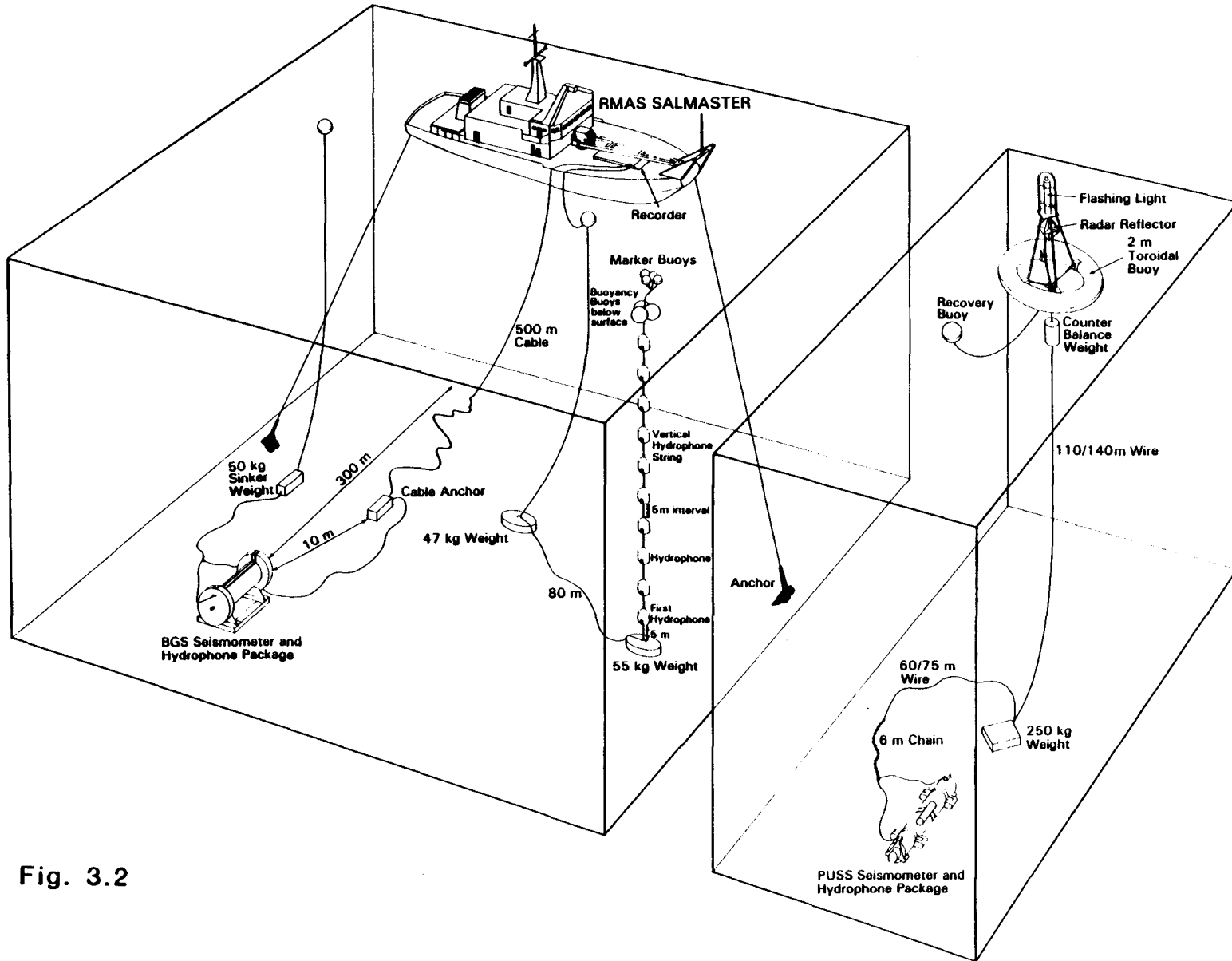


Fig. 3.2

Fig. 3.3

VHS - RECORDING CONFIGURATION

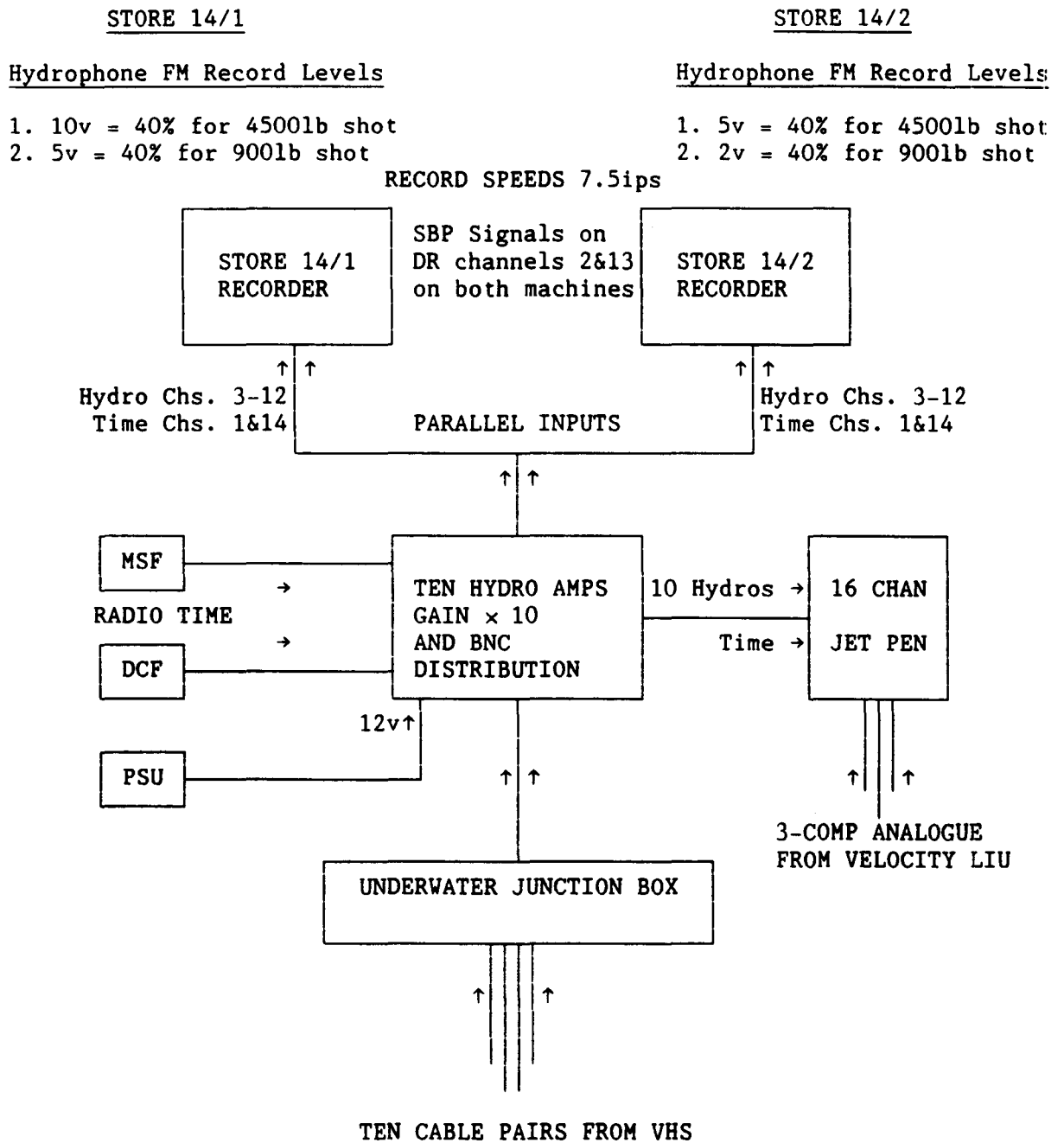


Fig. 3.4 Amplitude-Frequency response, VHS hydrophone

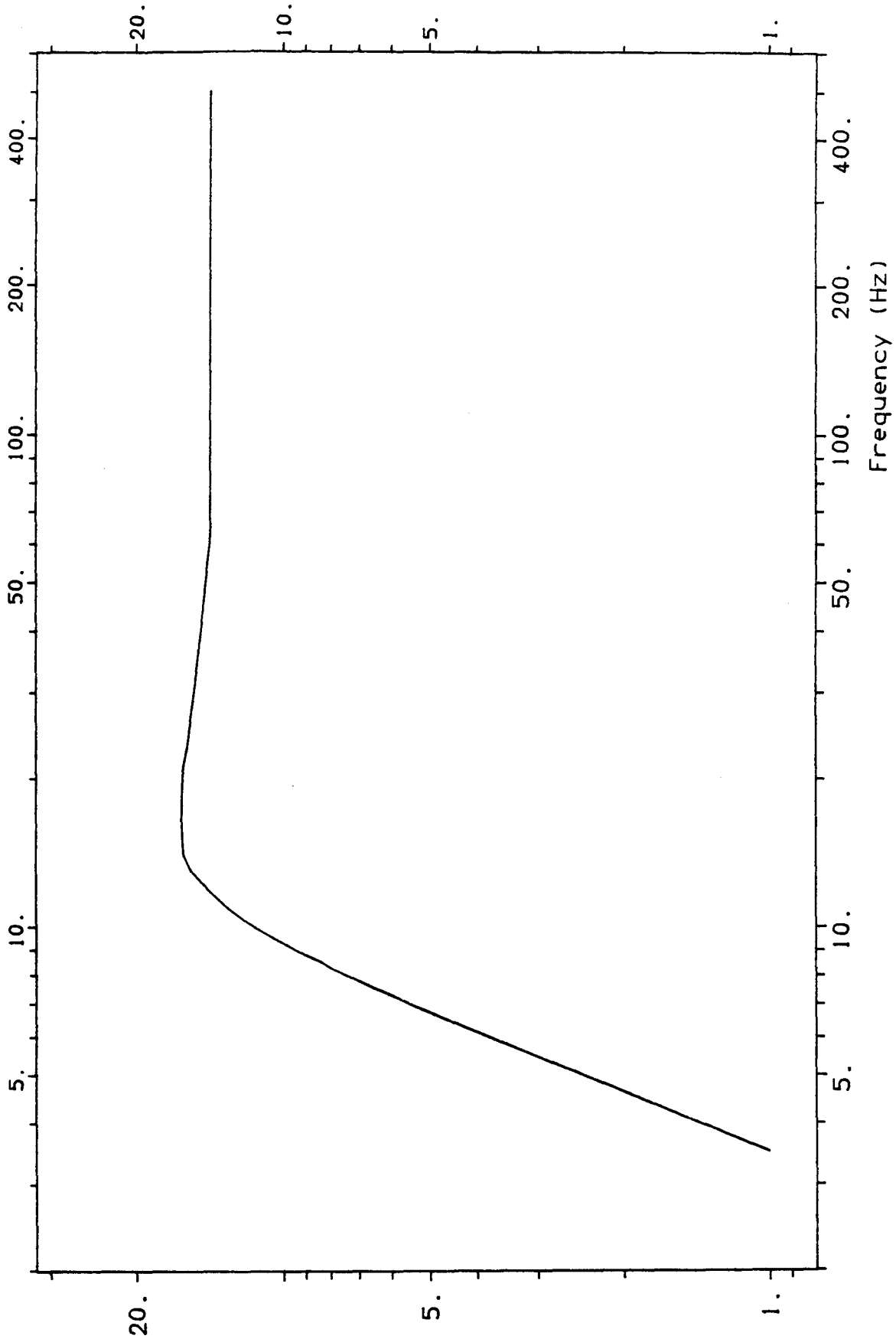
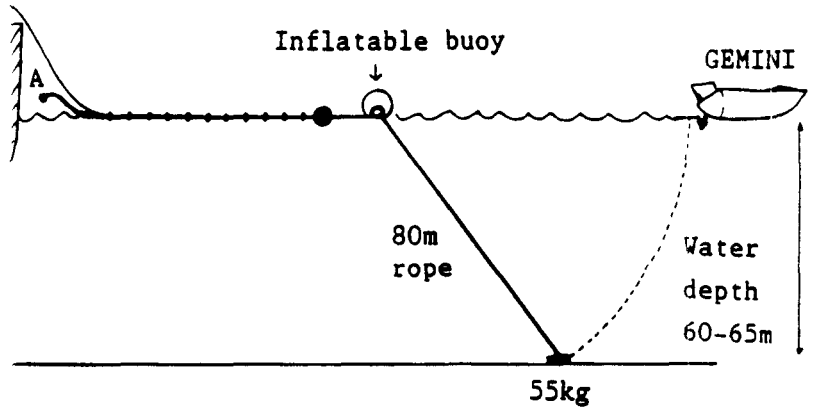


Fig. 3.5

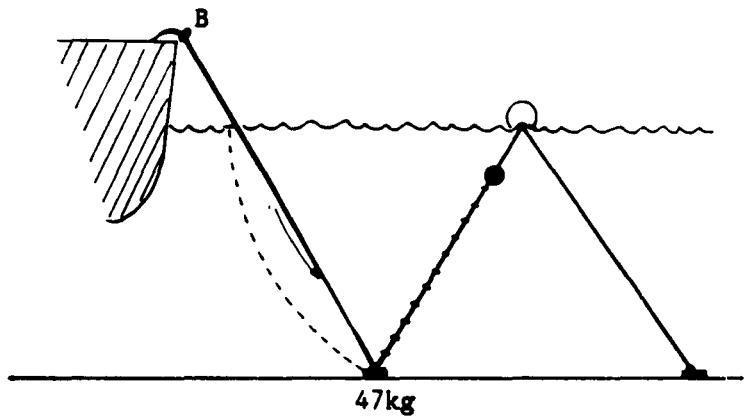
Step 1

GEMINI takes 55Kg weight attached to 80m of sinking rope, tows VHS out to the extent of point A and drops weight to sea-bed.



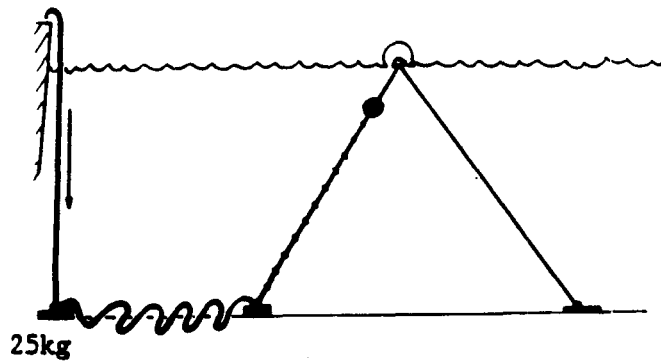
Step 2

47Kg weight attached at point A and lowered to sea-bed.



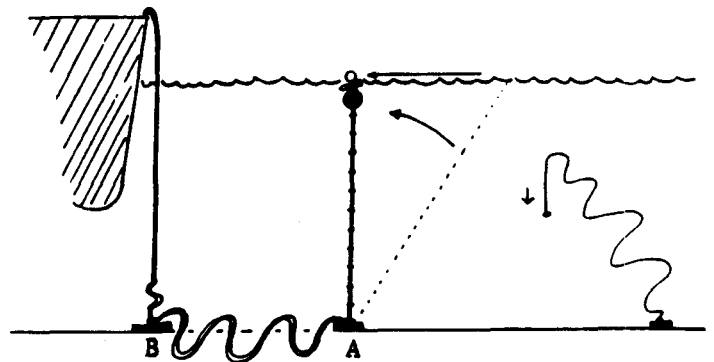
Step 3

25kg weight attached at point B and lowered to sea bed.



Step 4

Inflatable buoy, with attached sinking rope, are detached from the marker floats which move across surface as VHS adopts vertical attitude. Rope sinks when detached from buoy.



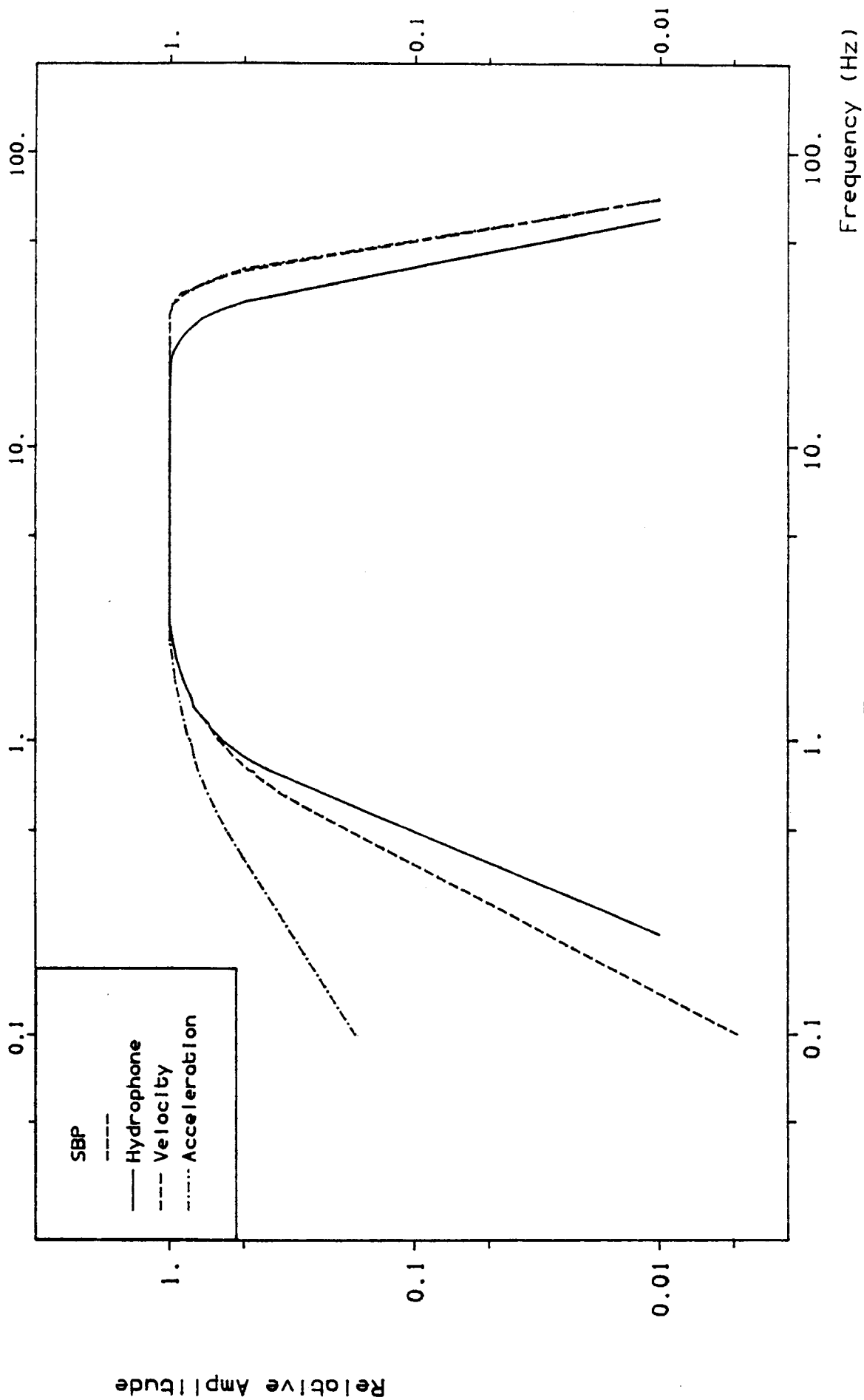


Fig. 3.7

System arrangement at BGS station

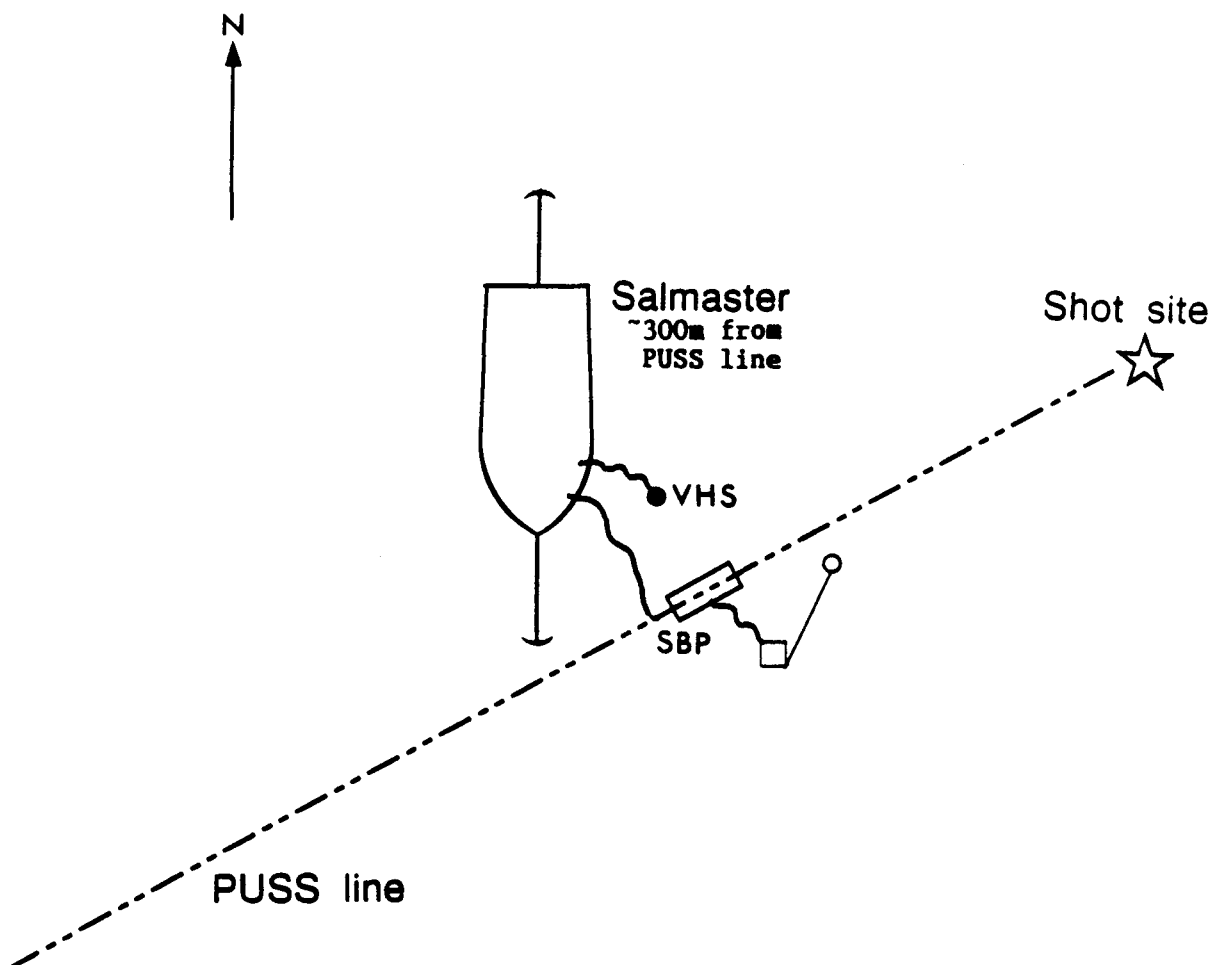
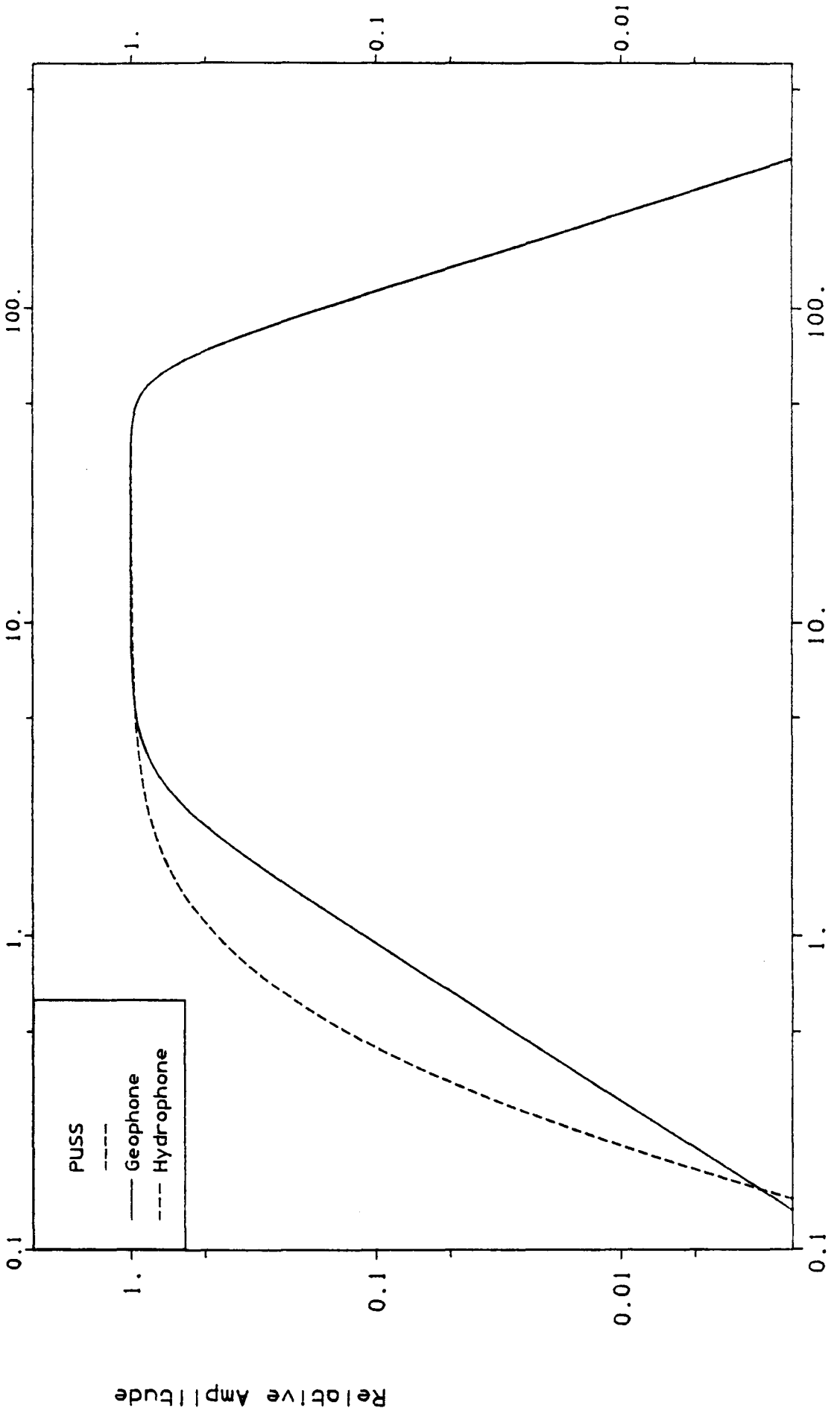


Fig. 3.8



Frequency (Hz)

Fig. 3.9

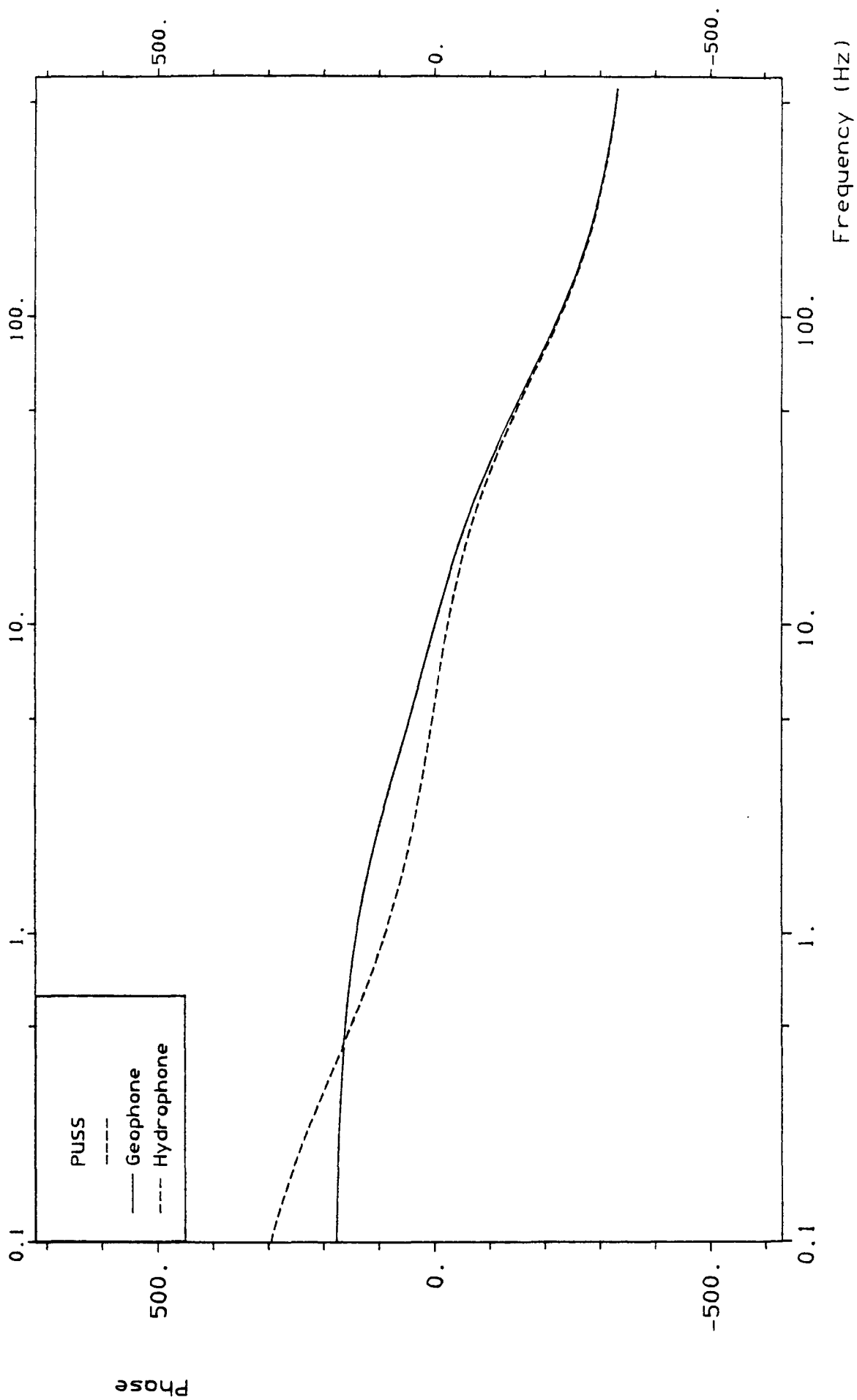


Fig. 3.10

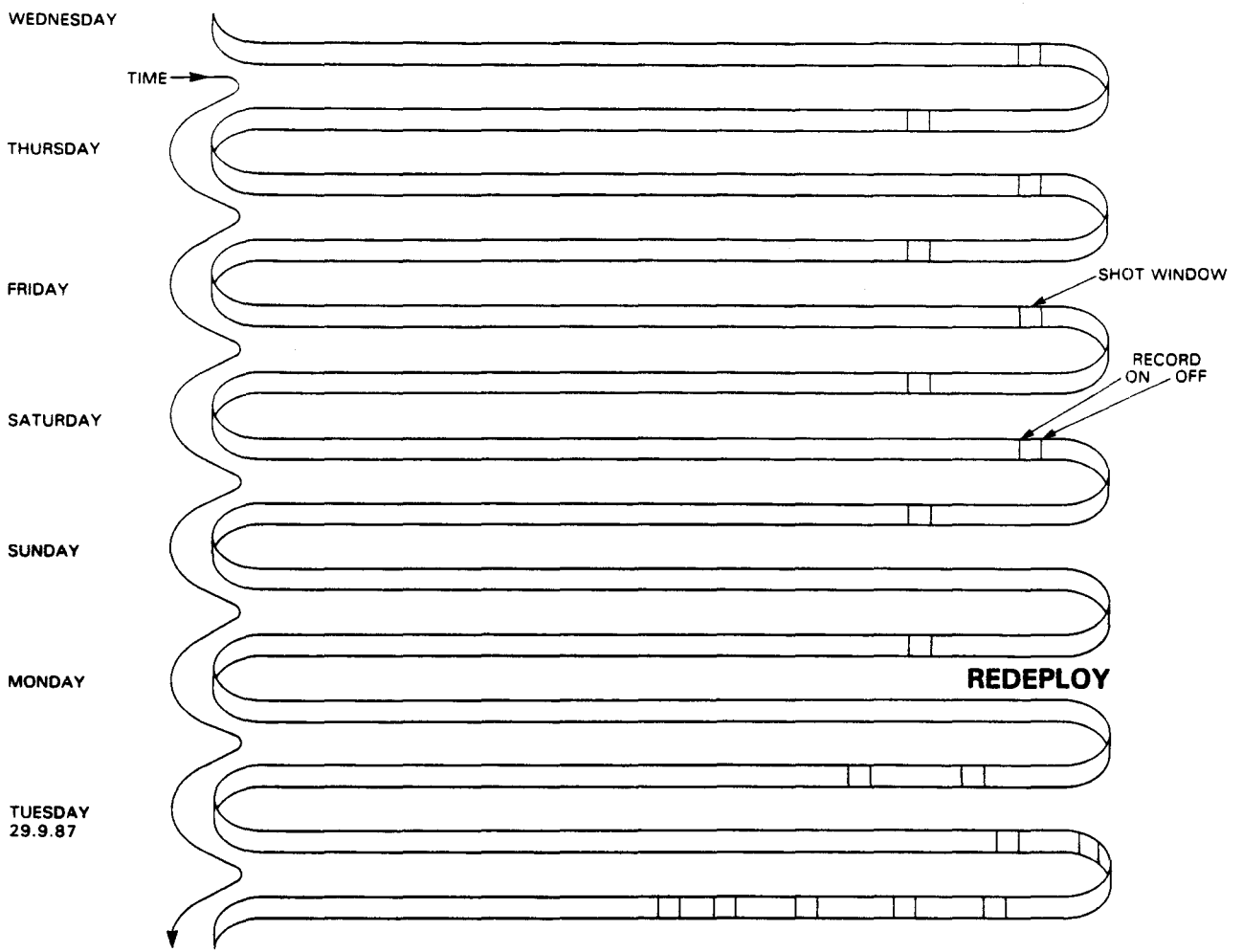


Fig. 4.1

Fig. 4.2

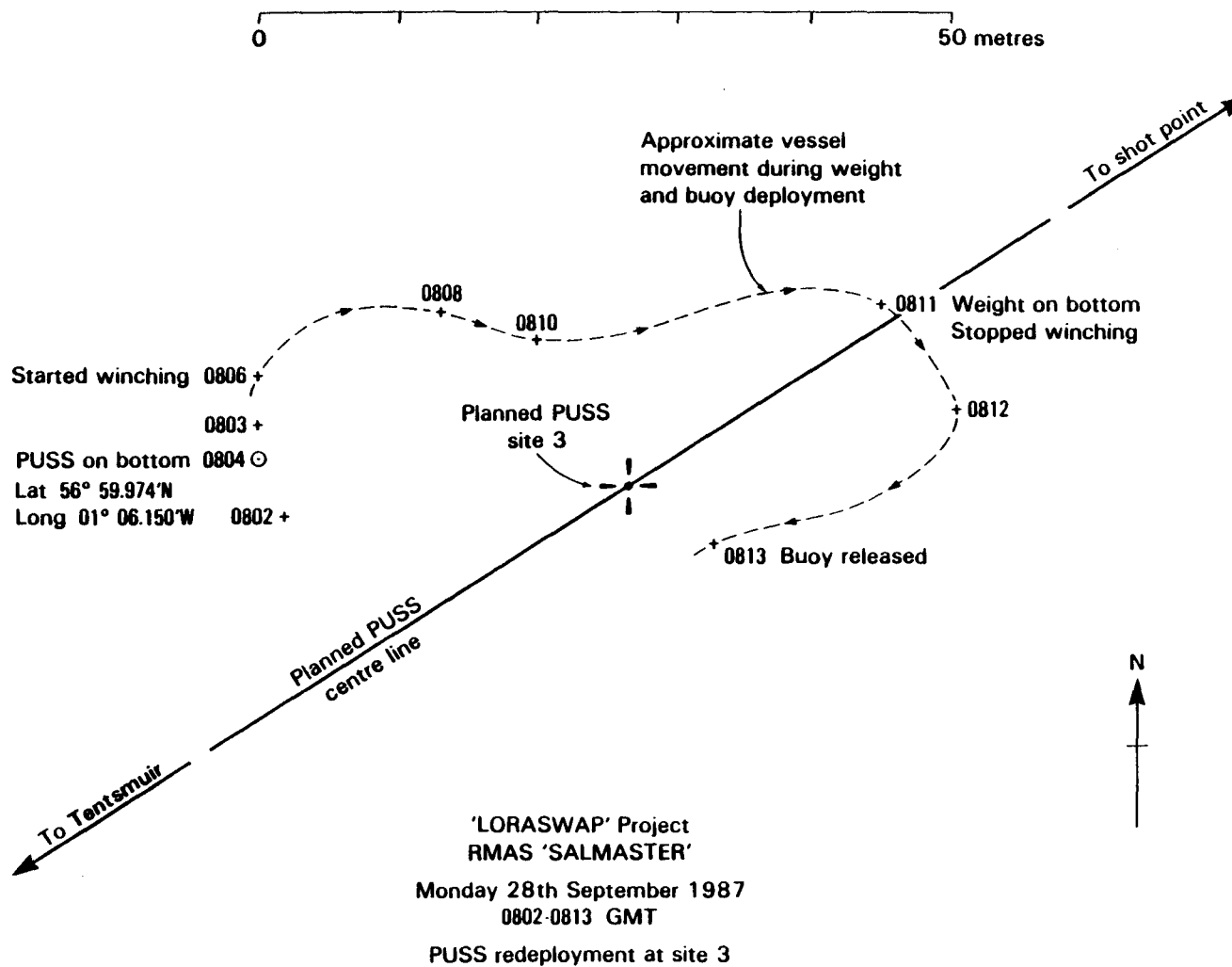
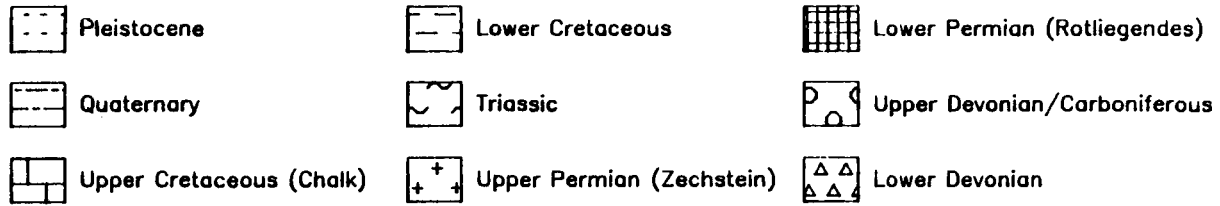
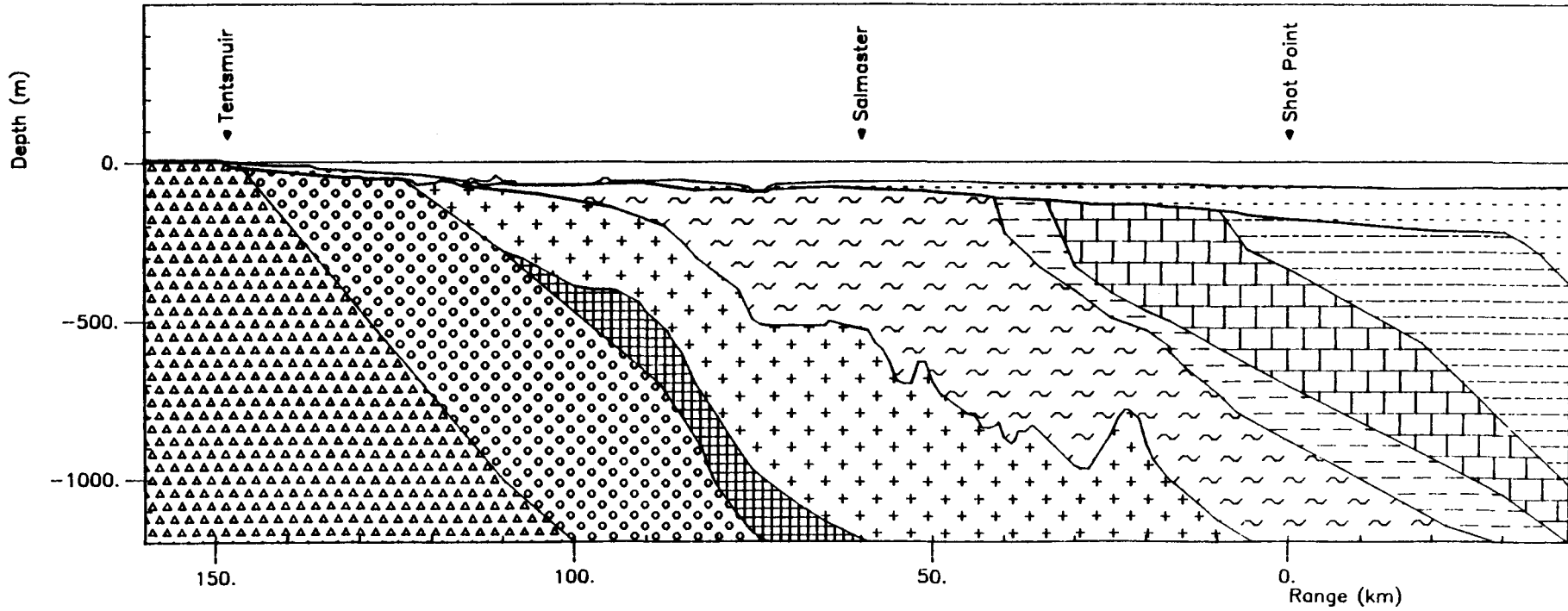


Fig. 6.1



68



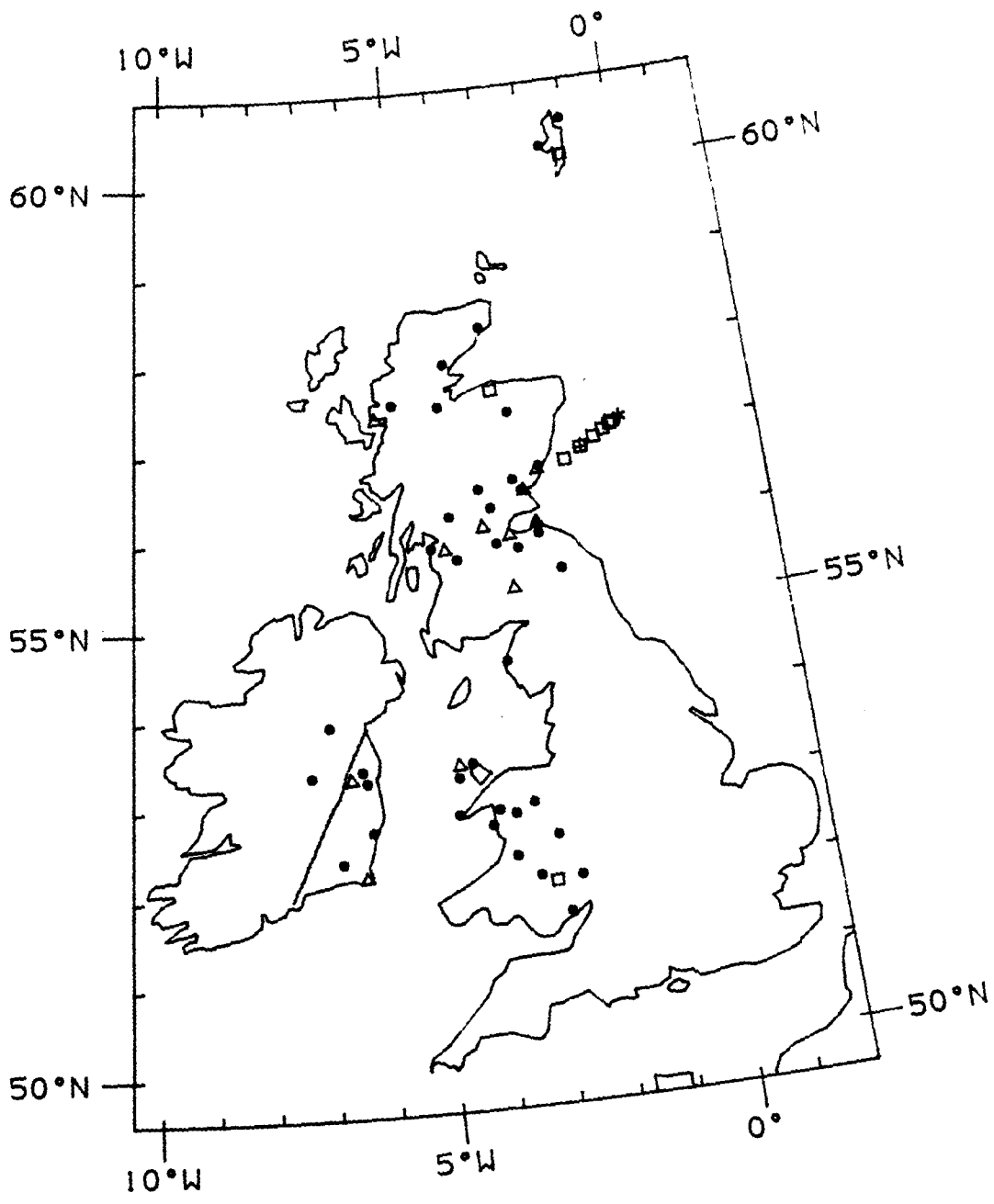


Fig 7.1

Fig. 7.2 Travel time vs range (4500lb charge)

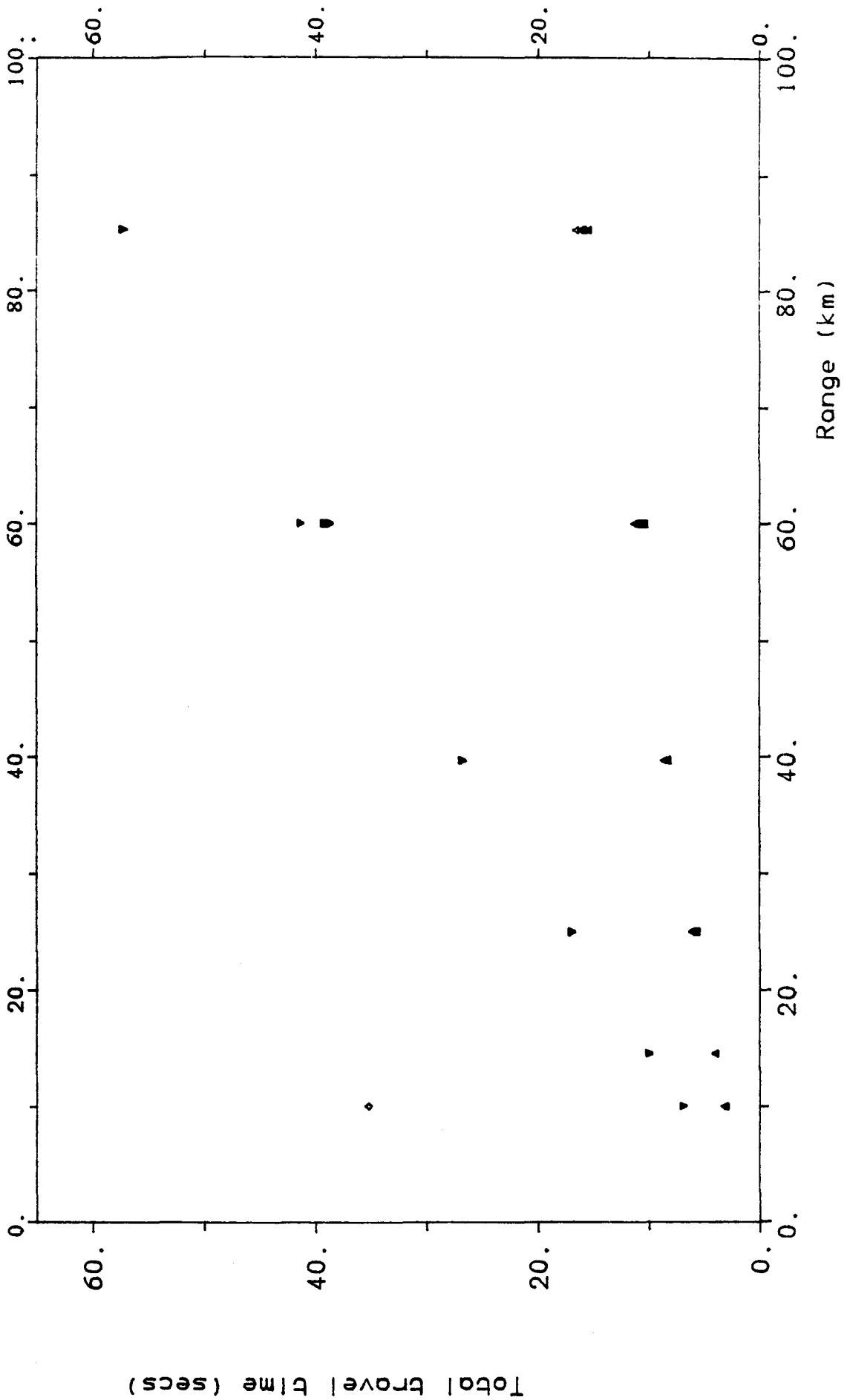


Fig. 7.3 Travel time vs range (900 lb charge)

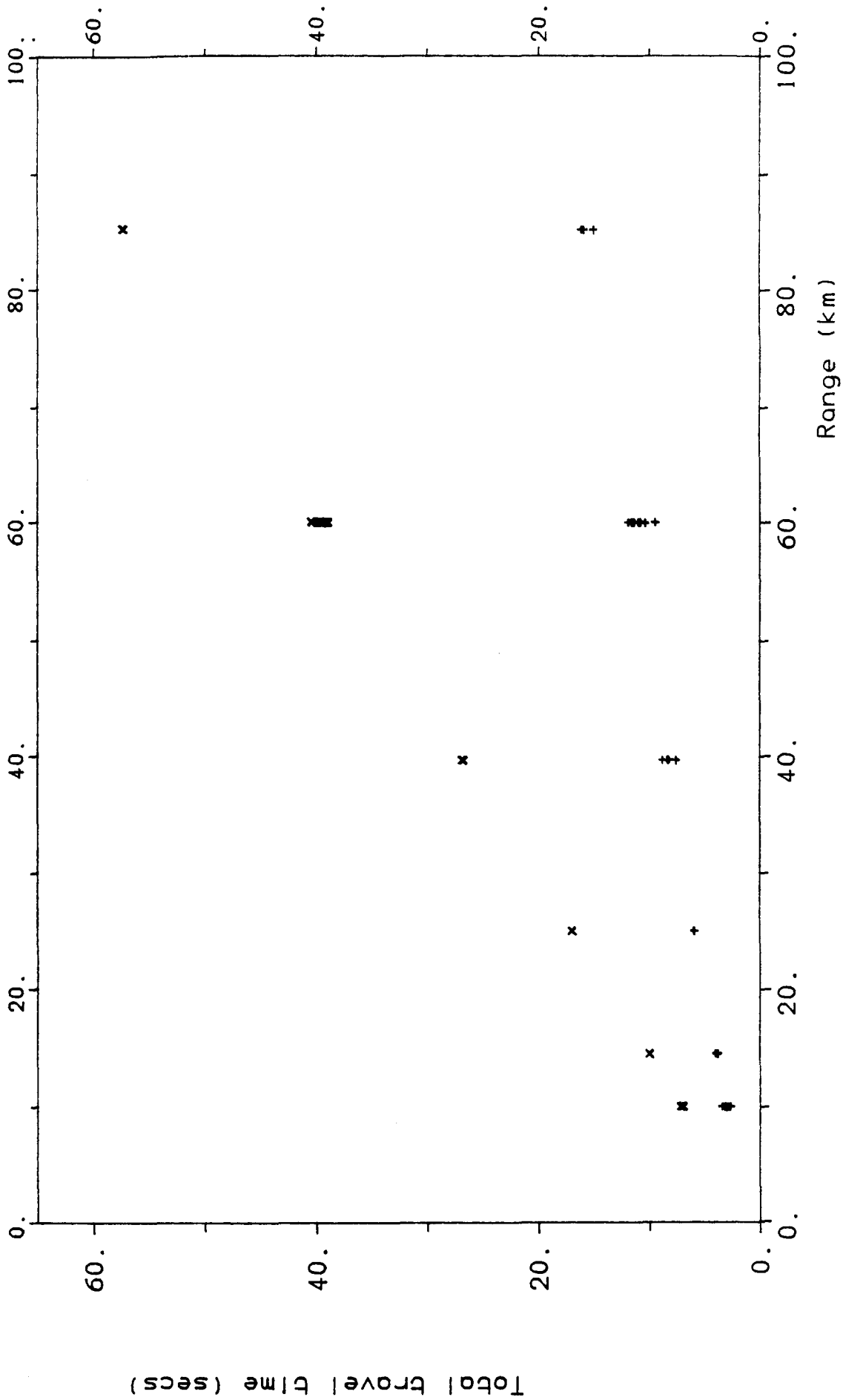


Fig. 7.4 Apparent velocity vs range (4500lb charge)

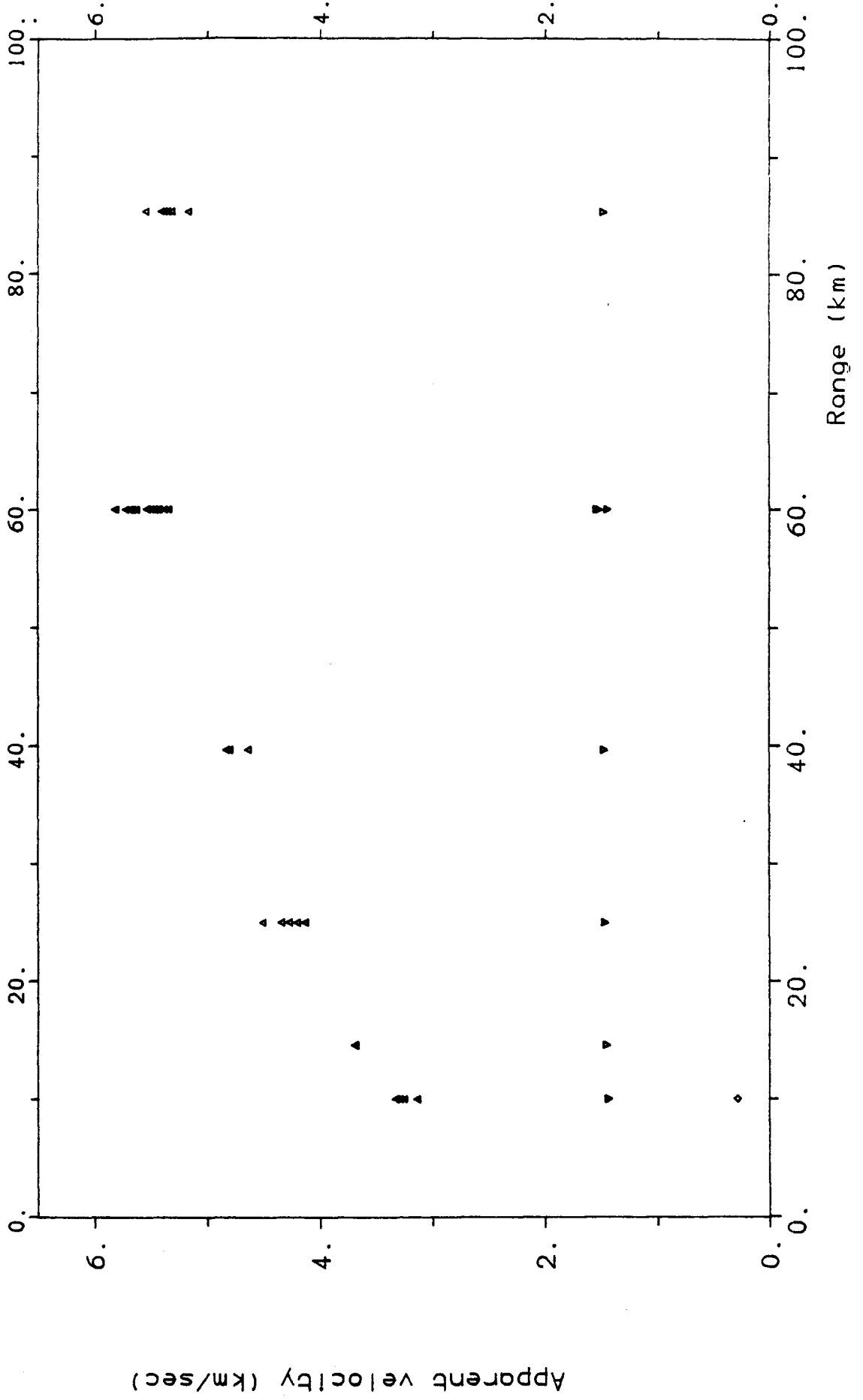


Fig. 7.5 Apparent velocity vs range (900 lb charge)

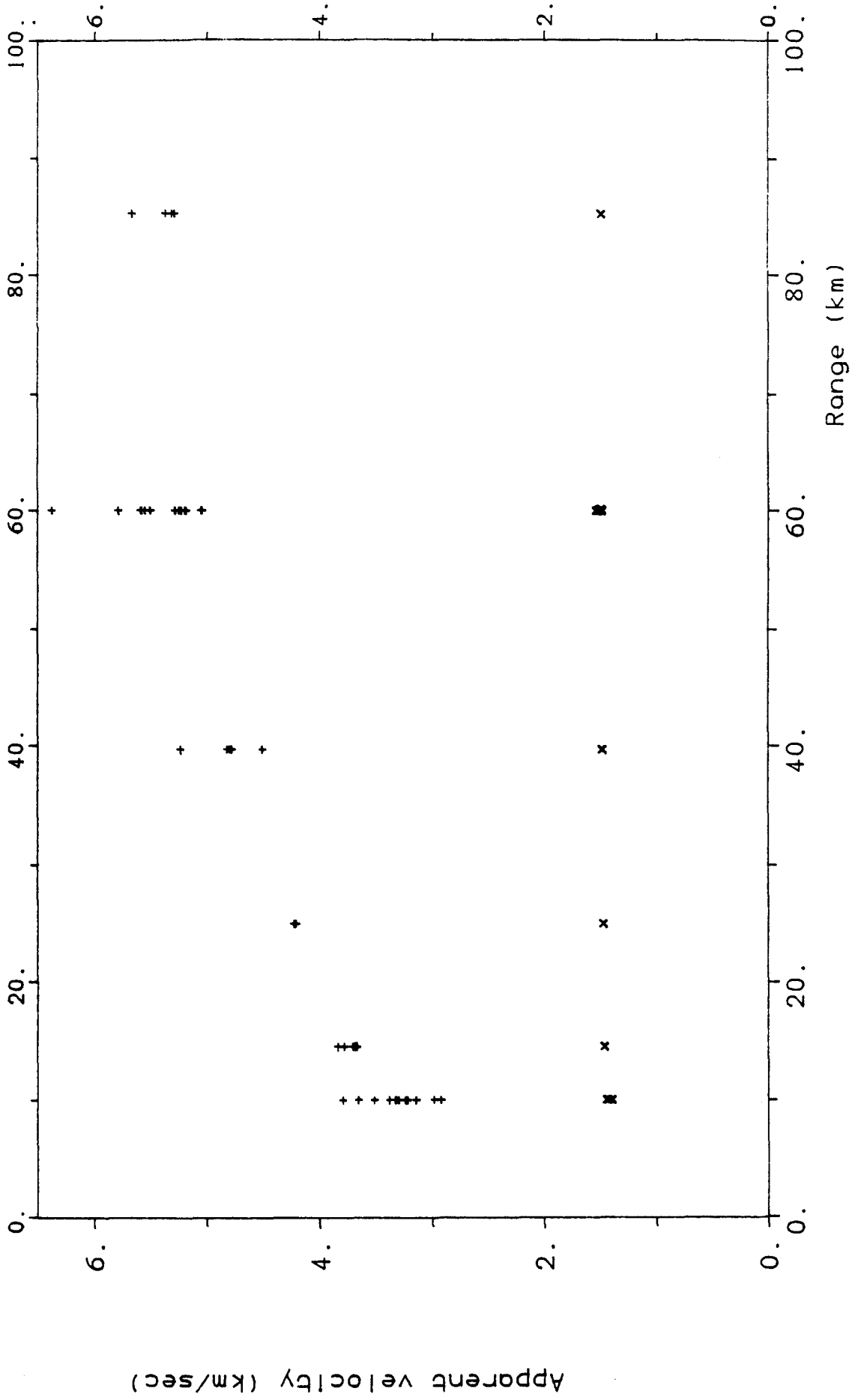


Fig. 7.6 Maximum amplitude vs range (4500lb charge)

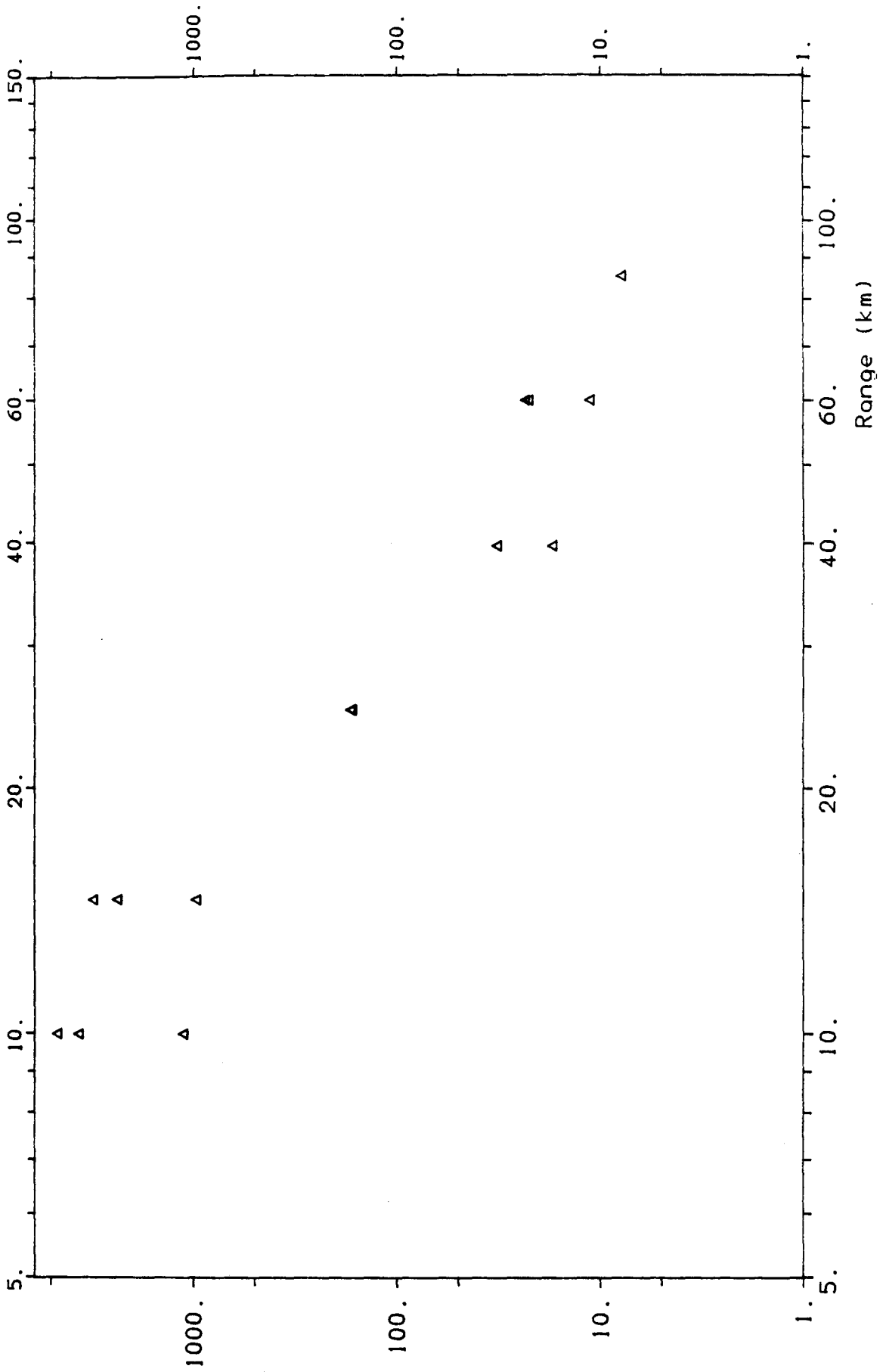


Fig. 7.7 Maximum amplitude vs range (900lb charge)

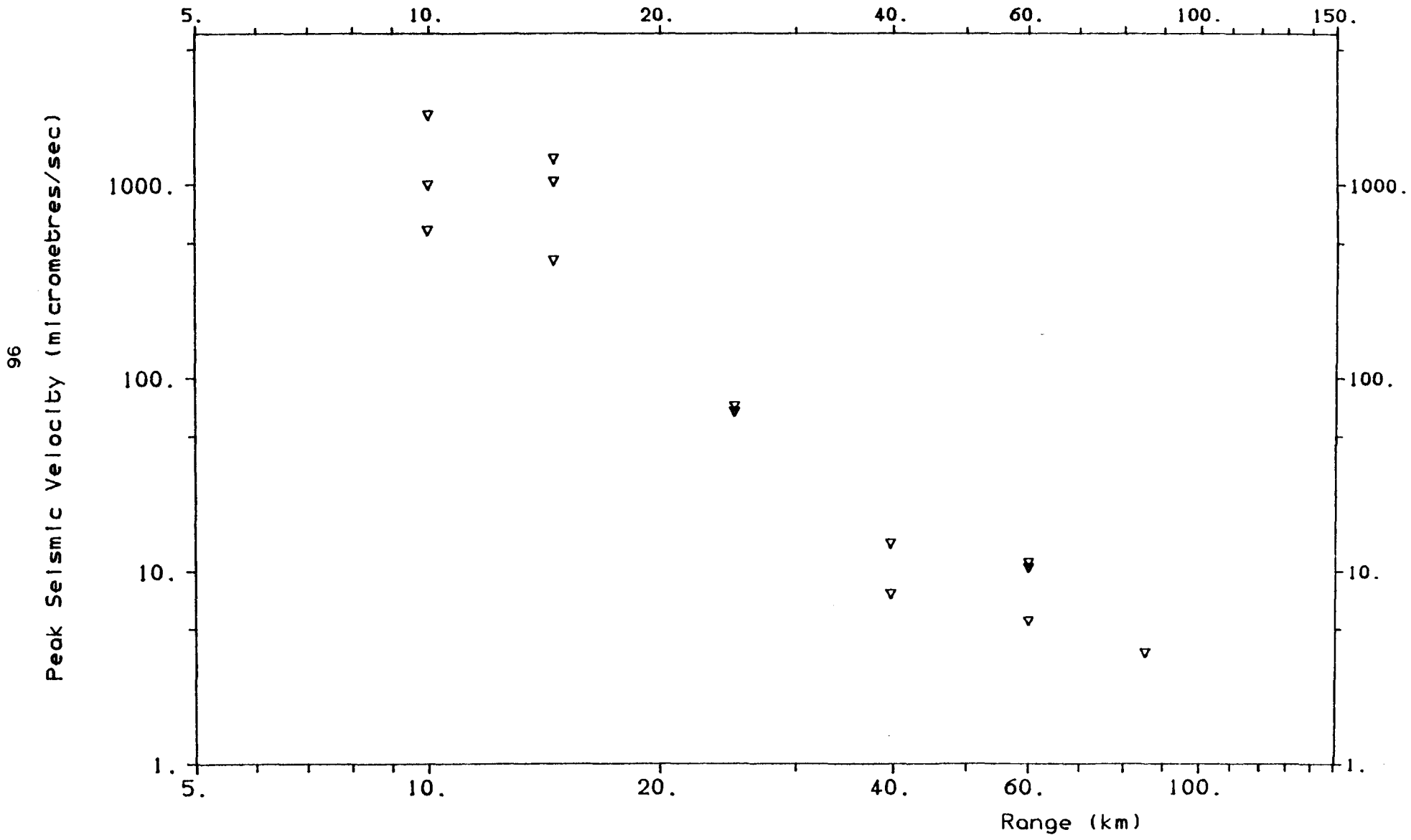


Fig. 7.8 Amplitude vs Range (4500lb charge)

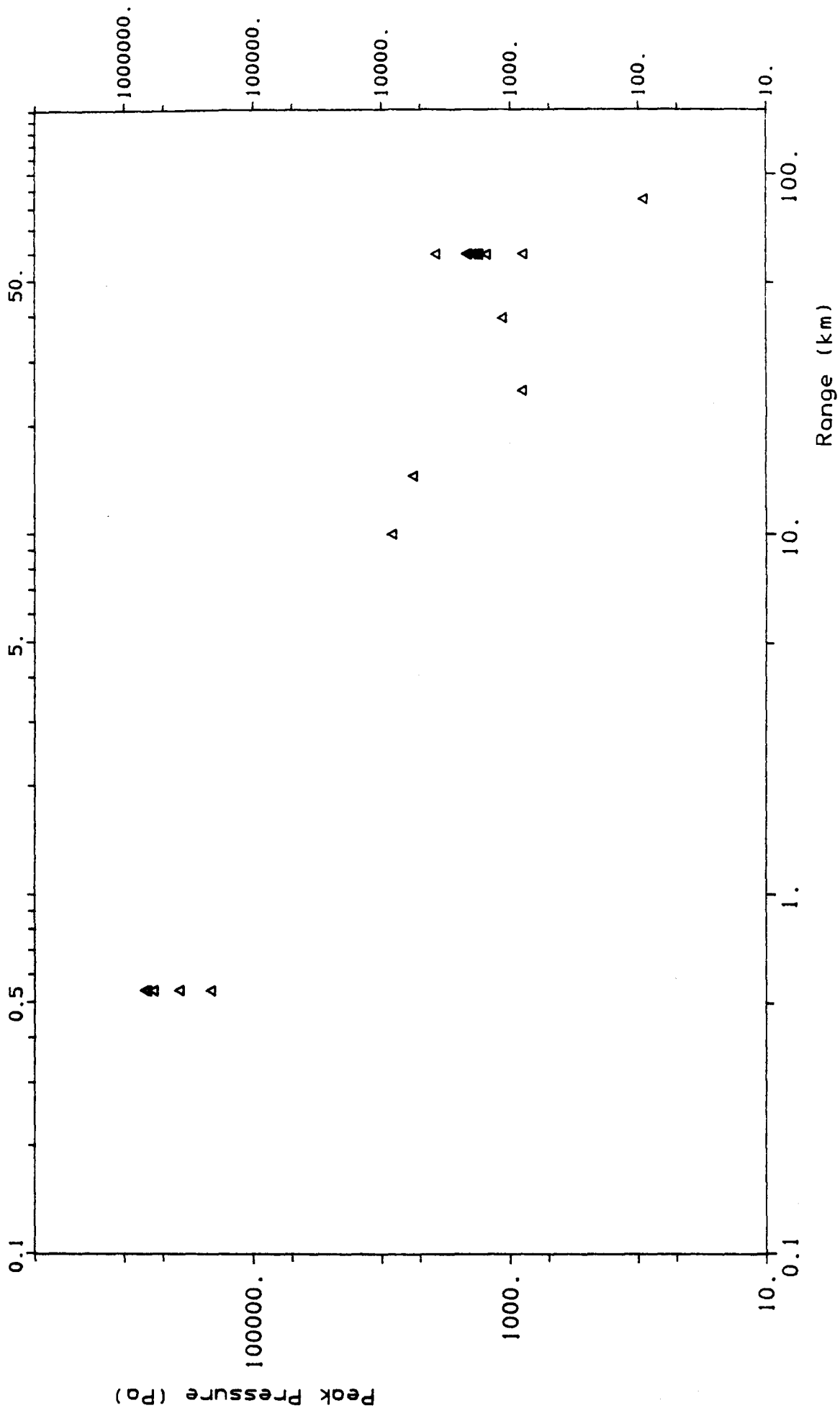


Fig. 7.9 Maximum amplitude vs range (9001b)

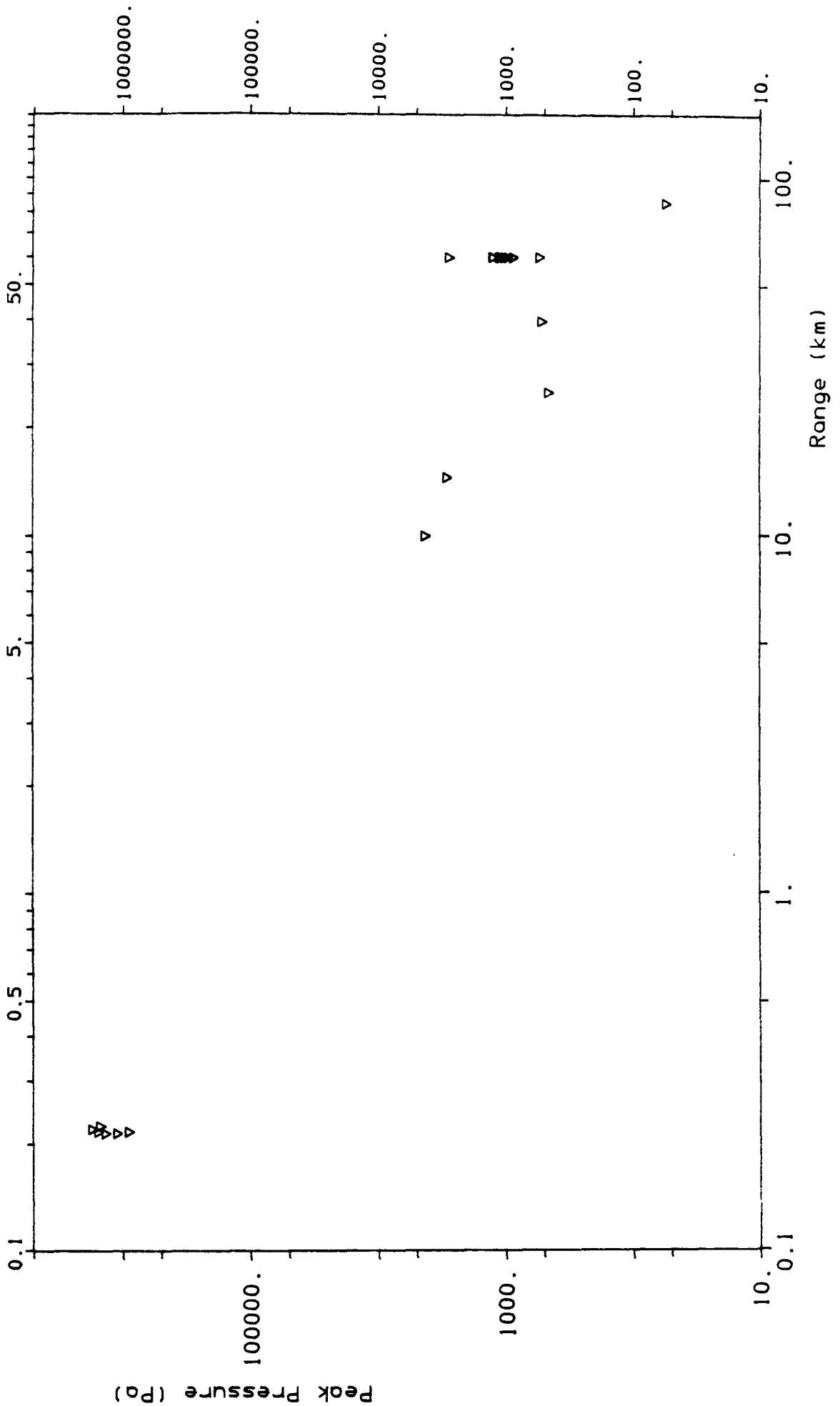


Fig. 8.1 4500lb charge MPa

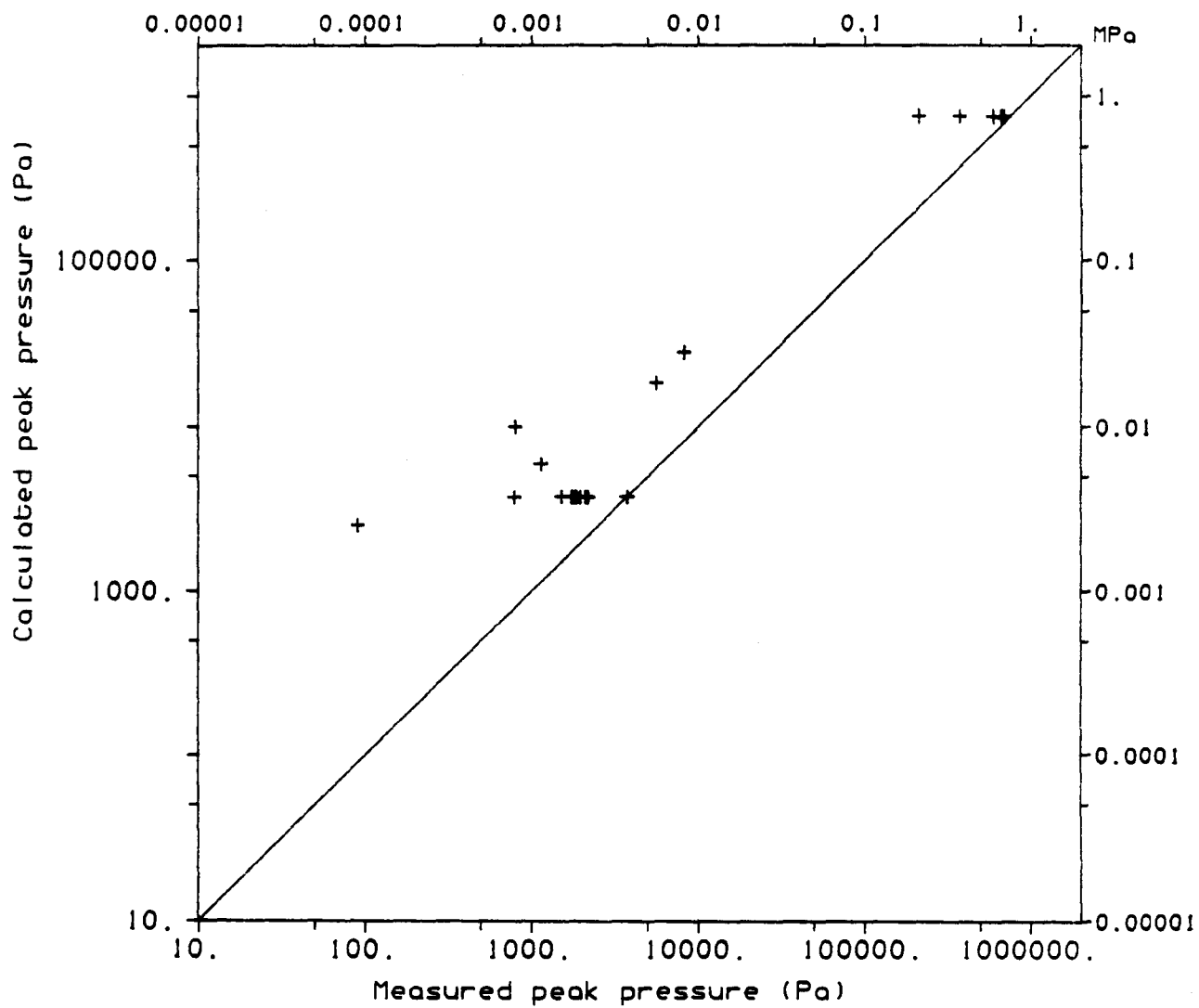
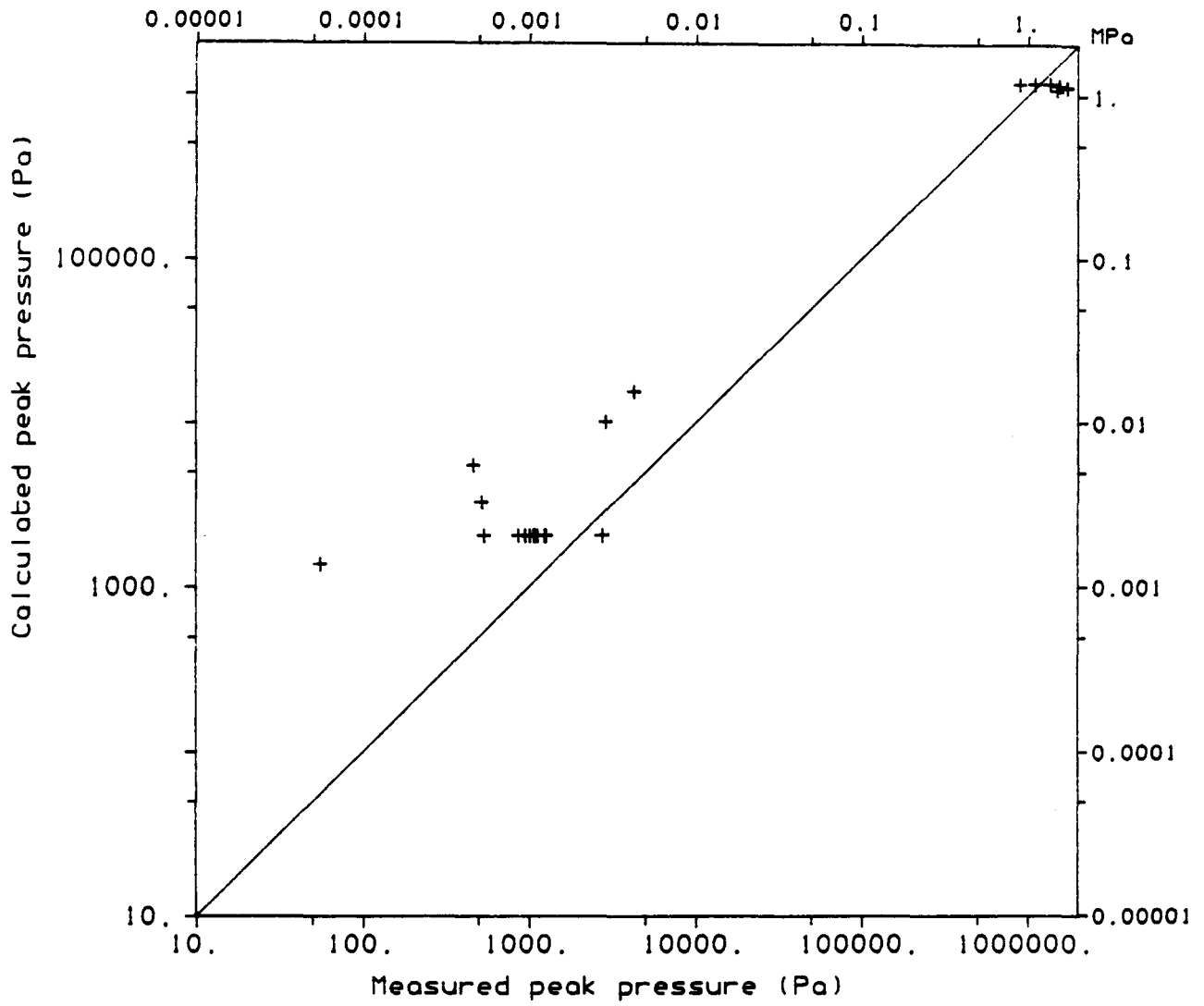


Fig. 8.2 900lb charge MPa



Appendix A: Proposed schedule for LORASWAP experiment

Thurs 17 Sep Local equipment onto Salmaster
 Sat 19 Sep Salmaster to put to sea and proceed to shot point
 Sun-Tues 20-22 Sep Salmaster to lay moorings at shot point, deploy PUSSES, deploy BGS Sea Bottom Package and hydrophones, wait at anchor.
 Mon 21 Sep Goosander to collect charges and proceed to shot point.
 Tues 22 Sep Goosander to prepare charge, deploy pressure gauges and shot timing gear.

All equipment deployment and preparations at sea were scheduled to take place with a view to detonating the 2 tonne charge at the first available detonation time window on 23 September.

Window No	Date	PUSS time window GMT	detonation time window GMT
1	Wed 23 Sep	11.50 - 12.00	11.52 - 11.54
2	Wed 23 Sep	13.50 - 14.00	13.52 - 13.54
3	Thu 24 Sep	11.50 - 12.00	11.52 - 11.54
4	Thu 24 Sep	13.50 - 14.00	13.52 - 13.54
5	Fri 25 Sep	11.50 - 12.00	11.52 - 11.54
6	Fri 25 Sep	13.50 - 14.00	13.52 - 13.54
7	Sat 26 Sep	11.50 - 12.00	11.52 - 11.54
8	Sat 26 Sep	13.50 - 14.00	13.52 - 13.54
9	Sun 27 Sep	13.50 - 14.00	13.52 - 13.54

Mon 28 Sep Disconnect and buoy off BGS Sea Bottom Package. Pull up PUSSES. If shot not detonated and weather forecast favourable: replace batteries, reprogram shot windows and redeploy PUSSES. Reconnect Salmaster to BGS Sea Bottom Package and VHS.

1	Tue 29 Sep	11.00 - 11.10	11.02 - 11.04
2		11.50 - 12.00	11.52 - 11.54
3		13.15 - 13.25	13.17 - 13.19
4		13.30 - 13.40	13.32 - 13.34
5		13.45 - 13.55	13.47 - 13.49

6	14.00 - 14.10	14.02 - 14.04
7	15.20 - 15.30	15.22 - 15.24
8	16.00 - 16.10	16.02 - 16.04
9	16.30 - 16.40	16.32 - 16.34

APPENDIX B: LOG OF DEPLOYMENT OF SEA BED INSTRUMENTS

(1) LOG OF DEPLOYMENT OF BGS SEABOTTOM PACKAGE 22:Sep:1987

TIME/GMT	ACTION/COMMENT
16:23:30	Final preparations for deployment
16:26:-	Gemini ready, outboard
16:27:20	Gemini in water
16:28:30	First length of rope taken outboard with Gemini
16:30:07	Gemini out 30° to port from stern
16:30:32	Package outboard, gemini ~ 60°
16:33:20	Gemini ~ 60
16:33:50	Lowering package to sea surface
16:34:08	Greasy pin slipped, package at sea surface
16:34:33	Lowering away rope and cable
16:34:40	Gemini ~ 45°
16:35:00	Weight (decoupling) outboard
16:35:42	Gemini 30° astern
16:36:29	Rope at 50 m mark at sea surface
16:36:43	60 m mark at fairlead, decoupling weight and package on bottom indicated
16:37:47	61 m reported water depth and ship bearing 190°
16:38:36	Shackling retrieval rope and weight
16:38:55	Starting to heave ship forward
16:39:30	Gemini alongside port fairlead
16:40:24	Preparing to put weight overboard into Gemini
16:40:40	+10 m heaved forward
16:41:12	Weight in Gemini, paying out retrieval weight/rope and cable simultaneously.
16:43:20	Gemini ~ 60°, retrieval buoy outboard, lowering weight from Gemini, +29 m heaved.
16:44:20	+30 m heaved forward, still paying out cable, it is now being deployed through an open fairlead aft.
16:46:45	+34 m heaved forward, cable entangled on deck at approximately ROV lashing position.

16:47:00 Cable now OK
16:47:20 +40 m heaved forward
16:47:30 Retrieval buoy entwined in cable and submerged.
16:47:34 +45 m heaved, 100 m of cable left on deck
16:47:55 +49 m heaved, stopped heaving forward
16:48:03 +50 m, 2 fluorescent buoys outboard
16:48:19 +53 m offset (a container vessel passed close by taking a look)
16:48:53 Heaving forward recommences
16:49:30 Gemini aft ~ 40 ft behind us
16:49:50 Cable all deployed, Gemini ~ 30° to port moving away from
ship ~ 50 m away
16:50:32 Stopping heaving forward, deployment complete

(2) Table log of deployment of PUSSEs (second deployment)

PUSS 1 (INSTRUMENT 9) REDEPLOYED

28.09.87 AT POSITION 3

TIME/GMT	ACTION/COMMENT
07:47:00	PUSS ready for deployment
08:01:36	Deployment commencing
08:02:11	PUSS in the water
08:02:30	PUSS away, paying out wire
08:03:48	Water depth 70 m
08:04:00	PUSS DOWN - POSITION FIX. Weight outboard, stopped paying out wire
08:05:00	Shackling weight onto wire
08:05:23	Finished fixing position - water 70 m
08:06:00	+3 m moved since PUSS down position
08:06:35	Order to heave forward, weight away
08:06:49	Paying out wire and heaving forward
08:07:35	+5 m heaved forward
08:07:52	+10 m heaved forward
08:08:15	+15 m heaved forward
08:08:32	Buoy outboard +20 m heaved forward
08:09:25	Stopped paying out wire for a while until 30 m heaved forward
08:09:38	Steady at 20 m from PUSS position
08:10:20	Steady at 20 m from PUSS position
08:10:30	+25 m heaved forward
08:10:42	+31 m heaved forward, paying out remainder of wire
08:10:48	+34 m heaved forward
08:10:55	+39 m stopping heaving
08:11:04	Weight on bottom +43 from PUSS
08:11:22	+48 m from PUSS site
08:11:32	+50 m from PUSS site
08:12:00	+52m steady, all wire out
08:12:25	+48 m from PUSS site

08:12:45 +45 m from PUSS site
08:12:50 Buoy outboard
08:13:00 +40 m from PUSS site
08:13:24 Buoy away +35 m from PUSS site

PUSS 2 (instrument 10) REDEPLOYED

28.09.87 AT POSITION 1

TIME/GMT	ACTION/COMMENT
05:18:32	PUSS ready to deploy
05:44:03	125 m off firing line
05:46:00	Slight swing on anchor, OK to proceed with deployment
05:46:40	PUSS outboard
05:47:28	PUSS away, paying out wire, 74 m water depth
05:49:30	PUSS DOWN, POSITION FIX
05:49:50	Preparing weight
05:51:00	Shackling weight to wire, position fixing complete
05:53:00	Swung +10 m since we put PUSS down
05:53:10	Weight away
05:53:25	Using swing on anchor to move forward
05:53:58	+15 m moved by swinging
05:54:40	Preparing buoy
05:55:07	+20 m moved by swinging, weight down
05:55:50	+30 m moved by swinging
05:56:20	Wire all out
05:56:39	+35 m from PUSS position
05:57:01	Buoy outboard
05:58:35	+40 m from PUSS site, buoy away
05:58:39	+42 m from PUSS site.

PUSS 3 (INSTRUMENT 11) REDEPLOYED

27.09.87 AT POSITION 2

TIME/GMT	ACTION/COMMENT
18:55:45	PUSS ready for deployment
18:59:46	Commencing deployment, drifting at 30 m/min.
19:01:00	PUSS outboard
19:02:15	PUSS in water
19:02:41	PUSS away, paying out wire as fast as possible as drift rate high
19:03:33	Drift rate 12 m/min
19:03:45	8 m/min drift, water depth 70 m
19:04:09	PUSS DOWN, POSITION FIX
19:04:55	Weight outboard
19:05:44	Position fix complete - 70 m water
19:06:50	Stopped drifting, +7 m drift from PUSS site
19:07:15	Weight away
19:07:35	Paying out rest of wire quickly, heaving forward
19:08:31	+10 m heaved forward
19:08:58	+15 m heaved forward
19:09:09	Weight on bottom
19:09:30	Buoy outboard
19:10:00	+20 m heaved forward
19:10:41	Wire all out, +25 m no drift
19:11:15	+30 m heaved forward
19:11:45	Buoy outboard
19:11:58	125 m heaved forward
19:12:15	Buoy away

PUSS 5 (INSTRUMENT 13) REDEPLOYED

27.09.87 AT POSITION 4

TIME/GMT	ACTION/COMMENT
16:09:30	Commencing deployment - PUSS outboard
16:09:50	PUSS in water
16:10:07	PUSS away
16:10:10	Paying out wire
16:11:26	Preparing weight
16:11:39	PUSS DOWN - POSITION FIX
16:12:45	Shackling weight - 67 m water depth
16:12:57	Fix complete
16:14:45	Having difficulty fixing weight on to wire, some delay
16:15:30	No drift at all
16:16:11	Weight away
16:16:40	Order to heave 50 m forward, paying out wire as fast as poss.
16:17:23	Stopped paying out wire
16:17:49	+5 m heaved forward
16:18:00	+10 m heaved forward
16:18:35	+15 m heaved forward
16:19:23	+20 m heaved forward
16:20:50	+30 m heaved forward, paying out rest of wire, stopped heaving
16:21:24	Weight on bottom
16:21:58	Wire all out
16:22:10	Buoy outboard
16:23:20	Paying out remainder of wire to allow weight to be taken by buoy
16:24:24	Buoy away

PUSS 6 (INSTRUMENT 14) REDEPLOYED

27.09.87 AT POSITION 5

TIME/GMT	ACTION/COMMENT
11:59:34	PUSS ready for deployment
12:00:00	PUSS off deck
12:00:12	PUSS outboard
12:00:38	PUSS in water
12:00:56	Water depth 54 m
12:02:30	Waiting for bridge to give "go ahead"
12:06:19	Manoeuvring bow to port as drifting off position
12:16:29	PUSS deployment commences
12:16:45	PUSS away - gressy pin slipped, lowering wire
12:20:24	Preparing weight
12:20:54	54 m water depth, weight outboard
12:21:40	Still drifting at 18 m/min to starboard, weight ready
12:22:05	PUSS DOWN - POSITION FIX paying out more wire
12:22:54	Shackling weight onto wire
12:23:13	Drift slowing - fix complete
12:24:30	Weight away, 54 m water depth
12:26:30	Buoy ready for deployment
12:27:05	Stopped drifting
12:27:36	Order to heave forward 50 m given, paying out wire
12:28:20	3 m heaved forward
12:29:00	+7 m heaved forward
12:29:10	+10 m heaved forward half of wire out
12:29:19	+13 m heaved forward
12:29:30	+15 m heaved forward
12:30:10	+20 m heaved forward
12:30:36	+25 m heaved forward
12:31:00	+30 m heaved forward
12:31:27	+35 m heaved forward
12:32:30	Stopped heaving forward

12:32:45 Paying out rest of wire +45 m from PUSS position
12:33:30 Weight down on bottom
12:35:15 Buoy outboard
12:36:00 Buoy away

Appendix C: Locations of sites at second deployment

Locations as on 29.9.87 when the 4500 lb and 900 lb charge were successfully detonated and recorded.

(1) SHOT POINT: SHACKLE RING

Class 5 mooring. Fix on shackle ring by approach of Salmaster to ring, locate ring between horns.

(a) First positioning of shot point.

Beacons: WHI, GIR, INV

Fixed at: 20.9.87

Depth: 76.25 m (including draught)

Fix: 57°06.972N 00°45.032W

$\sigma_N = .010$ $\sigma_W = .009$
 +9 m +5 m

Accuracy on fix: 20 fixes over 250s, $\sigma \sim 1.5$ m

Decca error: green 150 m, purple 80 m

Ship moving to shackle with heading of 80°

(b) Second positioning of shot point.

Beacons: WHI, GIR, INV

Fixed at: 14:02 on 30.9.87

Depth: 76 m (including draught)

Fix: (average of 2): 57°06.996N 00°45.040W

$\sigma_N = .003$ $\sigma_W = .001$
 +3 m +1m

Accuracy on fix: Seven fixes taken, average of first two accepted while Salmaster stationary with ring between the horns (anchor cable tension on buoy created slight movement).

Standard deviation over 2 fixes: $\sigma \sim 0.5$ m

Decca error: green 120 m, purple 90 m

Headings of ship on approach to shackle were 190° and 185° respectively

Final shot point position:

Simple average of fixes at deployment and recovery of shot moorings

$57^\circ 06.984\text{N}$ $00^\circ 45.036\text{W}$

$\sigma_N = .01$ $\sigma_W = .009$

± 9 m ± 5 m

Depth: $76.125 \pm .125$ m

Closure distances: 44 m in latitude, 8 m in longitude

Closure distance: 45 m

(2) PUSS LOCATIONS

SITE 1 (PUSS 2)

Fixed at: 05:49 on 28.9.87

No evidence of dragging

Beacons: WHI, GIR, INV

Depth: 74 m

Fix: 57°04.141N 00°53.424W

$\sigma_N = .002$ $\sigma_W = .003$
 +2 m +1.5 m

7 fixes taken over 62 s, $\sigma \sim 2$ m

Decca error: green 150 m, purple 15 m

Perpendicular distance from planned centre line: ~ 120 m

SITE 2 (PUSS 3)

Fixed at: 19:04 on 27.9.87

No evidence of dragging

Beacons: WHI, GIR, INV

Depth: 70 m

Fix: 57°02.882N 00°57.298W

$\sigma_N = .004$ $\sigma_W = .010$
 +4 m +5 m

6 fixes over 60 s, $\sigma \sim 1$ m

Decca error: green 150 m, purple 140 m

Perpendicular distance from planned centre line: 93 m

SITE 3 (PUSS 1)

Fixed at: 08:03:40 on 28.9.87

No evidence of dragging. Weight and chain tangled at recovery, weight layed NE of PUSS on deployment, vessel to SW on recovery, hence tangle.

Beacons: WHI, GIR, INV

Depth: 70 m

Fix: 56°59.974N 01°06.151W

$\sigma_N = .002$ $\sigma_W = .001$
 +2 m + .5m

7 fixes over 62 s, $\sigma \sim 1$ m

Decca error: green 150 m, purple 90 m

Perpendicular distance from planned centre line: 17 m

SITE 4 (PUSS 5)

Fixed at: 16:11:47 on 27.9.87

No evidence of dragging

Beacons: WHI, GIR, RED

Depth: 67 m

Fix: 56°55.794N 01°18.472W

$\sigma_N = .002$ $\sigma_W = .003$
 +2 m +1.5 m

6 Fixes over 53 s, $\sigma \sim 2$ m

Decca error: green 140 m, purple 20 m

Perpendicular distance from planned centre line: 91 m

SITE 5 (PUSS 6)

Fixed at: 12:21:56 on 27.9.87

Beacons: GIR, INV, RED

Depth: 54 m

Fix: 56°42.810N 01°56.500W

$\sigma_N = .001N$ $\sigma_W = .007$
 +1 m +3.5 m

9 fixes over 105 s, $\sigma \sim 2$ m

Decca error: green 450 m, (purple inappropriate)

Perpendicular distance from planned centre line:

(3) BGS/ARE LISTENING SITE

- 1 BGS sea bottom package (was fixed 22.9.87 during first deployment). No evidence of drag (anchor dragged by ship in winching suggests soft bottom).

Beacons: WHI, INV, RED

Depth: 61 m

Fix: 56°50.073N 01°35.537W

$\sigma_N = .002$ $\sigma_W = .006$
 +2 m +3 m

Accuracy on fix: 5 fixes over 46 s, $\sigma \sim 2$ m

Decca error: green 140 m

Ship's head: 190° (include correction for orientation rope angle)

2 VERTICAL HYDROPHONE STRING (VHS)

Fix obtained by extension to VHS using: (1) Sydelis offset from antenna to point on Salmaster port side, (2) measuring distance from point at Salmaster port side to VHS using rope, in calm conditions. Rope measured 69 m and gyro bearing was 133°.

Fixed at: 13:25:50 on 28.9.87

Beacons: WHI, INV, RED

Depth: 61.5 m at 12:45:00

Fix: using a grid Δ easting = +50 m, Δ northing = -47 m and assuming grid north = true north
56°50.123N 01°35.625W

Accuracy on fix: 1 fix with $\sigma \sim 2$ m

Decca error: green 135 m

3 ARE HYDROPHONE STRING

Deployed from Salmaster. Fixed for each of two shots separately. Syledis fix few minutes after shot to avoid any possible interference problems with on ship signal recording, Syledis being an active transmitting system.

(a) 4500 lb shot fix:

Fixed at: 11:00:00 on 29.9.87

Beacons: GIR, INV, RED

Depth: 61.5 m

Fix: 56°50.140N 01°35.715W

Accuracy on fix: 1 fix with $\sigma \sim 1$ m

Decca error: green 140 m

(b) 900 lb shot fix:

Fixed at: 15:37:55 on 29.9.87

Beacons: GIR, INV, RED

Depth: 61.5 m

Fix: 56°50.141N 01°35.729W

Accuracy on fix: 1 fix with $\sigma \sim .3$ m

Drift from first fix on ARE hydrophone at first shot is 14 m.

Decca error: not available.

SYLEDIS BEACONS

WHI: Whinnyfield

GIR: Girdleness

INV: Inverbervie

RED: Redhead

Appendix D: MODELS FOR COMPUTER SIMULATION

(1) ACOUSTIC MODELS

- (a) Model at shot-point to be used out to site PUSS 1**
- (b) Model for sites PUSS 2 and 3.**
- (c) Model for PUSS 4, BGS package and PUSS 5.**

(2) PARAMETERS OF PRELIMINARY SEISMIC MODELS

- a) Shot point central model (0 km range)**
- b) BGS site model (60 km range)**
- c) Tentsmuir hard rock site model (148km range)**

Table D1: Parameters of preliminary acoustic models

(a) Model at shot-point to be used out to site PUSS 1

Layer No	Type	Thickness m	Depth to Base, m	α km/s	β km/s	ρ g/cc	$\frac{1}{Q_\alpha}$	$\frac{1}{Q_\beta}$
1	Water	20	20	1.510	0	1.02	0	0
2	Water	20	40	1.4902	0	1.02	0	0
3	Water	35	75	1.480	0	1.02	0	0
4	sand (fine)	20	95	1.749	.195	1.94	.03	.06
5	silty sand	40	135	1.838	.751	1.77	.03	.06
6	gravelly muddy sand	∞	∞	1.838	.926	1.77	.03	.06

(b) Model for sites PUSS 2 & 3

Layer No	Type	Thickness m	Depth to Base, m	α km/s	β km/s	ρ g/cc	$\frac{1}{Q_\alpha}$	$\frac{1}{Q_\beta}$
1	Water	20	20	1.510	0	1.02	0	0
2	Water	20	40	1.4902	0	1.02	0	0
3	Water	30	70	1.480	0	1.02	0	0
4	sand (fine)	20	90	1.749	.195	1.94	.03	.06
5	silty sand	40	130	1.838	.751	1.77	.03	.06
6	gravelly muddy sand	∞	∞	1.838	.926	1.77	.03	.06

(c) Model for PUSS4, BGS package and PUSS 5

Layer No	Type	Thickness m	Depth to Base, m	α km/s	β km/s	ρ g/cc	$\frac{1}{Q_\alpha}$	$\frac{1}{Q_\beta}$
1	Water	20	20	1.510	0	1.02	0	0
2	Water	20	40	1.4902	0	1.02	0	0
3	Water	20	60	1.480	0	1.02	0	0
4	sand (fine)	20	80	1.749	.195	1.94	.03	.06
5	gravelly muddy sand	∞	∞	1.838	.926	1.77	.03	.06

Table D2 Parameters of preliminary seismic models.

(a) Shot-Point Central Model at 57°06.984'N 00°45.036'W (0 km range)

Layer No	Region	Type	Thickness km	Depth to bottom km	α km/s	σ	β km/s	ρ g/cc	$1/Q_\alpha$	$1/Q_\beta$
1	Sea	Water	0.075	0.075	1.4902	-	-	1.02	0	0
2	Sea bed	Fine sand	0.02	0.095	1.749 ¹	>0.49	0.195 ³	1.941 ¹⁶	0.03 ¹⁹	0.06 ²⁰
3	Sea bed	Silty/ gravelly muddy sand	0.119	0.214	1.838 ²	0.33 ⁴	0.926 ⁵	1.772 ¹⁶	0.03 ¹⁹	0.06 ²⁰
4	Shallow upper crust (SUC)	Tertiary, Eocene - Paleocene	0.124	0.338	1.851 ⁶	0.33 ⁴	0.932 ⁵	2.034 ¹⁷	0.008 ²³	0.025 ²¹
5	SUC	Upper Cretaceous through Triassic	0.762	1.100	2.626 ⁷	0.33 ⁴	1.323 ⁵	2.159 ¹⁷	0.008 ²³	0.025 ²¹
6	SUC	Permian Zechstein	0.900	2.000	5.115 ⁸	0.33 ⁴	2.577 ⁵	2.559 ¹⁷	0.017 ²³	0.05 ²¹
7	Upper crust (UC)	UC, Lower Permian and older	2.000	4.0	5.996 ¹¹	0.233 ¹⁰	3.548 ⁹	2.700 ¹⁷	0.002 ²²	0.004 ²³
8	UC	UC	5.0	9.0	6.238 ¹¹	0.233 ¹⁰	3.691 ¹²	2.739 ¹⁷	0.002 ²²	0.004 ²³
9	Mid crust (MC)	MC	9.0	18.0	6.373 ¹¹	0.224 ¹³	3.8 ¹³	2.761 ¹⁷	0.002 ²²	0.004 ²³
10	Lower crust (LC)	LC	13.0	31.0	7.00 ¹⁴	0.249 ¹⁴	4.046 ¹⁴	2.862 ¹⁷	0.002 ²²	0.004 ²³
11	Upper mantle (UM)	UM	24.0	55.0	8.10 ¹⁵	0.25 ¹⁸	4.677 ¹⁸	3.269 ¹⁸	0.002 ²²	0.005 ²³
12	Upper mantle (UM)	UM	20.0	75.0	8.3 ²⁴	0.25 ¹⁸	4.792 ¹⁸	3.334 ¹⁸	0.002 ²²	0.005 ²³
13	Upper mantle (UM)	UM	15.0	90.0	8.6 ²⁴	0.25 ¹⁸	4.965 ¹⁸	3.433 ¹⁸	0.002 ²²	0.005 ²³
14	Upper mantle (UM)	UM	∞	∞	8.9 ²⁴	0.25 ¹⁸	5.139 ¹⁸	3.531 ¹⁸	0.007 ²²	0.016 ²³

Table D2 Parameters of preliminary seismic models (cont.).

(b) BGS Site Model at 56°50.073'N 01°35.537'W (60 km range)

Layer No	Region	Type	Thickness km	Depth to bottom km	α km/s	σ	β km/s	ρ g/cc	$1/Q_\alpha$	$1/Q_\beta$
1	Sea	Water	0.060	0.060	1.4902	-	-	1.02	0	0
2	Sea bed	Fine sand	0.020	0.080	1.749 ¹	>0.49	0.195 ³	1.941 ¹⁶	0.03 ¹⁹	0.06 ²⁰
3	Sea bed	Silty/ gravelly muddy sand	0.040	0.120	1.838 ²	0.33 ⁴	0.926 ⁵	1.772 ¹⁶	0.03 ¹⁹	0.06 ²⁰
4	Shallow upper crust (SUC)	Triassic red marls & clays	0.430	0.550	2.427 ²⁵	0.33 ⁴	1.223 ⁵	2.127 ¹⁷	0.008 ²³	0.025 ²¹
5	SUC	Permian Zechstein	0.650	1.200	5.115 ²⁶	0.33 ⁴	2.577 ⁵	2.559 ¹⁷	0.017 ²³	0.05 ²¹
6	Upper crust (UC)	UC, Lower Permian and Carboniferous	1.600	2.8	3.840 ²⁷	0.233 ¹⁰	2.272 ⁵	2.354 ¹⁷	0.002 ²²	0.004 ²³
7	Upper crust (UC)	UC, Devonian	2.500	5.3	5.000 ²⁸	0.233 ¹⁰	2.959 ⁵	2.540 ¹⁷	0.002 ²²	0.004 ²³
8	Upper crust (UC)	UC, Silurian and older	3.700	9.0	6.238 ¹¹	0.233 ¹⁰	3.691 ¹²	2.739 ¹⁷	0.002 ²²	0.004 ²³
9	Mid crust (MC)	MC	9.0	18.0	6.373 ¹¹	0.224 ¹³	3.8 ¹³	2.761 ¹⁷	0.002 ²²	0.004 ²³
10	Lower crust (LC)	LC	13.0	31.0	7.00 ¹⁴	0.249 ¹⁴	4.046 ¹⁴	2.862 ¹⁷	0.002 ²²	0.004 ²³
11	Upper mantle (UM)	UM	24.0	55.0	8.10 ¹⁵	0.25 ¹⁸	4.677 ¹⁸	3.269 ¹⁸	0.002 ²²	0.005 ²³
12	Upper mantle (UM)	UM	20.0	75.0	8.3 ²⁴	0.25 ¹⁸	4.792 ¹⁸	3.334 ¹⁸	0.002 ²²	0.005 ²³
13	Upper mantle (UM)	UM	15.0	90.0	8.6 ²⁴	0.25 ¹⁸	4.965 ¹⁸	3.433 ¹⁸	0.002 ²²	0.005 ²³
14	Upper mantle (UM)	UM	∞	∞	8.9 ²⁴	0.25 ¹⁸	5.139 ¹⁸	3.531 ¹⁸	0.007 ²²	0.016 ²³

Table D2 Parameters of preliminary seismic models (cont.).

(c) Tentsmuir Hard Rock Site Model at 56°24.456'N 02°48.72'E (148 km range)

Layer No	Region	Type	Thickness km	Depth to bottom km	α km/s	σ	β km/s	ρ g/cc	$1/Q_\alpha$	$1/Q_\beta$
1	Shallow upper crust (SUC)	Lower Devonian, old red sandstone	0.3	0.3	3.772 ¹¹	0.33 ³⁰	1.9 ²⁹	2.343 ¹⁷	0.014 ²³	0.040 ³¹
2	SUC	Lower Devonian volcanics, basalt and sandstone	0.7	1.0	4.367 ¹¹	0.33 ³⁰	2.2 ³²	2.438 ¹⁷	0.007 ²³	0.020 ³¹
3	SUC	Lower Devonian	1.0	2.0	4.633 ¹¹	0.27 ³⁰	2.6 ³³	2.481 ¹⁷	0.015 ²³	0.040 ³⁴
4	Upper crust (UC)	Silurian and older	4.0	6.0	6.065 ¹¹	0.233 ¹⁰	3.589 ³⁵	2.711 ¹⁷	0.002 ²²	0.004 ²³
5	Mid crust (MC)	MC	12.0	18.0	6.373 ¹¹	0.224 ¹³	3.8 ¹³	2.761 ¹⁷	0.002 ²²	0.004 ²³
6	Lower crust (LC)	LC	13.0	31.0	7.00 ¹⁴	0.249 ¹⁴	4.046 ¹⁴	2.862 ¹⁷	0.002 ²²	0.004 ²³
7	Upper mantle (UM)	UM	24.0	55.0	8.10 ¹⁵	0.25 ¹⁸	4.677 ¹⁸	3.269 ¹⁸	0.002 ²²	0.005 ²³
8	Upper mantle (UM)	UM	20.0	75.0	8.30 ²⁴	0.25 ¹⁸	4.792 ¹⁸	3.334 ¹⁸	0.002 ²²	0.005 ²³
9	Upper mantle (UM)	UM	15.0	90.0	8.60 ²⁴	0.25 ¹⁸	4.965 ¹⁸	3.433 ¹⁸	0.002 ²²	0.005 ²³
10	Upper mantle (UM)	UM	110.0	200.0	8.90 ²⁴	0.25 ¹⁸	5.139 ¹⁸	3.531 ¹⁸	0.007 ²²	0.016 ²³
11	Upper mantle (UM)	UM	213.0	413.0	8.97 ³⁶	-	4.96	3.64	0.003	0.007 ³⁷
12	Upper mantle (UM)	UM	287.0	700.0	10.67	-	5.93	4.3	0.002	0.005
13	Upper mantle (UM)	UM	500.0	1200.0	11.71	-	6.5	4.77	0.001	0.002
14	Upper mantle (UM)	UM	∞	∞	12.79	-	6.92	5.22	0.001	0.002

Footnotes to parameters of preliminary seismic models

Footnotes to shot point central model

- 1: Although Thomson & Eden (1977) do not subdivide the "sand" category used in their borehole logs it will be defined as "fine sand" in order to extract α values from Hamilton (1980) and Allen (1988); $\alpha = 1.749$ km/s is similar to Schirmer's (1971) value of $\alpha = 1.725$ km/s for "sand",
- 2: Velocity calculated from Plio-Pleistocene one-way travel time in AMOCO Well 27/3-1 after allowing for 20 m of fine sand,
- 3: β from Jensen & Schmidt (1986) for sand at 20m,
- 4: $\sigma = 0.33$ is consistent with comparisons between β in layers below 0.6 km in model FF1 of the Firth of Forth (MacBeth & Burton 1986) and α in the Permian Zechstein and Lower Paleozoic base layers of AMOCO Well 27/3-1; also adopted for shallower layers and is consistent with $\sigma = 0.33$ in top 2 km of Midland Valley according to Assumpcao & Bamford (1978),
- 5: β derived from α ,
- 6: α velocity of Tertiary Eocene-Palaeocene, layer 3 of AMOCO Well 27/3-1,
- 7: Average α velocity of Upper Cretaceous through Triassic, layers 4 to 8, of AMOCO Well 27/3-1 with Triassic base evident in AMOCO Well extended down to 1100 m,
- 8: α velocity of Permian Zechstein, layer 9 of AMOCO Well 27/3-1, with layer placed at 900-2000 m depth range,
- 9: β obtained by Rayleigh wave velocity inversion, predominantly in the Midland Valley, for Region G, layer 2 of MacBeth & Burton (1985, Fig.13),
- 10: σ given by Assumpcao & Bamford (1978) for approximately 2-9 km depth in the Midland Valley,
- 11: α derived from β ,
- 12: β values of Region G, layers 3 & 4 of MacBeth & Burton (1985, Fig.13) combined through slowness average,
- 13: β values of Region G, layers 5 & 6 of MacBeth & Burton (1985, Fig.13) combined to give layer to depth 18 km - the approximate horizon indicated by Assumpcao & Bamford (1978) for $\sigma = .224$ between 9-18 km depth in the Midland Valley,

- 14: α from Bamford *et al.* (1978) for layer extending from 18 to 31 km beneath the Midland Valley; β inferred from σ using Assumpção & Bamford (1978) value in this layer,
- 15: α from Bamford *et al.* (1976) for Midland Valley sub-Moho,
- 16: ρ from Hamilton (1980) and Hamilton *et al.* (1982),
- 17: ρ following Stuart's (1978) use of Nafe & Drake (1965) for lower crust in the North Sea, $\rho = (\alpha + 10.8)/6.22$; noting that Colette *et al.* (1970) suggest $\rho = 2.4$ g/cc for top 5 km in the North Sea.
- 18: ρ following Stuart's (1978) use of Birch (1961) for the upper mantle lid layer in the North Sea and of an implicit $\sigma = 0.25$; $\alpha = \sqrt{3}\beta$, $\rho = (\alpha + 1.87)/3.05$,
- 19: $1/Q_\alpha$ from Hamilton (1972),
- 20: $1/Q_\beta$ adapted from Hamilton (1976c), using log decrement approximately 0.2 for both sand and silty sand,
- 21: $1/Q_\beta$ adapted from Evan's (1981) Hedgehog inversion of Rayleigh wave attenuation in the Carboniferous of the Midland Valley, noting MacBeth & Burton's (1987) more general model of 0.02 - 0.09 in the upper 400m, < 0.01 between 400 - 800m and 0.04 below 800m,
- 22: $1/Q_\alpha$ values typical for continental crust and lithosphere (e.g. Burton 1977),
- 23: Q_α obtained from Q_β or vice versa using $Q_\beta = (4/3)(\beta/\alpha)^2 Q_\alpha$. Note when $\sigma = .25$, $\alpha = \sqrt{3}\beta$, $Q_\alpha = 2.25 Q_\beta$,
- 24: α values typical for continental crust and lithosphere (e.g. Ryaboy (1966), MacBeth & Panza (1988)),

Additional footnotes for BGS site model

- 25: α velocity of Triassic, layer 8 of AMOCO Well 27/3-1; with depth to 550 m inferred from BGS 1:250000 map of Marr Bank solid geology,
- 26: α velocity of Permian Zechstein, layer 9 of AMOCO Well 27/3-1, with layer placed at 650-1200 m depth range,
- 27: α average interval velocities (R W Gatliff, personal communication) of Lower Permian (Rotliegendes sandstones) and Carboniferous combined; with layer at 1200-2800 m inferred from BGS 1:250000 map of Marr Bank solid geology,
- 28: α average interval velocity of Devonian (R W Gatliff, personal communication), with layer at 2800-5300 m inferred from BGS 1:250000 maps of Tay-Forth and Marr Bank solid geology,

Additional footnotes for Tentsmuir model

- 29: β from Evan's (1981) inversion of Rayleigh wave velocities in the Old Red Sandstone,
- 30: σ from Assumpcao & Bamford (1978) for depths less than 2 km in the Midland Valley,
- 31: $1/Q_{\beta}$ from Evan's (1981) inversion of Rayleigh wave amplitudes in the Old Red Sandstone,
- 32: β from Evan's (1981) Devonian Lavas and Old Red Sandstone inversions,
- 33: β from Evan's (1981) Devonian Lavas inversion,
- 34: $1/Q_{\beta}$ from MacBeth & Burton's (1987) general model of $1/Q_{\beta}$ below 800 m,
- 35: β values of Region G, layers 2 & 3, of MacBeth & Burton (1985, Fig.13) combined through slowness average,
- 36: α , β , ρ adapted from J-B A' model (e.g. see Ben Menahem & Singh (1981)) for all layers below 200 km depth,
- 37: $1/Q_{\beta}$ adapted from typical lithospheric model (e.g. see Ben Menahem & Singh (1981)) for all layers below 200 km.

Appendix E: Data inventory

Table E1: List of sites known to have detected the 4500lb explosion.

Instrument codes: X,Y,Z velocity components where Z is the vertical and X & Y are horizontal, (= NS and EW components for land stations); z = Z low gain; H = hydrophone; A = acceleration; P = pressure gauge; p = air pressure

Q = quality of signal. 1 = recorded and visible; 2 = recorded, good signal to noise; - = MSF/DCF not received; N = level information not given.

* shot point location; † not confirmed. These sites bracket a temporary array of 72 stations which detected the 4500lb explosion. (Q = 2) See Fig. 7.1.

DIAS = Dublin Institute of Advanced Studies

(a) Instruments deployed at sea for the LORASWAP experiment

Code	Lat.	Long.	Inst.	Q	Site.
	57.1164*	-0.7500*	2x6H	2	ARE pressure gauges (Goosander)
PU1	57.06902	-0.89040	XYZH	2	PUSS 10
PU2	57.04803	-0.95497	XYZH	2	PUSS 11
PU3	56.99957	-1.10252	XYZH	2	PUSS 9
PU4	56.92990	-1.30786	XYZH	2	PUSS 13
VHS	56.83538	-1.59375	10H	2	Vertical Hydrophone String (Salmaster) & ARE Vertical hydrophone string
BGS	56.83455	-1.59228	XYZHA	2	BGS sea bottom package (Salmaster)
PU5	56.71350	-1.94166	XYZH	2	PUSS 14

(b) Instruments deployed on land by BGS for the LORASWAP experiment.

Code	Lat.	Long.	Ht.	Inst.	Q	Site.
GMA	56.0348	-3.6943		2 XYZ		1- Grangemouth
GMB	56.0337	-3.6952		2 XYZ		1- Grangemouth
LHS	56.0276	-2.6226		42 XYZz		2- Lochhouses (near Dunbar)
LUA	56.6328	-2.5157		55 XYZz		2- Newbarns, Lunan Bay
LUB	56.6730	-2.4687		3 Z		2- Boddin Point
TMA	56.4076	-2.8120		3 XYZz		2 Tents Muir Forest (sand)
TMB	56.4211	-2.8633		10 Z		2 Tents Muir (Quarry)
WHK	56.0274	-2.6515	180	Z		2 Whitekirk (near Dunbar)

(c) Permanent land stations with a clear record of the 4500lb explosion

Code	Lat.	Long.	Ht. (m)	Inst.	Q	Site.
DCN♦	53.3439	-7.2767	150	Z	N	Croghan (DIAS)
DDK♦	53.3869	-6.3392	85	Z	N	Dunsink Obs. (DIAS)
DLE♦	53.2872	-6.5436	140	XYZ	N	Lyons Estate (DIAS)
DMK♦	53.2553	-6.2644	280	Z	N	Kilmashogue (DIAS)
DMU♦	53.8989	-6.9106	280	Z	N	Kingscourt (DIAS)
EAB	56.1881	-4.3400	250	Z	2	Aberfoyle LOWNET
EAU	55.8444	-3.4547	350	Z	2	Auchinoon LOWNET
EBH	56.2481	-3.5081	375	Z	2	Black Hill LOWNET
EBL	55.7733	-3.0436	365	Z	2	Broad Law LOWNET
ECB♦	52.3661	-6.7811	125	Z	N	Carrickbyrne (DIAS)
ECP♦	52.1800	-6.3689	5	XYZ	N	Carnsore Pt. (DIAS)
EDI	55.9233	-3.1861	125	XYZ	2	Edinburgh LOWNET
EDU	56.5475	-3.0142	275	z	1	Dundee LOWNET (gain set low for LORASWAP)
ELO	56.4706	-3.7119	495	Z	2	Logiealmond LOWNET
ESK	55.3167	-3.2050	263	XYZp	2	Eskdalemuir ESKDALEMUIR
ESY	55.9177	-2.6144	328	Z	2	Stoney Path LOWNET
ETA♦	52.6958	-6.2100	140	Z	N	Tara Hill (DIAS)
HAE	52.0376	-2.5475	224	Z	1	Alders End HEREFORD
HCG	52.3224	-3.6567	511	Z	1	Craig Goch HEREFORD
HGH	51.6380	-2.8064	210	Z	1	Gray Hill HEREFORD
HLM	52.5169	-2.8878	259	Z	1	Long Mynd HEREFORD
HTR	52.0790	-3.2697	329	Z	1	Trewern Hill HEREFORD
KAC	57.4999	-5.2982	330	Z	2	Achnashellach KYLE
KYL	57.3370	-5.6530	105	XYZ	2	Kyle KYLE
LRW	60.1360	-1.1779	100	XYZz	2	Lerwick SHETLAND
MCD	57.5827	-3.2541	280	XYZz	2	Coleburn Distillery MORAY
MCH	51.9977	-2.9983	229	XYZz	1	Michaelchurch HEREFORD
MDO	57.4410	-4.3630	366	Z	2	Dochfour MORAY
MLA	58.3050	-3.3640	190	Z	2	Latheron MORAY
MME	57.3150	-2.9650	455	Z	2	Meikle Cairn MORAY
MVH	57.9232	-4.1816	198	Z	2	Achvaich MORAY
PCA	55.7000	-4.2550	305	Z	2	Carrot PAISLEY
PGB	55.8100	-4.4780	200	XYZ	2	Glenifferbraes PAISLEY
PMS	55.8460	-4.7440	351	Z	2	Muirshiel PAISLEY
SBD	52.9055	-3.2588	497	Z	1	Bryn Du HEREFORD
WAL	60.2576	-1.6133	170	Z	2	Walls SHETLAND
WBR	52.8560	-3.8941	340	Z	2	Bronaber FFESTINIOG
WCB	53.3782	-4.5465	135	XYZ	2	Church Bay NORTH WALES
WFB	52.6830	-4.0378	325	Z	1	Fairbourne FFESTINIOG
WME	53.3966	-4.3034	130	Z	2	Myndd Eilian NORTH WALES
WVR	52.7974	-3.6051	580	Z	1	Vyrnwy FFESTINIOG
XDE	54.5058	-3.4897	291	Z	1	Dent ESKDALEMUIR
XSO	55.4925	-2.2511	495	Z	2	Sourhope ESKDALEMUIR
YEL	60.5509	-1.0830	200	Z	1	Yell SHETLAND
YRC	53.2506	-4.5741	24	Z	1	Rhoscolyn NORTH WALES
YRH	52.8335	-4.6289	300	Z	1	Rhiw FFESTINIOG

Appendix E2 : Inventory of PUSS data from 4500lb and 900lb explosions

(a) 4500 lb charge

All records start at 11^h 52^m 05^s

Site	Inst.ID	Channel	Q	Comments
1	10			<i>Record length = 90s</i> <i>First arrival 31.5s from start of record</i> <i>Water wave arrival 35.2s from start of record</i>
		Hydr.	2	Clear seismic and water wave arrival.
		Z	2	Clear seismic and water wave arrival.
		X	2	Clear seismic and water wave arrival.
		Y	2	Clear seismic and water wave arrival.
2	11			<i>Record length = 90s</i> <i>First arrival 32.2s from start of record</i> <i>Water wave arrival 38.2s from start of record</i>
		Hydr.	2	Clear seismic and water wave arrival.
		Z	2	Clear seismic and water wave arrival.
		X	2	Clear seismic and water wave arrival.
		Y	2	Clear seismic and water wave arrival.
3	9			<i>Record length = 120s</i> <i>First arrival 34.0s from start of record</i> <i>Water wave arrival 45.2s from start of record</i>
		Hydr.	2	Clear water wave arrival, no seismics.
		Z	1	Clear water wave arrival, no detectable seismics. Very weak signal, poor signal to noise ratio.
		X	2	Clear seismic arrival and very strong, asymmetric water wave arrival.
		Y	2	Clear seismic and water wave arrival.

4 13

Record length = 120s
First arrival 36.5s from start of record
Water wave arrival 55.05s from start of record

Hydr. 2 Clear seismic and water wave arrival.
Z 2 Clear seismic and water wave arrival.
X 2 Clear water wave arrival, no seismic.
Y 2 Clear seismic and water wave arrival.

5 14

Record length = 150s
First arrival 44.1s from start of record
Water wave arrival 85.6s from start of record

Hydr. 2 Clear seismic and water wave arrival.
Z 2 Clear water wave arrival, weak seismics. Weak signal with spiky noise. Data terminates at 140.5s from start of record. Noise is still in evidence after this time.
X 2 Faulty instrument, periodic noise obscures trace. Fairly clear water wave arrival. No trace of seismics.
Y 2 Clear seismic and water wave arrival.

(b) 900lb shot

All records start at 15^h 22^m 05^s

Site	Inst.ID	Channel	Q	Comments
1	10			<i>Record length = 90s</i> <i>First arrival 28.6s from start of record</i> <i>Water wave arrival 32.5s from start of record</i>
		Hydr.	2	Clear seismic and water wave arrival
		Z	2	Clear seismic and water wave arrival
		X	2	Clear seismic and water wave arrival
		Y	2	Clear seismic and water wave arrival
<hr/>				
2	11			<i>Record length = 90s</i> <i>First arrival 29.5s from start of record</i> <i>Water wave arrival 35.6s from start of record</i>
		Hydr.	2	Clear seismic and water wave arrival
		Z	2	Clear seismic and water wave arrival
		X	2	Clear seismic and water wave arrival
		Y	2	Clear seismic and water wave arrival
<hr/>				
3	9			<i>Record length = 120s</i> <i>First arrival 31.5s from start of record</i> <i>Water wave arrival 42.6s from start of record</i>
		Hydr.	2	Clear water wave arrival, no seismic
		Z	1	Very weak signal, seismic arrival not visible Clear water wave arrival.
		X	1	Periodic interference, seismic first arrival obscured. Clear water wave arrival.
		Y	2	Clear seismic and water wave arrival
<hr/>				
4	13			<i>Record length = 120s</i>

First arrival 33.8s from start of record
Water wave arrival 52.4s from start of record

Hydr. 2 Clear seismic and water wave arrival
Z (2) Some periodic interference to signal. Clear seismic and water wave arrival.
X 2 Clear water wave arrival, no seismics
Y 2 Clear seismic and water wave arrival

5 14

Record length = 120s
First arrival 41.7s from start of record
Water wave arrival 82.9s from start of record

Hydr. 1 Clear water wave arrival, poor signal to noise ratio.
Z 1 Clear water wave arrival, very weak signal, spiky noise.
X 1 Faulty instrument, periodic noise obscures trace. Fairly clear water wave arrival. No trace of seismics.
Y 2 Clear seismic and water wave arrival

Appendix F: Display of the data

F1: Whole of the available record.

F.1.1 PUSS 10 at 9.982 km, 4500lb shot
F.1.2 PUSS 11 at 14.543 km, 4500lb shot
F.1.3 PUSS 09 at 25.002 km, 4500lb shot
F.1.4 PUSS 13 at 39.705 km, 4500lb shot
F.1.5 BGS SBP (accn) at 60.035 km, 4500lb shot
F.1.6 BGS SBP (vel) at 60.035 km, 4500lb shot
F.1.7 PUSS 14 at 85.291 km, 4500lb shot
F.1.8 Tentsmuir at 148km (filtered) 4500lb shot

F.1.9 PUSS 10 at 9.982 km, 900lb shot
F.1.10 PUSS 11 at 14.543 km, 900lb shot
F.1.11 PUSS 09 at 25.002 km, 900lb shot
F.1.12 PUSS 13 at 39.705 km, 900lb shot
F.1.13 BGS SBP (accn) at 60.035 km, 900lb shot
F.1.14 BGS SBP (vel) at 60.035 km, 900lb shot
F.1.15 PUSS 14 at 85.291 km, 900lb shot

F2: Acoustic arrivals (2 second window)

F.2.1 PUSS 10 at 9.982 km, 4500lb shot
F.2.2 PUSS 11 at 14.543 km, 4500lb shot
F.2.3 PUSS 09 at 25.002 km, 4500lb shot
F.2.4 PUSS 13 at 39.705 km, 4500lb shot
F.2.5 BGS SBP (accn) at 60.035 km, 4500lb shot
F.2.6 BGS SBP (vel) at 60.035 km, 4500lb shot
F.2.7 BGS VHS (1-5) at 60.062 km, 4500lb shot
F.2.8 BGS VHS (6-10) at 60.062 km, 4500lb shot
F.2.9 PUSS 14 at 85.291 km, 4500lb shot

F.2.10 PUSS 10 at 9.982 km, 900lb shot
F.2.11 PUSS 11 at 14.543 km, 900lb shot
F.2.12 PUSS 09 at 25.002 km, 900lb shot
F.2.13 PUSS 13 at 39.705 km, 900lb shot
F.2.14 BGS SBP (accn) at 60.035 km, 900lb shot
F.2.15 BGS SBP (vel) at 60.035 km, 900lb shot
F.2.16 BGS VHS (1-5) at 60.062 km, 900lb shot
F.2.17 BGS VHS (6-10) at 60.062 km, 900lb shot
F.2.18 PUSS 14 at 85.291 km, 900lb shot

F3: Seismic arrivals (2 second window)

F.3.1 PUSS 10 at 9.982 km, 4500lb shot
F.3.2 PUSS 11 at 14.543 km, 4500lb shot
F.3.3 PUSS 09 at 25.002 km, 4500lb shot
F.3.4 PUSS 13 at 39.705 km, 4500lb shot
F.3.5 BGS SBP (accn) at 60.035 km, 4500lb shot
F.3.6 BGS SBP (vel) at 60.035 km, 4500lb shot
F.3.7 PUSS 14 at 85.291 km, 4500lb shot
F.3.8 Tentsmuir at 148km (filtered) 4500lb shot

F.3.9 PUSS 10 at 9.982 km, 900lb shot
F.3.10 PUSS 11 at 14.543 km, 900lb shot
F.3.11 PUSS 09 at 25.002 km, 900lb shot
F.3.12 PUSS 13 at 39.705 km, 900lb shot
F.3.13 BGS SBP (accn) at 60.035 km, 900lb shot
F.3.14 BGS SBP (vel) at 60.035 km, 900lb shot
F.3.15 PUSS 14 at 85.291 km, 900lb shot (5 sec window)

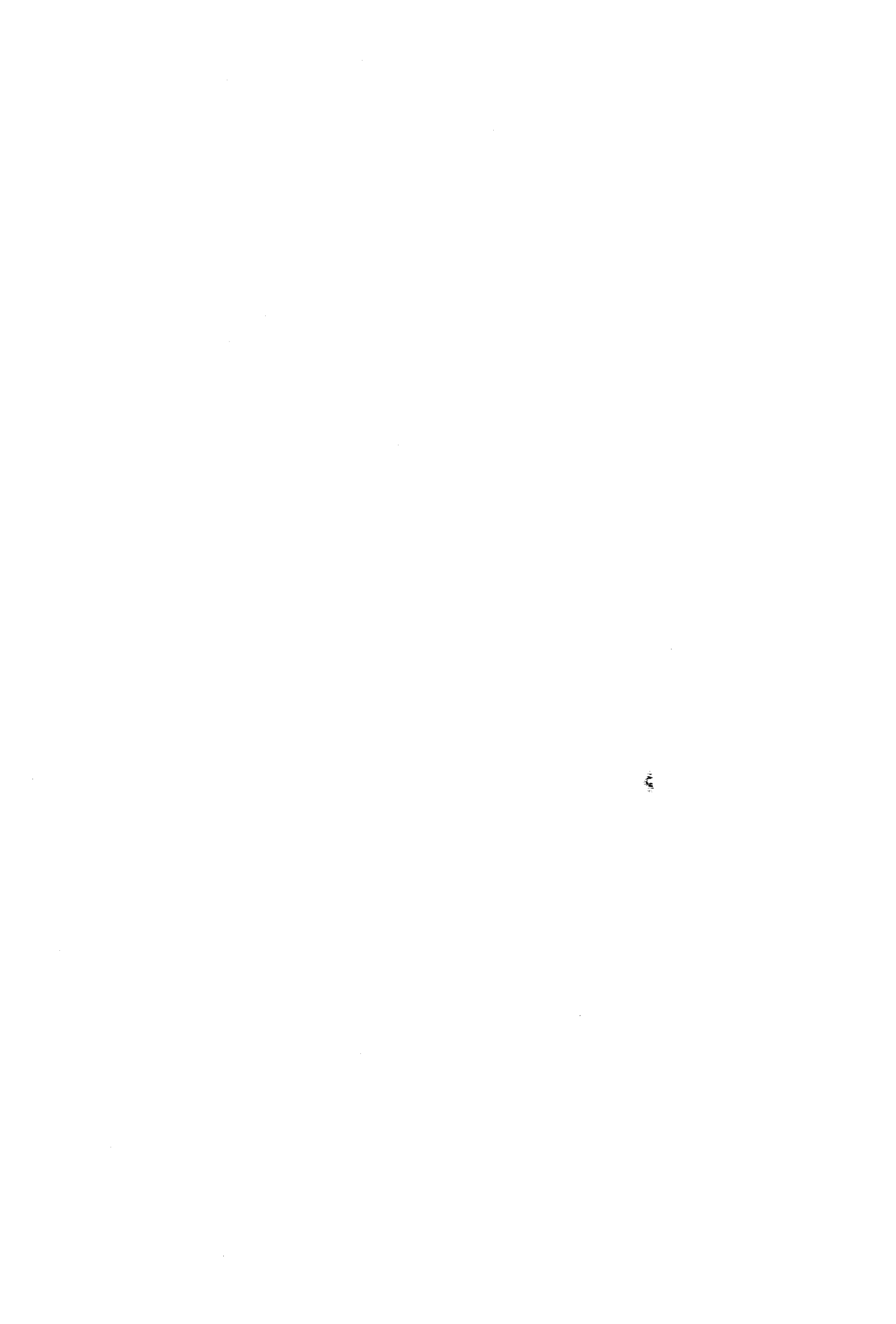


Fig. F.1.1

PUSS 10, RANGE=9.982 KM, 4500LB SHOT

135

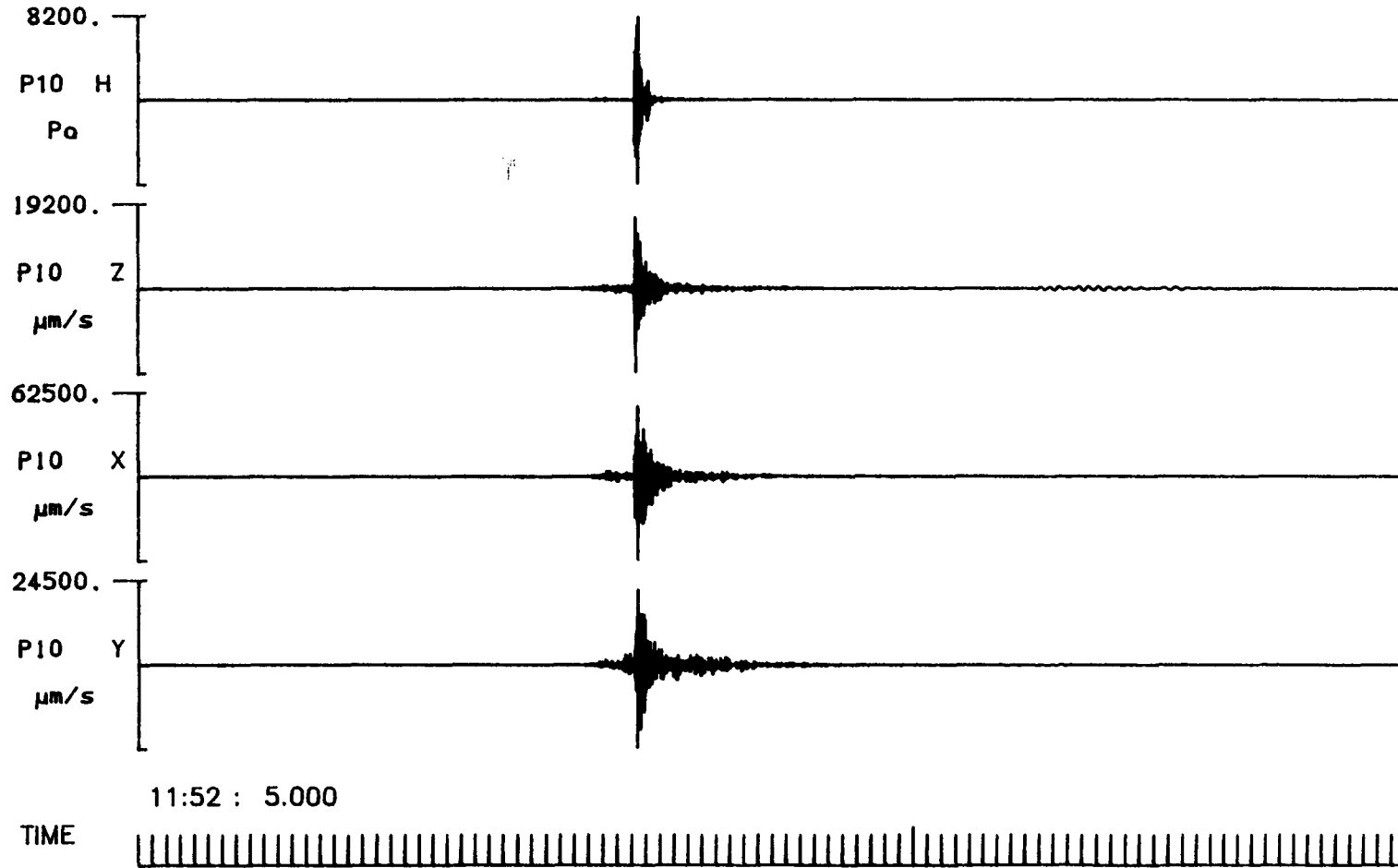


Fig. F.1.2

PUSS 11, RANGE=14.543 KM, 4500LB SHOT

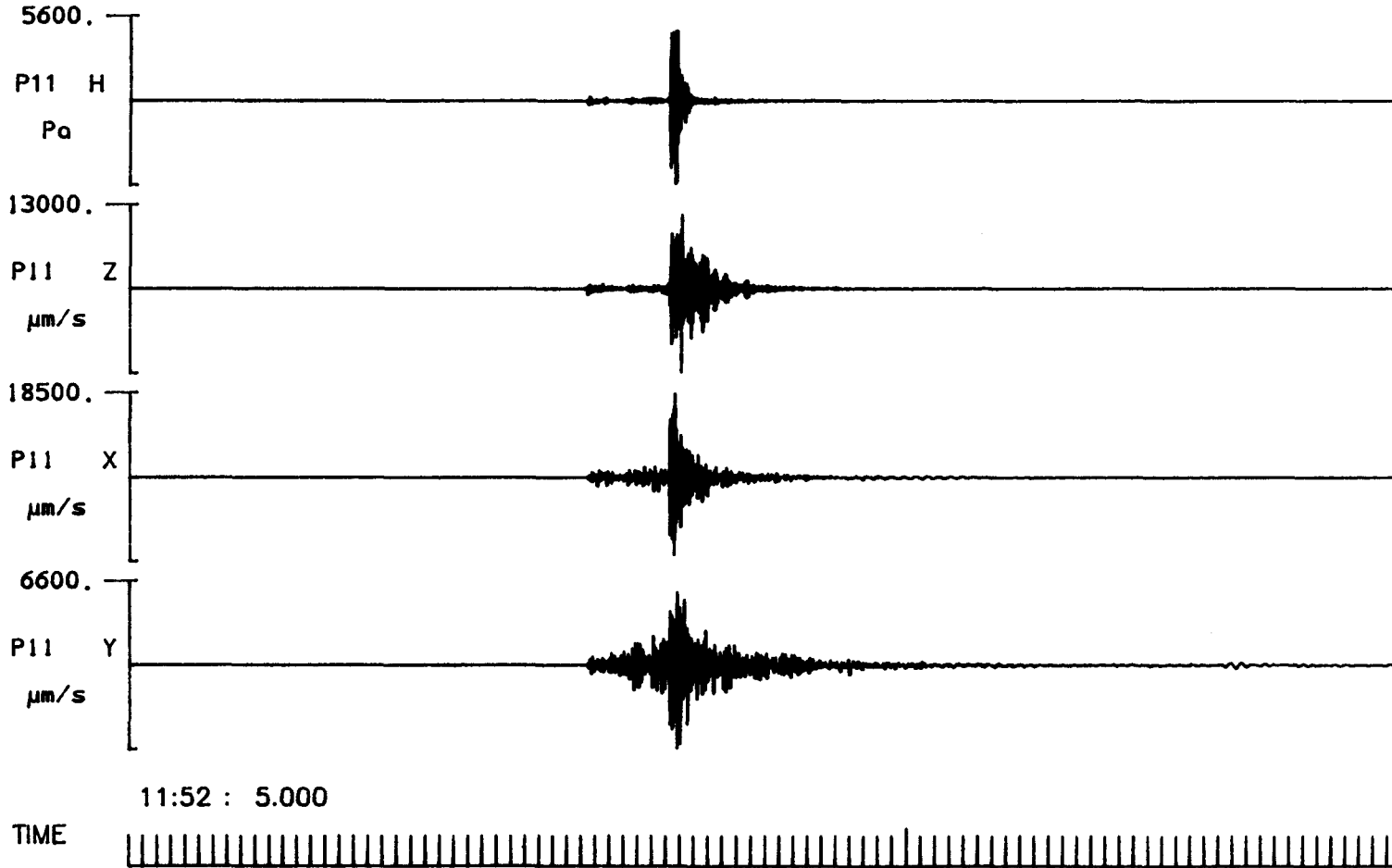


Fig. F.1.1.3

PUSS 09, RANGE=25.002 KM, 4500LB SHOT

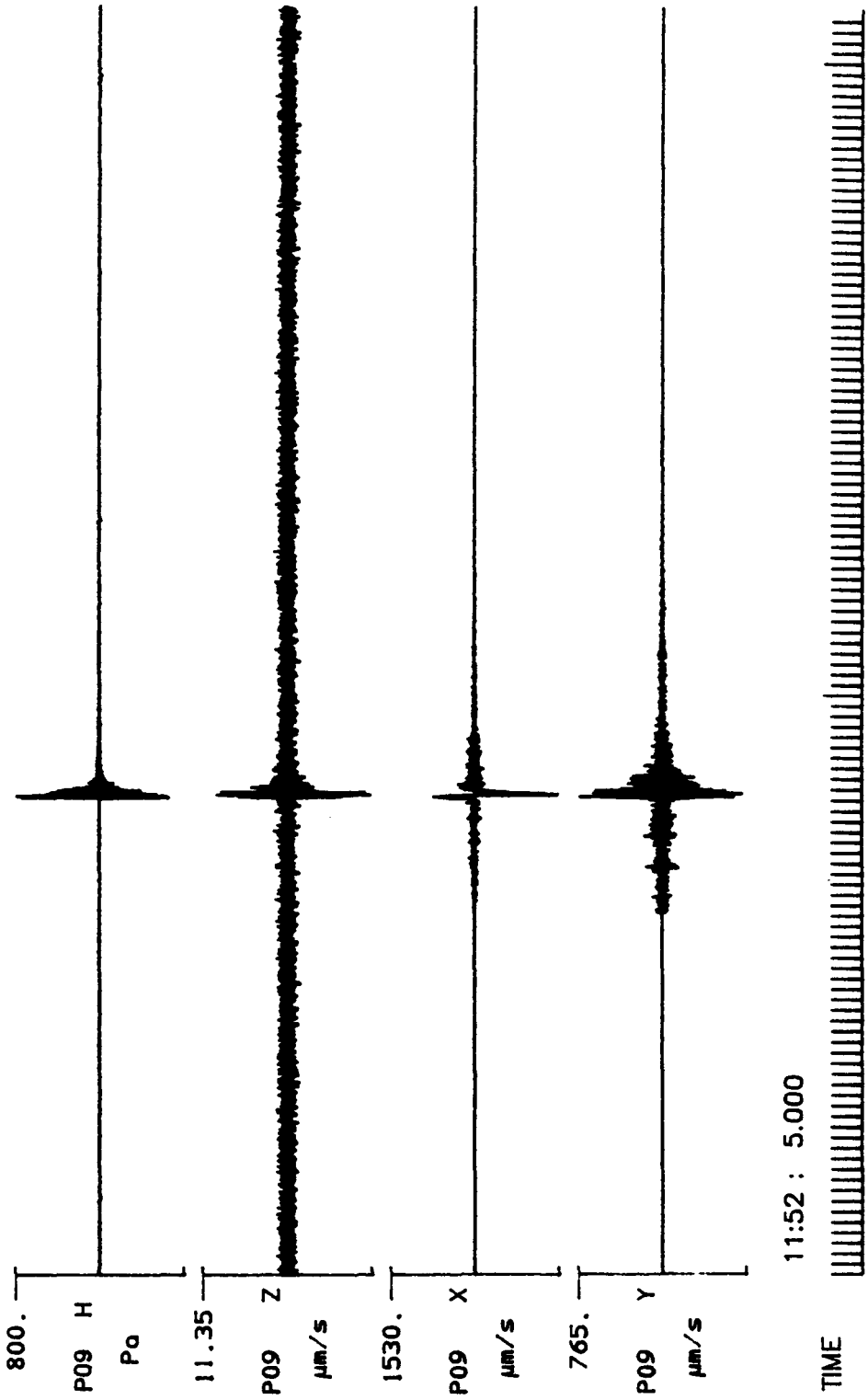


Fig. F.1.4

PUSS 13, RANGE=39.705 KM, 4500LB SHOT

138

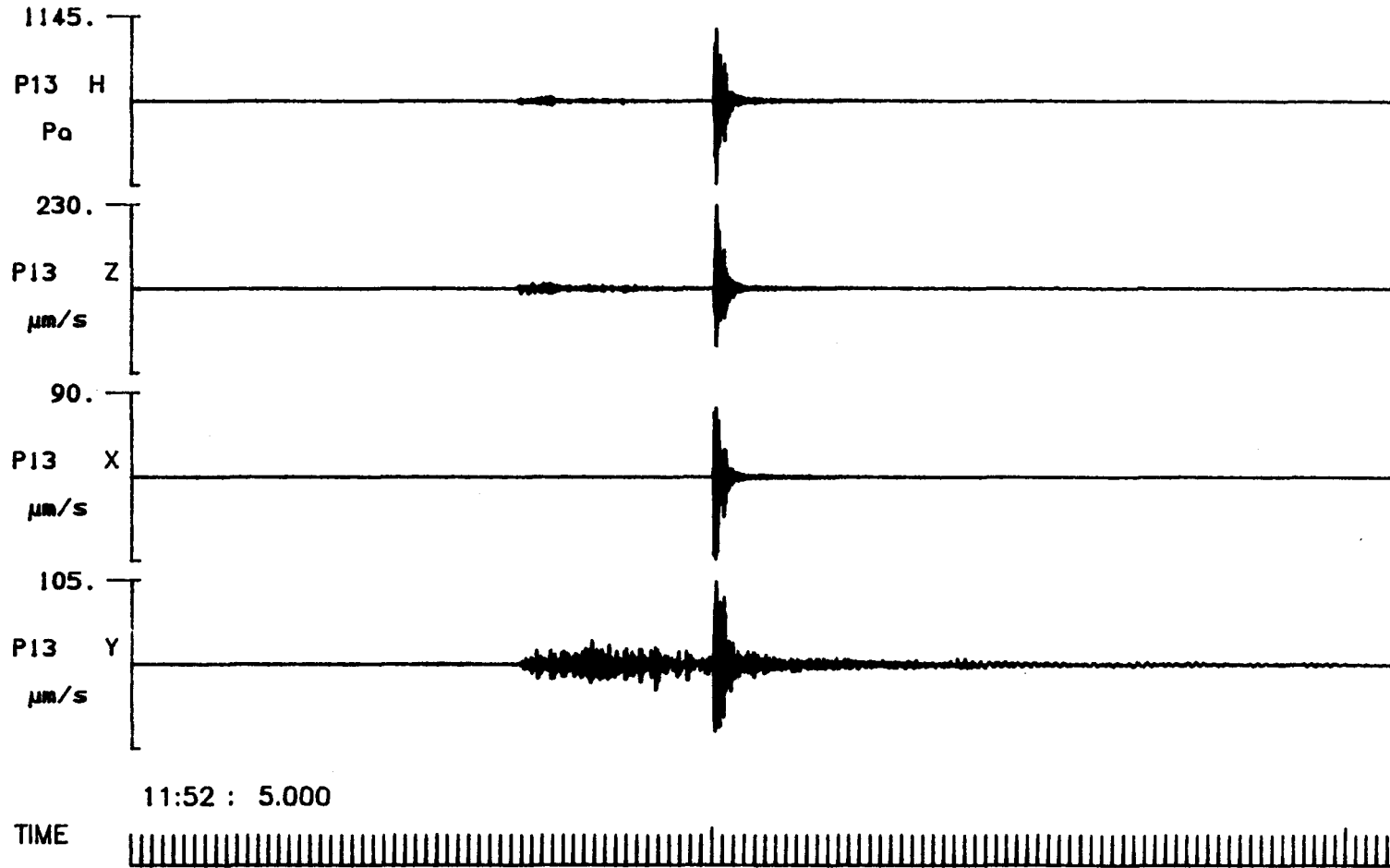


Fig. F.1.5

BGS Sea Bottom Package RANGE=60.035 KM, 4500LB SHOT

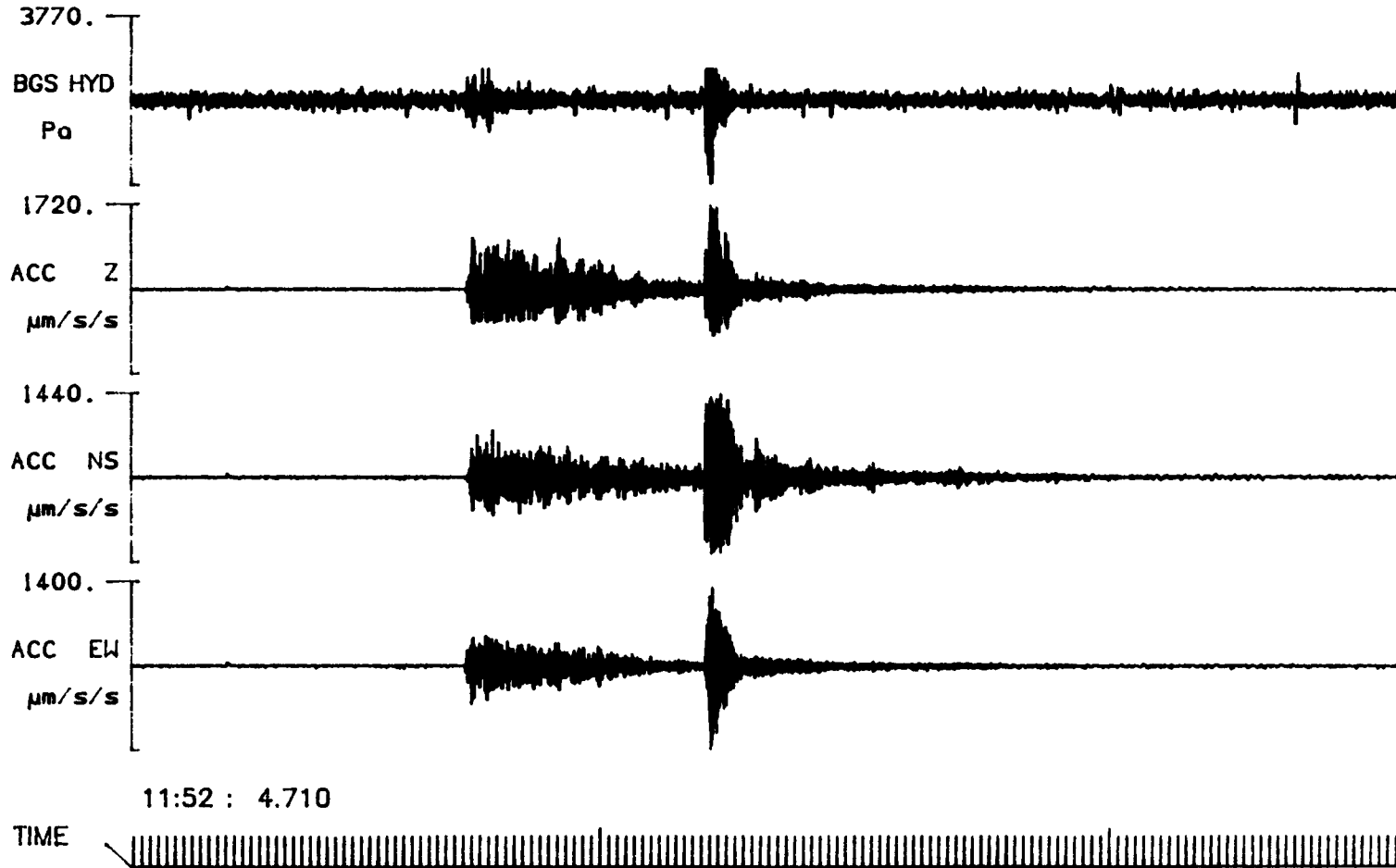


Fig. F.1.6

BGS Sea Bottom Package RANGE=60.035 KM, 4500LB SHOT

140

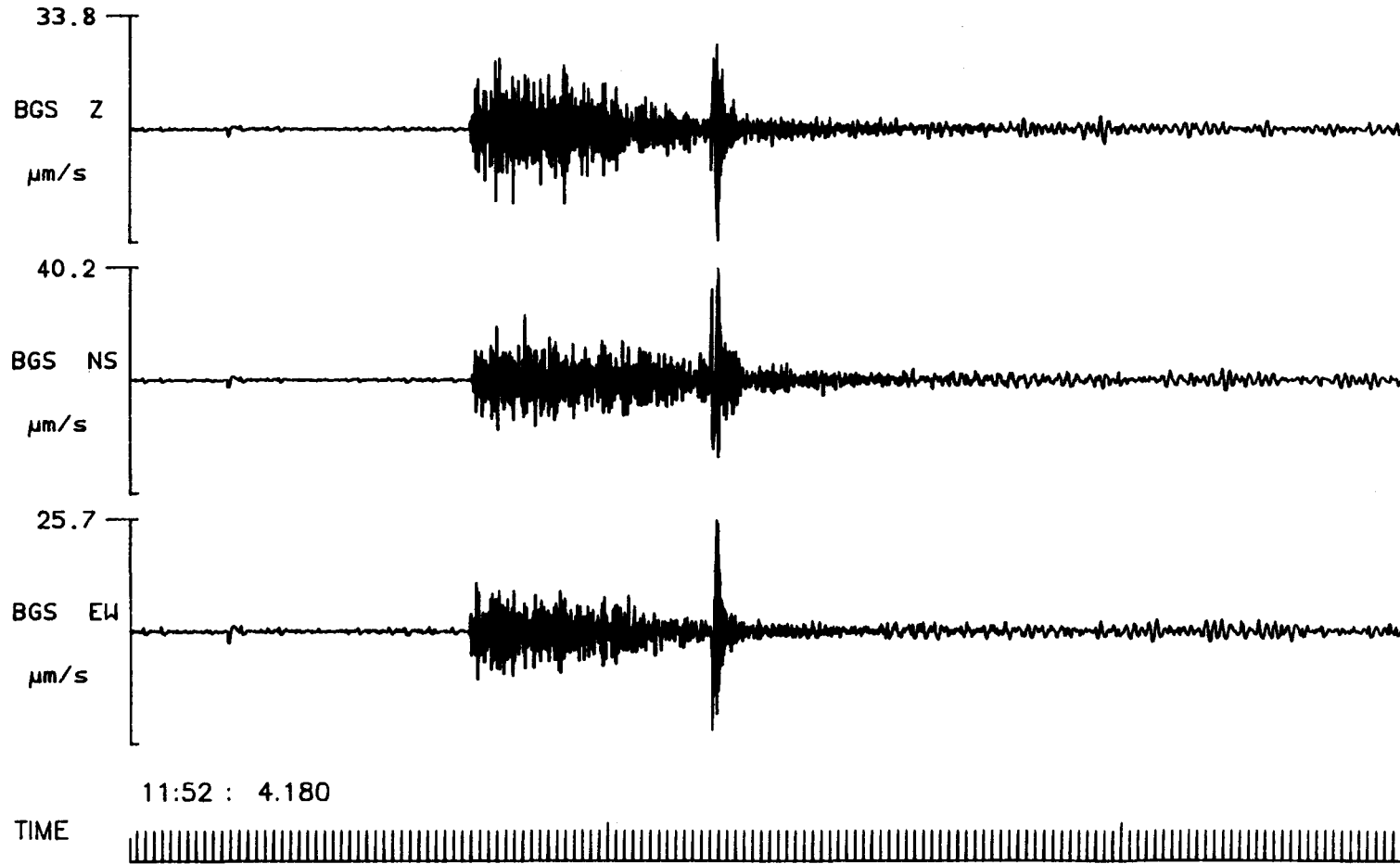


Fig. F.1.7

PUSS 14, RANGE=85.291 KM, 4500LB SHOT

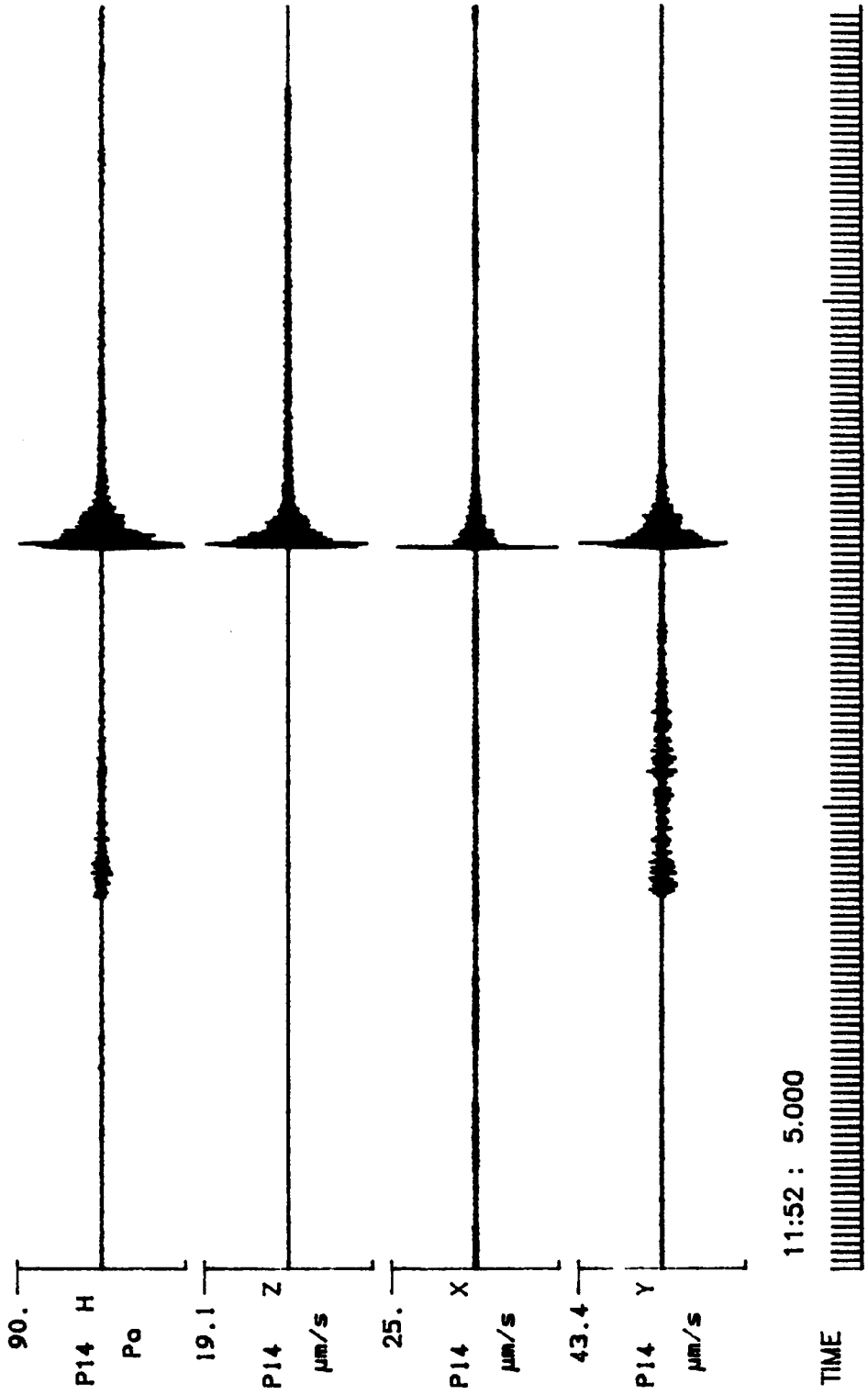


Fig. F.1.8

Tentsmuir, 4500LB SHOT Filtered at 8Hz

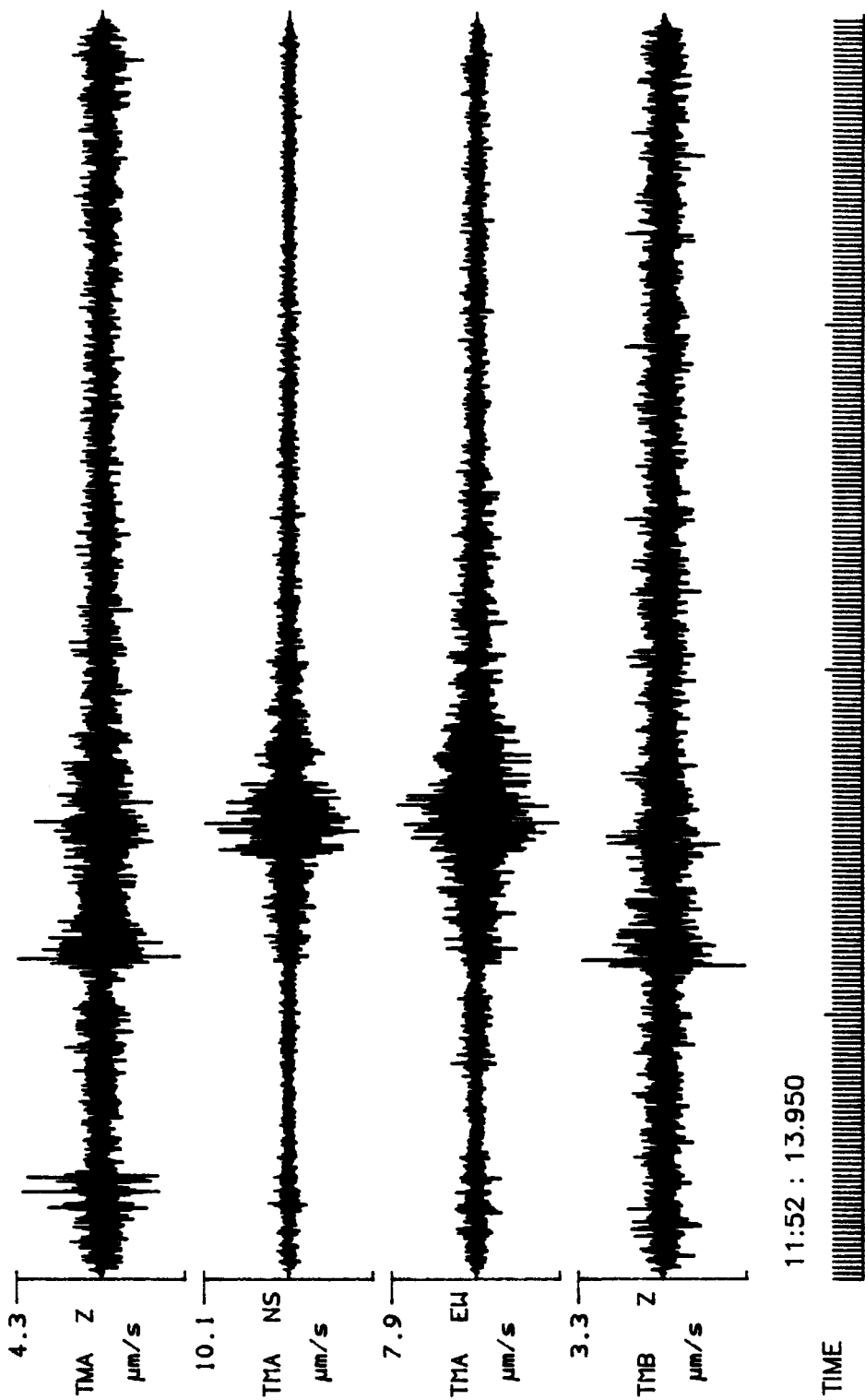


Fig. F.1.9

PUSS 10, RANGE=9.982 KM, 900LB SHOT

143

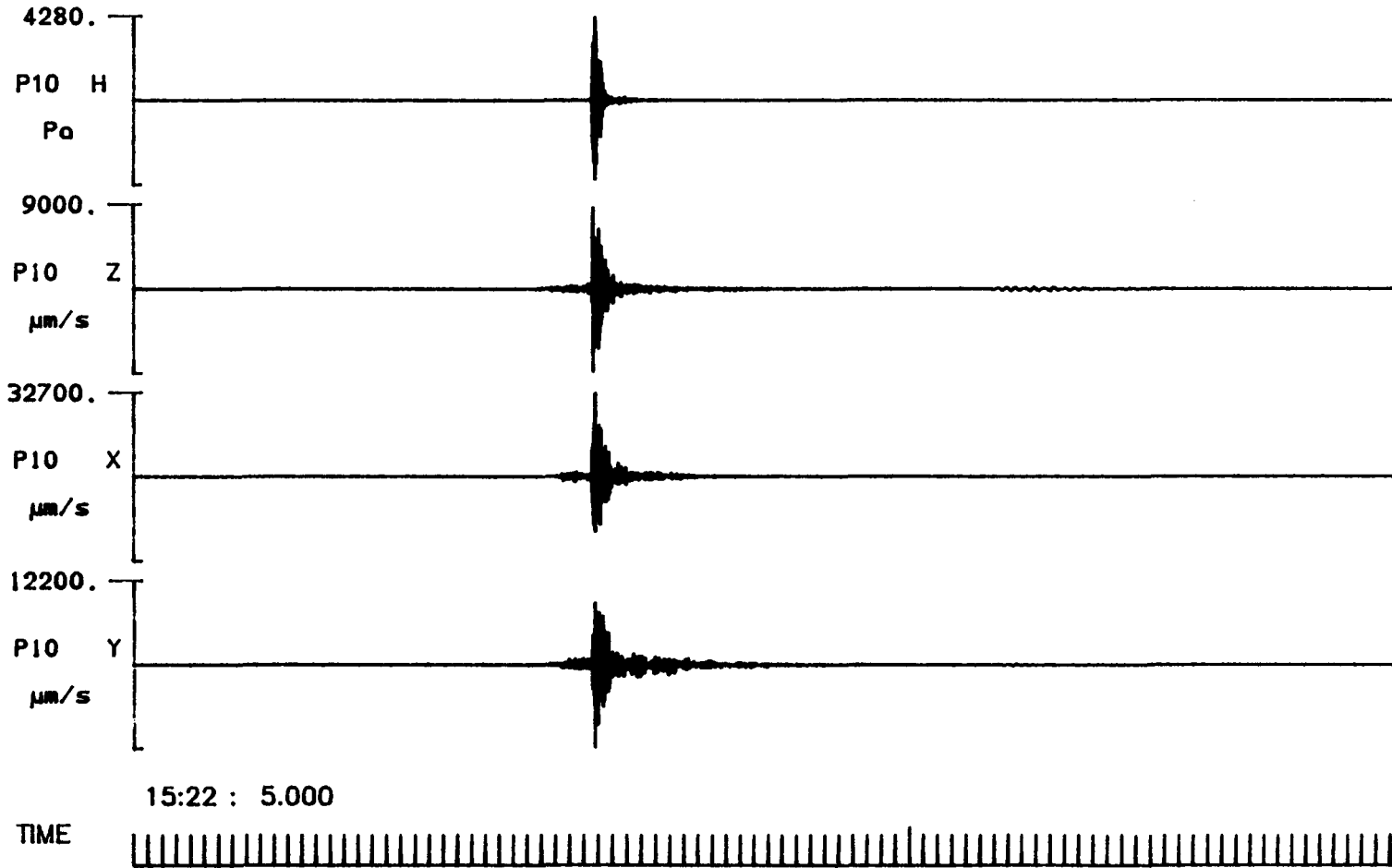
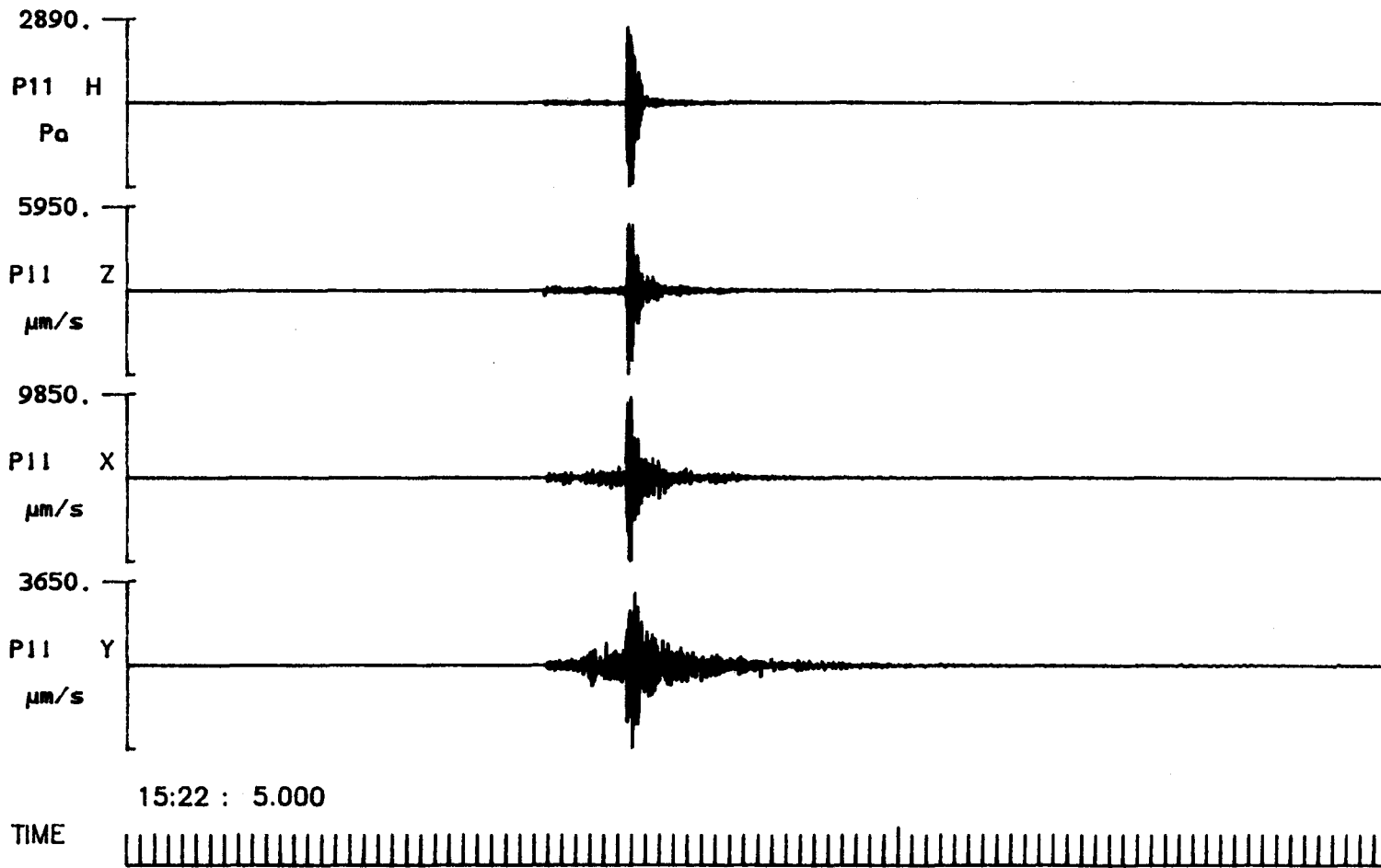


Fig. F.1.10

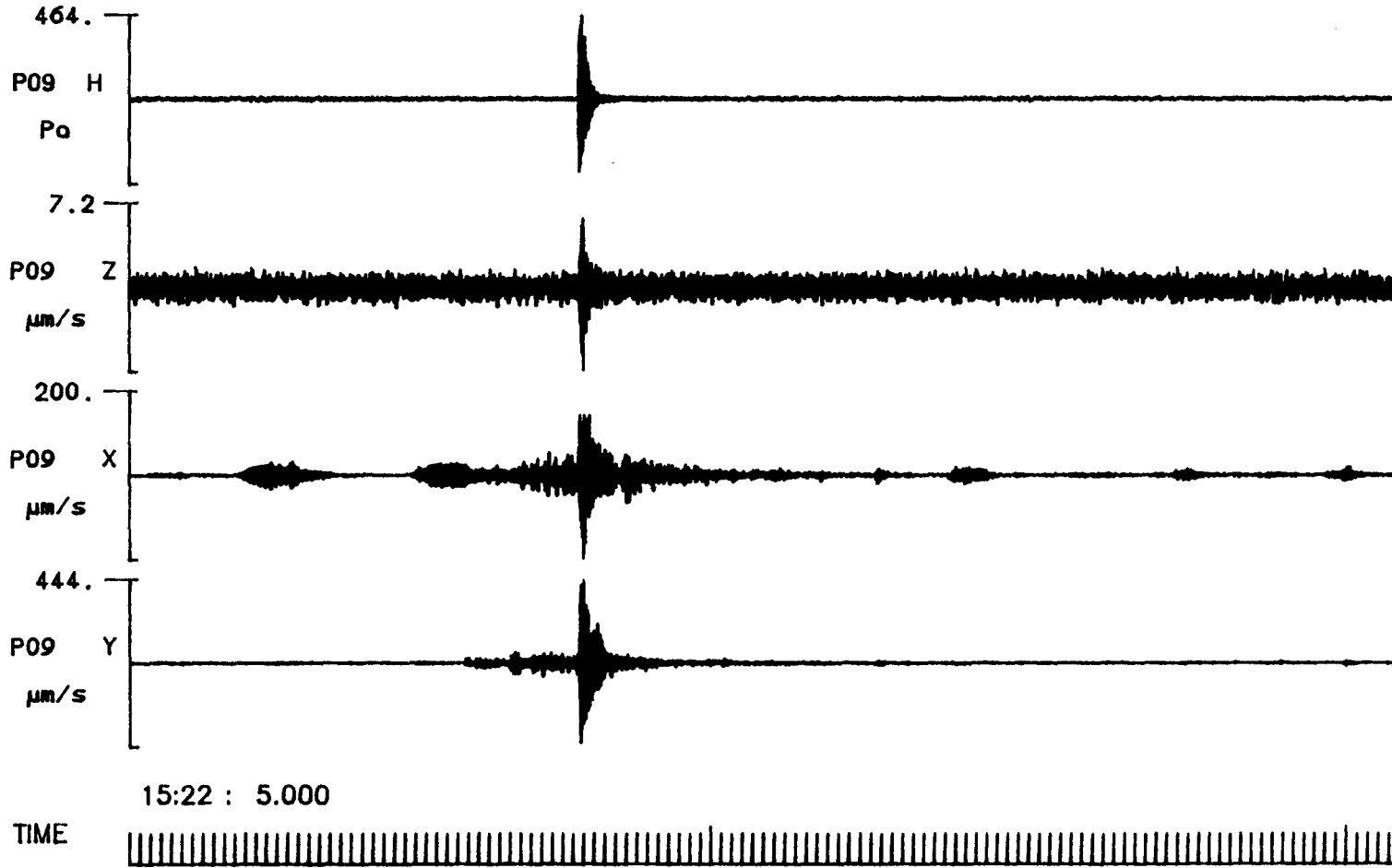
PUSS 11, RANGE=14.543 KM, 900LB SHOT



144

Fig. F.1.11

PUSS 09, RANGE=25.002 KM, 900LB SHOT



145

Fig. F.1.12

PUSS 13, RANGE=39.705 KM, 900LB SHOT

146

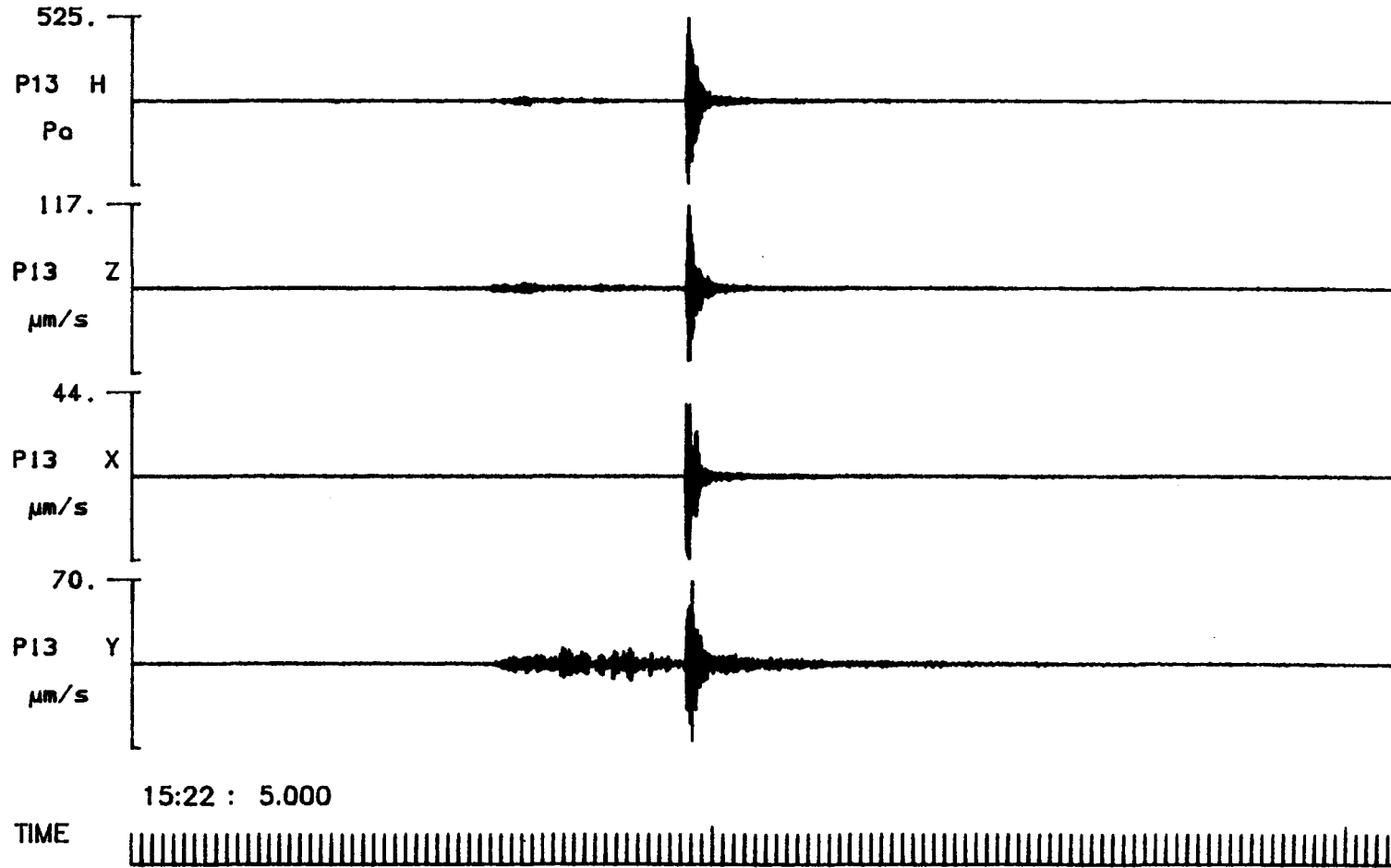
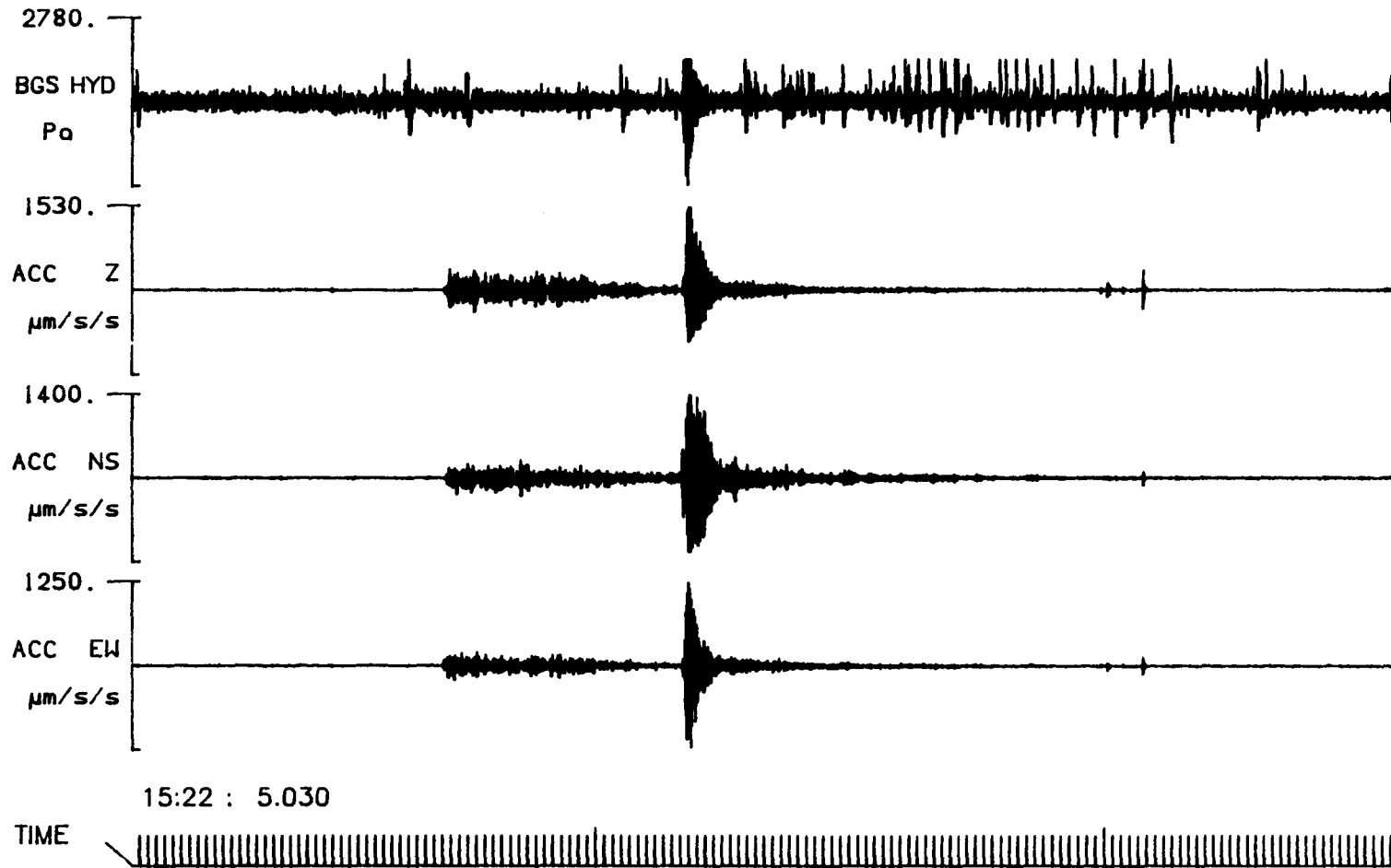


Fig. F.1.13

BGS Sea Bottom Package RANGE=60.035 KM, 900LB SHOT



147

Fig. F.1.14

BGS Sea Bottom Package RANGE=60.035 KM, 900LB SHOT

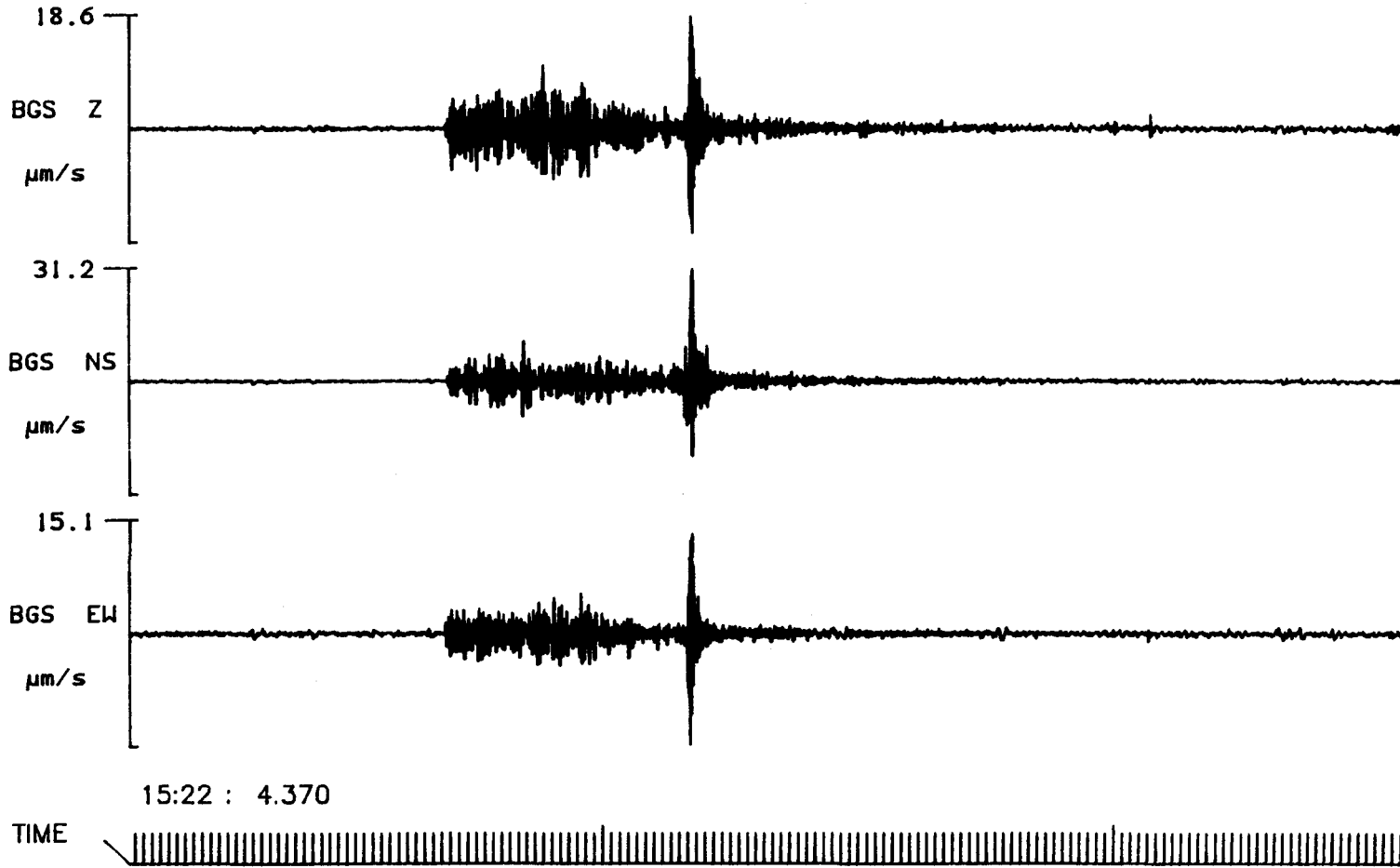


Fig. F.1.15

PUSS 14, RANGE=85.291 KM, 900LB SHOT

149

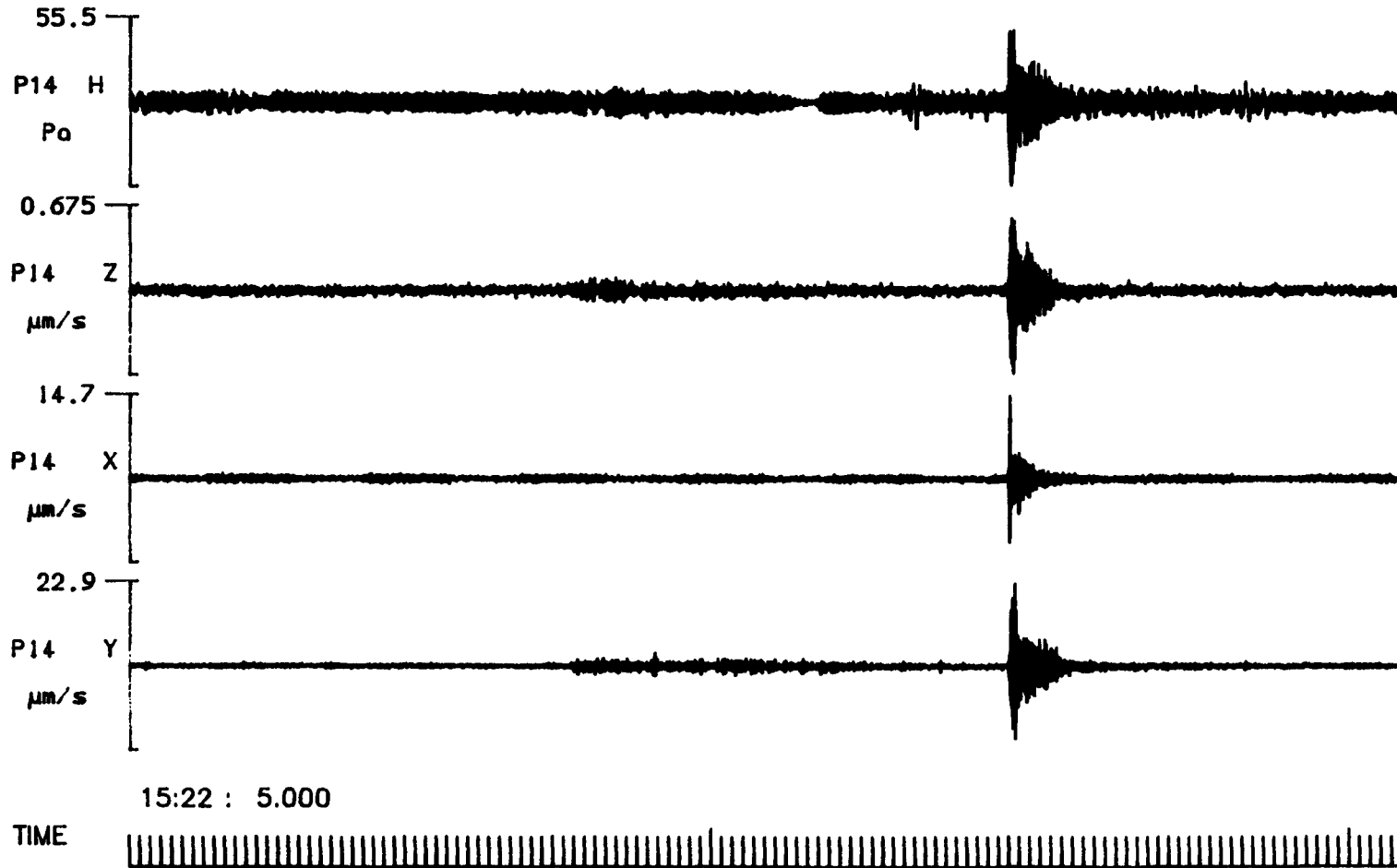


Fig. F.2.1

PUSS 10, RANGE=9.982 KM, 4500LB SHOT ACOUSTIC ARRIVAL

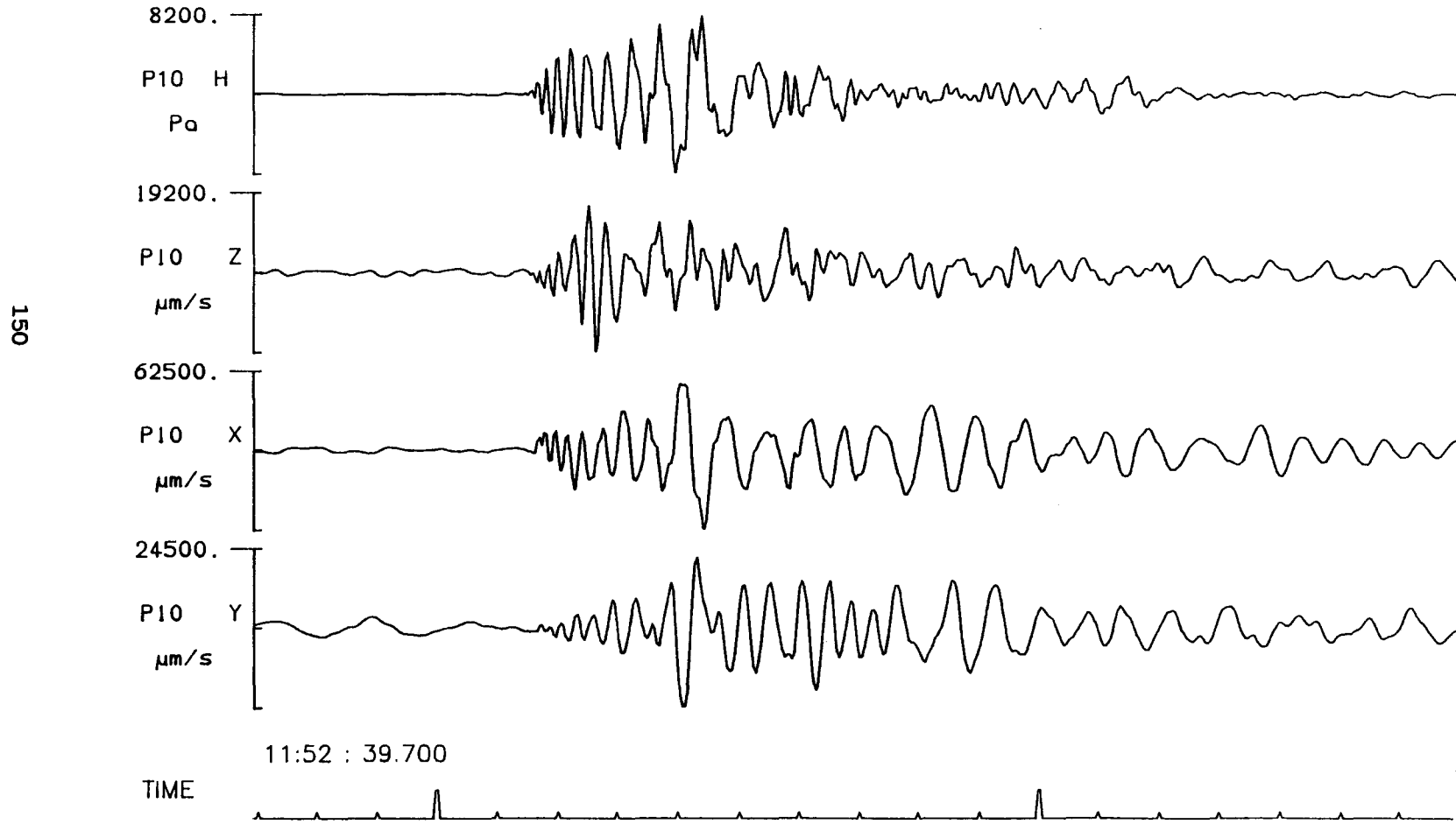


Fig. F.2.2

PUSS 11, RANGE=14.543 KM, 4500LB SHOT ACOUSTIC ARRIVAL

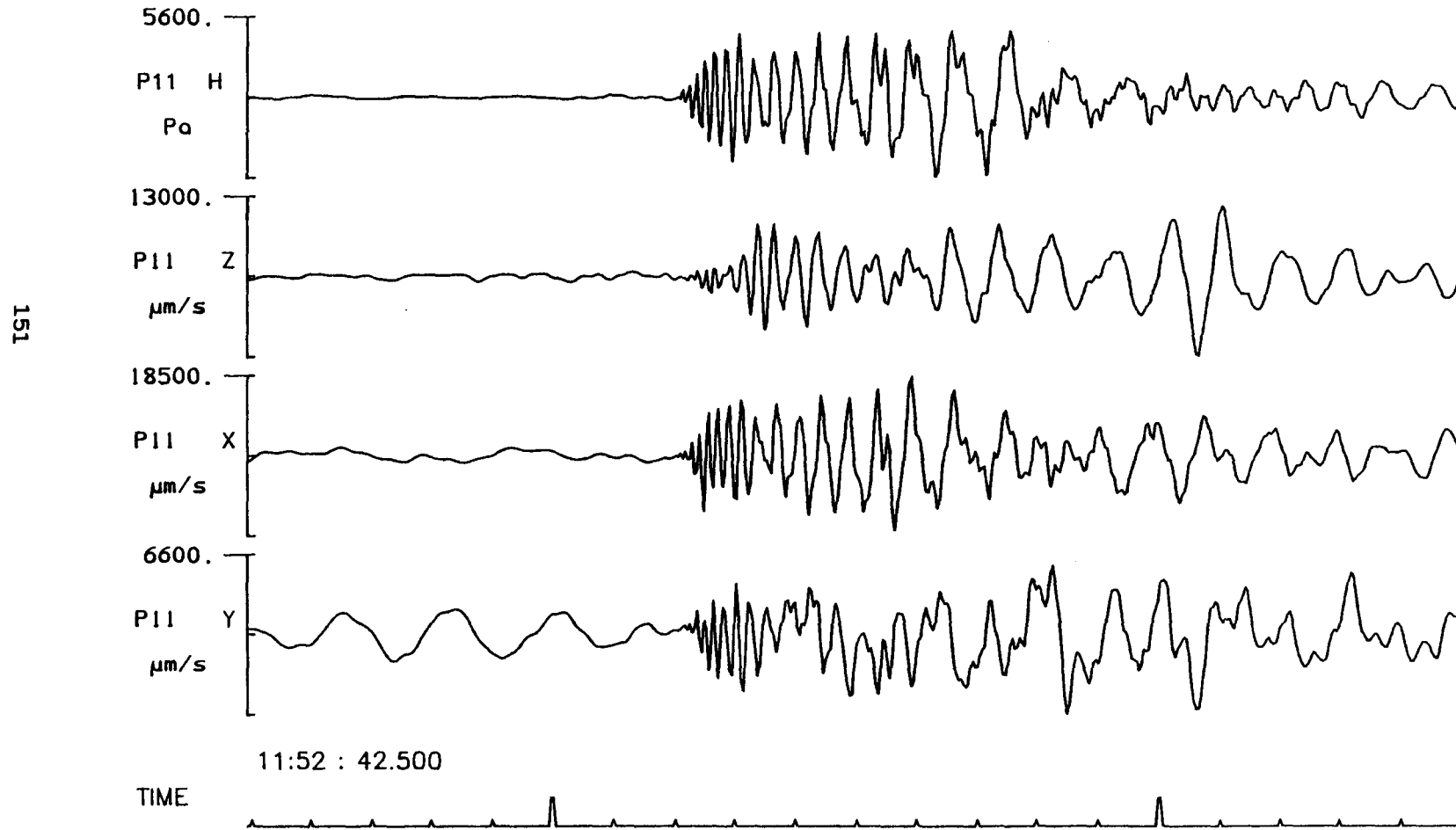


Fig. F.2.3

PUSS 09, RANGE=25.002 KM, 4500LB SHOT ACOUSTIC ARRIVAL

152

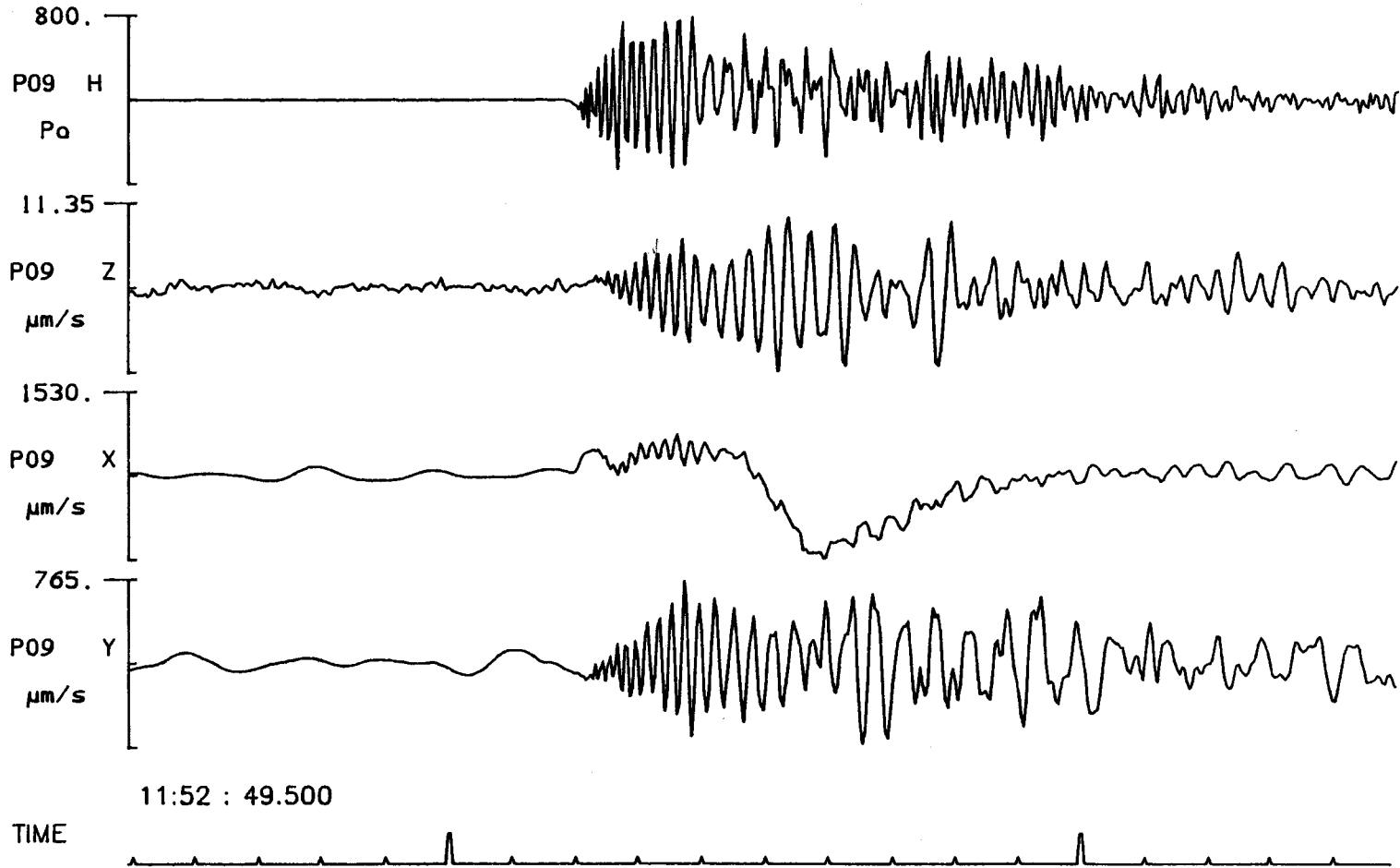


Fig. F.2.4

PUSS 13, RANGE=39.705 KM, 4500LB SHOT ACOUSTIC ARRIVAL

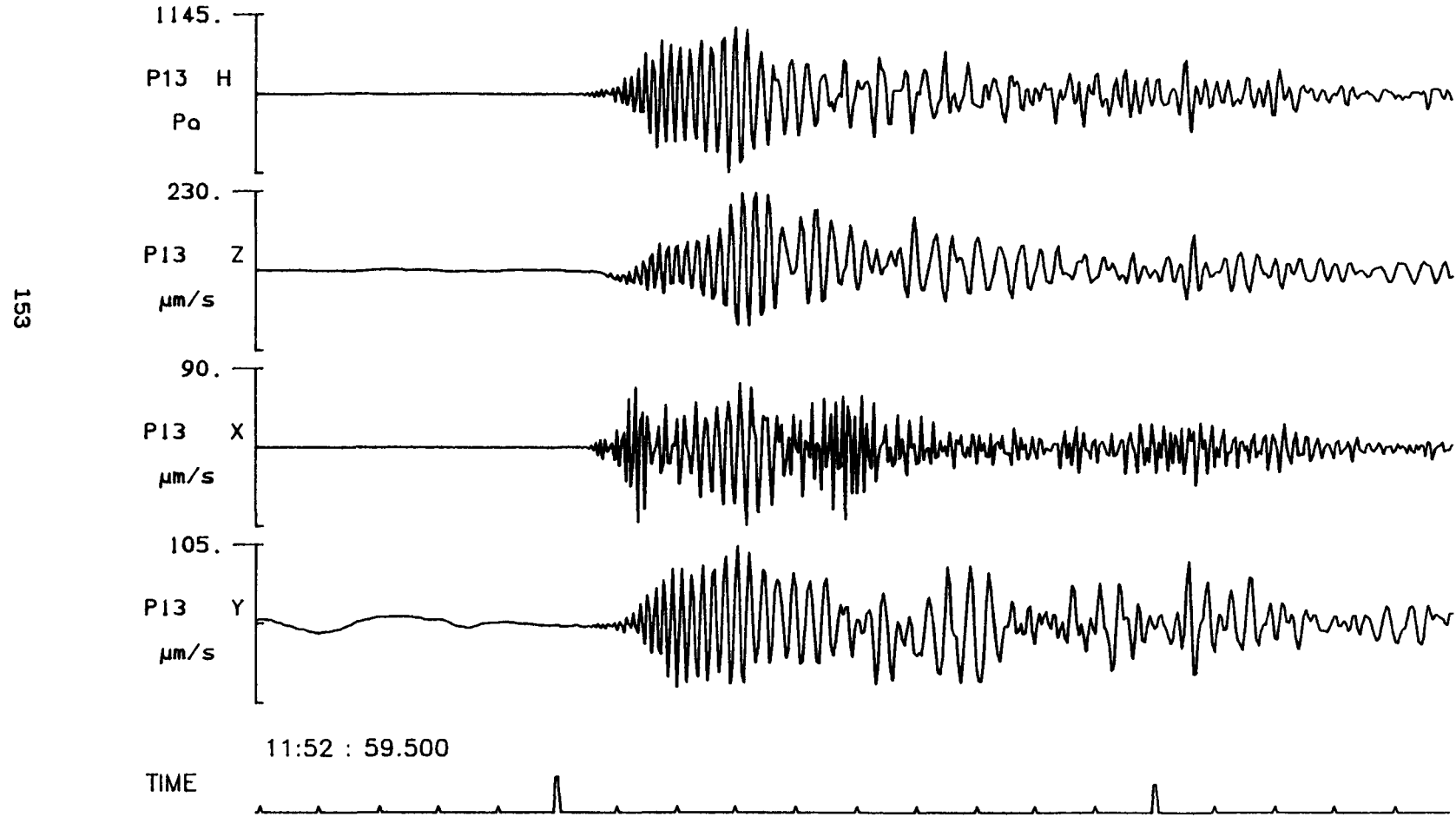


Fig. F.2.5

BGS Sea Bottom Package RANGE=60.035 KM, 4500LB SHOT ACOUSTIC ARRIVAL

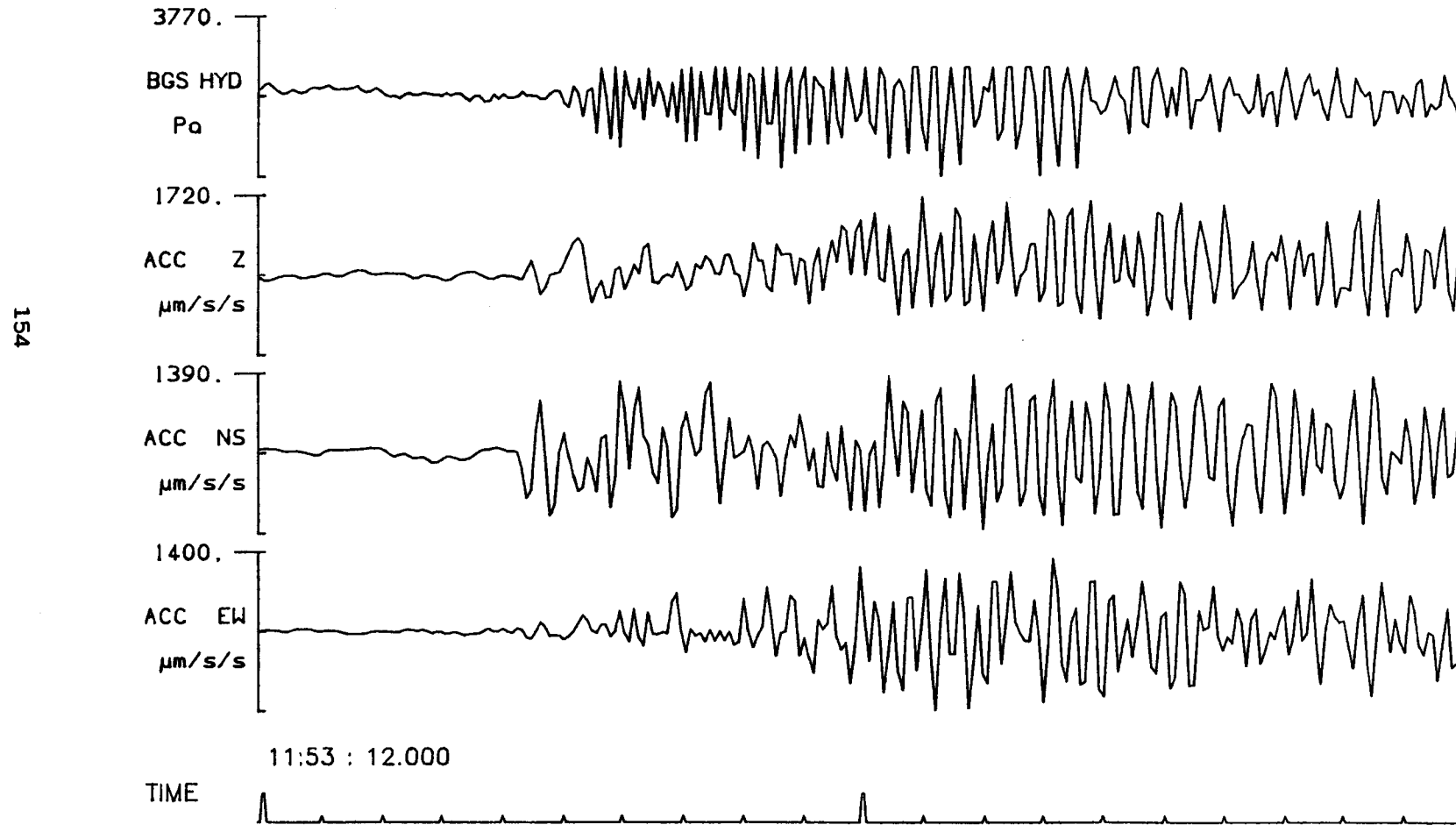


Fig. F.2.6

BGS Sea Bottom Package RANGE=60.035 KM, 4500LB SHOT ACOUSTIC ARRIVAL

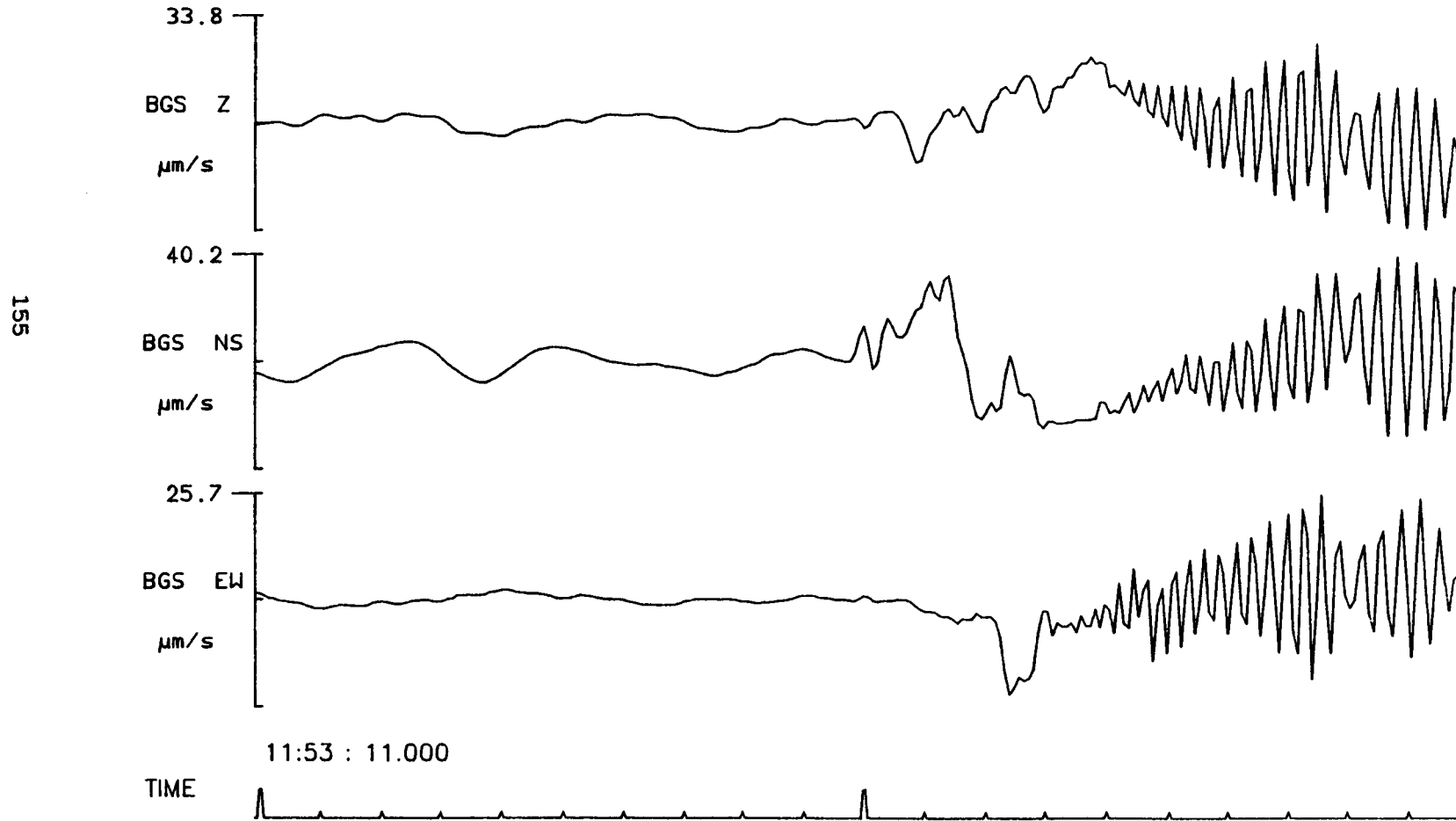


Fig. F.2.7

BGS Sea Vertical Hydrophone String RANGE=60.062 KM, 4500LB SHOT 1 - 5

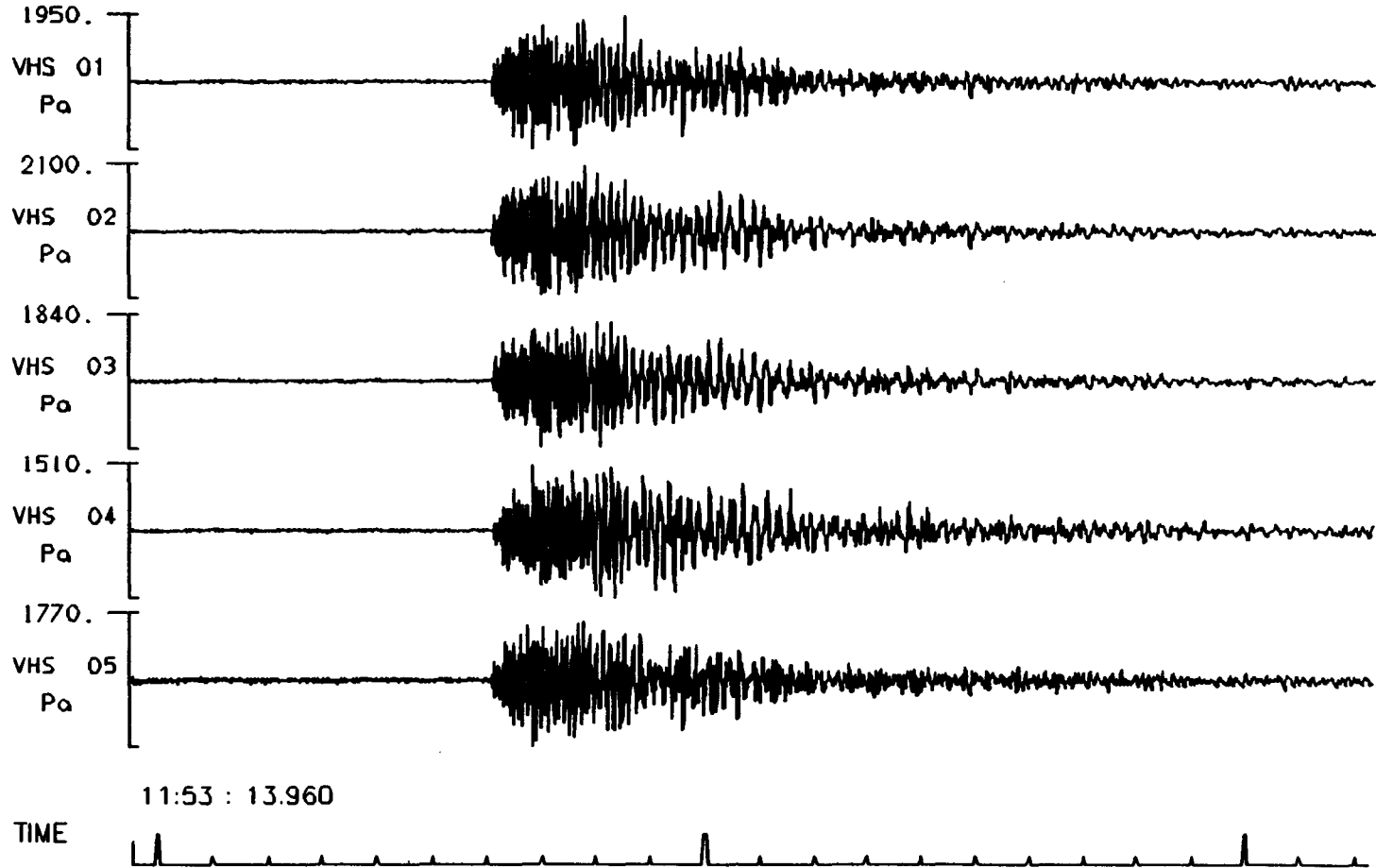


Fig. F.2.8

BGS Sea Vertical Hydrophone String RANGE=60.062 KM, 4500LB SHOT 6 - 10

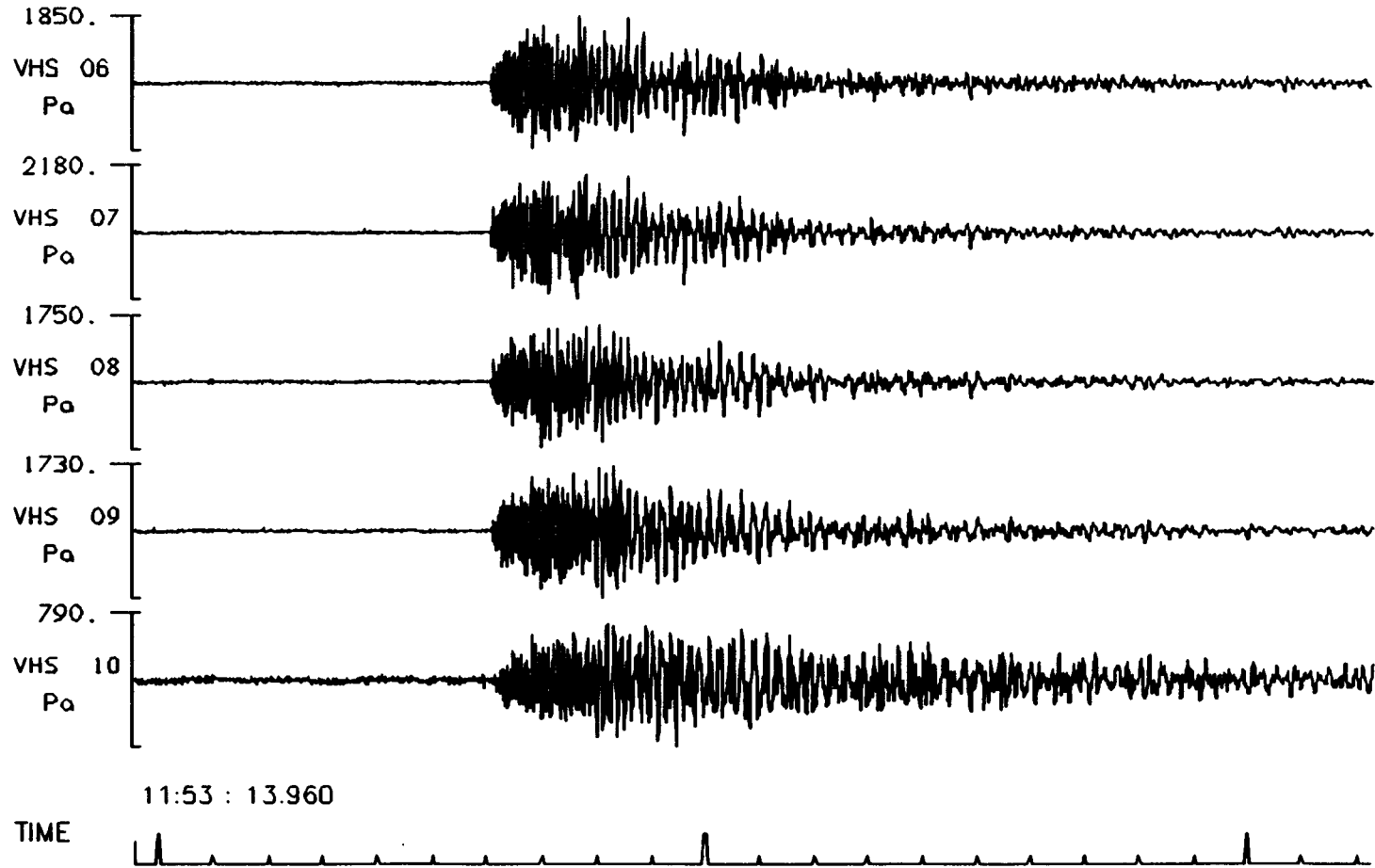


Fig. F.2.9

PUSS 14, RANGE=85.291 KM, 4500LB SHOT ACOUSTIC ARRIVAL

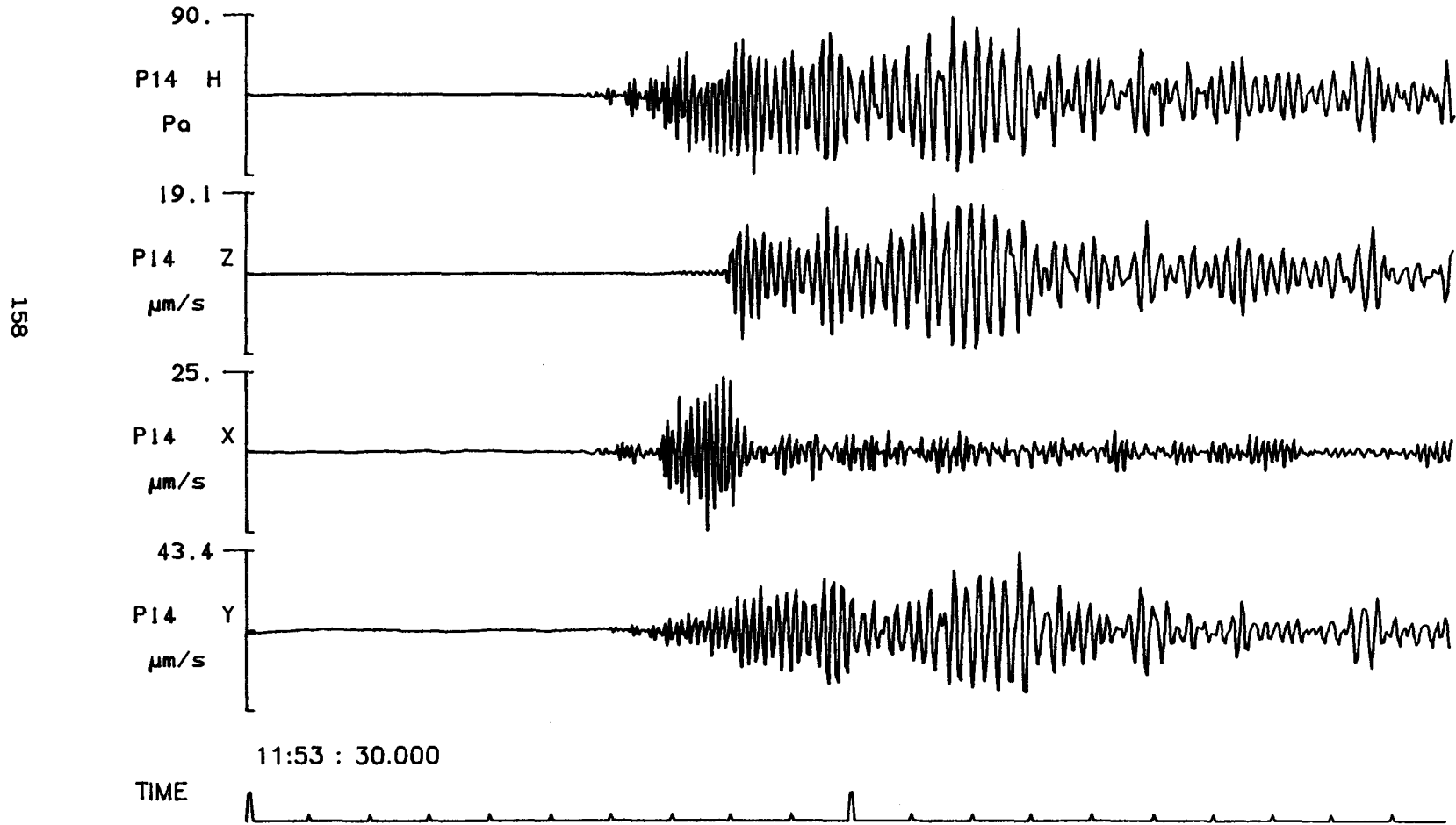


Fig. F.2.10

PUSS 10, RANGE=9.982 KM, 900LB SHOT ACOUSTIC ARRIVAL

159

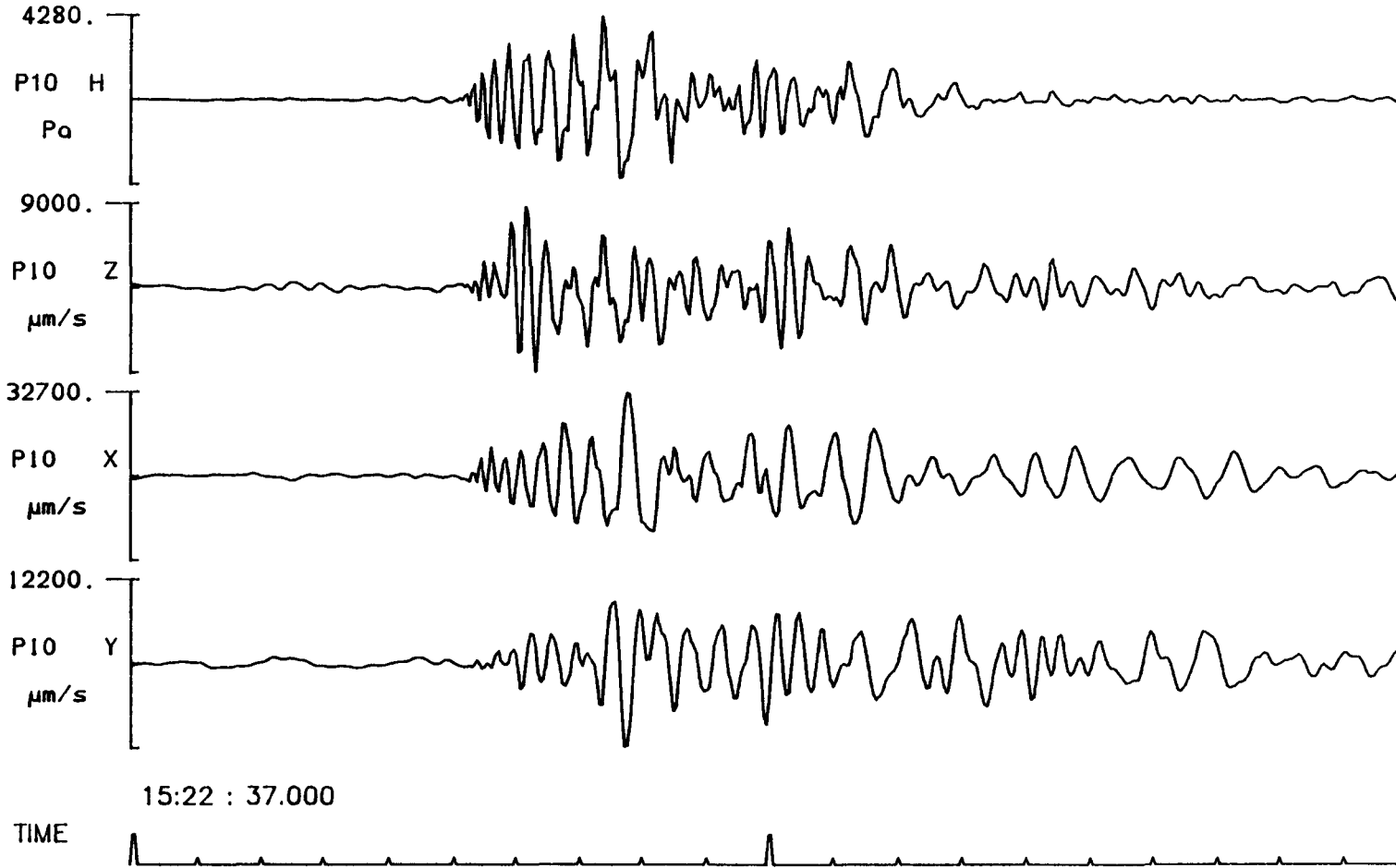


Fig. F.2.11

PUSS 11, RANGE=14.543 KM, 900LB SHOT ACOUSTIC ARRIVAL

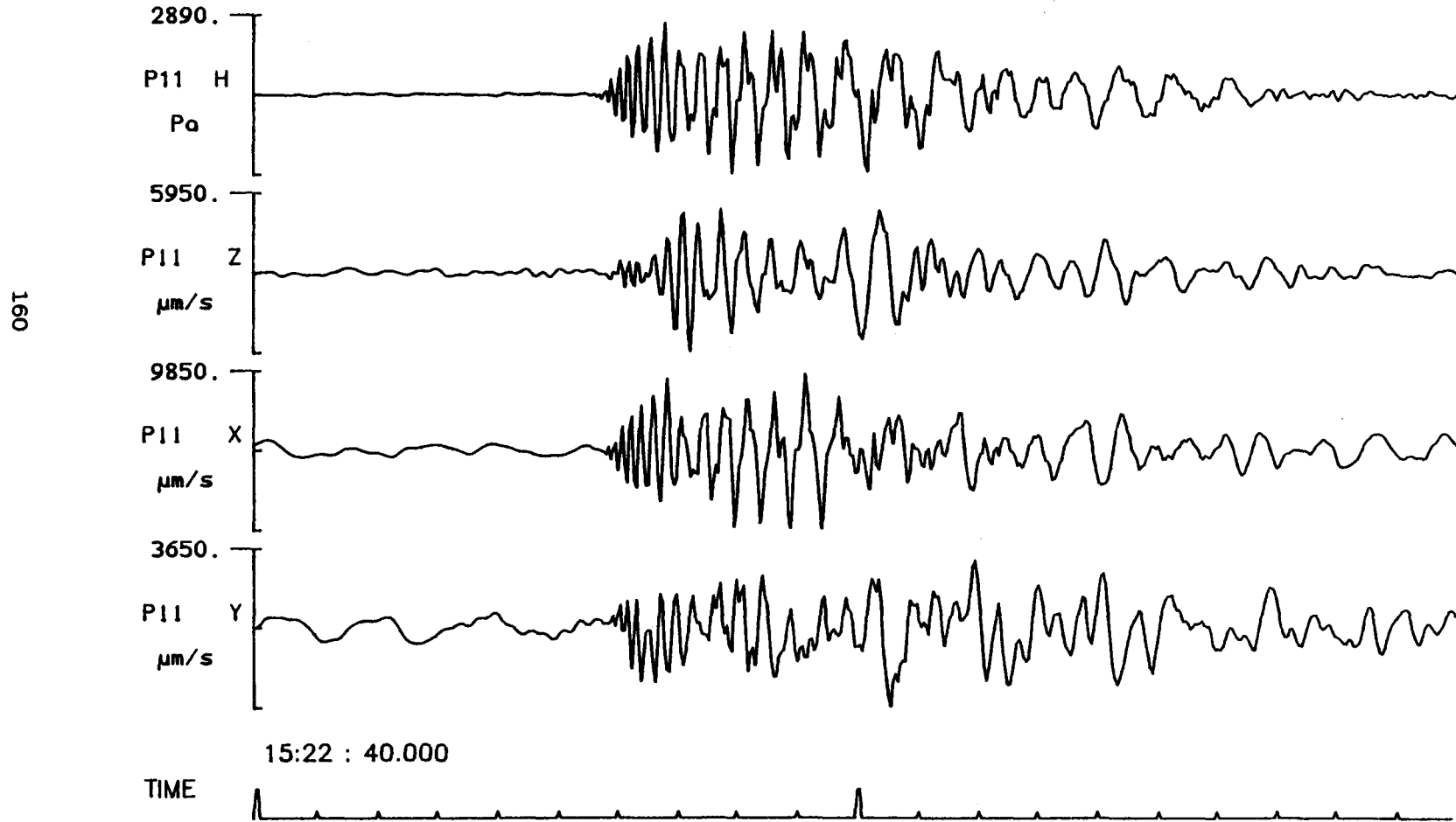
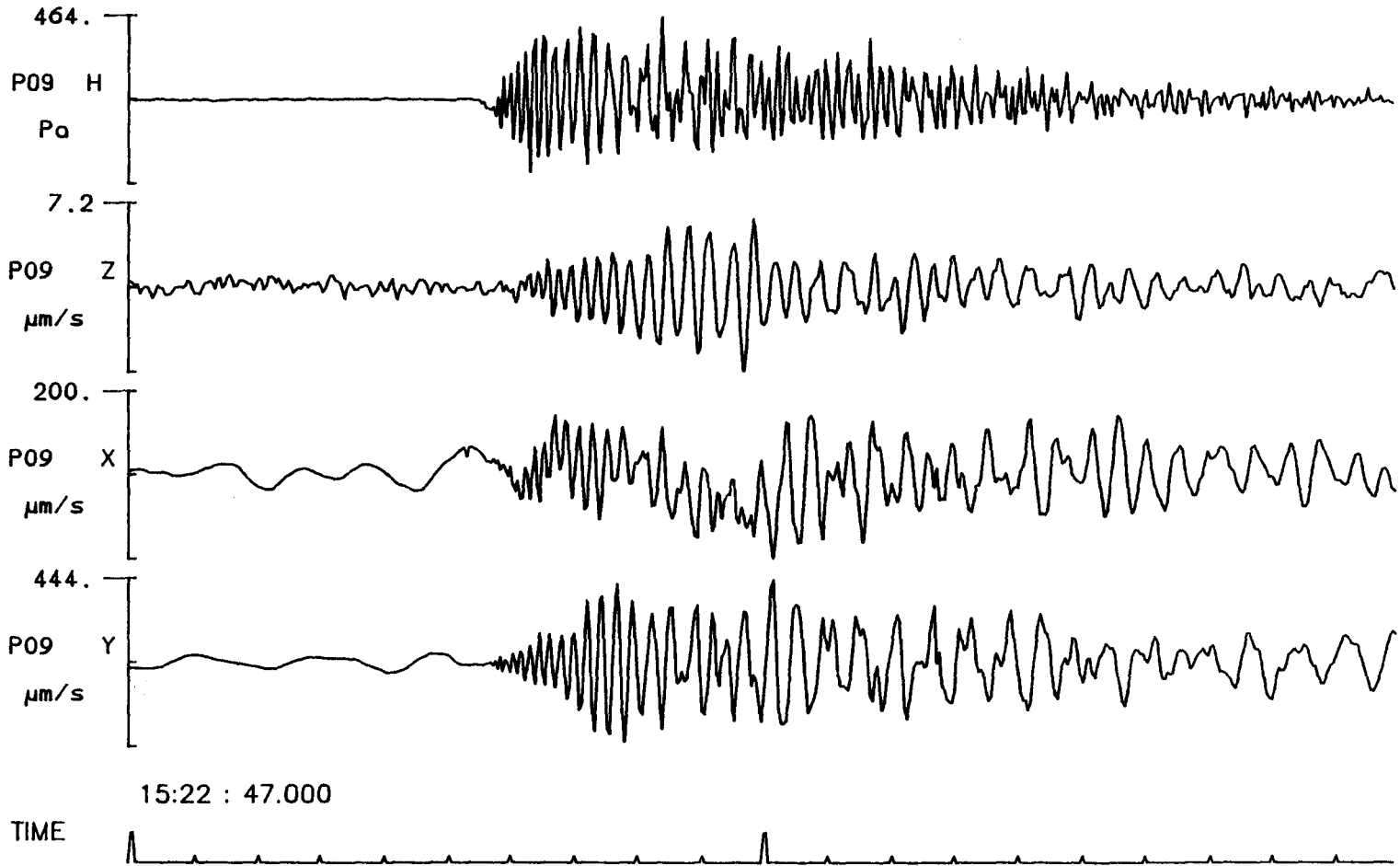


Fig. F.2.12

PUSS 09, RANGE=25.002 KM, 900LB SHOT ACOUSTIC ARRIVAL



161

Fig. F.2.13

PUSS 13, RANGE=39.705 KM, 900LB SHOT ACOUSTIC ARRIVAL

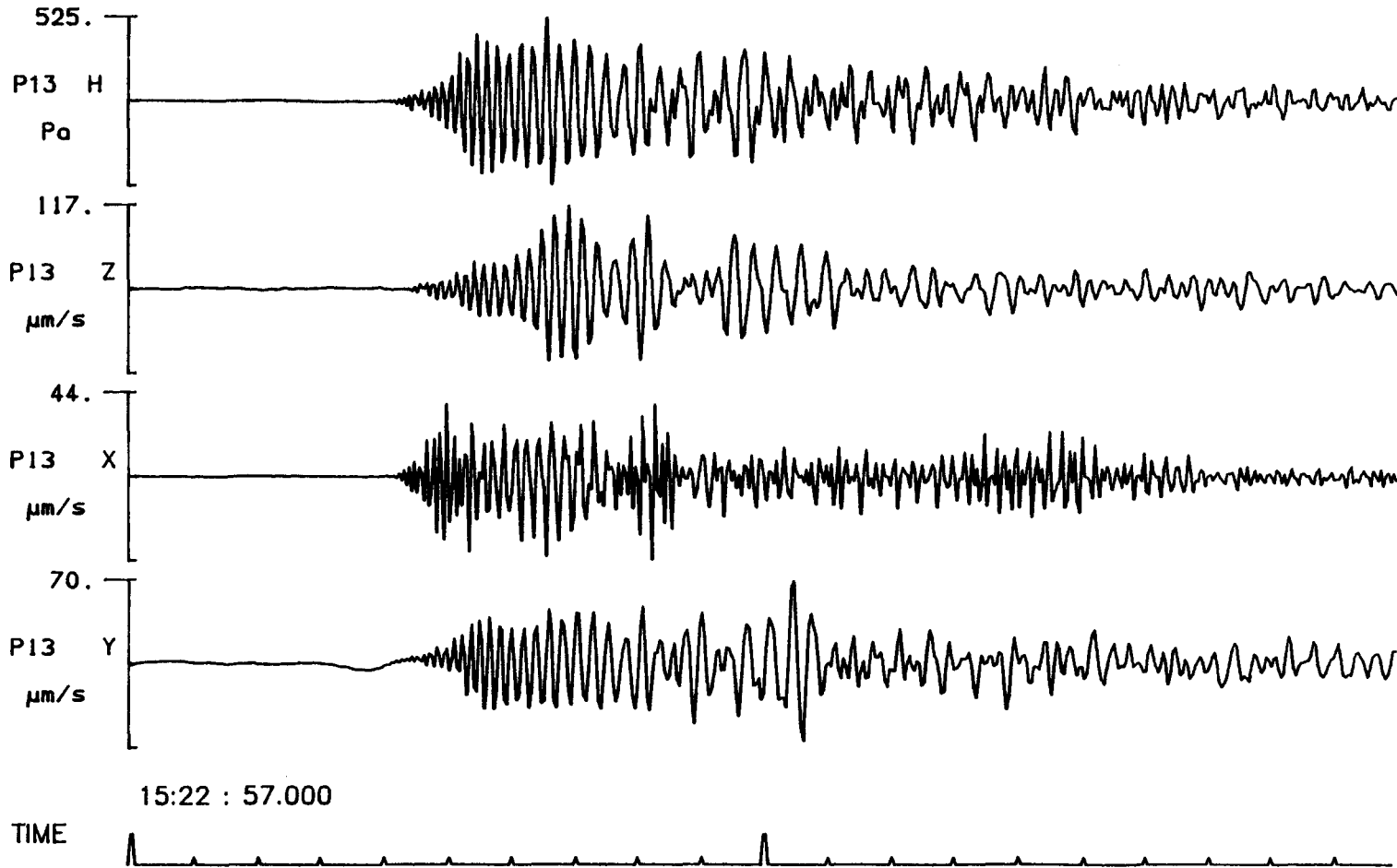


Fig. F.2.14

BGS Sea Bottom Package RANGE=60.035 KM, 900LB SHOT ACOUSTIC ARRIVAL

163

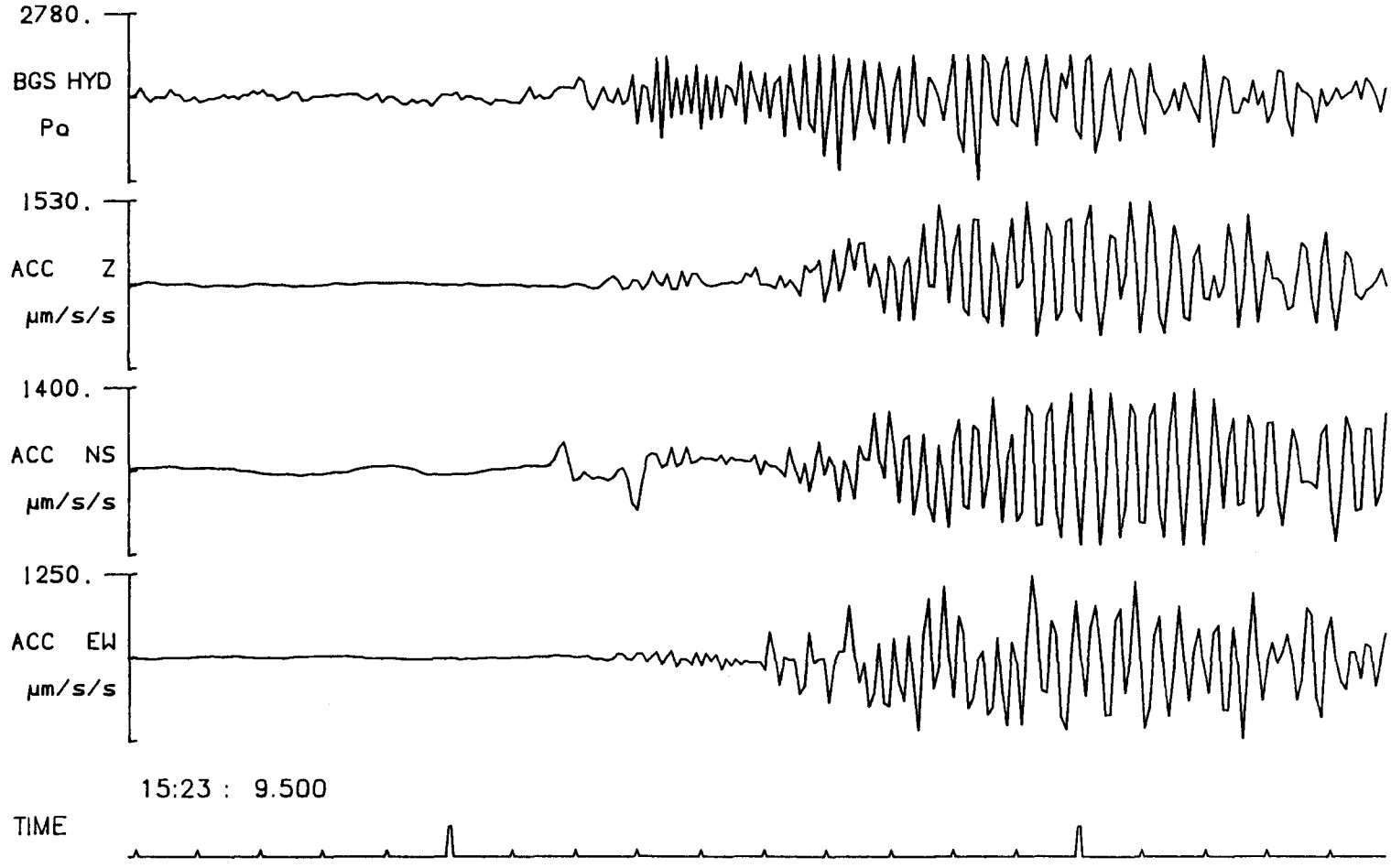


Fig. F.2.15

BGS Sea Bottom Package RANGE=60.035 KM, 900LB SHOT ACOUSTIC ARRIVAL

164

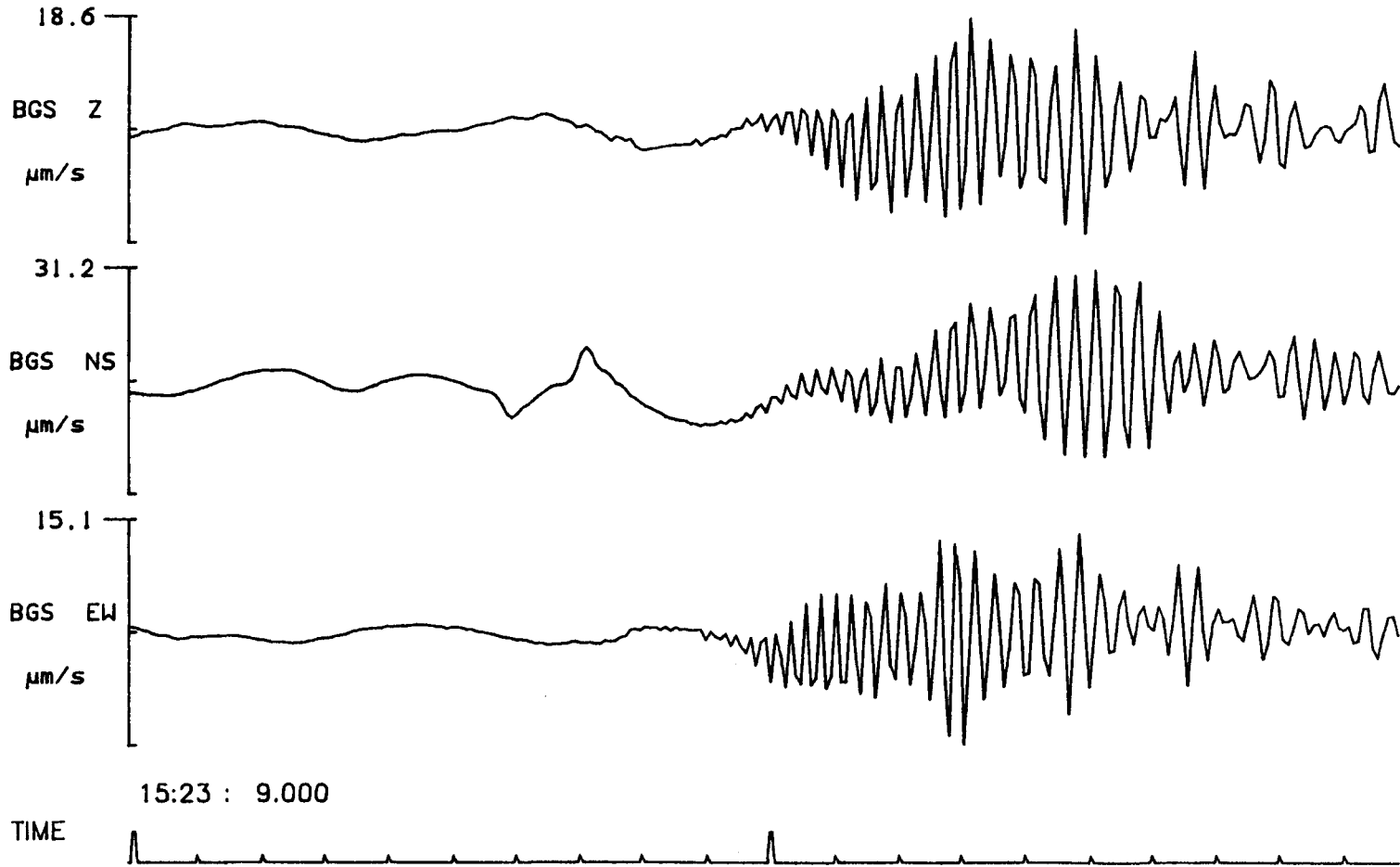


Fig. F.2.16

BGS Sea Vertical Hydrophone String RANGE=60.062 KM, 900LB SHOT 1 - 5

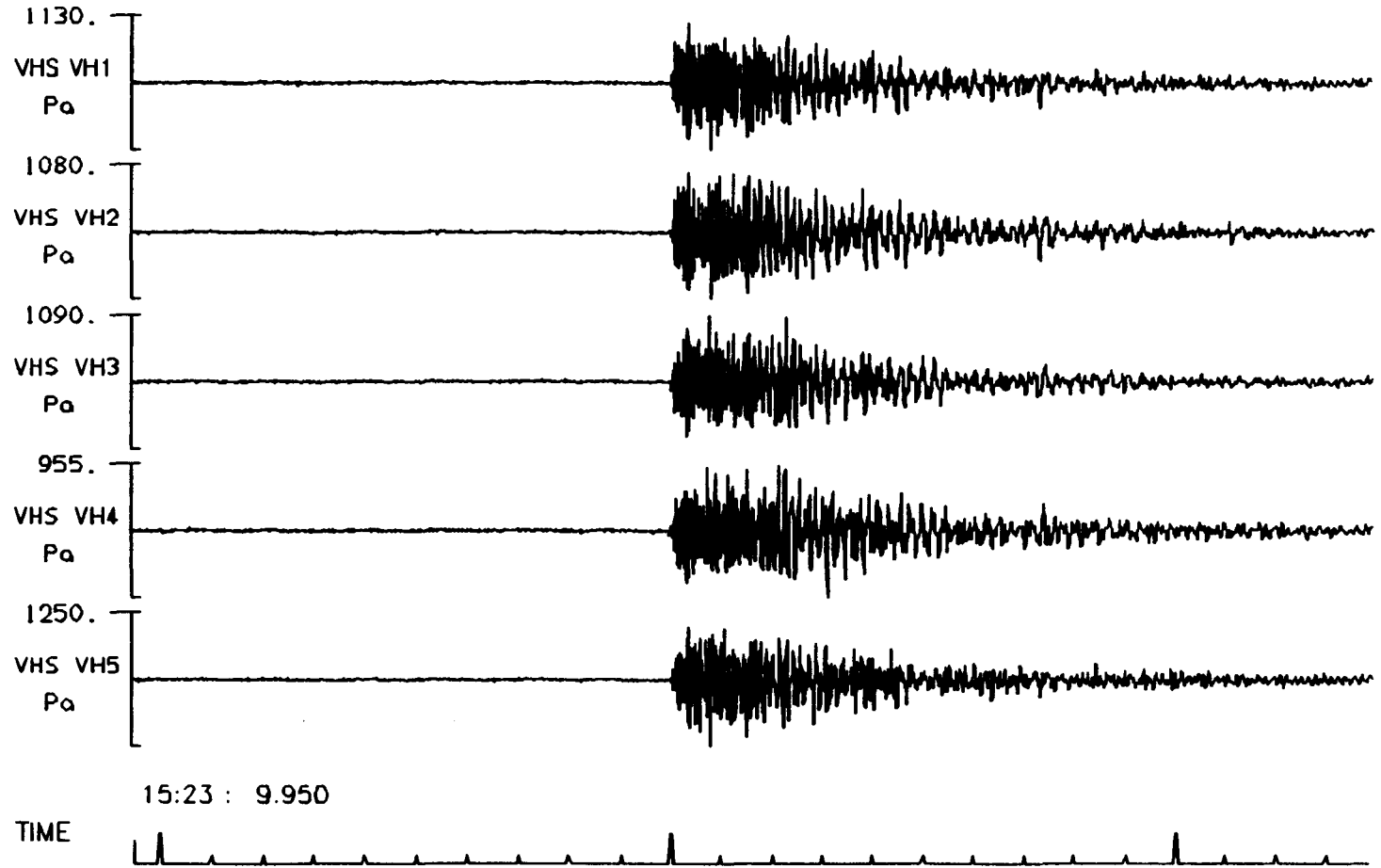


Fig. F.2.17

BGS Sea Vertical Hydrophone String RANGE=60.062 KM, 900LB SHOT 6 - 10

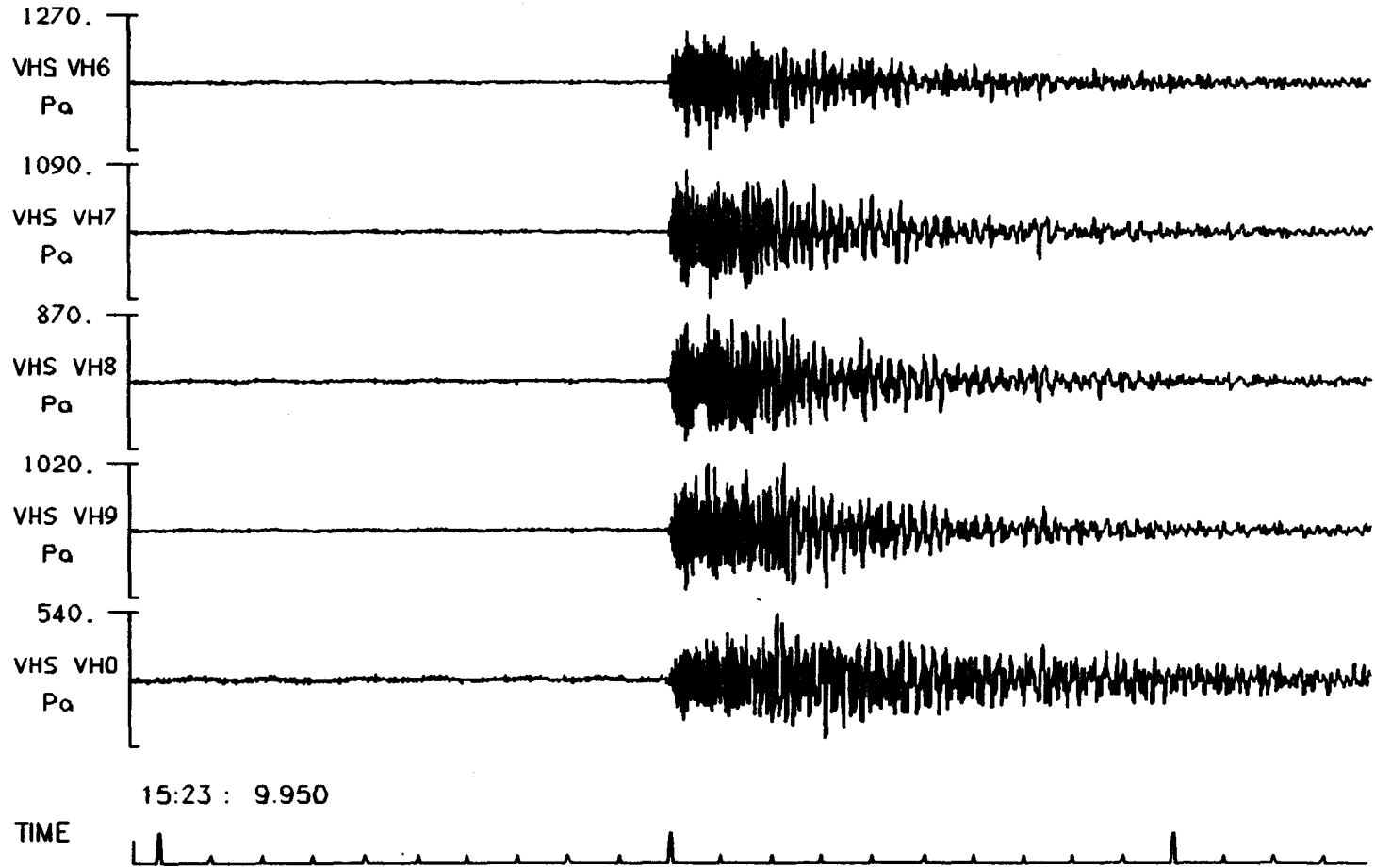


Fig. F.2.18

PUSS 14, RANGE=85.291 KM, 900LB SHOT ACOUSTIC ARRIVAL

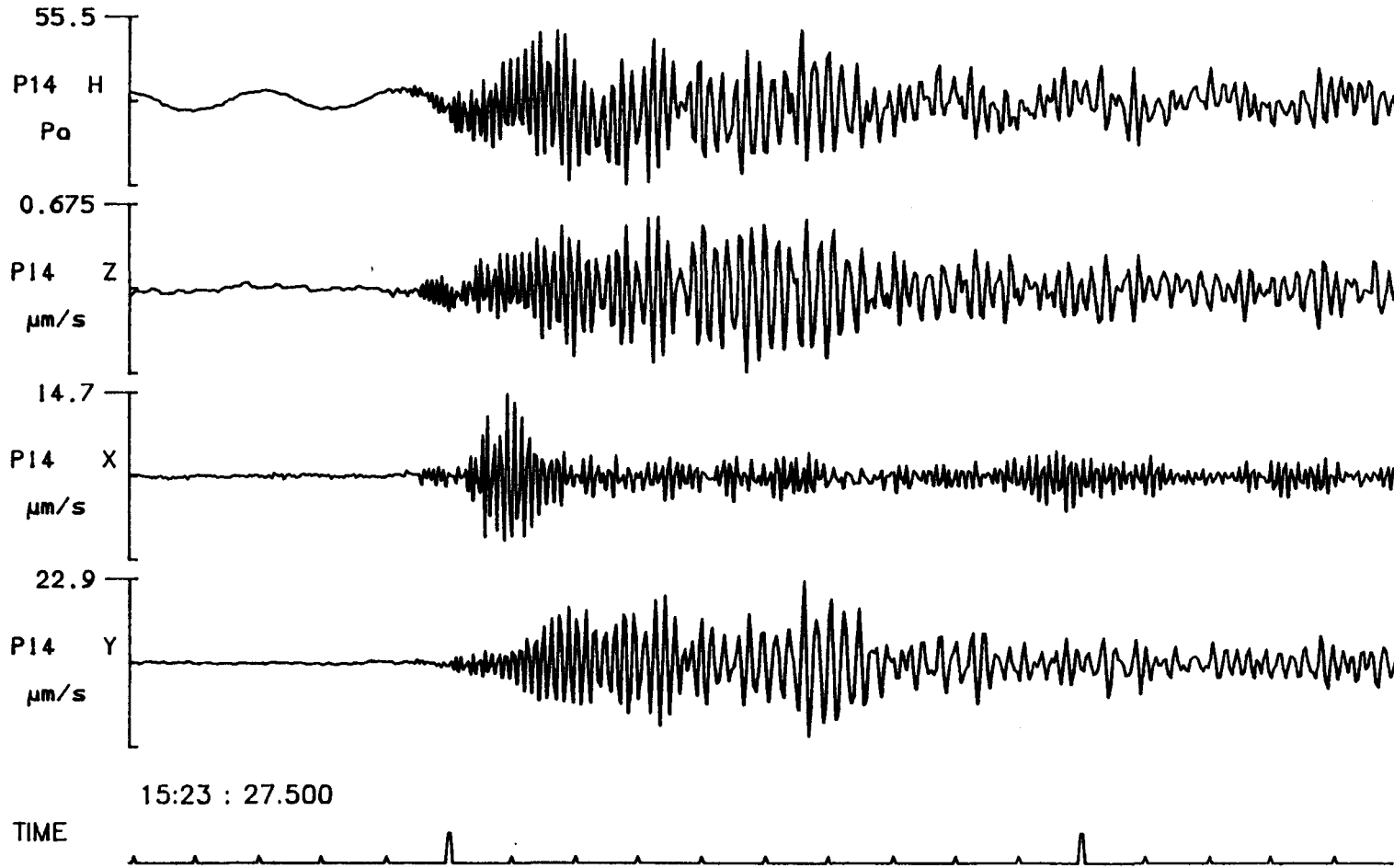


Fig. F.3.1

PUSS 10, RANGE=9.982 KM, 4500LB SHOT SEISMIC ARRIVAL

168

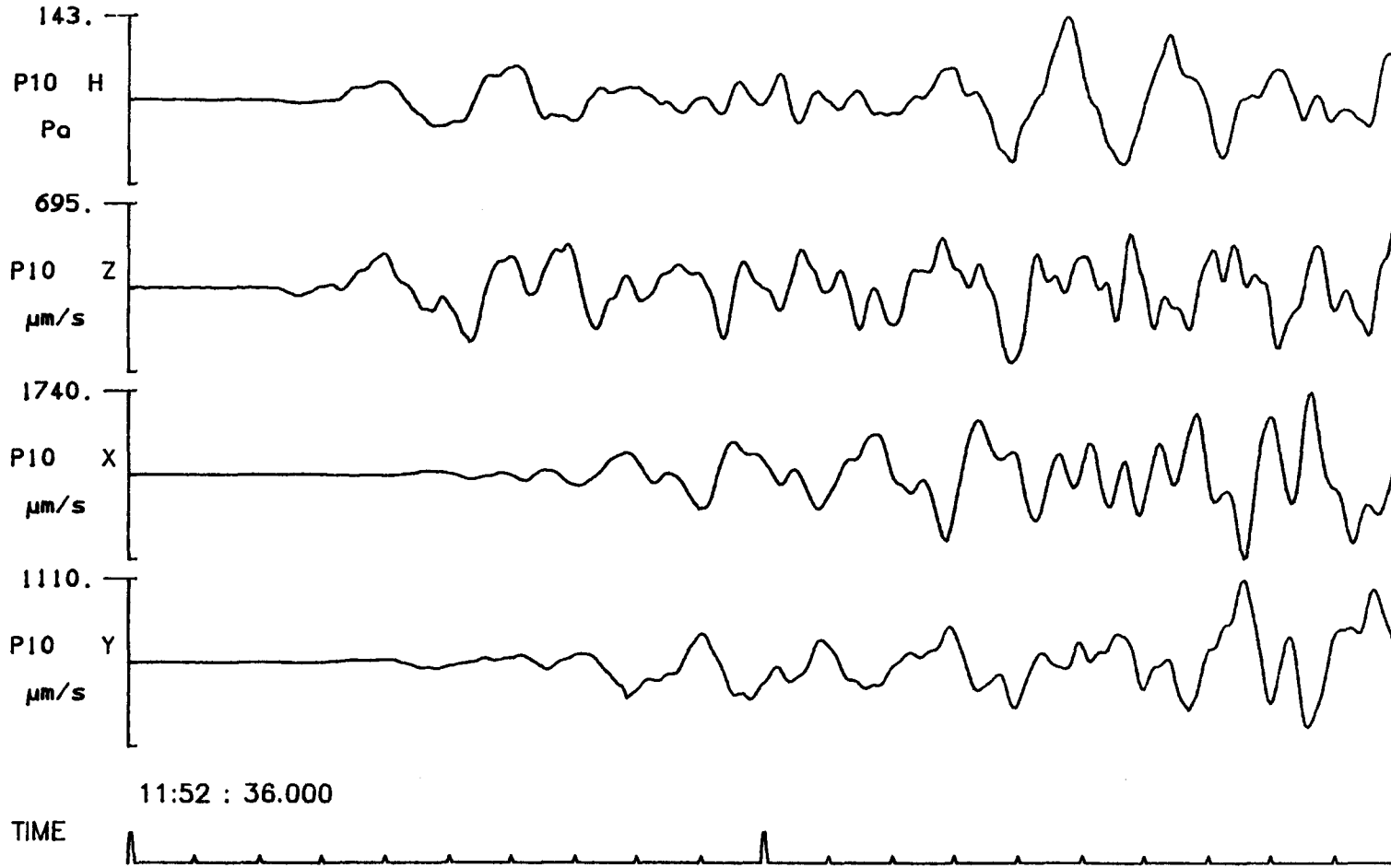


Fig. F.3.2

PUSS 11, RANGE=14.543 KM, 4500LB SHOT SEISMIC ARRIVAL

169

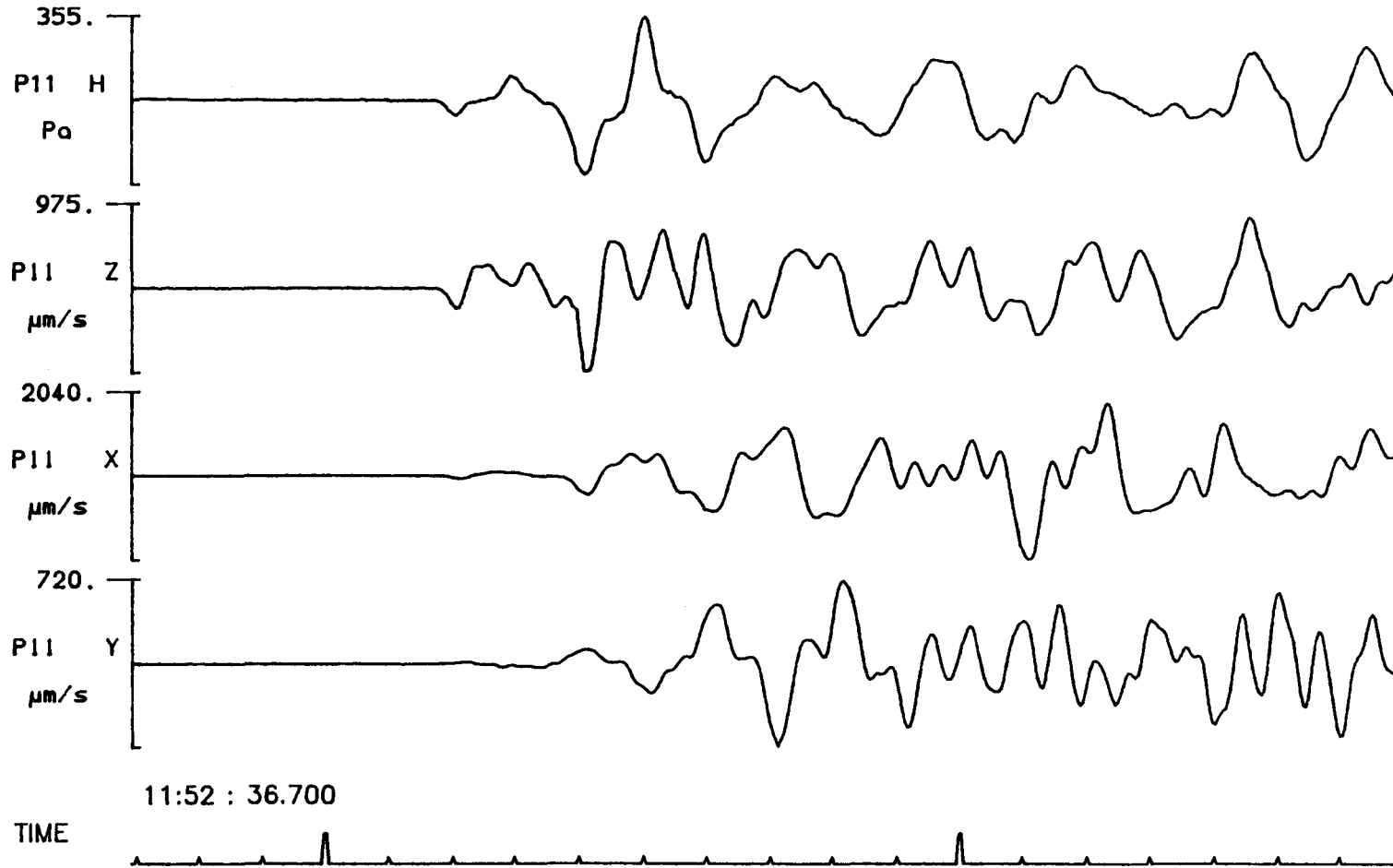


Fig. F.3.3

PUSS 09, RANGE=25.002 KM, 4500LB SHOT SEISMIC ARRIVAL

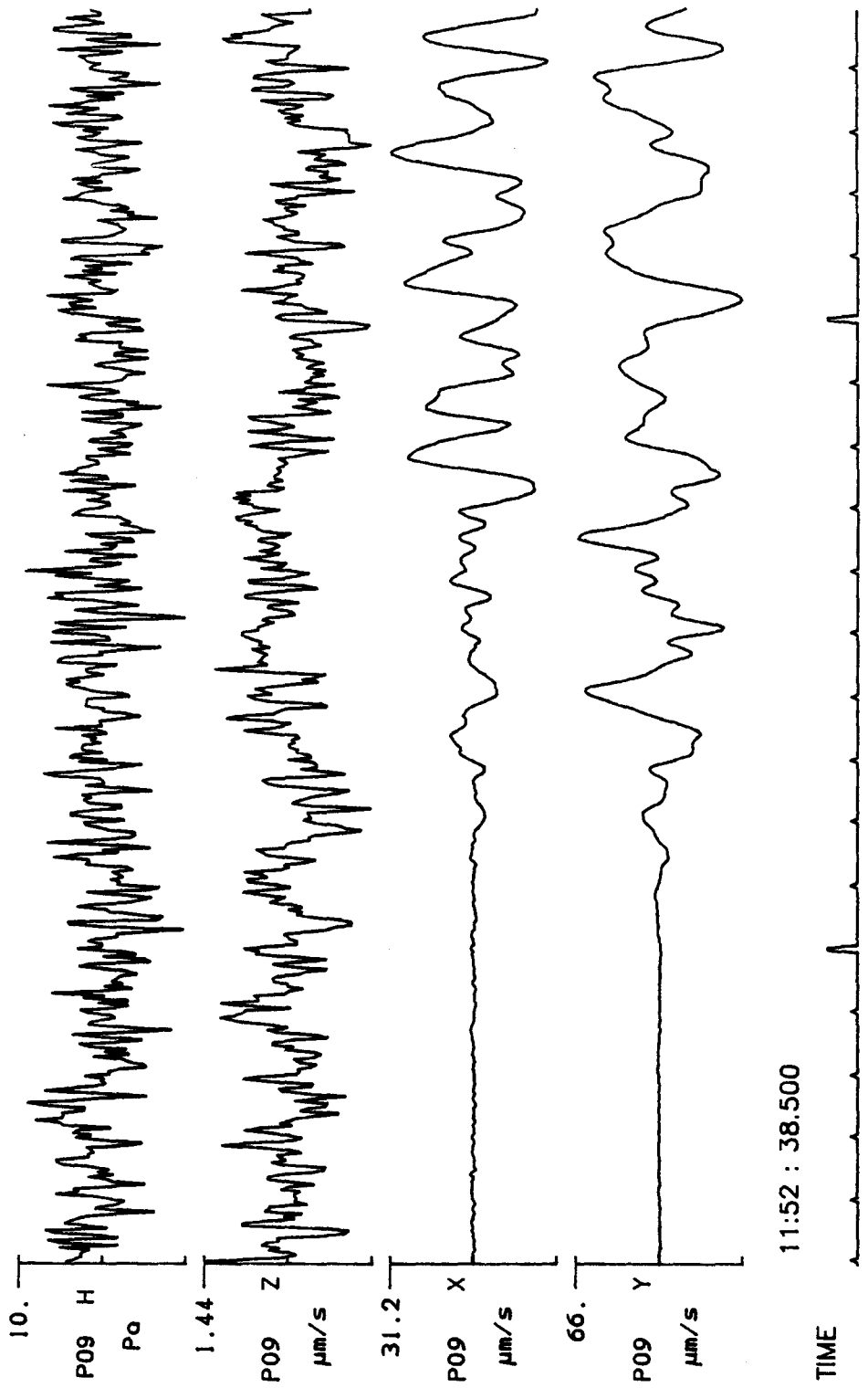


Fig. F.3.4

PUSS 13, RANGE=39.705 KM, 4500LB SHOT SEISMIC ARRIVAL

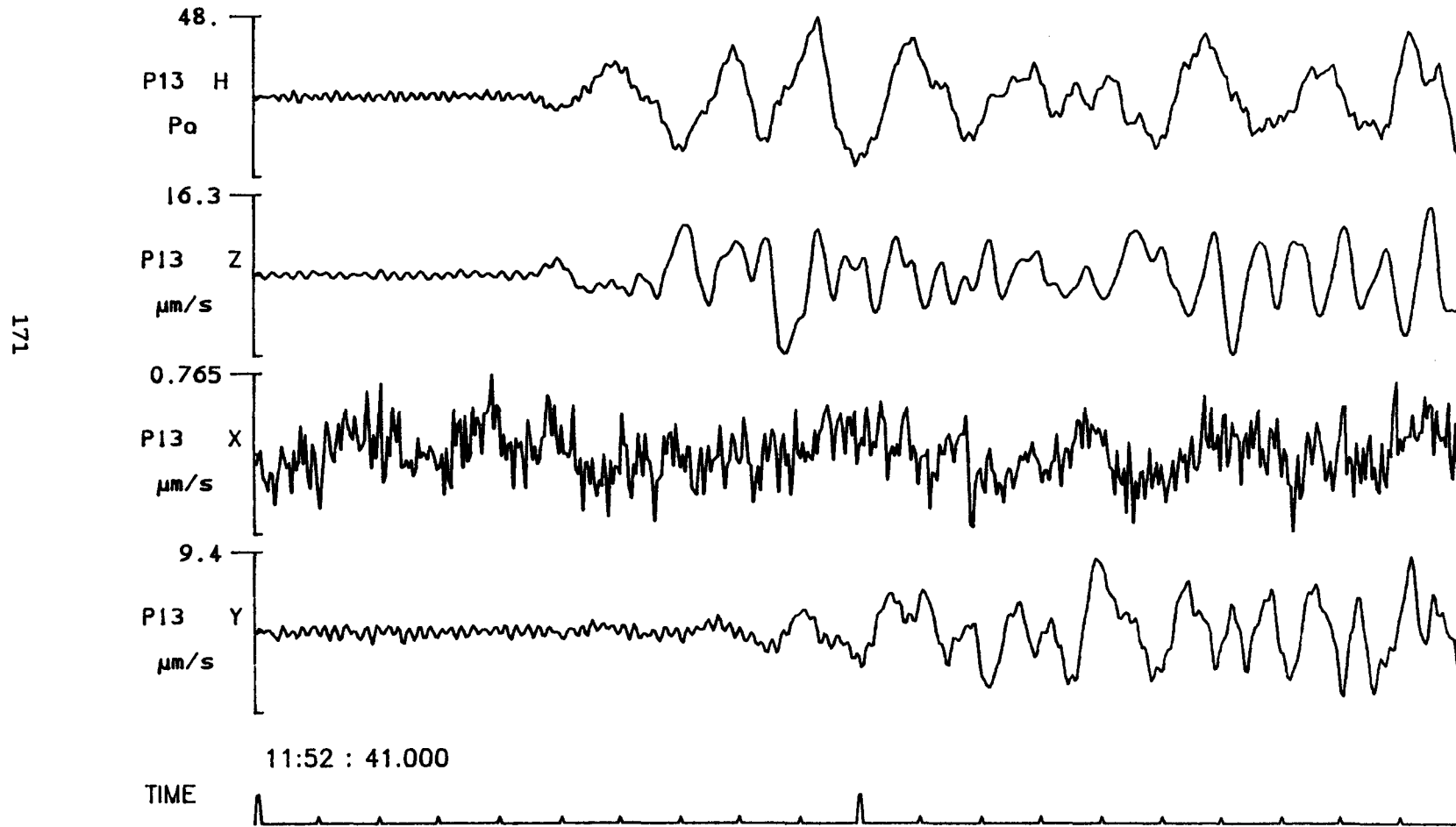


Fig. F.3.5

BGS Sea Bottom Package RANGE=60.035 KM, 4500LB SHOT SEISMIC ARRIVAL

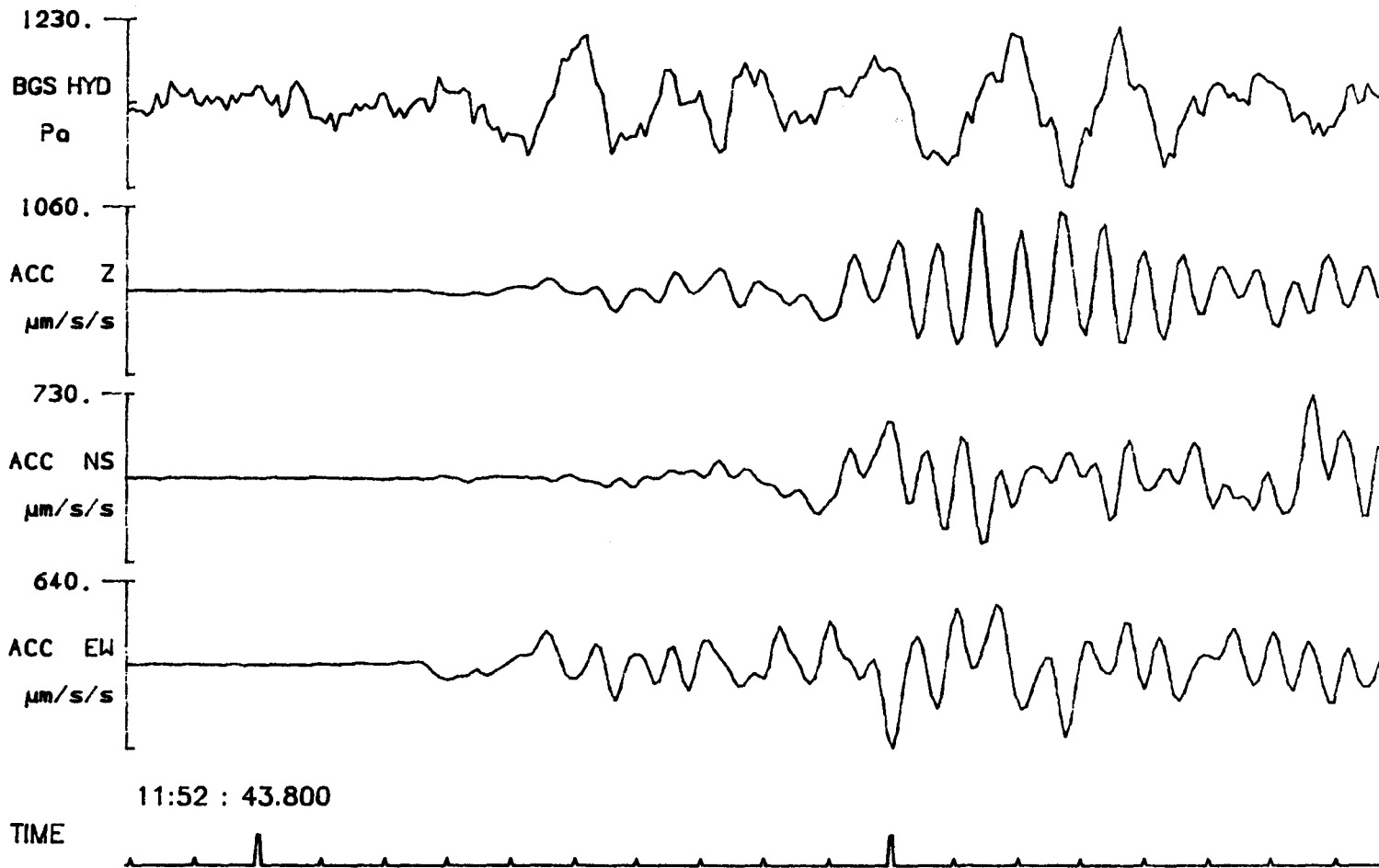


Fig. F.3.6

BGS Sea Bottom Package RANGE=60.035 KM, 4500LB SHOT SEISMIC ARRIVAL

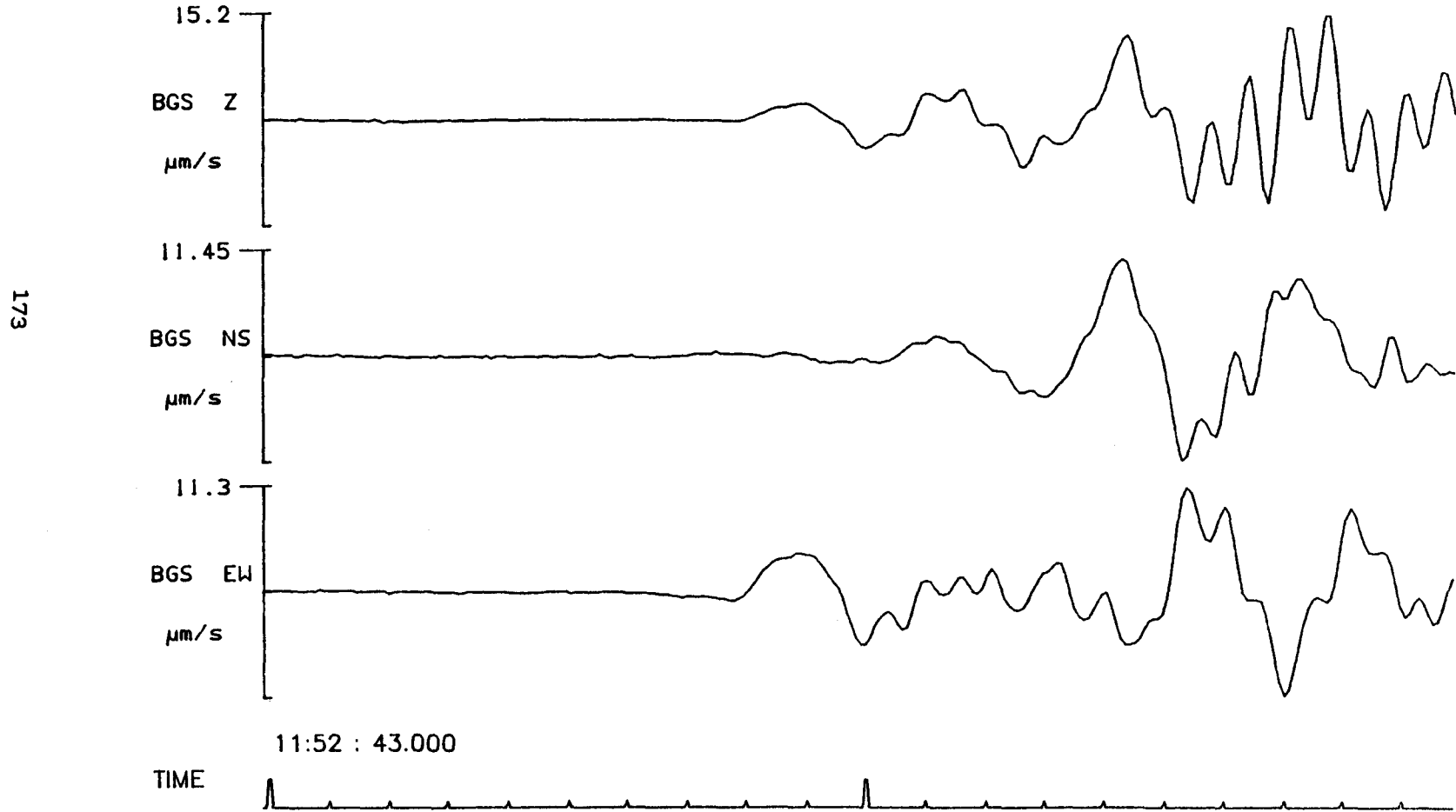


Fig. F.3.7

PUSS 14, RANGE=85.291 KM, 4500LB SHOT SEISMIC ARRIVAL

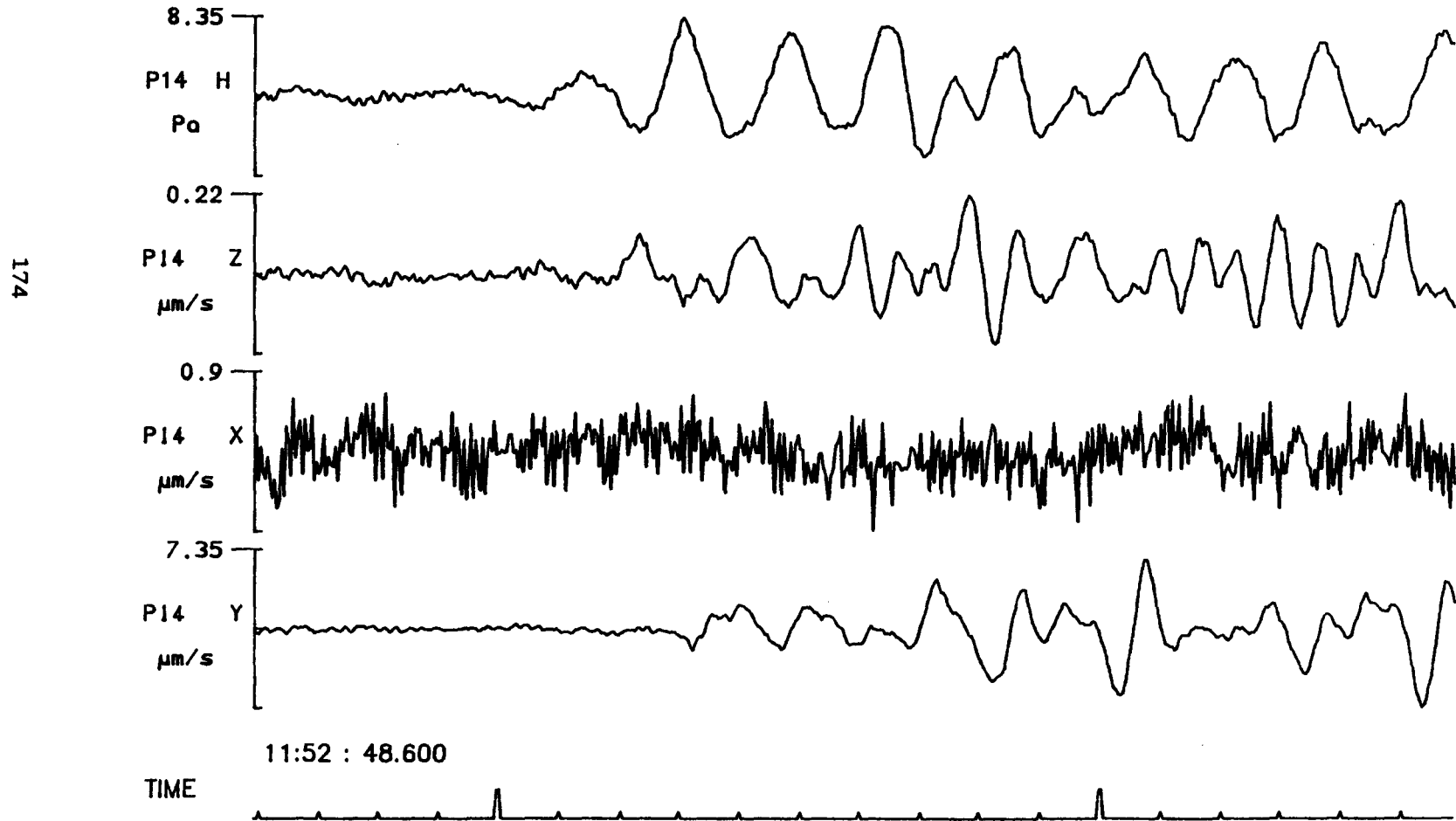


Fig. F.3.8

Tentsmuir, 4500LB SHOT, seismic arrival, Filtered at 8Hz

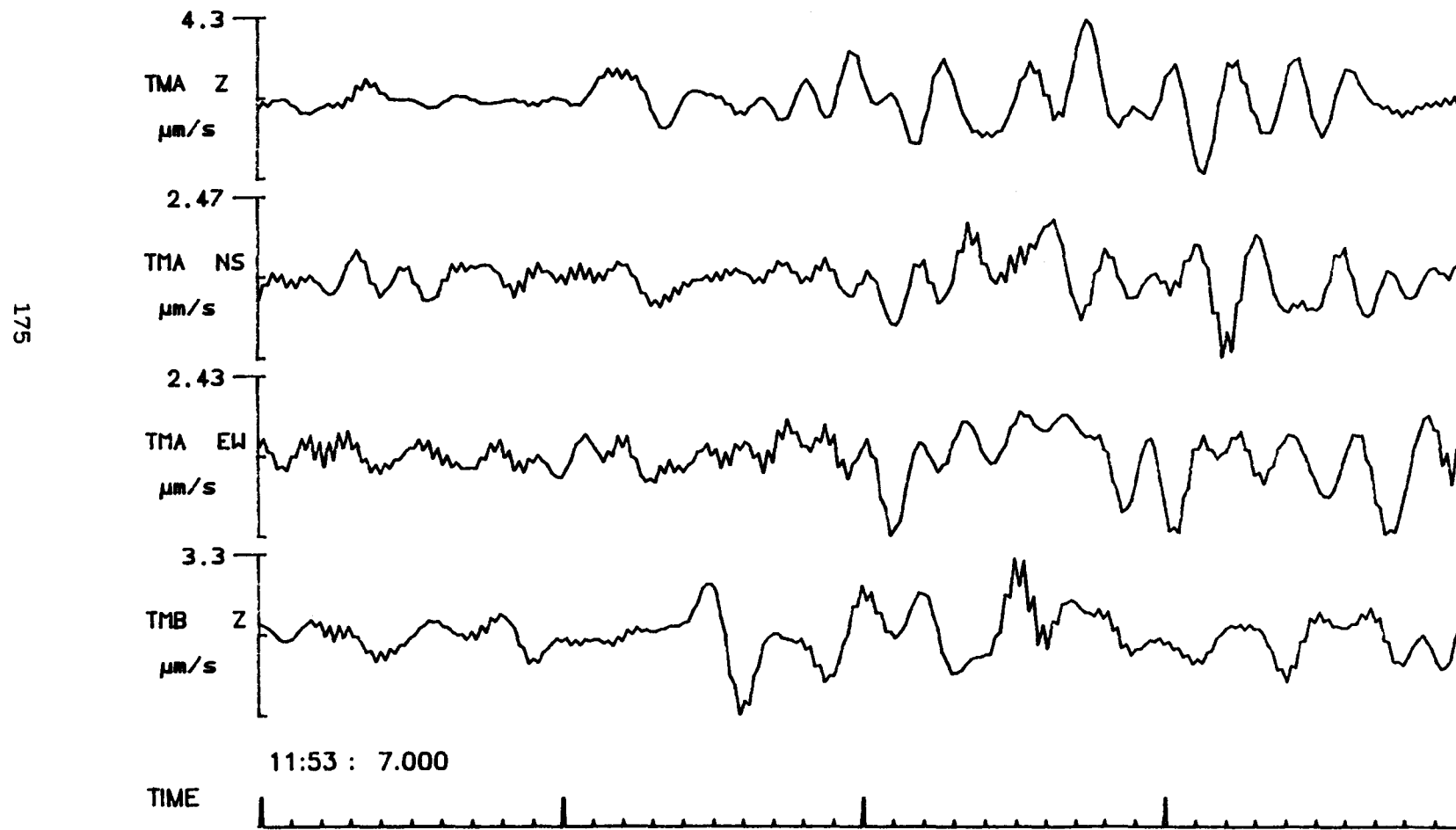


Fig. F.3.9

PUSS 10, RANGE=9.982 KM, 900LB SHOT SEISMIC ARRIVAL

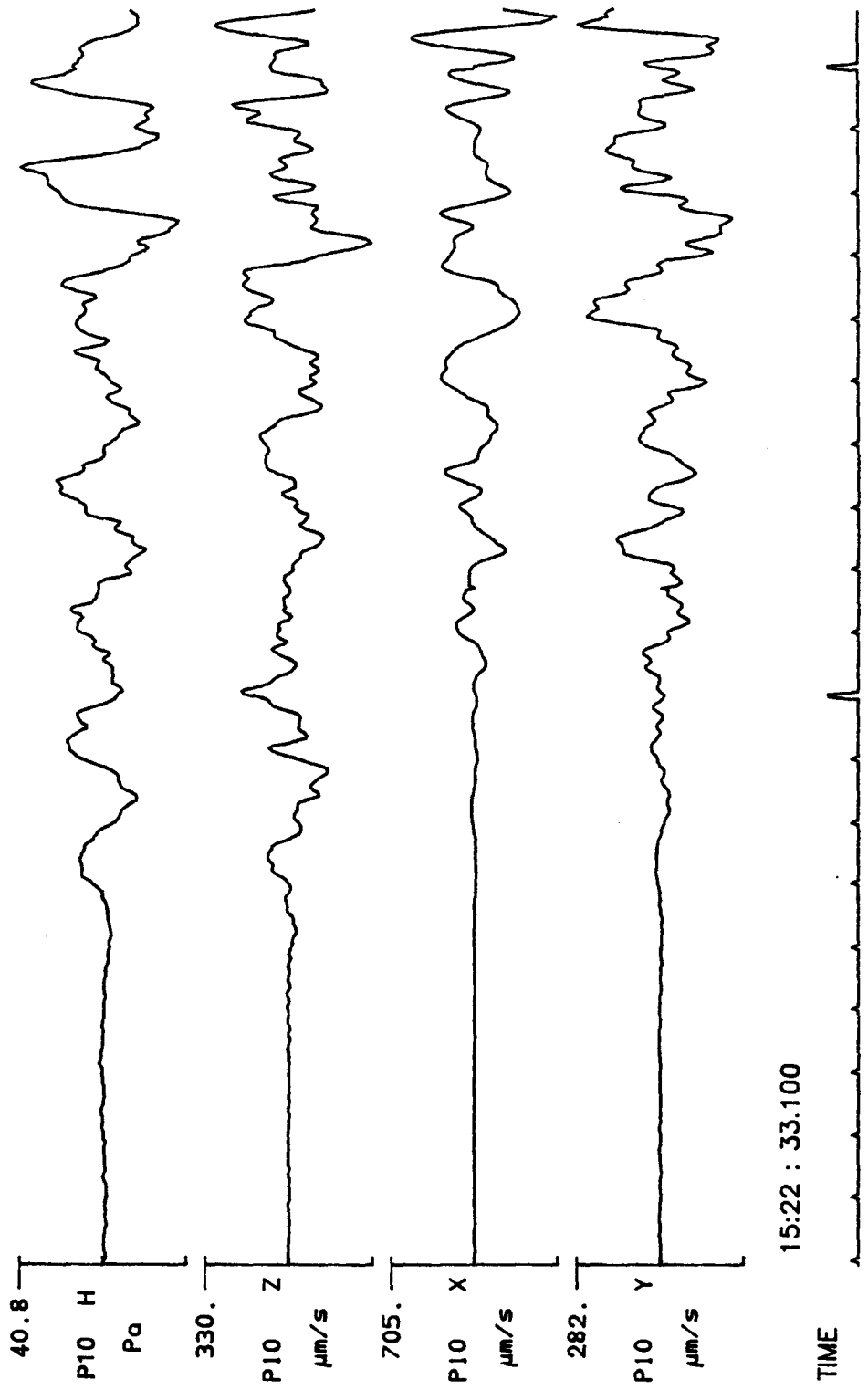


Fig. F.3.10

PUSS 11, RANGE=14.543 KM, 900LB SHOT SEISMIC ARRIVAL

177

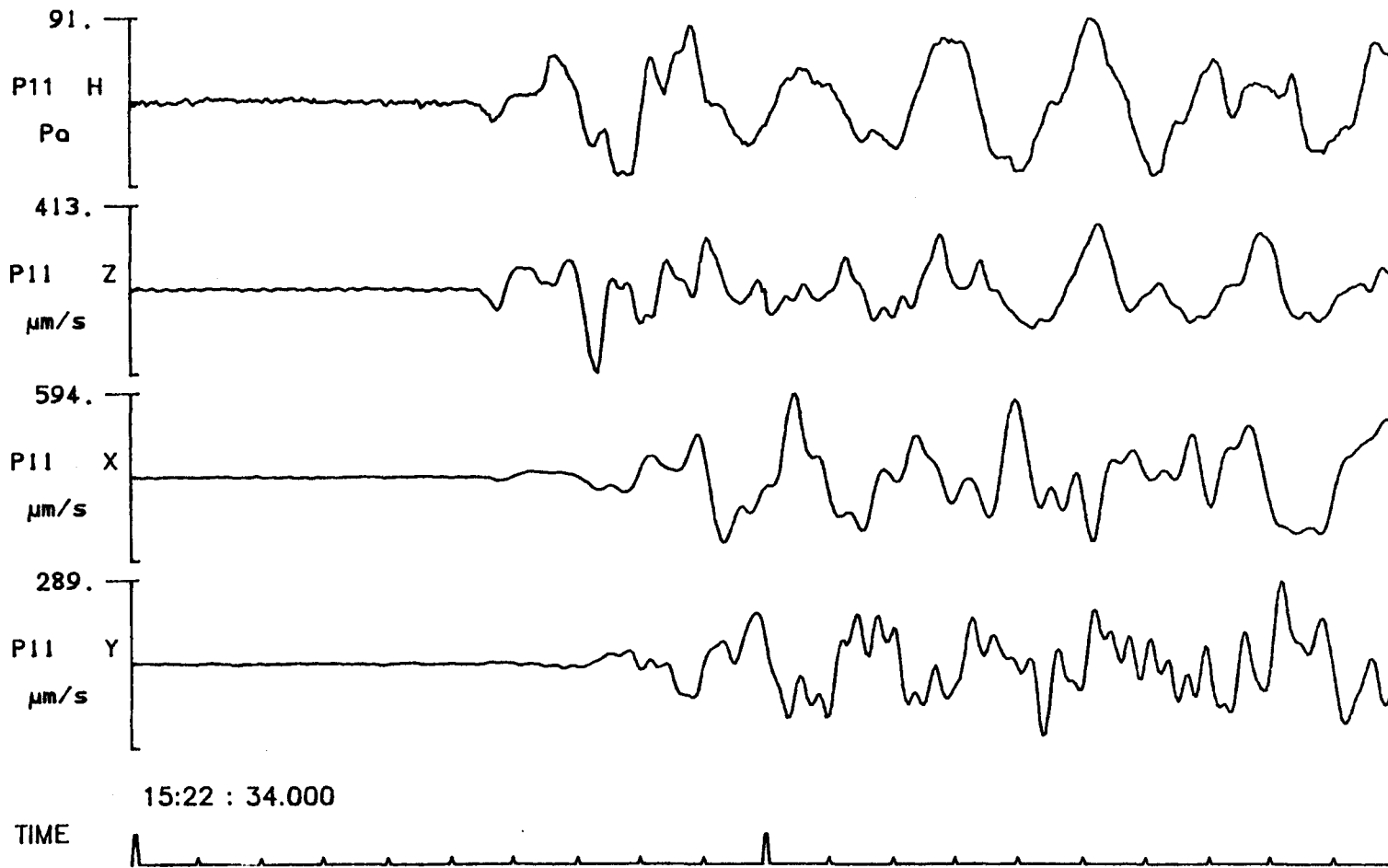


Fig. F.3.11

PUSS 09, RANGE=25.002 KM, 900LB SHOT SEISMIC ARRIVAL

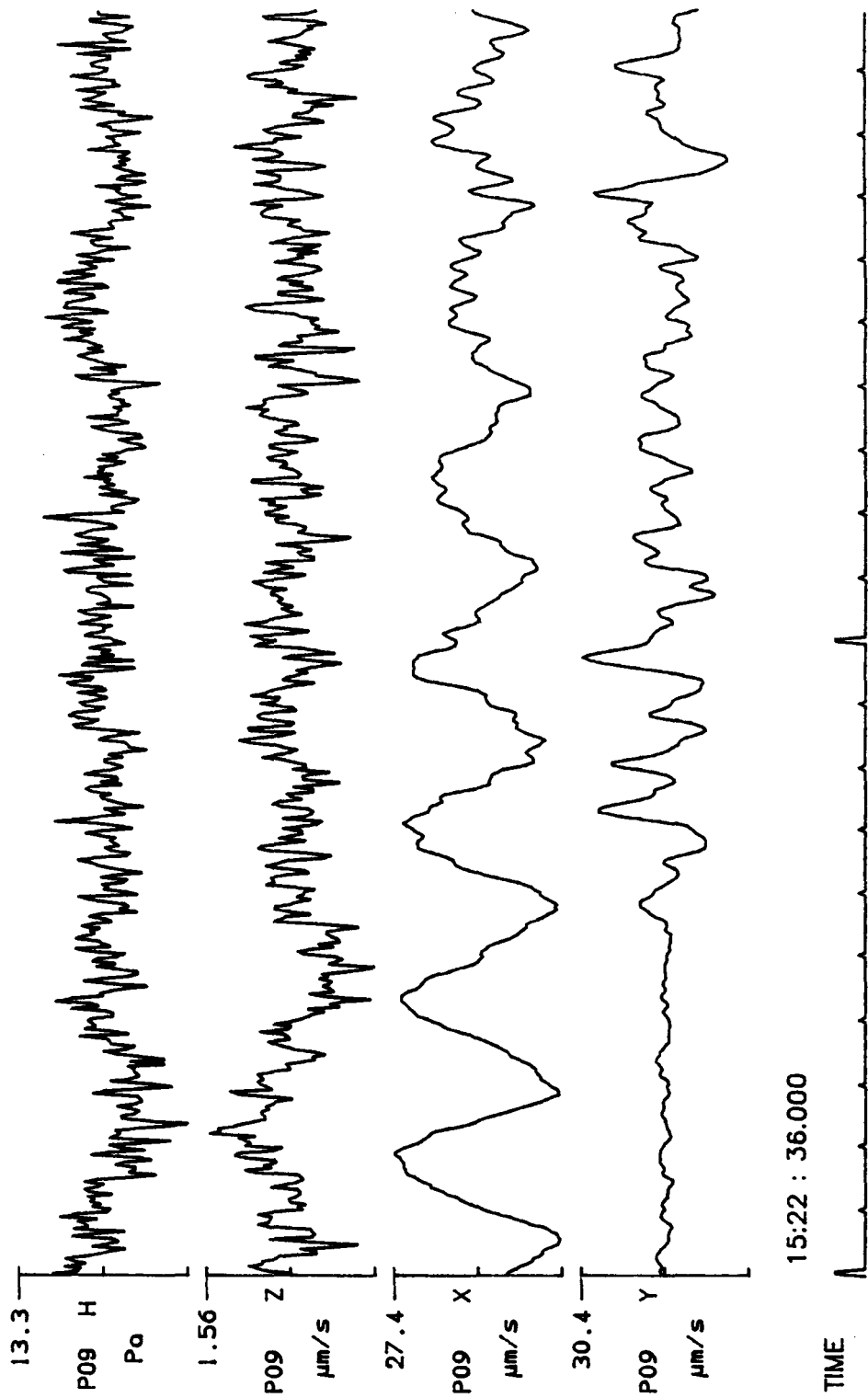


Fig. F.3.12

PUSS 13, RANGE=39.705 KM, 900LB SHOT SEISMIC ARRIVAL

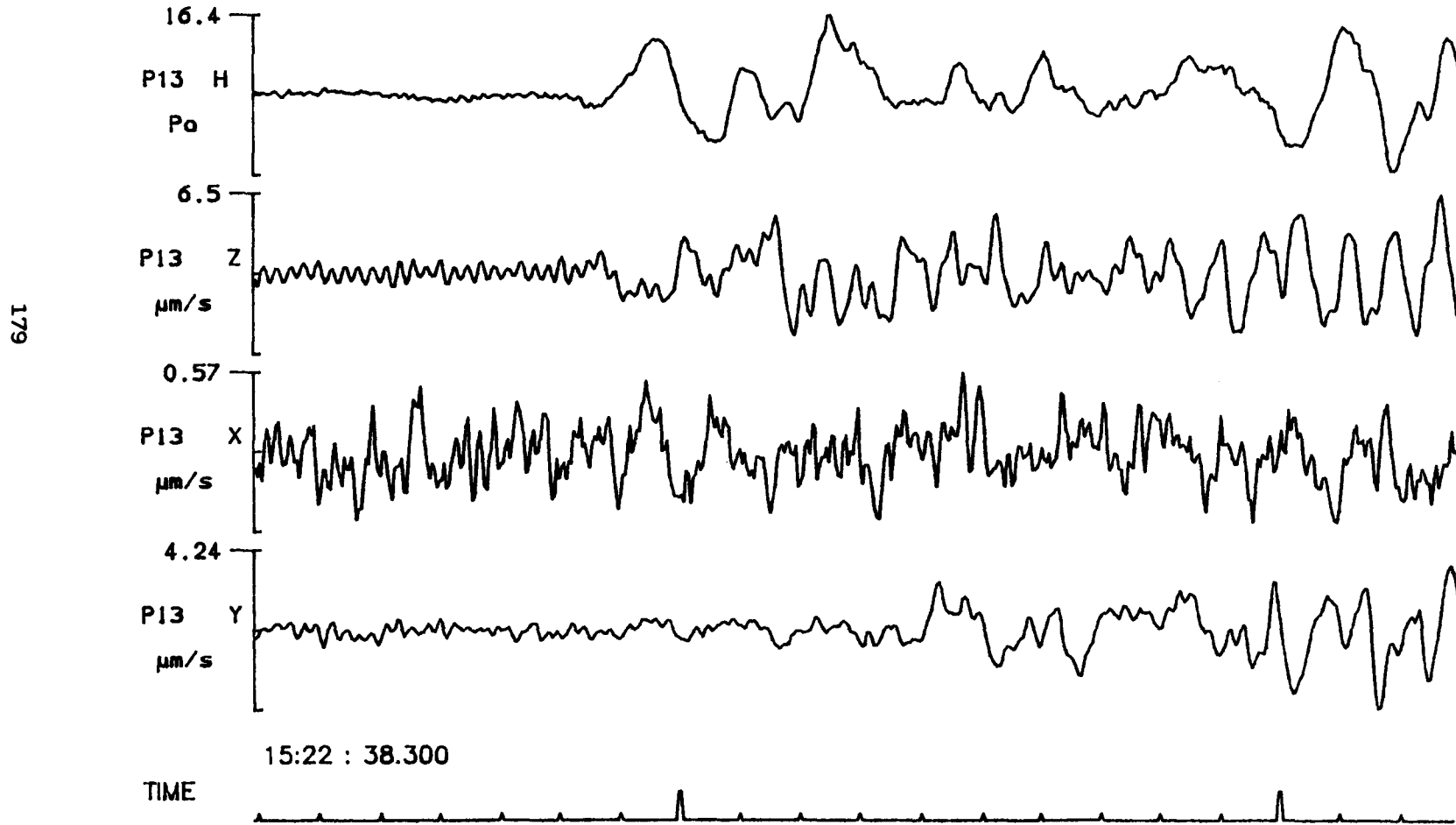


Fig. F.3.13

BGS Sea Bottom Package RANGE=60.035 KM, 900LB SHOT SEISMIC ARRIVAL

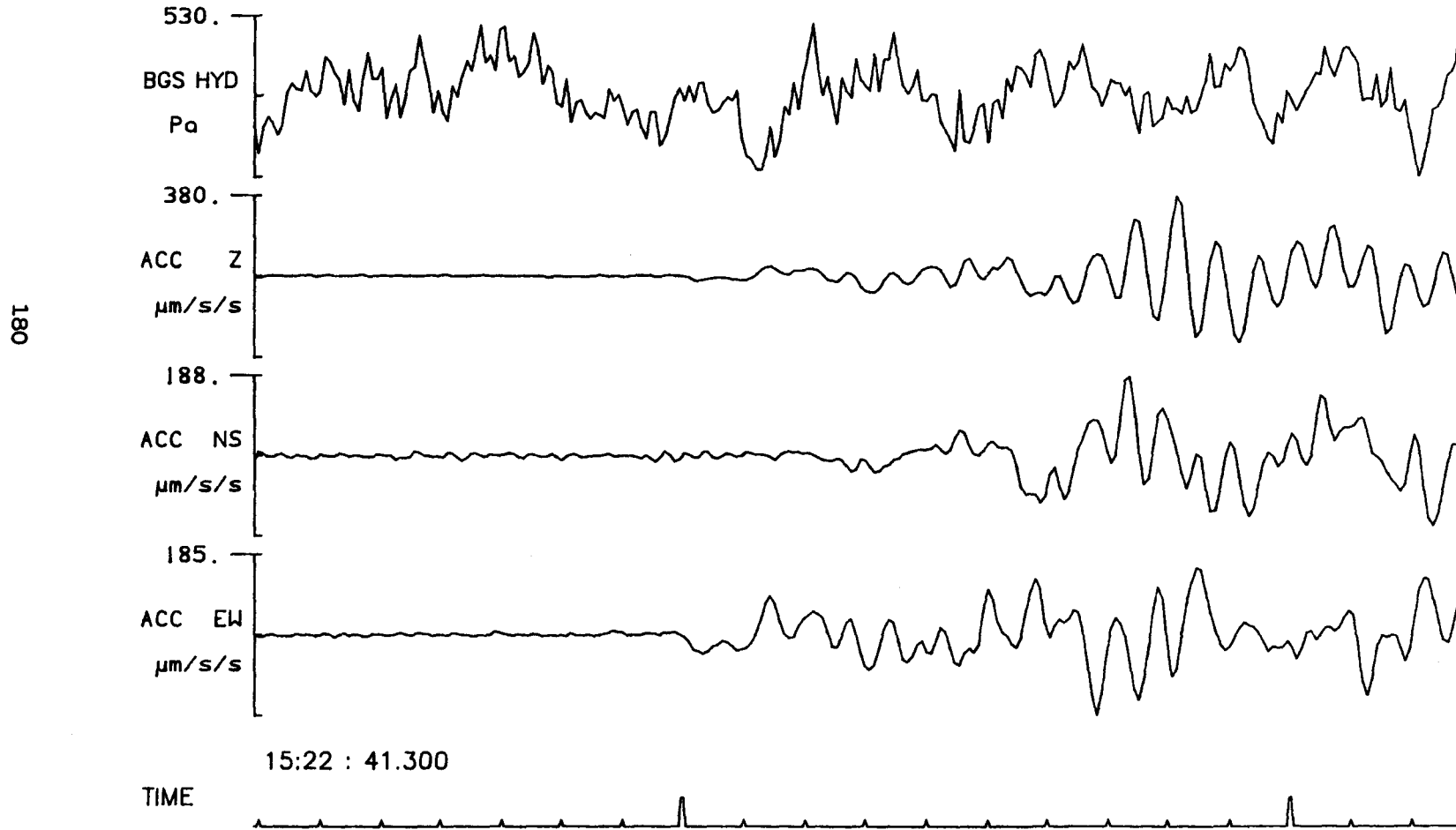


Fig. F.3.14

BGS Sea Bottom Package RANGE=60.035 KM, 900LB SHOT SEISMIC ARRIVAL

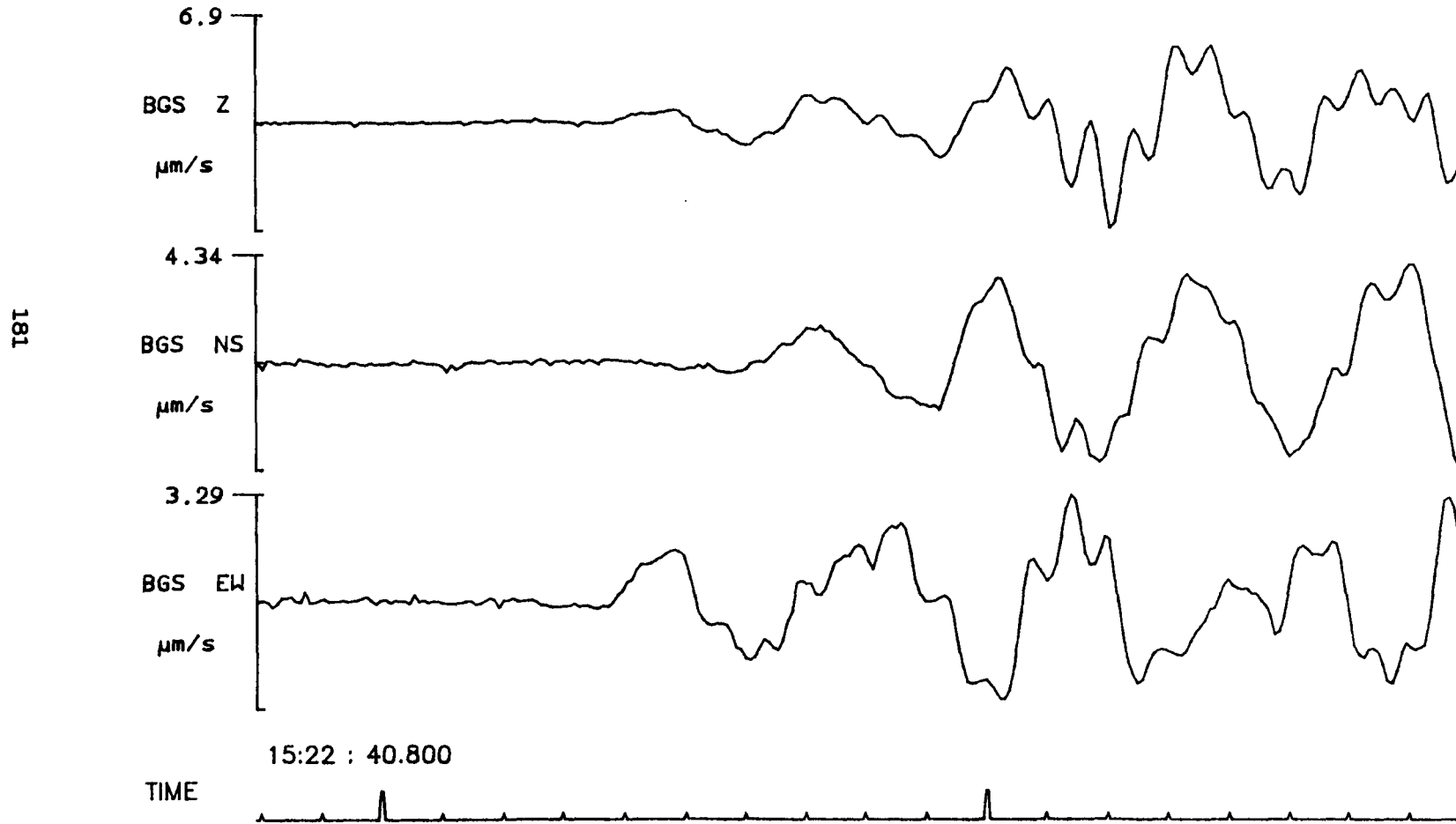


Fig. F.3.15

PUSS 14, RANGE=85.291 KM, 900LB SHOT SEISMIC ARRIVAL

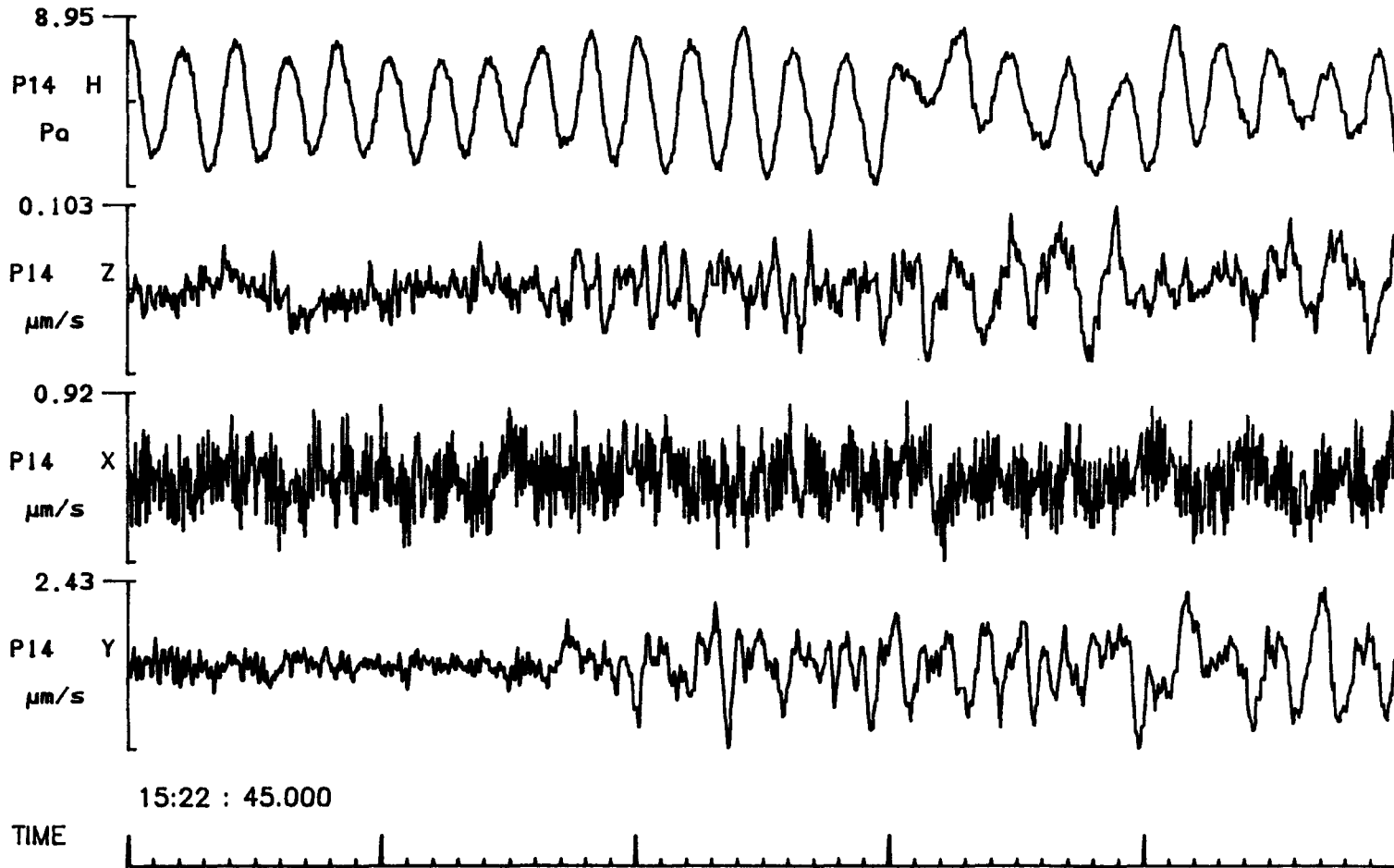


Fig. F.3.1

PUSS 10, RANGE=9.982 KM, 4500LB SHOT SEISMIC ARRIVAL

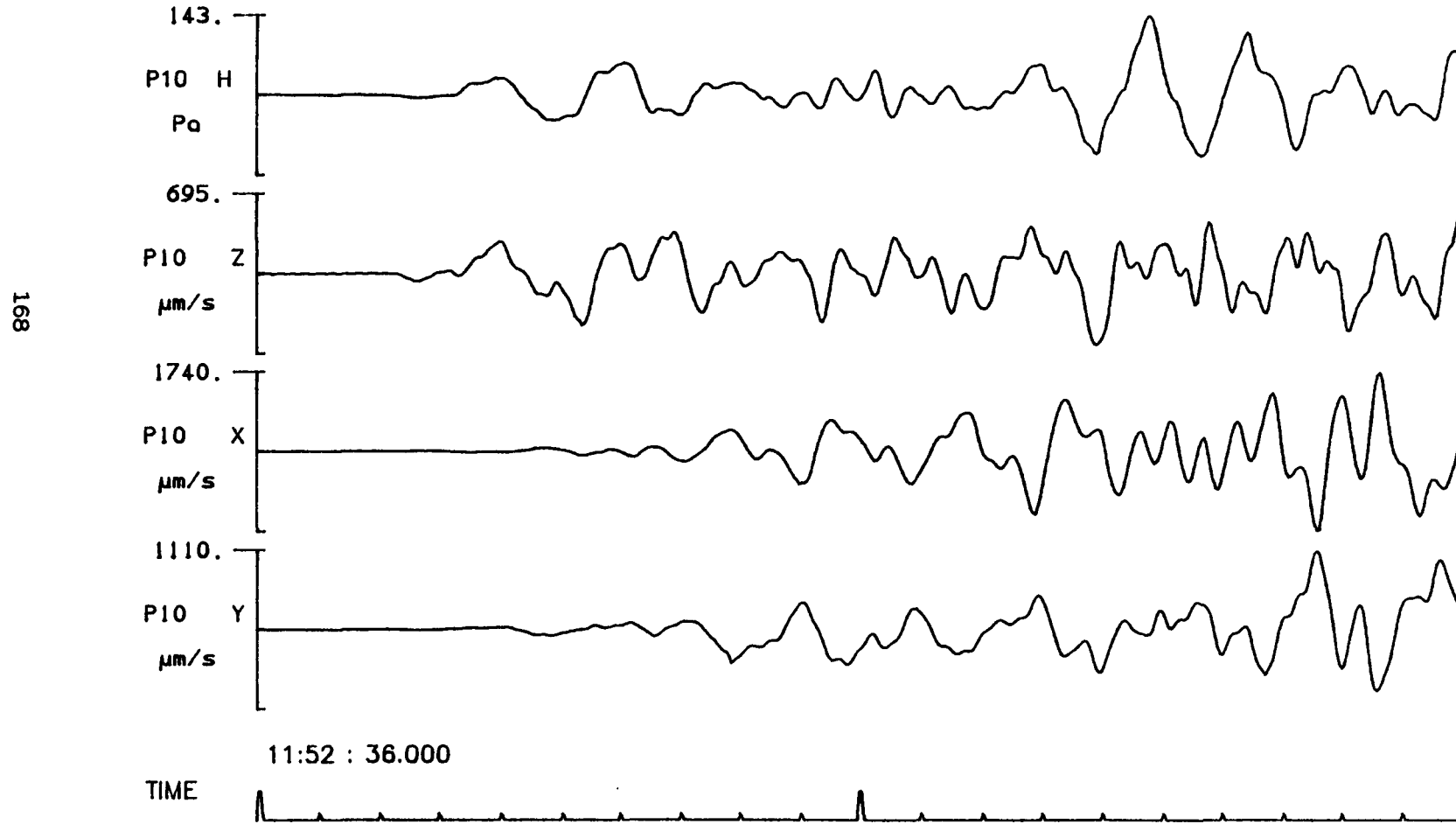


Fig. F.3.2

PUSS 11, RANGE=14.543 KM, 4500LB SHOT SEISMIC ARRIVAL

169

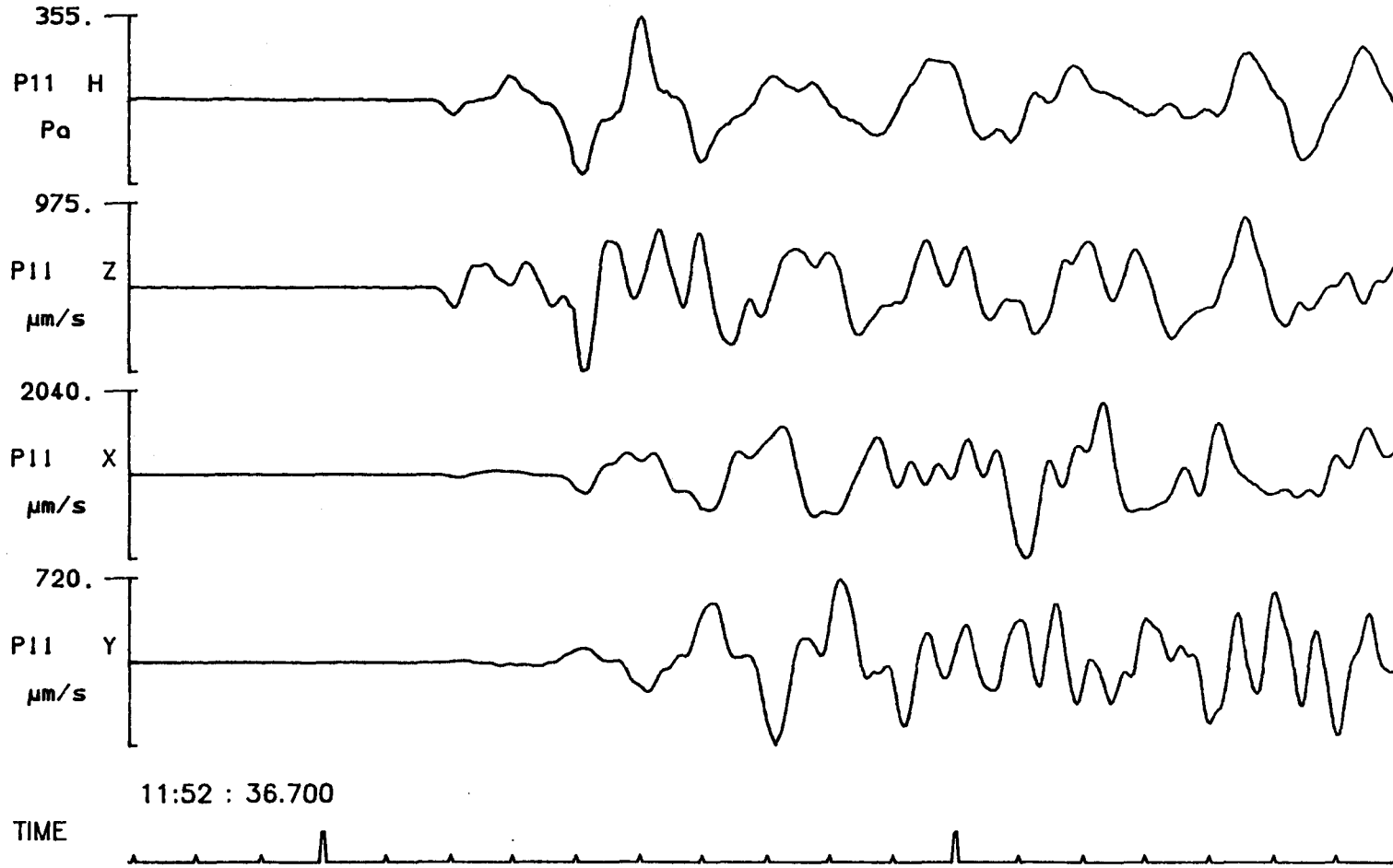


Fig. F.3.3

PUSS 09, RANGE=25.002 KM, 4500LB SHOT SEISMIC ARRIVAL

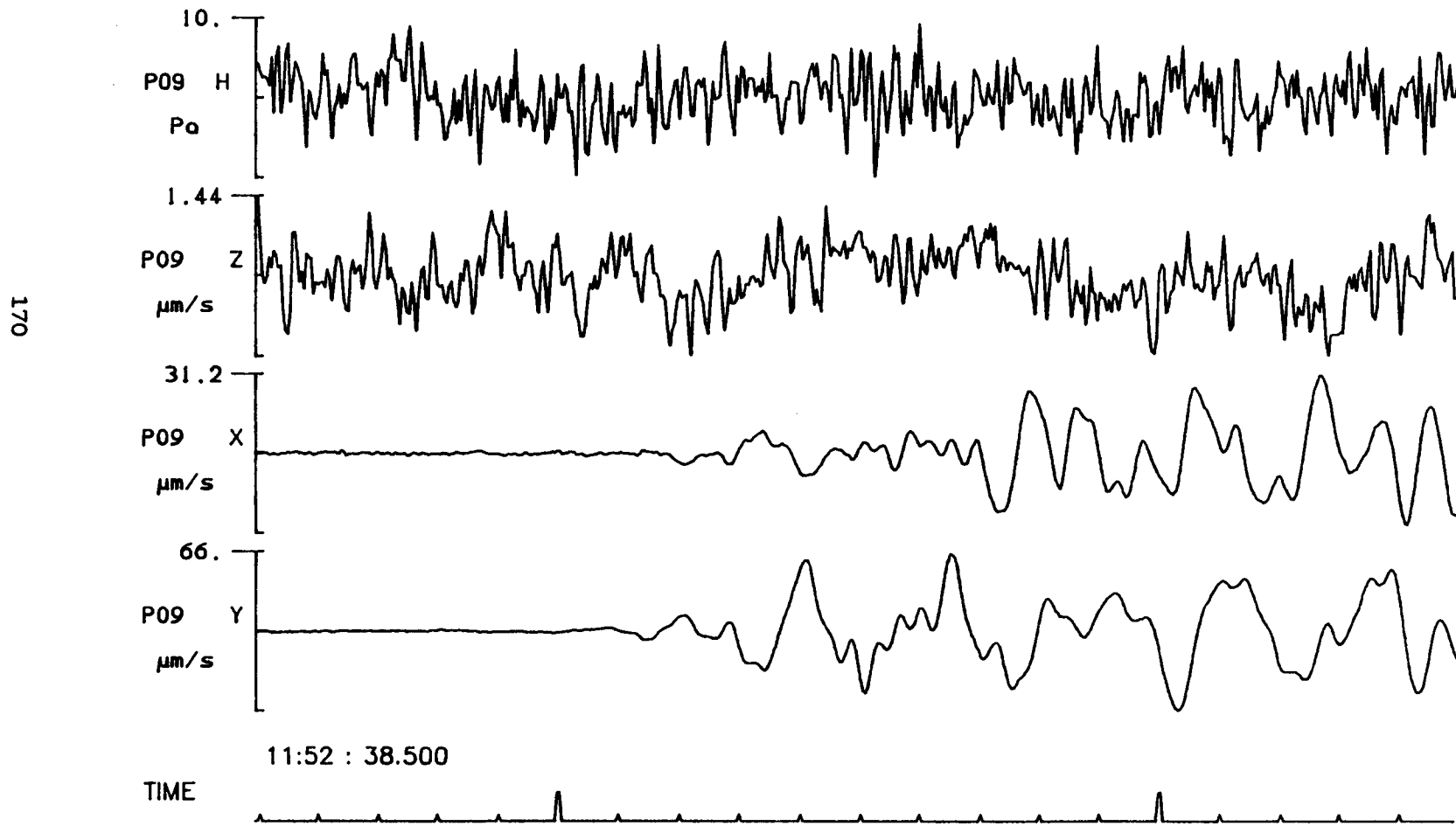


Fig. F.3.4

PUSS 13, RANGE=39.705 KM, 4500LB SHOT SEISMIC ARRIVAL

171

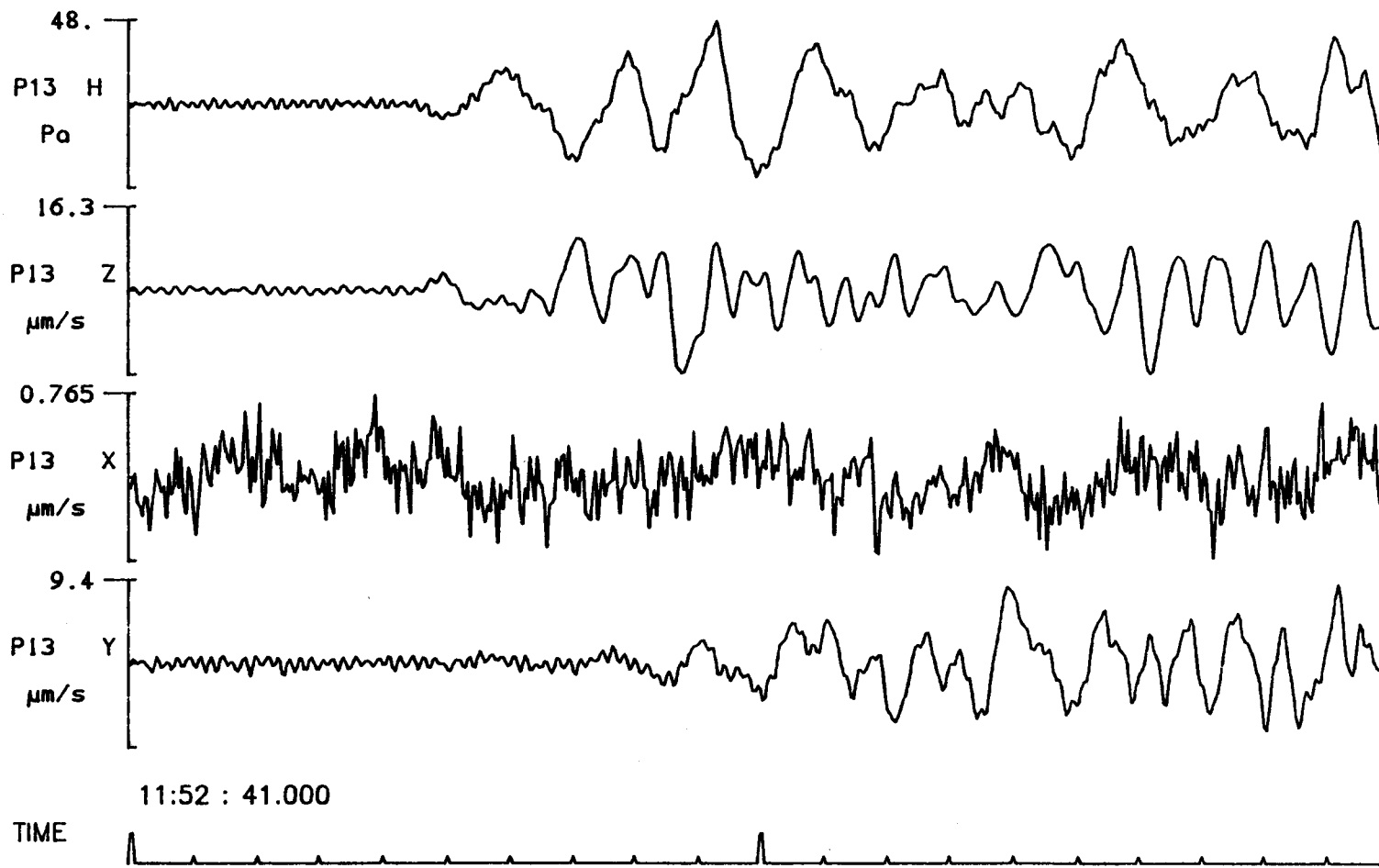
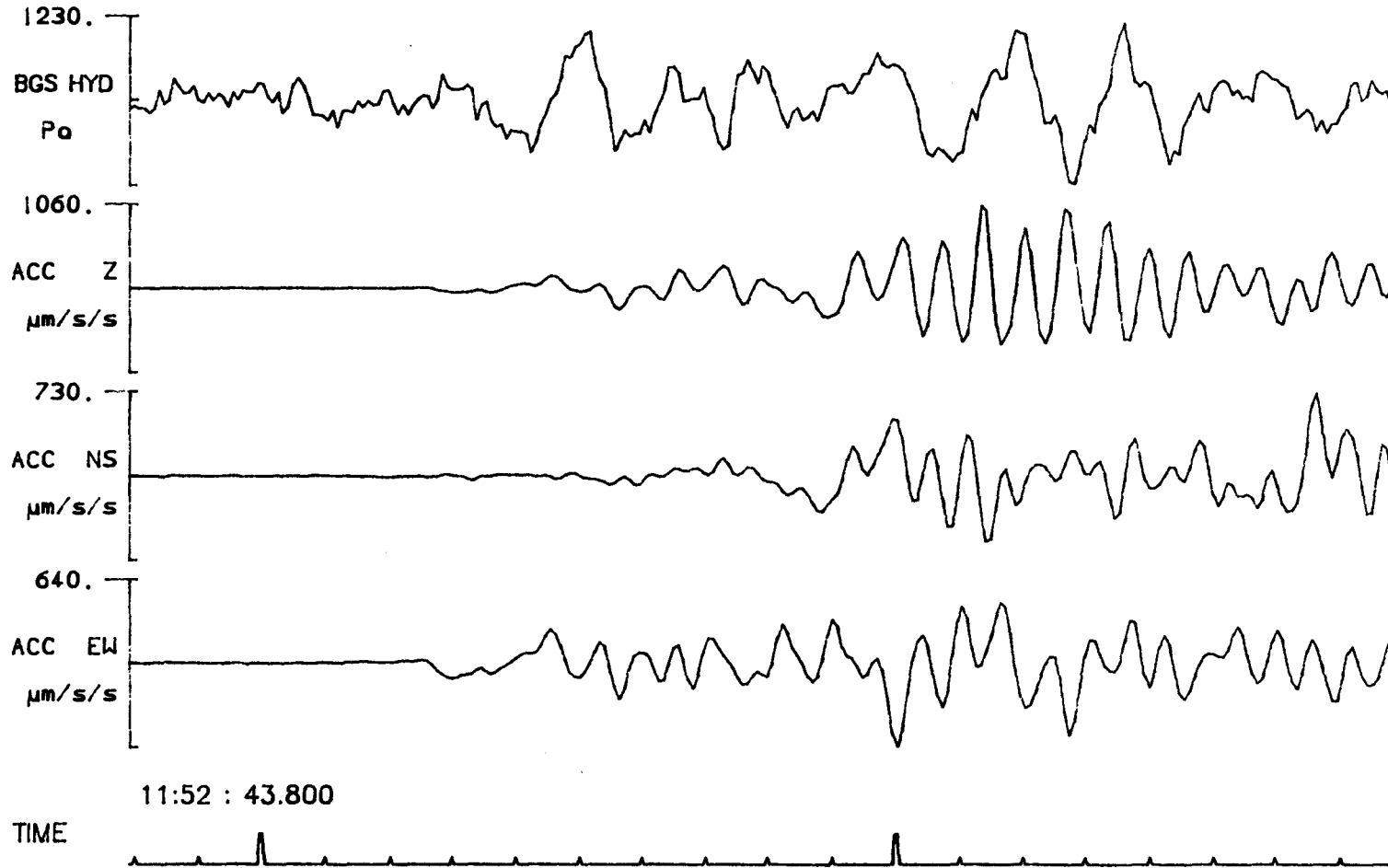


Fig. F.3.5

BGS Sea Bottom Package RANGE=60.035 KM, 4500LB SHOT SEISMIC ARRIVAL



172

Fig. F.3.6

BGS Sea Bottom Package RANGE=60.035 KM, 4500LB SHOT SEISMIC ARRIVAL

173

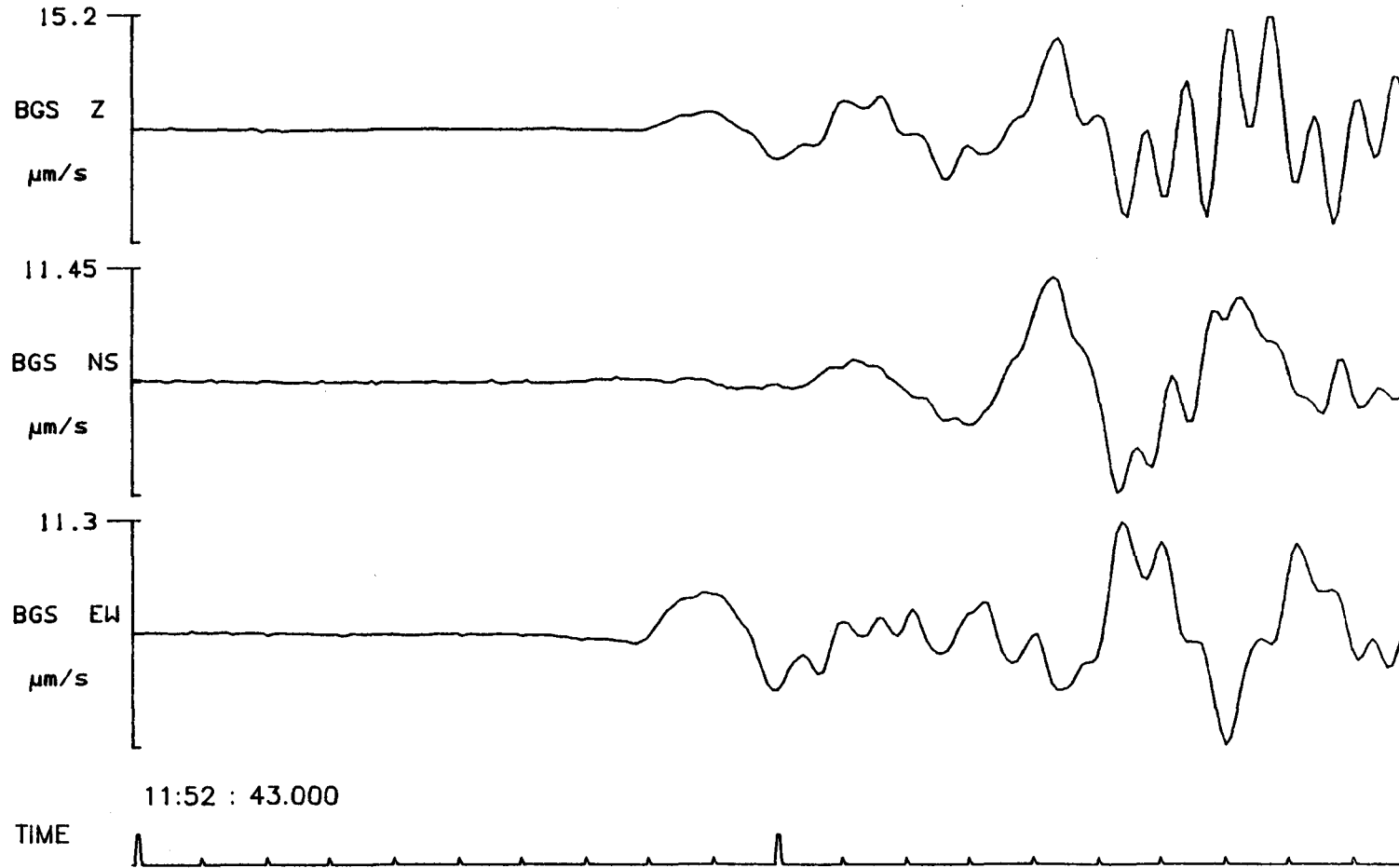


Fig. F.3.7

PUSS 14, RANGE=85.291 KM, 4500LB SHOT SEISMIC ARRIVAL

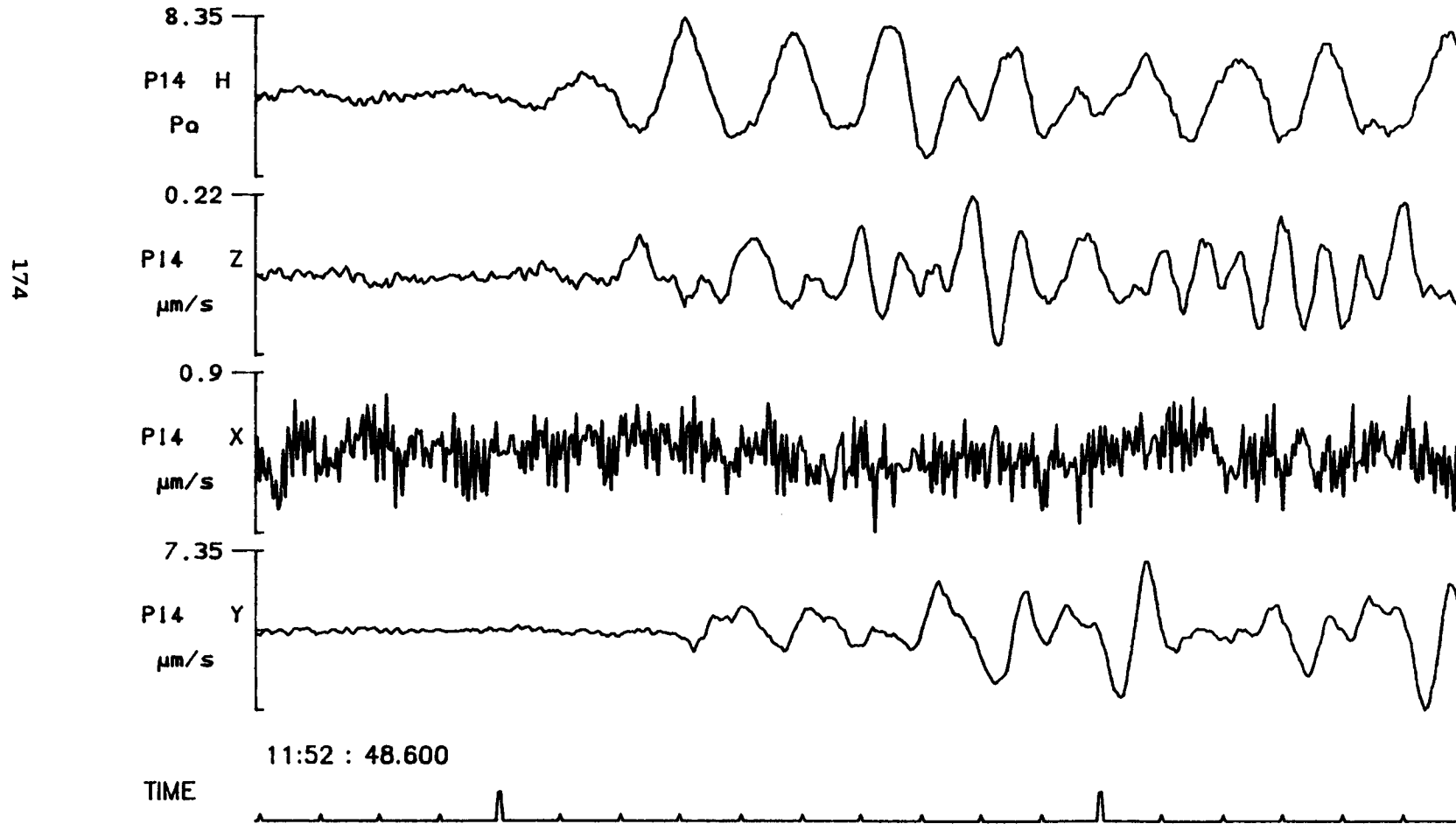


Fig. F.3.8

Tentsmuir, 4500LB SHOT, seismic arrival, Filtered at 8Hz

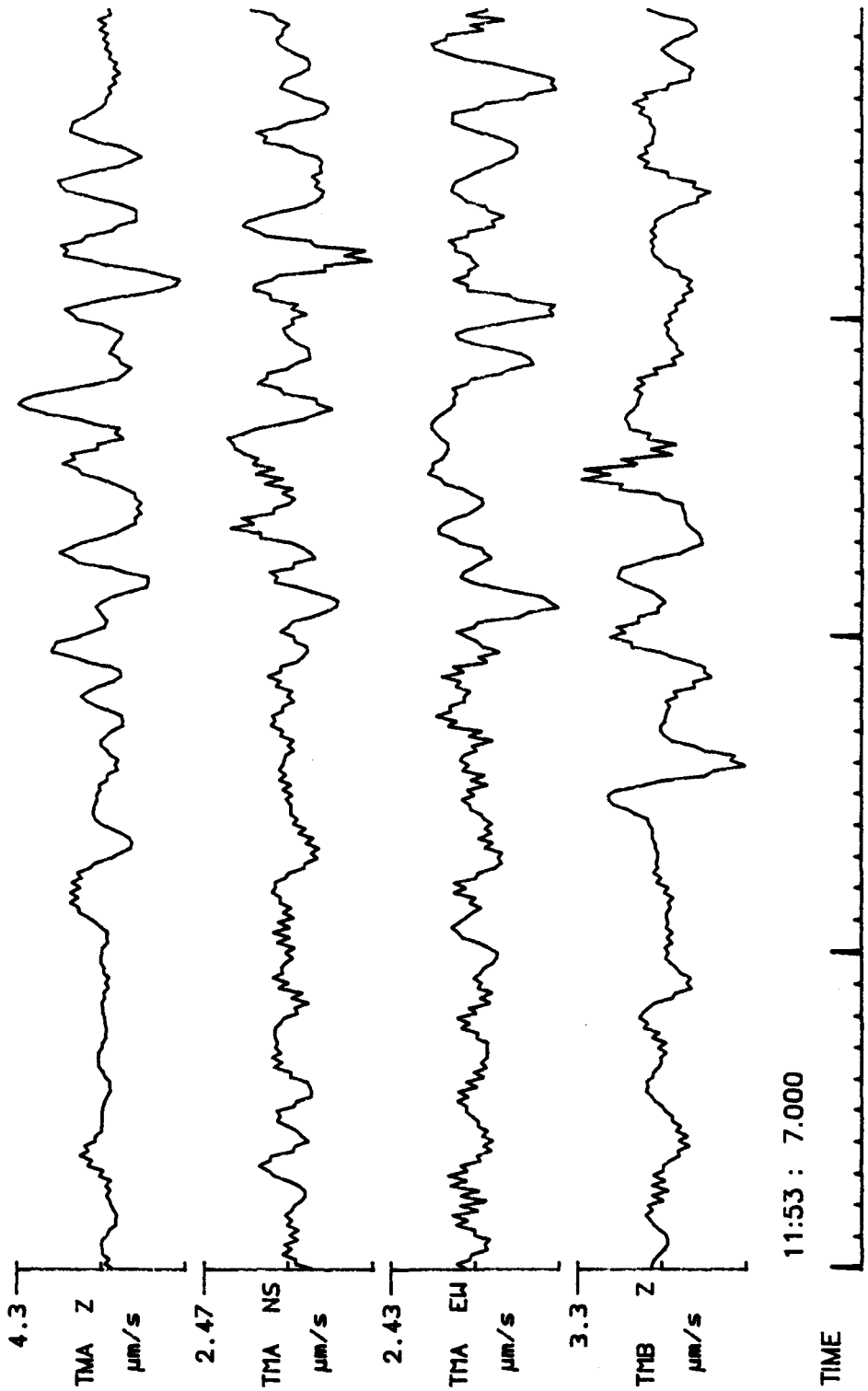


Fig. F.3.9

PUSS 10, RANGE=9.982 KM, 900LB SHOT SEISMIC ARRIVAL

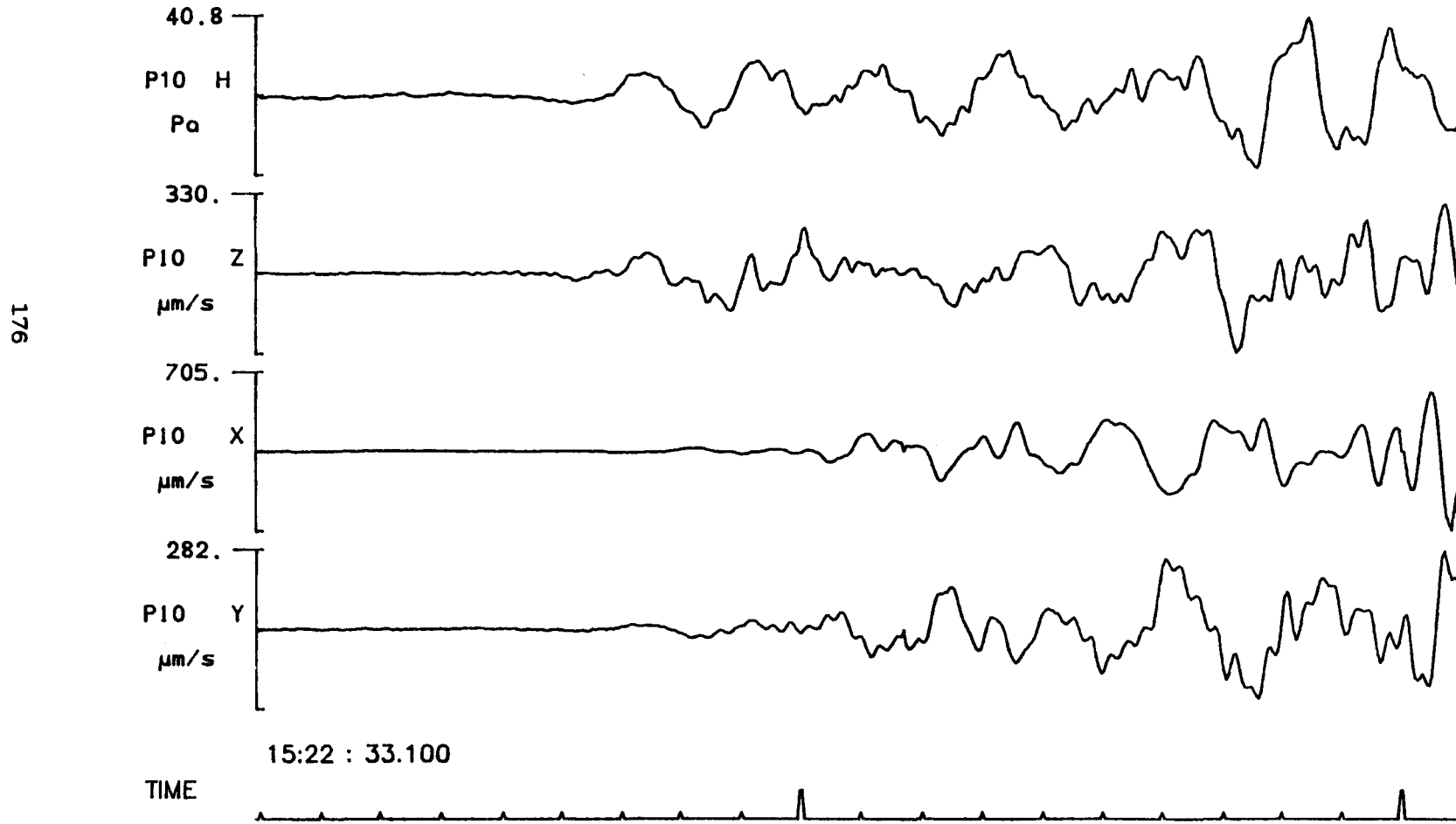


Fig. F.3.10

PUSS 11, RANGE=14.543 KM, 900LB SHOT SEISMIC ARRIVAL

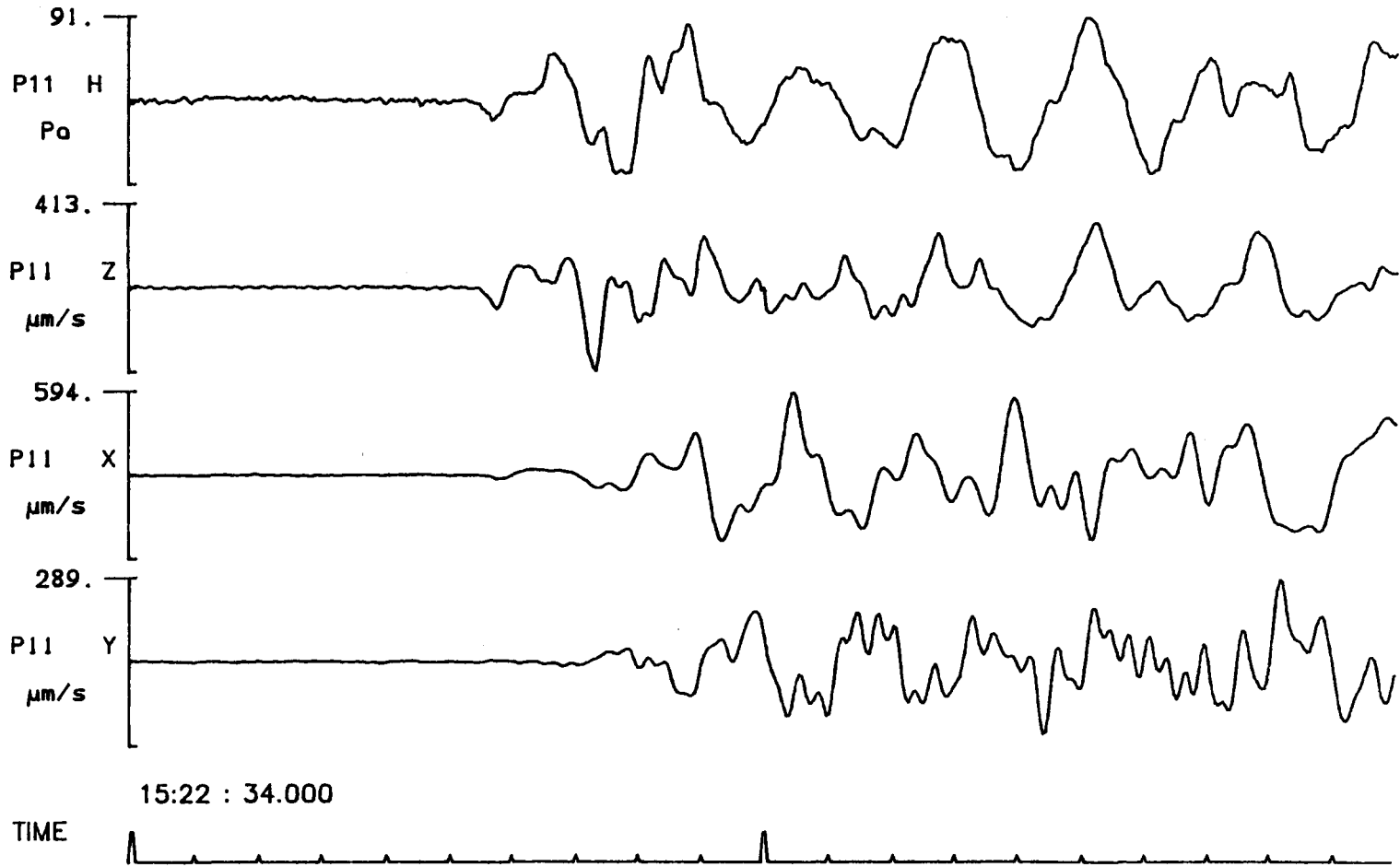


Fig. F.3.11

PUSS 09, RANGE=25.002 KM, 900LB SHOT SEISMIC ARRIVAL

178

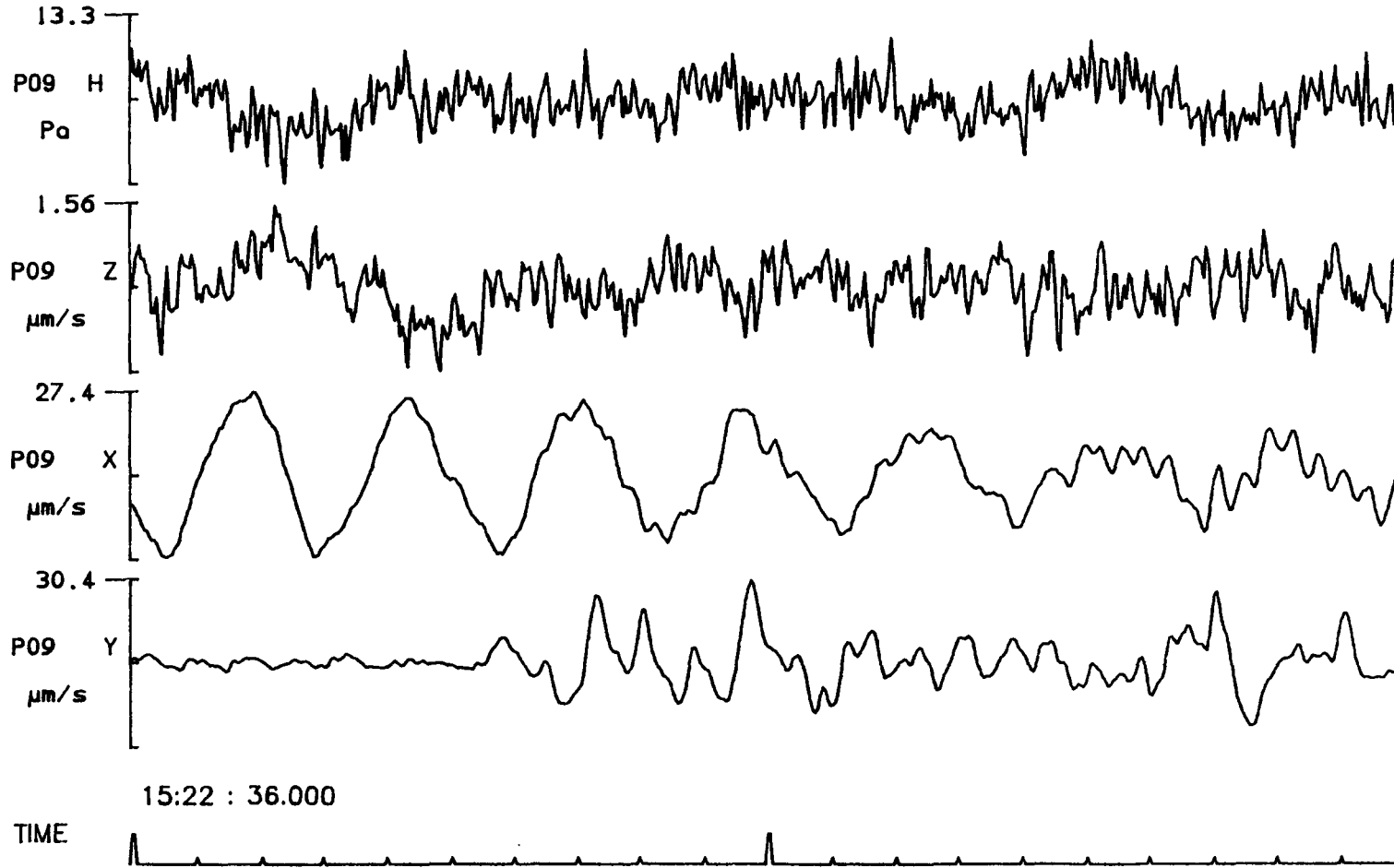


Fig. F.3.12

PUSS 13, RANGE=39.705 KM, 900LB SHOT SEISMIC ARRIVAL

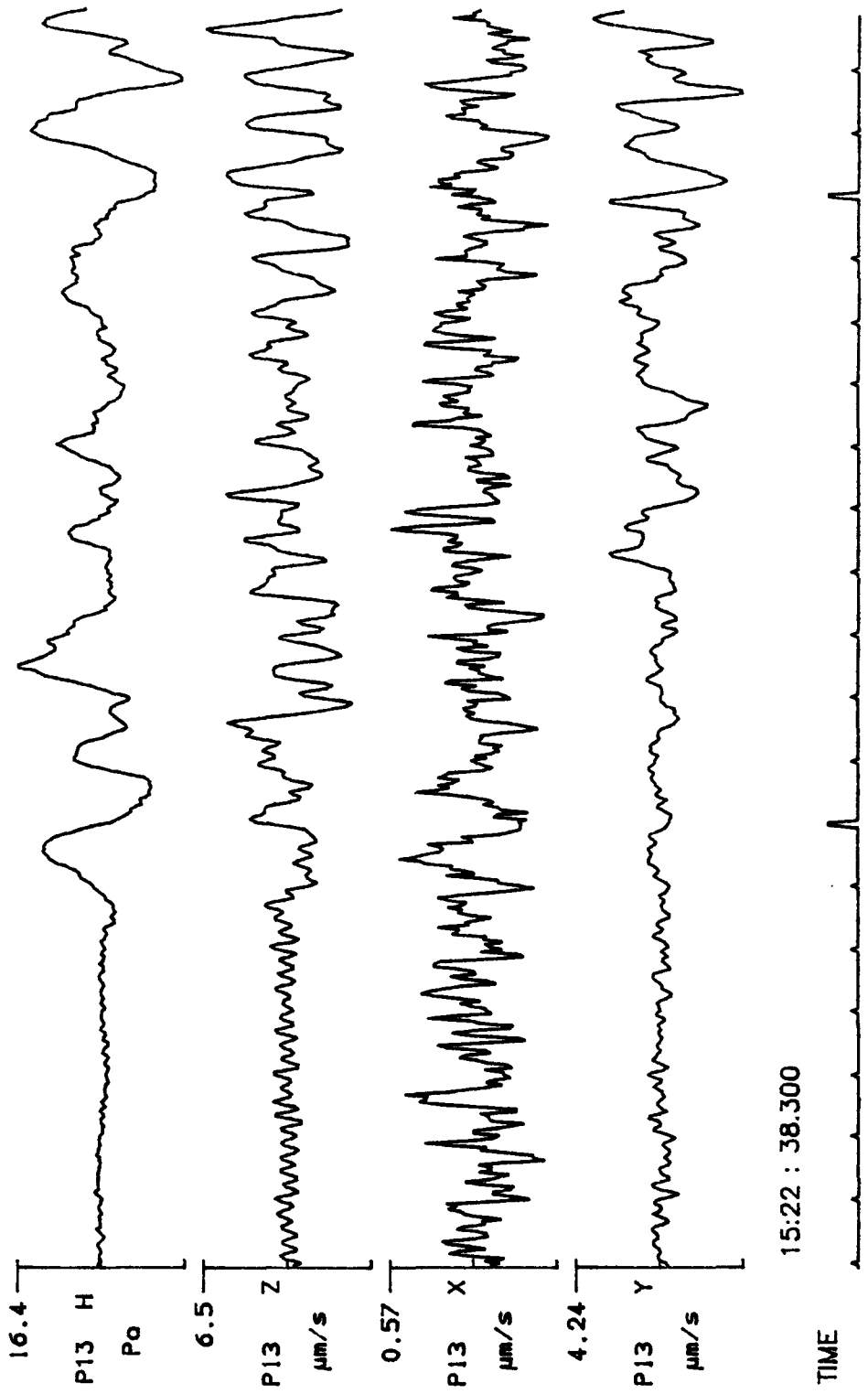


Fig. F.3.13

BGS Sea Bottom Package RANGE=60.035 KM, 900LB SHOT SEISMIC ARRIVAL

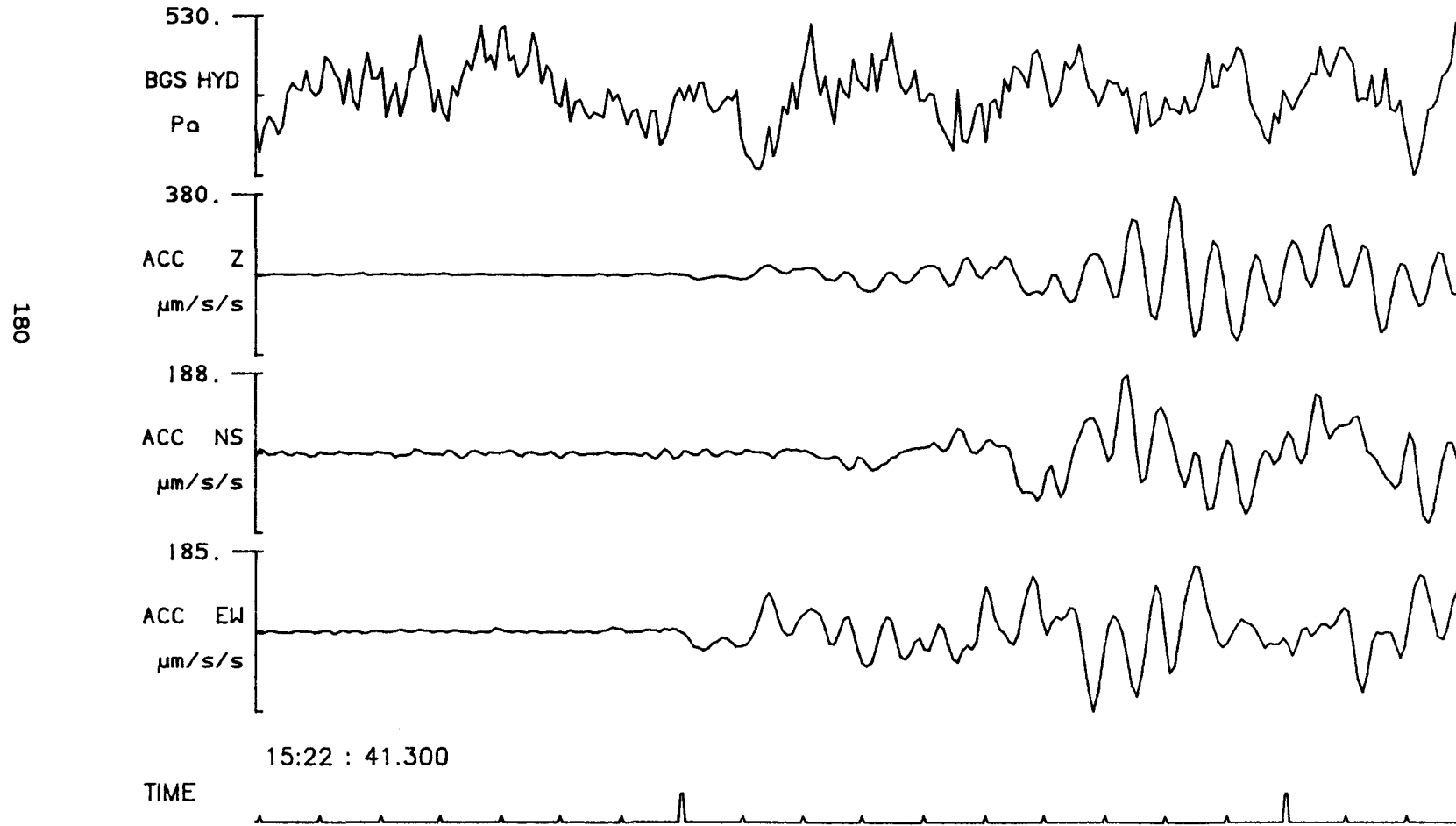


Fig. F.3.14

BGS Sea Bottom Package RANGE=60.035 KM, 900LB SHOT SEISMIC ARRIVAL

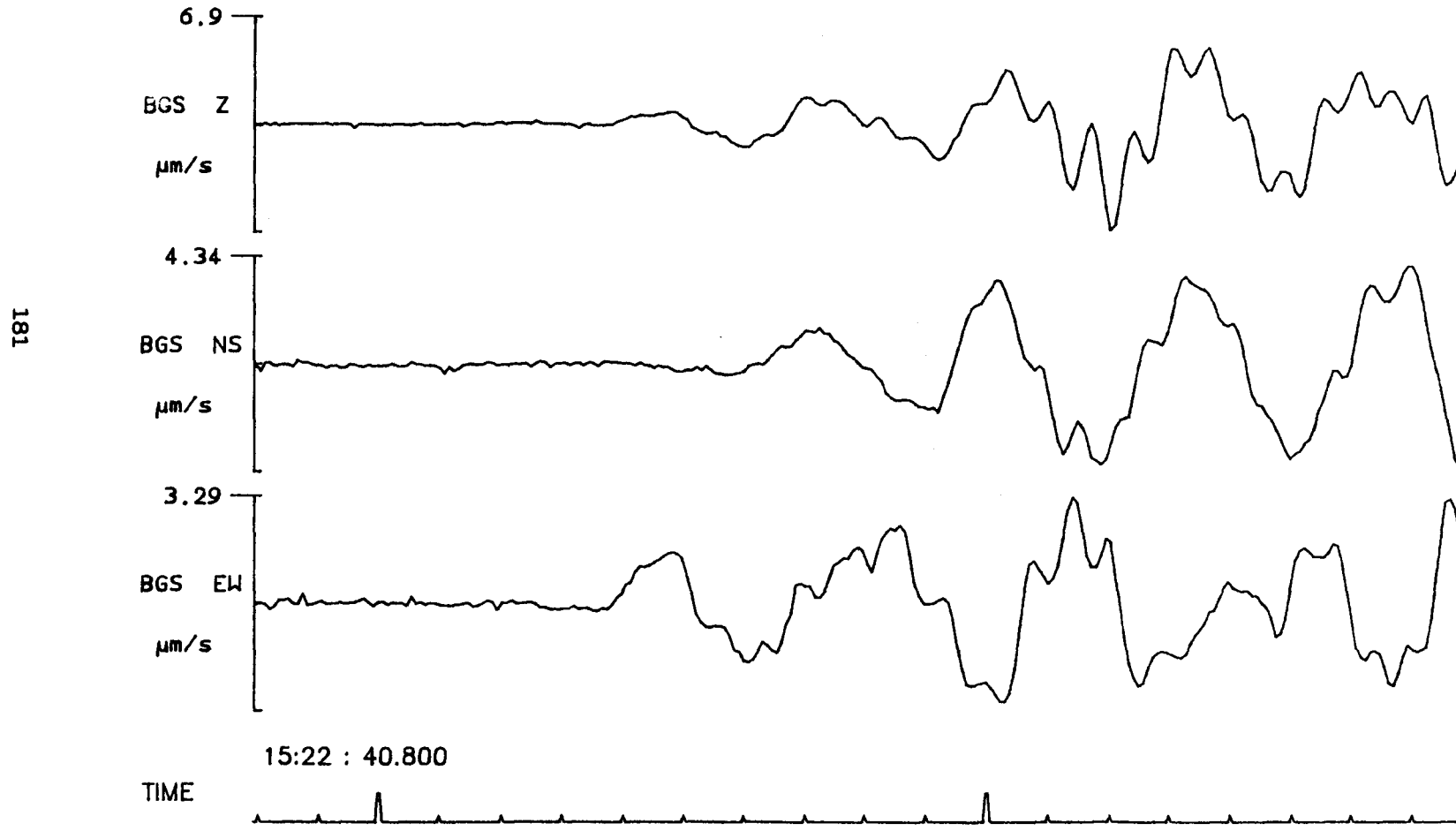
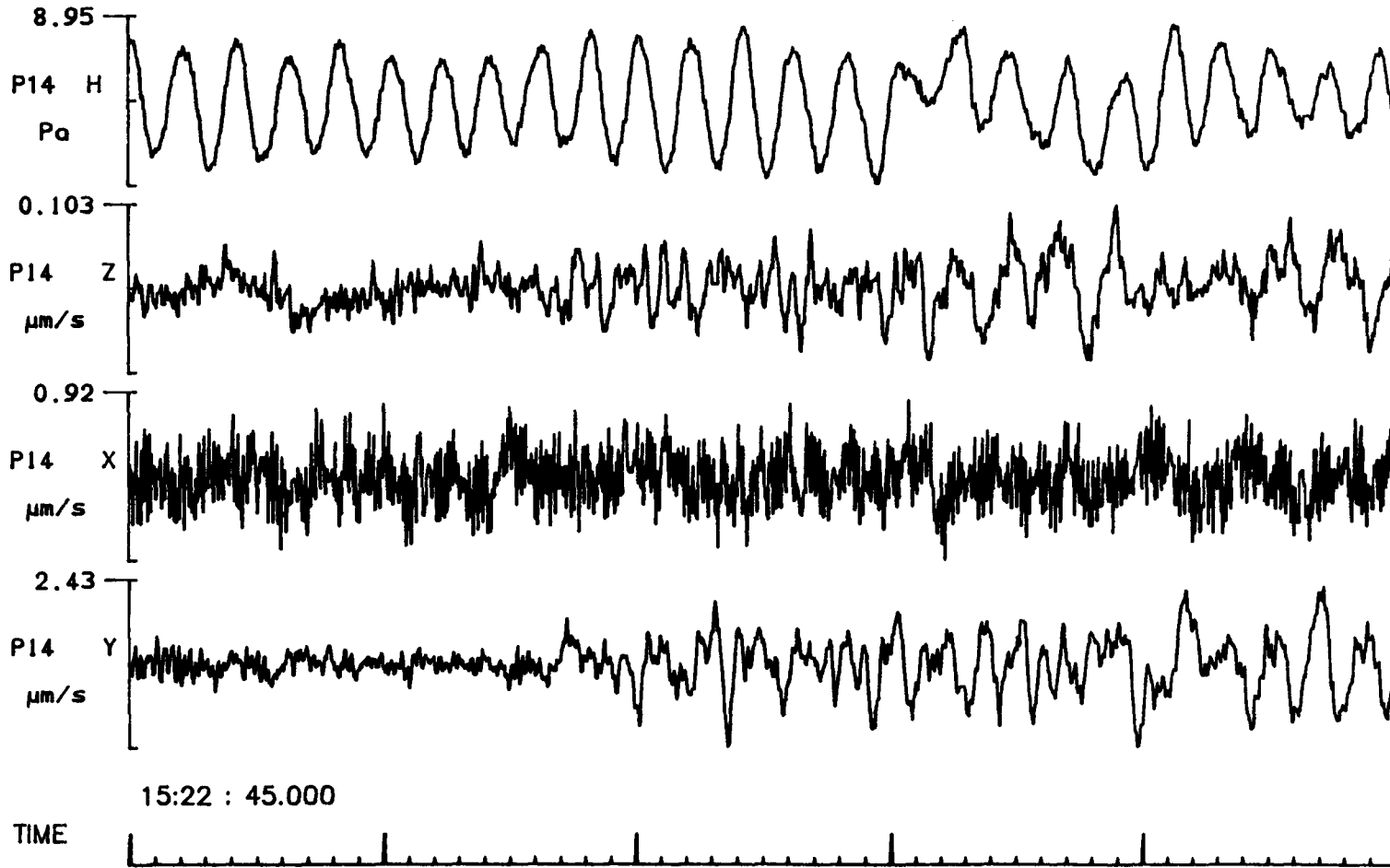


Fig. F.3.15

PUSS 14, RANGE=85.291 KM, 900LB SHOT SEISMIC ARRIVAL



Appendix G: Picking list for travel time determinations

Filename = name of file on magnetic tape. (suffix S. indicates that the record has been despiked and zeroed before processing.); N = number of the datum in the file corresponding to the pick; DT = elapsed time in seconds equivalent to N.

Shot timing:

4500lb shot time = 11:52:33.2252(+1ms)
 900lb shot time 15:22:30.5910(+1ms)

Start of record = 11:52:05.0

Filename	N	ΔT	Type of arrival
H10G1S.	7995	31.227	seismic
H10G1S.	8997	35.141	acoustic
Z10G1S.	7995	31.230	seismic
Z10G1S.	8999	35.152	acoustic
Z10G1S.	16237	63.426	interface? not a sharp arrival
X10G1S.	8004	31.266	seismic?
X10G1S.	8013	31.301	seismic -
X10G1S.	8042	31.414	seismic (main signal)
X10G1S.	8998	35.148	weak acoustic arrival?
X10G1S.	9002	35.164	main acoustic arrival
X10G1S.	9005	35.176	2nd acoustic arrival? +
Y10G1S.	7996	31.234	seismic (weak 1st break)
Y10G1S.	8042	31.414	seismic (main signal)
Y10G1S.	8998	35.148	acoustic (weak arrival)
Y10G1S.	9003	35.168	acoustic (main arrival)
Y10G1S.	9006	35.180	acoustic (2nd arrival +)
H11G1S.	8236	32.168	seismic
H11G1S.	9781	38.203	acoustic
Z11G1S.	8237	32.176	seismic
Z11G1S.	9784	38.215	acoustic
X11G1S.	8239	32.180	seismic
X11G1S.	9781	38.203	acoustic
Y11G1S.	8236	32.168	seismic
Y11G1S.	9784	38.215	acoustic
H09G1S.	11569	45.191	acoustic, first break
H09G1S.	11573	45.207	acoustic, start of main signal
Z09G1S.	11573	45.207	acoustic first break
Z09G1S.	11579	45.230	acoustic, start of main signal
X09G1S.	8752	34.188	seismic first break
X09G1S.	8778	34.289	seismic, main arrival
X09G1S.	11578	45.227	acoustic HF arrival
X09G1S.	11570	45.195	acoustic? large +ve pulse before HF arrival
Y09G1S.	8648	33.781	seismic ? possible first break
Y09G1S.	8703	33.996	seismic (break)
Y09G1S.	8727	34.090	seismic, main signal
Y09G1S.	11570	45.195	acoustic, first break
Y09G1S.	11576	45.219	acoustic, main signal onset

Start of record = 11:52:05.0

Filename	N	ΔT	Type of arrival
H13G1S.	9333	36.457	seismic, first break (noisy)
H13G1S.	14089	55.035	acoustic, first break
H13G1S.	14102	55.086	acoustic, 2nd arrival
Z13G1S.	14090	55.039	acoustic, first break (HF)
Z13G1S.	14098	55.070	acoustic? 2nd arrival (LF)
Z13G1S.	14102	55.086	acoustic, main signal (HF)
Z13G1S.	9334	36.461	seismic
X13G1S.	14090	55.039	acoustic, first break
X13G1S.	14102	55.086	acoustic?, 2nd arrival?
Y13G1S.	14094	55.055	acoustic, first break
Y13G1S.	14103	55.090	acoustic, 2nd arrival
Y13G1S.	9347	36.512	seismic, 1st break? (noisy)
Y13G1S.	9422	36.805	seismic ? (noisy)
H14G1S.	11168	43.625	seismic, poss. 1st break
H14G1S.	11312	44.188	seismic, main signal
H14G1S.	11459	44.762	seismic, poss 2nd arr.
H14G1S.	21899	85.543	acoustic, 1st break
H14G1S.	21912	85.594	acoustic, HF, ?2nd arr.
Z14G1S.	11268	44.016	seismic? poss lf precursor?
Z14G1S.	11314	44.195	seismic, main signal, low signal/noise
Z14G1S.	21901	85.551	acoustic, 1st break
Z14G1S.	21910	85.586	acoustic, HF arrival
X14G1S.			no visible seismic arrival
X14G1S.	21894	85.523	acoustic, 1st break ,mf
X14G1S.	21903	85.559	acoustic, main signal onset, (not clear)
X14G1S.	21916	85.609	acoustic, HF onset (not clear)
Y14G1S.	11340	44.297	seismic, main signal
Y14G1S.	11288	44.094	seismic,? poss lf precursor?
Y14G1S.	21889	85.504	acoustic ? weak precursor?
Y14G1S.	21903	85.559	acoustic, MF arrival
Y14G1S.	21912	85.594	acoustic, HF arrival

Start of record = 15:22:05.0

Filename	N	ΔT	Type of arrival
H10G2S.	7308	28.547	seismic? (very weak)
H10G2S.	7327	28.621	seismic? +ve
H10G2S.	7344	28.688	seismic (main signal)
H10G2S.	8321	32.504	acoustic, weak 1st break
H10G2S.	8326	32.523	acoustic (main signal last possible posn)
Z10G2S.	7225	28.223	seismic? very weak
Z10G2S.	7251	28.324	seismic? very weak
Z10G2S.	7279	28.434	seismic, 1st clear arrival
Z10G2S.	7320	28.594	seismic, 2nd arrival main signal
Z10G2S.	7346	28.695	seismic ? possible 3rd arrival
Z10G2S.	8324	32.516	acoustic, initial onset weak
Z10G2S.	8330	32.539	acoustic, possible 2nd arrival
Z10G2S.	8342	32.586	acoustic, main signal
X10G2S.	7341	28.676	seismic, first break
X10G2S.	7427	29.012	seismic 2nd arrival
X10G2S.	8321	32.504	acoustic, first break (v.weak)
X10G2S.	8327	32.527	acoustic main arrival
X10G2S.	8387	32.762	acoustic? 2nd arrival
Y10G2S.	7320	28.594	seismic first break
Y10G2S.	7365	28.770	seismic 2nd arrival
Y10G2S.	7409	28.941	seismic ? 3rd arrival
Y10G2S.	8325	32.520	acoustic first break
Y10G2S.	8336	32.563	acoustic 2nd arr.
Y10G2S.	8378	32.727	acoustic main signal
H11G2S.	7523	29.383	seismic
H11G2S.	7539?	29.445	seismic
H11G2S.	7559	29.523	seismic
H11G2S.	9100	35.543	acoustic
Z11G2S.	7564/8	29.543	seismic (unclear)
		29.559	
Z11G2S.	9106	35.566	acoustic
X11G2S.	7564	29.543	seismic
X11G2S.	9108	35.574	acoustic
Y11G2S.	7564	29.543	seismic
Y11G2S.	9100/1	35.543	acoustic
		35.547	
H09G2S.	10893	42.551	acoustic, first break
H09G2S.	10898	42.570	acoustic, main signal
Z09G2S.	10903	42.590	acoustic (noisy)
X09G2S.	8066	31.508	seismic? obscured by noise
X09G2S.	10896	42.563	acoustic, first break
Y09G2S.	8073	31.535	seismic, main signal
Y09G2S.	10895	42.559	acoustic, first break
Y09G2S.	10898	42.570	acoustic, main signal

Start of record = 15:22:05.0

Filename	N	ΔT	Type of arrival
H13G2S.	8491	33.168	seismic, LF precursor
H13G2S.	8661	33.832	seismic, MF arrival
H13G2S.	8671	33.871	seismic, main signal
H13G2S.	13413	52.395	acoustic, first break
H13G2S.	13416	52.406	acoustic, main signal
Z13G2S.	8678	33.898	seismic, main signal, low signal/noise
Z13G2S.	13417	52.410	acoustic, poss weak precursor
Z13G2S.	13425	52.441	acoustic, main signal
X13G2S.	13415	52.402	acoustic, poss weak precursor
X13G2S.	13418	52.414	acoustic, main signal onset
X13G2S.			no seismic signal present
Y13G2S.	8679	33.902	seismic, poss 1st break , noisy
Y13G2S.	8807	34.402	seismic, main signal onset, (high mag)
Y13G2S.	13388	52.297	acoustic, LF precursor
Y13G2S.	13418	52.414	acoustic, weak arrival 1st break hf
Y13G2S.	13430	52.461	acoustic main signal
Y13G2S.	13425	52.441	acoustic, 2nd arr.?
H14G2S.	21224	82.906	acoustic, first break
H14G2S.	21232	82.938	acoustic, main signal onset
Z14G2S.	10403	40.637	seismic ?? poss arr.
Z14G2S.	10685	41.738	seismic, main signal (v.weak)
Z14G2S.	21223	82.902	acoustic, 1st break
Z14G2S.	21235	82.949	acoustic, main signal onset
X14G2S.			seismic arrival not pickable
X14G2S.	21230	82.930	acoustic, possible 1st break
X14G2S.	21236	82.953	acoustic, hf onset
X14G2S.	21249	83.004	acoustic, main signal onset
Y14G2S.	10618	41.477	seismic ??
Y14G2S.	10664	41.656	seismic, main signal , v noisy
Y14G2S.	21213	82.863	acoustic, ? 1st break
Y14G2S.	21233	82.941	acoustic, HF onset

BGS Sea bottom package: acceleration
 Start of record = 11:52:04.71

Filename	N	ΔT	Type of arrival
HBAG1S.	5072	39.625	seismic arrival, v noisy
HBAG1S.	8677	67.789	acoustic, main signal onset
HBAG1S.	8674	67.766	acoustic, poss 1st break?
ZBAG1S.	5056	39.500	seismic, 1st break
ZBAG1S.	5063	39.555	seismic, 2nd arr
ZBAG1S.	5074	39.641	seismic, main signal
ZBAG1S.	8669	67.727	acoustic, 1st break
ZBAG1S.	8683	67.836	acoustic, HF arrival?
NSBAG1S.	5046	39.422	seismic ? poss 1st break (displacement)
NSBAG1S.	5065	39.570	seismic arr.
NSBAG1S.	5087	39.742	seismic arr., main signal onset
NSBAG1S.	5097	39.820	seismic, main signal arr.
NSBAG1S.	8640	67.500	acoustic, weak lf arrival?
NSBAG1S.	8668	67.719	acoustic, main arrival
EWBAG1S.	5046	39.422	seismic, 1st break (LF)
EWBAG1S.	5056	39.500	seismic, 2nd arrival
EWBAG1S.	5063	39.555	seismic, main signal onset
EWBAG1S.	5074	39.641	seismic arr.?
EWBAG1S.	8641	67.508	acoustic, weak HF
EWBAG1S.	8669	67.727	acoustic, main signal

BGS Sea bottom package: acceleration
 Start of record = 15:22:05.03

Filename	N	ΔT	Type of arrival
HBAG2S.	4604	35.969	seismic??
HBAG2S.	8331	65.086	acoustic, 1st break
HBAG2S.	8344	65.188	acoustic, 2nd arr
HBAG2S.	8357	65.289	acoustic, HF onset
ZBAG2S.	4732	36.969	seismic, 1st break
ZBAG2S.	4758	37.172	seismic 2nd arr?
ZBAG2S.	4799	37.492	seismic, 3rd. main signal
ZBAG2S.	8330	65.078	acoustic, (slope change)
ZBAG2S.	8340	65.156	acoustic, poss. arr.
ZBAG2S.	8375	65.430	acoustic, main signal
NSBAG2S.	4482	35.016	seismic??
NSBAG2S.	4760	37.188	seismic, 1st break?
NSBAG2S.	4802	37.516	seismic, main signal
NSBAG2S.	8335	65.117	acoustic, 1st break
NSBAG2S.	8352	65.250	acoustic 2nd. arr.
EWBAG2S.	4732	36.969	seismic, main signal
EWBAG2S.	8343	65.180	acoustic, 1st break
EWBAG2S.	8349	65.227	acoustic arr. weak
EWBAG2S.	8365	65.352	acoustic arr.
EWBAG2S.	8380	65.469	acoustic, main signal
EWBAG2S.	8387	65.523	acoustic arr.

BGS Sea bottom package: velocity
 Start of record = 11:52:04.18

Filename	N	ΔT	Type of arrival
ZBVG1S.	5069	39.602	seismic, main signal
ZBVG1S.	5080	39.688	seismic arrival
ZBVG1S.	8679	67.805	acoustic, 1st break?
ZBVG1S.	8733	68.227	acoustic, HF
NSBVG1S.	5048	39.438	seismic, poss 1st break LF
NSBVG1S.	5076	39.656	seismic, weak arr. lf
NSBVG1S.	5083	39.711	seismic, LF arrival
NSBVG1S.	5117	39.977	seismic, main signal?
NSBVG1S.	8677	67.789	acoustic, 1st break?
NSBVG1S.	8730	68.203	acoustic, HF arrival
NSBVG1S.	8700	67.969	acoustic ?
EWBVG1S.	5045	39.414	seismic, 1st break, LF
EWBVG1S.	5069	39.602	seismic, main signal
EWBVG1S.	5092	39.781	seismic, main signal, 2nd arr.?
EWBVG1S.	8692	67.906	acoustic, LF
EWBVG1S.	8708	68.031	acoustic arr.?
EWBVG1S.	8720	68.125	acoustic, HF onset

BGS Sea bottom package: velocity
 Start of record = 15:22:04.37

Filename	N	ΔT	Type of arrival
ZBVG2S.	4738	37.016	seismic, first break
ZBVG2S.	4827	37.711	seismic arr. mf
ZBVG2S.	8362	65.328	acoustic, poss weak arrival
ZBVG2S.	8369	65.383	acoustic, poss. weak arr.
ZBVG2S.	8385	65.508	acoustic, poss. weak arr.
ZBVG2S.	8395	65.586	acoustic, main HF onset
NSBVG2S.	4745	37.070	seismic, poss 1st break, (ch slope)
NSBVG2S.	4758	37.172	seismic, arr. main onset
NSBVG2S.	4833	37.758	seismic arr.?
NSBVG2S.	8344	65.188	acoustic, 1st break?
NSBVG2S.	8384	65.500	acoustic, HF onset
EWBVG2S.	4736	37.000	seismic arr. main signal onset
EWBVG2S.	4758	37.172	seismic arr.?
EWBVG2S.	8350	65.234	acoustic, poss. weak arr.
EWBVG2S.	8372	65.406	poss weak arr. alternate posn.
EWBVG2S.	8374	65.422	acoustic, poss. weak arr.
EWBVG2S.	8387	65.523	acoustic, main HF onset

BGS VHS

Start of record = 11:53:13.96

Filename	N	ΔT	Type of arrival
hy01g1S.	1313	0.652	acoustic, first break
hy02g1S.	1311	0.651	acoustic, first break
hy03g1S.	1313	0.652	acoustic, first break
hy04g1S.	1314	0.653	acoustic, first break
hy05g1S.	1314	0.653	acoustic, first break
hy06g1S.	1313	0.652	acoustic, first break
hy06g1S.	1325	0.658	acoustic ? 2nd arrival?
hy07g1S.	1313	0.652	acoustic, 1st break
hy08g1S.	1312	0.652	acoustic, 1st break
hy09g1S.	1313	0.652	acoustic, 1st break
hy09g1S.	1297	0.644	acoustic, HF?
hy10g1S.	1322	0.657	acoustic, main signal (noisy)
hy10g1S.	1315	0.653	acoustic, HF? poss 1st break

BGS VHS

Start of record = 15:23:09.95

Filename	N	ΔT	Type of arrival
hy01g2S.	2111	1.049	acoustic, first break
hy01g2S.	2115	1.051	acoustic, main signal
HY02g2S.	2106	1.047	acoustic, first break
HY02g2S.	2122	1.055	acoustic, main signal
hy03g2S.	2106	1.047	acoustic, first break
hy03g2S.	2115	1.051	acoustic, 2nd arrival
HY04g2S.	2108	1.048	acoustic, first break
HY04g2S.	2117	1.052	acoustic 2nd arrival?
HY04g2S.	2123	1.055	acoustic, main signal onset.
hy05g2S.	2111	1.049	acoustic, first break
hy05g2S.	2121	1.054	acoustic, 2nd arrival
hy06g2S.	2115	1.051	acoustic, main signal
hy06g2S.	2100	1.044	acoustic, ? possible 1st break, v.weak
hy07g2S.	2094	1.041	acoustic, first break? low amplitude
hy07g2S.	2106	1.047	acoustic? possible arrival (phase change)
hy07g2S.	2114	1.051	acoustic, main signal
hy08g2S.	2094	1.041	acoustic, poss. 1st break (ch slope)
hy08g2S.	2107	1.047	acoustic, onset of HF
hy08g2S.	2112	1.050	acoustic, poss arrival? (ch amp)
hy08g2S.	2116	1.052	acoustic, main signal onset
hy09g2S.	2062	1.025	acoustic? poss weak arrival? from sea bed?
hy09g2S.	2082	1.035	acoustic ? poss weak HF arrival?
hy09g2S.	2094	1.041	acoustic, ? 1st break
hy09g2S.	2105	1.046	acoustic, onset of HF
hy09g2S.	2110	1.049	acoustic, 2nd arrival
hy09g2S.	2114	1.051	acoustic, main signal
hy10g2S.	2082	1.035	acoustic, ? poss HF
hy10g2S.	2088	1.038	acoustic, poss arrival?
hy10g2S.	2096	1.042	acoustic, possible arrival?
hy10g2S.	2107	1.047	acoustic, main signal, NB amplitude down.
hy10g2S.	2113	1.050	acoustic main arrival

Appendix H: Photographic record of the experiment.

Cover	RMAS Salmaster from Forth Road Bridge (Fergus I. McTaggart)
Frontispiece	Flags flown by RMAS Salmaster.
collage	British Geological Survey equipment container being loaded onto RMAS Salmaster Foredeck of RMAS Salmaster at sea.
Plate 1	Shot point mooring buoys on foredeck of RMAS Salmaster.
Plate 2	Orange shot point buoy and crate containing MSF radio time receiver for signal timing on analogue tape data recorders.
Plate 3	Recording Laboratory for hydrophone strings and the BGS Sea Bottom Package in portacabin between decks on RMAS Salmaster.
Plate 4	Checking and testing laboratory for Pull-Up Sea-bottom Seismometers (PUSSes) on RMAS Salmaster
Plate 5	Syledis computer for high accuracy navigation and positioning at sea.
Plate 6	Qubit monitor of Syledis navigational system mounted on the Bridge of RMAS Salmaster.
Plate 7	Qubit monitor screen in action. Note the target position at the centre of the bulls-eye, the current position of RMAS Salmaster some 1200m north and the line representing a section of the experiment great circle from the shot point to Tentsmuir.
Plate 8	PUSS, pressure sealed tube end.
Plate 9	PUSS, tube end removed.
Plate 10	PUSS instrumentation wired up at sea for testing and setting of recording time windows prior to deployment.
Plate 11	Final preparations of PUSS on deck immediately prior to deployment. Note quarter tonne anchor weights in background.
Plate 12	PUSS tube on deck fully prepared for deployment. Note hydrophone strapped to the tube and the dumb-bell weights at both ends of the tube.
Plate 13	PUSS being lowered into the sea at deployment.
Plate 14	Toroidal buoy used to mark the position of PUSS deployment for eventual retrieval. Note the radar reflector and flashing lamp installed on the superstructure.
Plate 15	PUSS toroidal buoy at deployment.

- Plate 16 PUSS buoy at sea with gemini and gemini crew. The gemini was vital to many manoeuvres during deployment and retrieval of the experiment equipment.
- Plate 17 BGS Sea Bottom Package ready for deployment. Note the stripes parallel to the cylinder axis intended to aid visual measurement of its alignment on the sea bed.
- Plate 18 BGS Sea Bottom Package junction to signal cable.
- Plate 19 BGS Sea Bottom Package sea-bed anchor and signal cable.
- Plate 20 BGS Sea Bottom Package signal cable, sealable junction box and flotation buoys for cable end. Note that sealable junction may be jettisoned overboard and subsequently retrieved if RMAS Salmaster needed to abandon position with the BGS Sea Bottom Package left on the sea-bed. RMAS Salmaster
- Plate 21 Signal cable, flotation buoys and sealable junction box of the BGS Sea Bottom Package manhandled by gemini crew.
- Plate 22 BGS Vertical Hydrophone String coiled on drum ready for deployment.
- Plate 23 Sea Owl.
- Plate 24 Fixing detonators to the 2 ton charge prior to deployment.
- Plate 25 Inching the 2 ton charge across the deck of RMAS Goosander at deployment.
- Plate 26 Deploying the 2 ton charge from RMAS Goosander.
- Plate 27 Submersion of the 2 ton charge from RMAS Goosander.
- Plate 28 Deployment of shot timing hydrophone RMAS Goosander.
- Plate 29 Sea surface effect of the 2 ton explosion : stage 1.
- Plate 30 Sea surface effect of the 2 ton explosion : stage 2.
- Plate 31 Deployment of the 900lb charge.
- Plate 32 Sea surface effect of the 900lb explosion : stage 1.
- Plate 33 Sea surface effect of the 900lb explosion : stage 2.

Plate 1



Plate 2



Plate 3



Plate 4

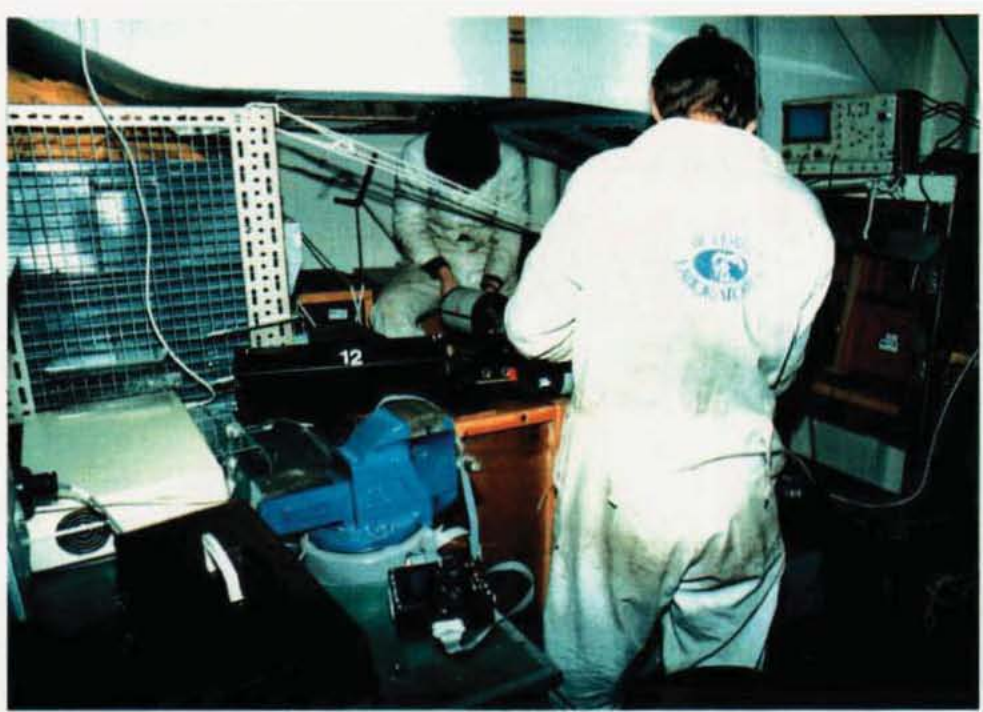


Plate 5



Plate 6



Plate 7



Plate 8



Plate 9



Plate 10

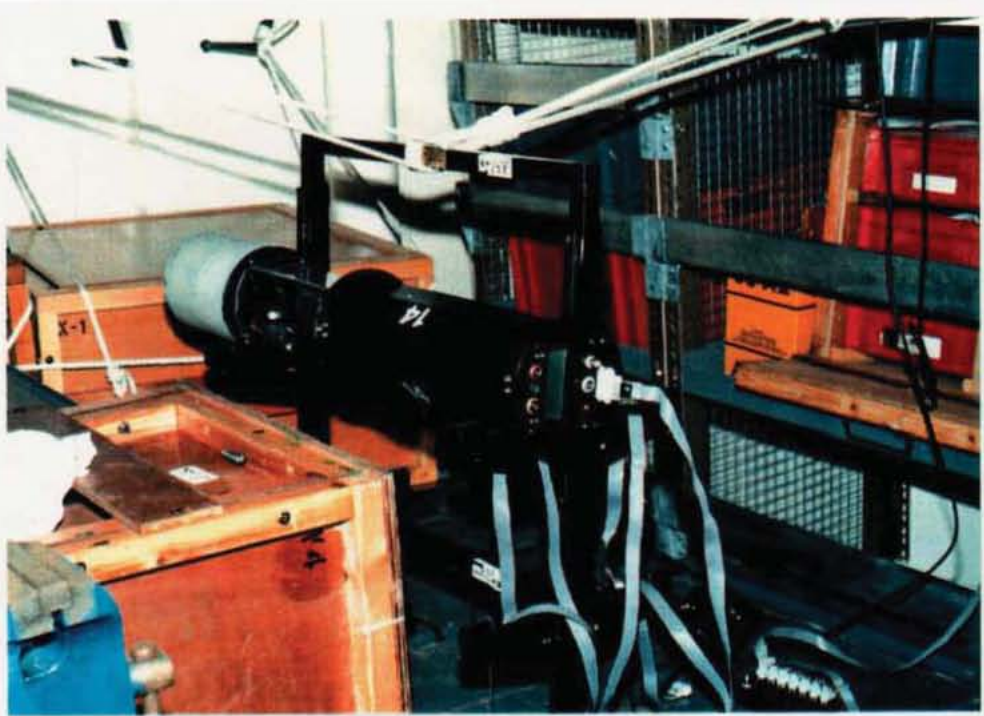


Plate 11

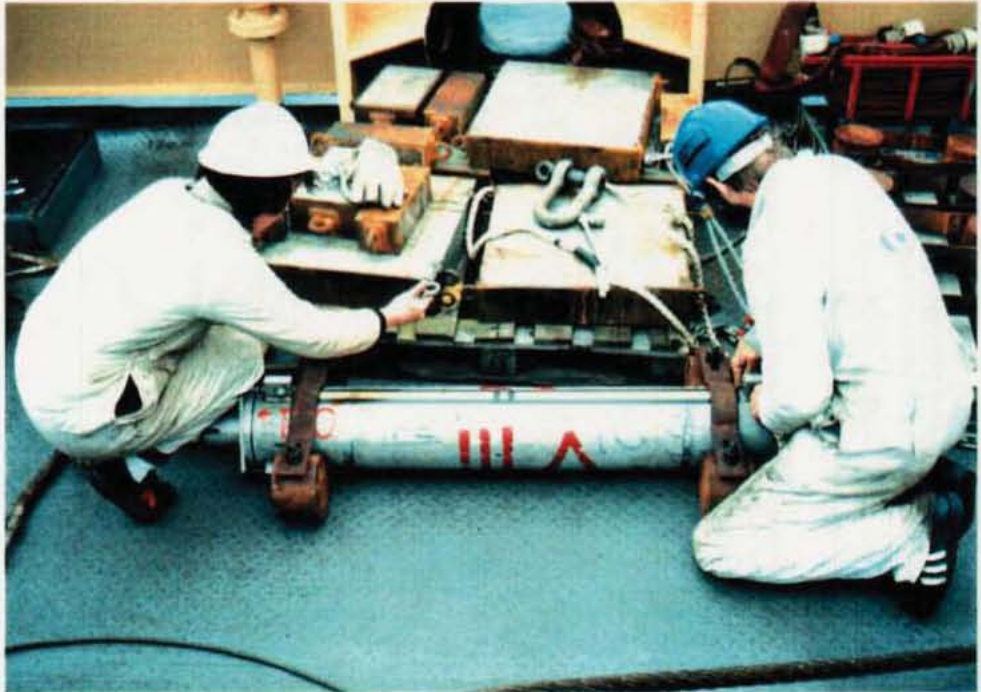


Plate 12

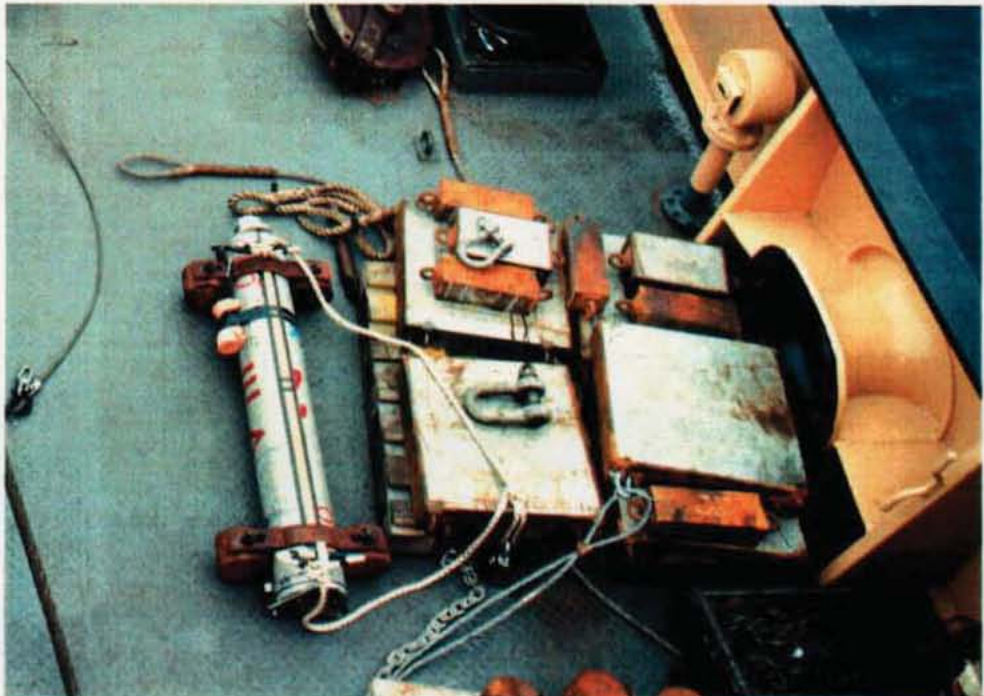


Plate 13

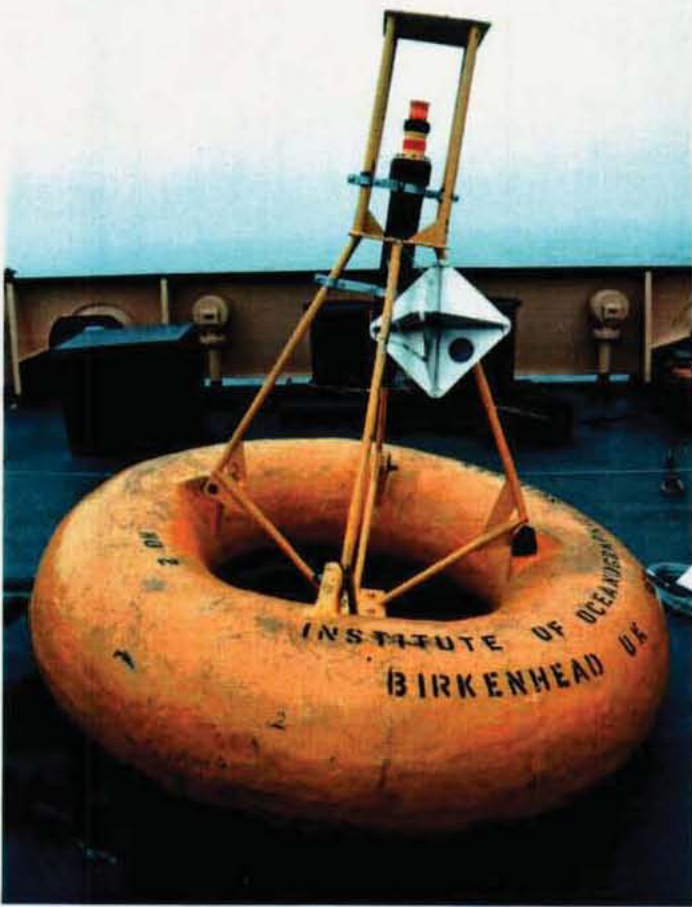


Plate 14



Plate 15

Plate 16



Plate 17

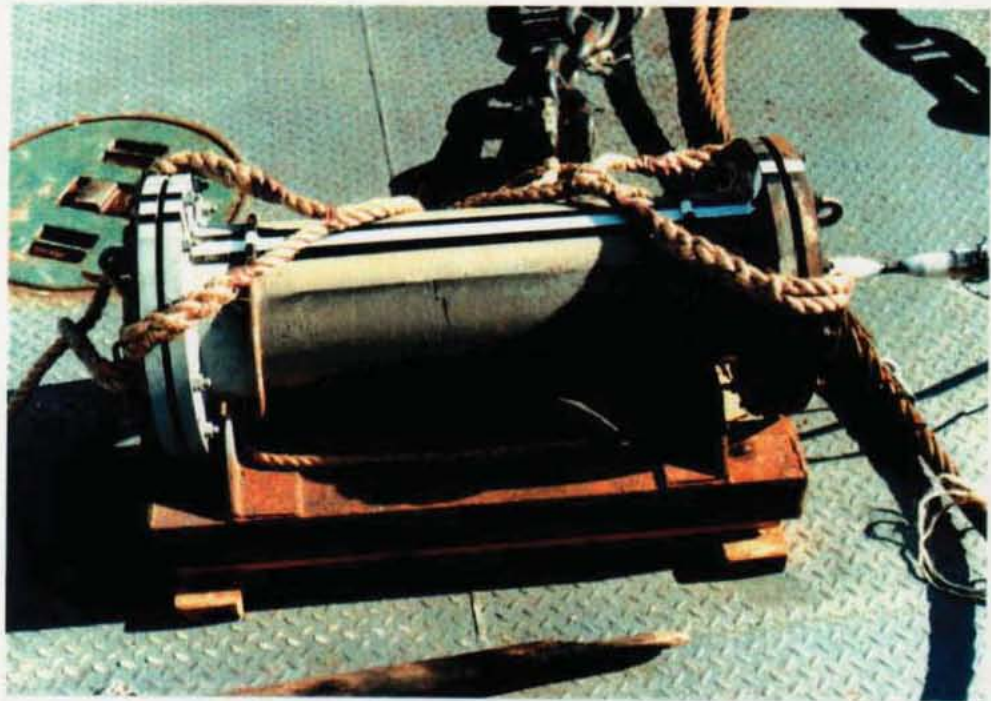
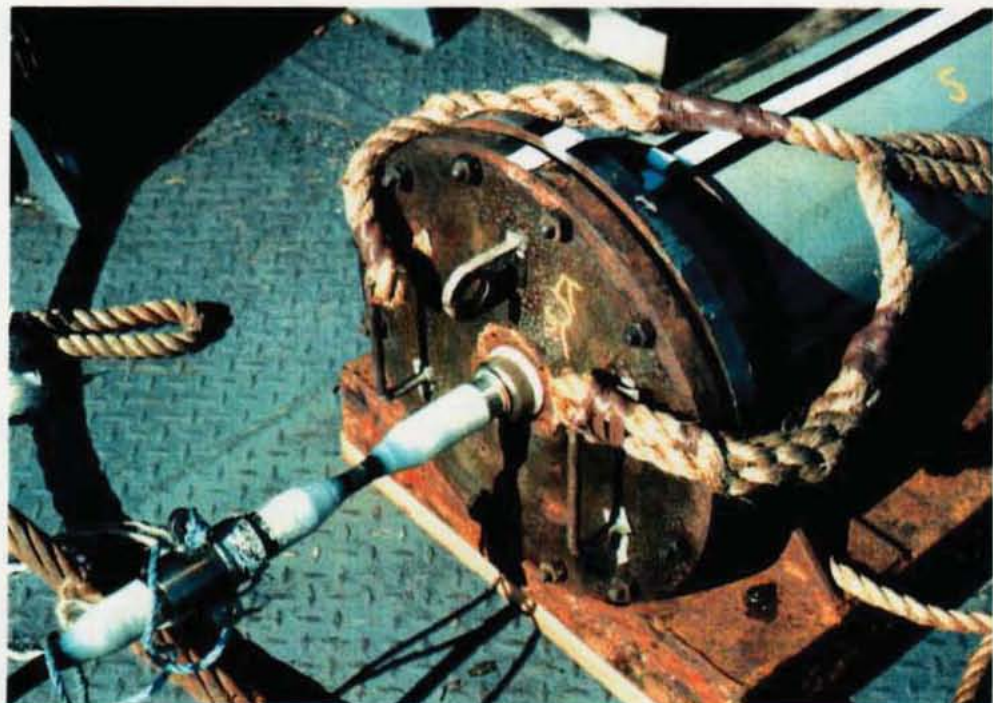


Plate 18



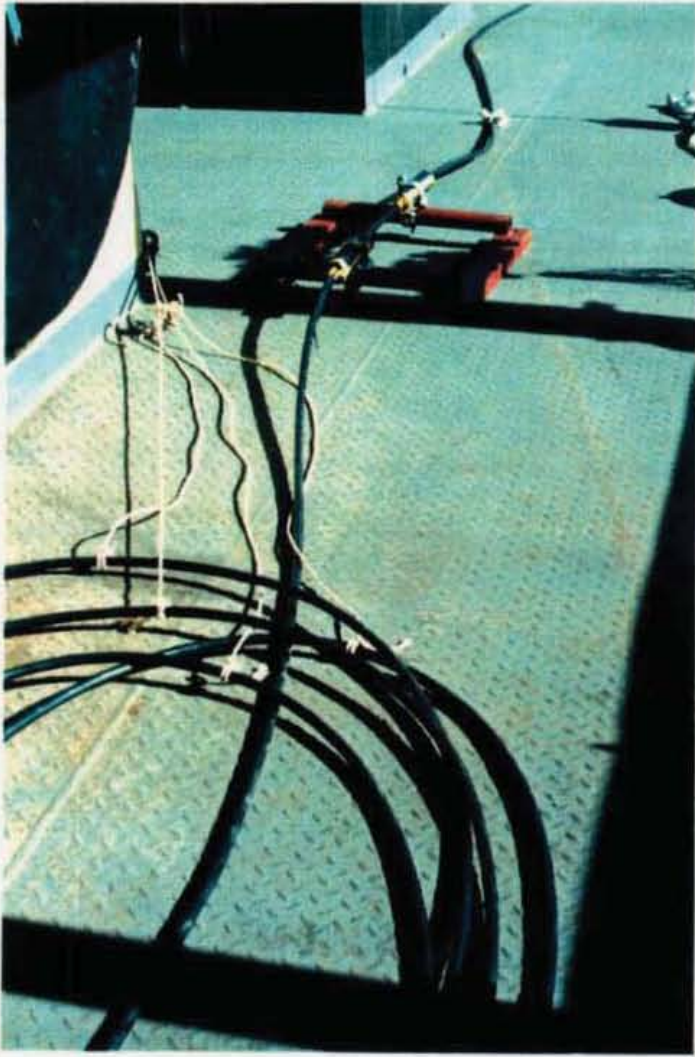


Plate 19

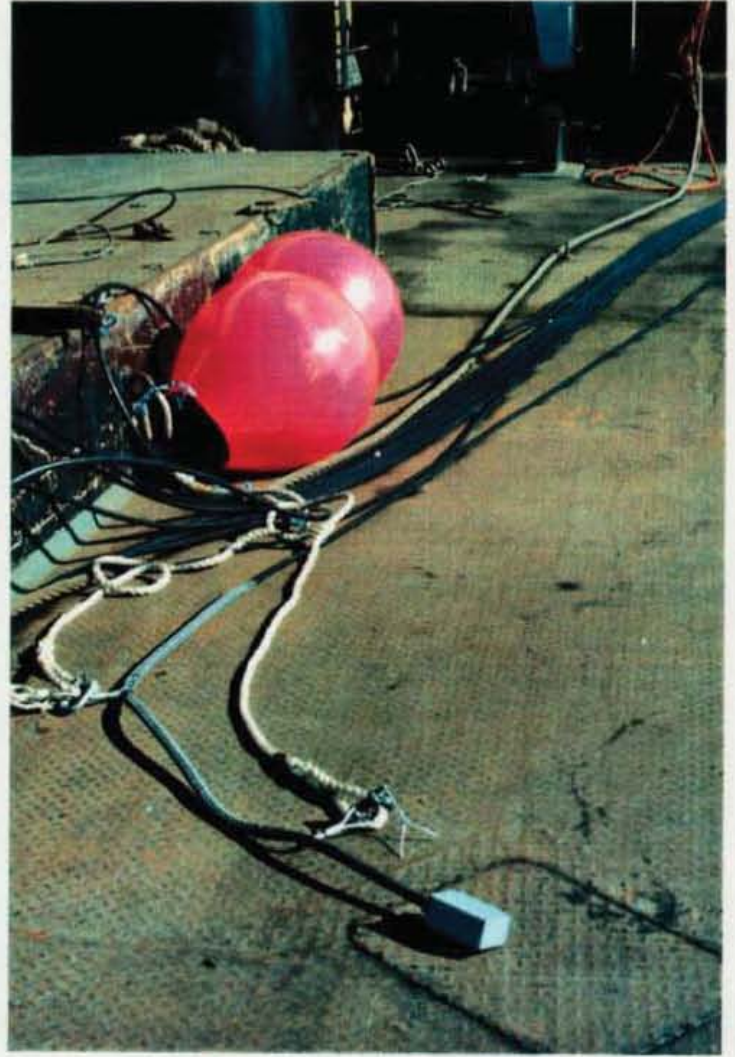


Plate 20



Plate 21

Plate 22



Plate 23

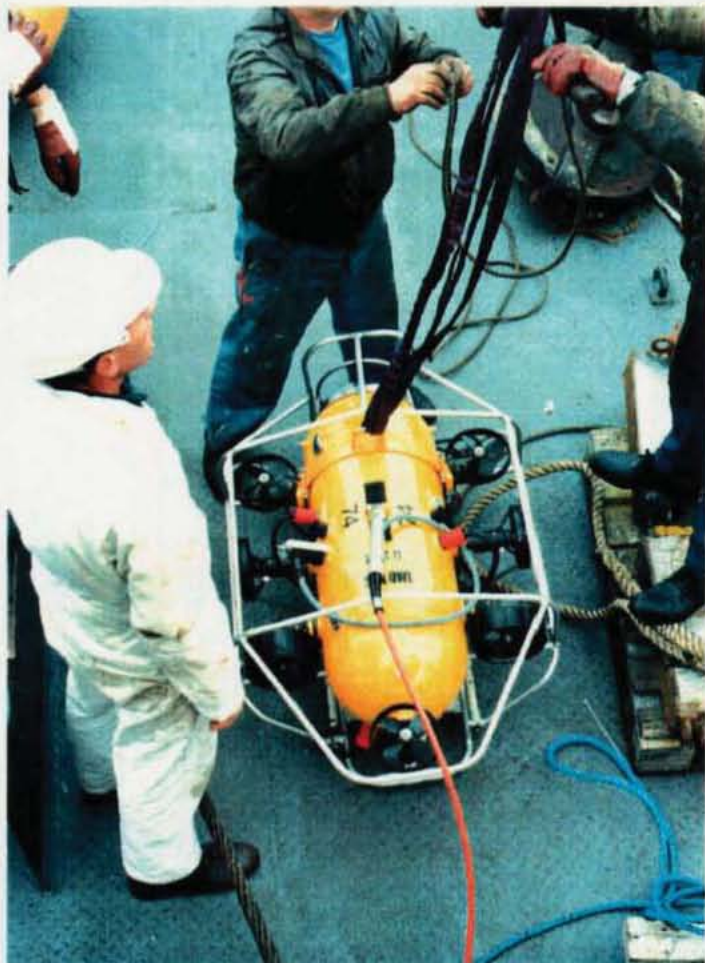


Plate 24



Plate 25



Plate 26

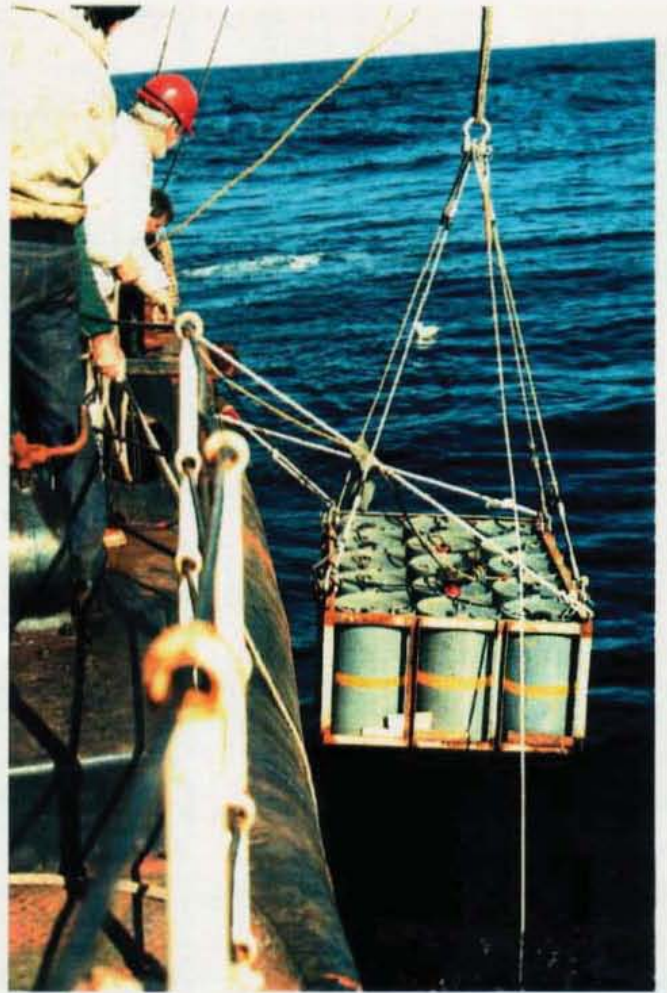


Plate 28



Plate 27

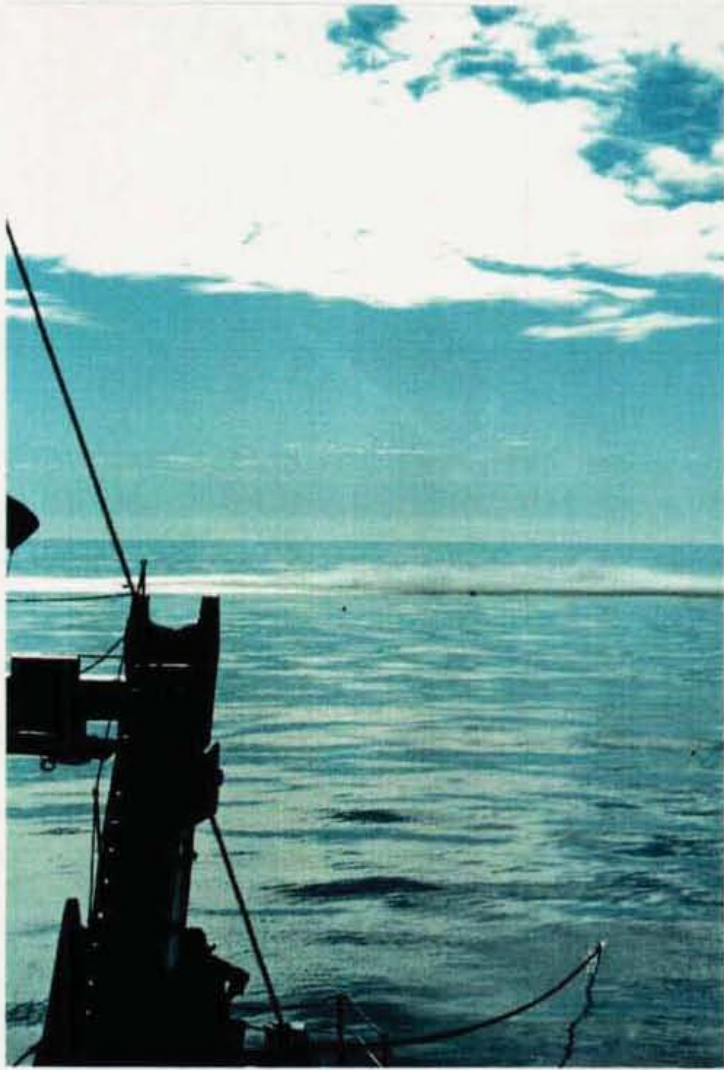


Plate 29

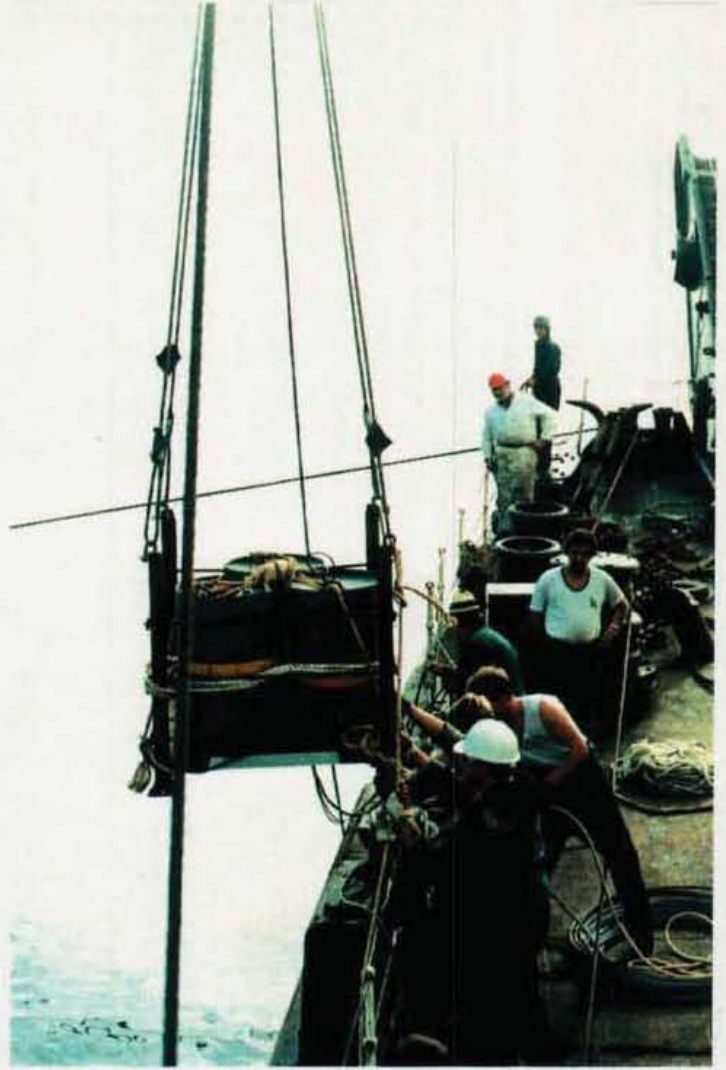


Plate 31

Plate 30

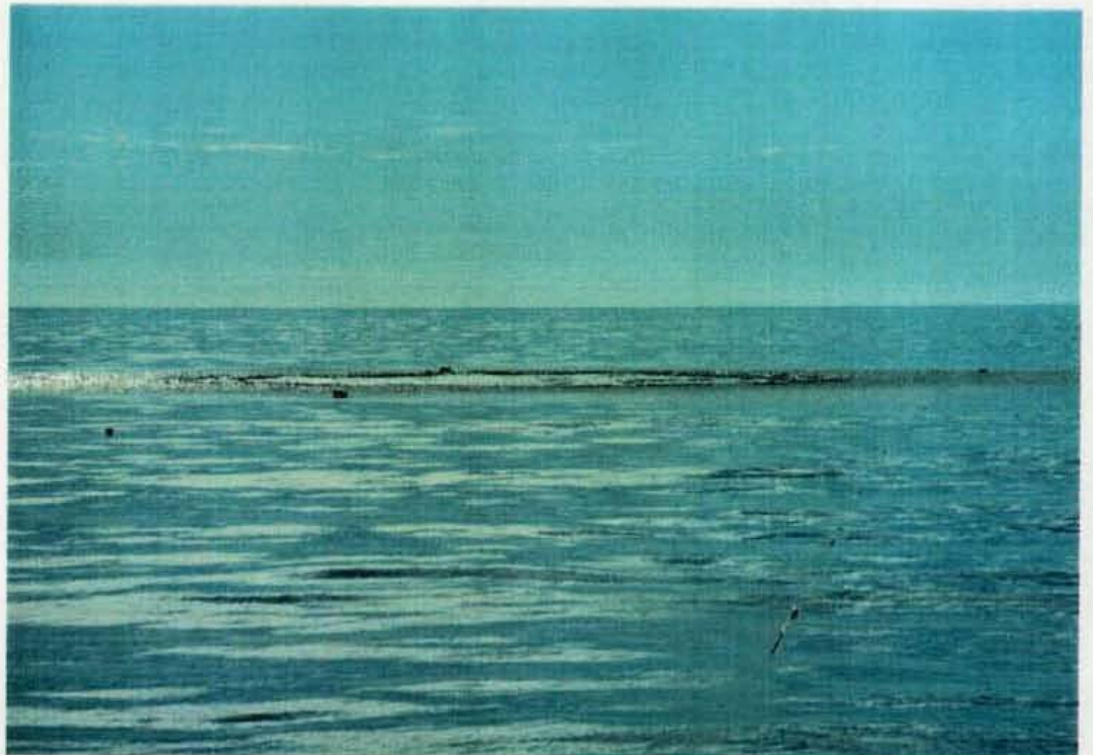


Plate 32



Plate 33

